The Investigation of Targets for Therapy in Brain Tumours

A thesis submitted for the degree of Ph.D.

by Paula Kinsella, BSc, MSc.

2011

This work was carried out under the supervision of

Dr. Verena Amberger-Murphy,

Dr. Niall Barron,

and

Prof. Martin Clynes

National Institute for Cellular Biotechnology

School of Biotechnology

Dublin City University

I hereby certify that this material, which I now submit for assessment on the programme of study leading to the award of PhD is entirely my own work and has not been taken from the work of others save and to the extent that such work has been cited and acknowledged within the text of my work.

Signed:_____ ID N0.:_____

Date:_____

Acknowledgements

I am extremely grateful to my supervisor Verena, from whom I have learnt so much, and is a constant source of inspiration in both her work ethic and strive for perfection.

I would like to sincerely thank Martin for all of his help and support throughout the years, and for giving me the opportunity to carryout this work. I would also like to thank Niall for his invaluable expertise and knowledge in molecular biology, without which the molecular section of my thesis would have been quite difficult. I'd like to thank Rob for initially introducing me to cancer research, with a very exciting lecture during my masters degree many years ago now.

I would like to thank Professor Michael Farrell for his encouragement and enthusiasm. The collaboration with both Michael and Rachel from Beaumont Hospital has been invaluable, and given us direct access to patient samples, making this work more clinically relevant.

I'd like to thank all of my colleagues in the NICB for their help and support over the years. A big thank you to both Carol and Yvonne, who were always willing to help despite the stationary crisis. Thanks to Mairead whose financial juggling played an important role. I'd also like to thank Cancer Research Ireland for providing the funding for this work.

A heart felt thanks to my friends and family who have given me support and advice throughout my Ph.D, they have kept me grounded and have always been there to show me the lighter side of life. I am eternally grateful for having someone as wonderful as Kev in my life, he is a constant source of strength when I need it most; his patience and understanding are invaluable.

Table of Contents

Abbreviations

%	-	Percent
2^o GBM	-	Secondary Glioblastoma
ABC	-	ATP-Binding Cassette
Am	-	Anti-miRNA
Ast	-	Astrocytoma
ATP	-	Adenosine Triphosphate
BBB	-	Blood Brain Barrier
BCB	-	Blood Cerebral spinal fluid Barrier
BCL2	-	B-cell CLL/Lymphoma 2
BCL11B	-	B-cell CLL/lymphoma 11B
BCNU	-	Carmustine
BCR-Abl	-	Breakpoint Cluster Region Abelson (C-Abl oncogene 1)
BCRP	-	Breast Cancer Resistant Protein
Bp	-	Base pair
BSA	-	Bovine Serum Albumin
CCNU	-	Lomustine (Marketed under the name CeeNU in US)
CDKN1A	-	Cyclin-Dependent Kinase Inhibitor 1A
cDNA	-	Complementary DNA
CED	-	Convection-Enhanced Delivery
CI	-	Combination Index
CM	-	Conditioned Media
CML	-	Chronic Myelogenous Leukemia
CNS	-	Central Nervous System
CSF	-	Cerebrospinal Fluid
Ctr	-	Control
Ct	-	Cycle Threshold
DAB	-	3,3' Diaminobenzidine
DCC	-	Deleted in Colorectal Cancer
dH2O	-	Distilled water
DIANA	-	DNA Intelligent Analysis
DMEM	-	Dulbecco’s Modified Eagle’s Medium
DMSO	-	Dimethyl Sulphoxide

DNA	-	Deoxyribonucleic Acid
dNTP	-	Deoxynucleotide Triphosphate (N = A, C, T, G)
Doc	-	Docetaxel
DTT	-	Dithiothreitol
EDTA	-	Ethylene Diamine Tetraacetic Acid
EGFR	-	Epidermal Growth Factor Receptor
El	-	Elacridar
ERBB	-	EGFR
Erl	-	Erlotinib
FFPE	-	Formalin Fixed Paraffin embedded
GBM	-	Glioblastoma Multiforme WHO grade IV
Gef	-	Gefitinib
GF	-	Growth Factor
GFAP	-	Glial Fibrillary Acidic Protein
GSH	-	Glutathione
HCA	-	Hierarchical Clustering Analysis
HIF-1α	-	Hypoxia Inducible transcription factor-1α
H_2O_2	-	Hydrogen Peroxide
HRP	-	Horseradish Peroxidase
IAP	-	Inhibitor of Apoptosis
IC_{50}	-	Inhibitory concentration of 50%
IGF1R	-	Insulin like Growth Factor-1 Receptor
IHC	-	Immunohistochemistry
Imt	-	Imatinib
kDa	-	KiloDaltons
LOH	-	Loss of Heterozygosity
MAPK	-	Mitogen Activated Protein Kinase
MAP4K4	-	Mitogen Activated Protein Kinase Kinase Kinase Kinase 4
MET	-	MNNG (N-Methyl-N'-nitro-N-nitroso-guanidine) HOS Tranforming gene
MDR	-	Multiple Drug Resistance
mg	-	MilliGram
MGMT	-	O6-Methylguanine-DNA methyltransferase

MMP	-	Matrix Metalloproteinase
MRP	-	Multidrug Resistance Protein
mRNA	-	Messenger RNA
µg	-	MicroGrams
µM	-	MicroMolar
miRNA	-	MicroRNA
ml	-	MilliLitre
mM	-	MilliMolar
MTOR	-	Mammalian Target of Rapamycin
NaCl	-	Sodium Chloride
NBD	-	Nuclear Binding Domain
NEAA	-	Non-Essential Amino Acids
ng	-	NanoGrams
NHA	-	Normal Human Astrocyte
NSCLC	-	Non-Small Cell Lung cancer
nM	-	Nano Molar
OA	-	Oligoastrocytoma
OD	-	Oligodendroglioma
PBS	-	Phosphate Buffered Saline
P53	-	Protein 53
P70s6K	-	Ribosomal protein S6 kinase 1
PCA	-	Principle Components Analysis
PCR	-	Polymerase Chain Reaction
PCV	-	Procarbazine, CCNU, and Vincristine
PD	-	Primer-Dimer
PDGFR	-	Platelet Derived Growth Factor Receptor
Pgp	-	P-glycoprotein
PI3K	-	Phosphoinositol 3 Kinase
PIP_3	-	Phosphoinositol 3,4,5-triphosphate
PMSF	-	Phenylmethanesulfonylfluoride
Pm	-	Pre-mRNA
PNP	-	Paranitrophenol phosphate
PPC	-	Peak Plasma Concentration
Pre-mRNA	-	Precursor mRNA

PTKs	-	Protein Tyrosine Kinases
PTEN	-	Phosphatase and Tensin Homolog
PTPRD	-	Protein Tyrosine Phosphatase Receptor D
qRT-PCR	-	Quantitative Real Time PCR
RISC	-	RNA Induced Silencing Complex
RNA	-	Ribonucleic Acid
RNase	-	Ribonuclease
RNasin	-	Ribonuclease Inhibitor
ROS	-	Reactive Oxygen Species
Rpm	-	Revolutions Per Minute
RQ	-	Relative Quantity
RTKs	-	Receptor Tyrosine Kinases
RT-PCR	-	Reverse Transcriptase PCR
SCF	-	Stem Cell Factor
SDS	-	Sodium Doedesyl Sulphate
SEMA6D	-	SEMaphorin 6D
SMAD5	-	SMAD family member 5
SNP	-	Single Nucleotide Polymorphism
NaOH	-	Sodium Hydroxide
SiRNA	-	Small Interfering RNA
S6K1	-	p70S6 Kinase 1
SNP	-	Single nucleotide polymorphism
SRC	-	Sarcoma
STAT	-	Signal Transducer and Activator of Transcription
TBS-T	-	Tris Buffer Saline Tween
TKI	-	Tyrosine Kinase Inhibitor
TLDA	-	Taqman Low Density Array
TMA	-	Tissue Microarray
Tmz	-	temozolomide
TP53INP1	-	Tumour Protein 53 Inducible Nuclear Protein 1
Tris-HCL	-	Tris (hydroxymethyl) Aminomethane
UHP	-	Ultra High Pure Water
UTR	-	Untranslated Region
VEGFR	-	Vascular Endothelial Growth Factor

WHO	-	World Health Organisation
XIAP	-	X-linked Inhibitor of Apoptosis

Abstract

Gliomas are among the most difficult of tumours to treat. Their highly invasive nature leads to recurrence even after aggressive therapy including surgery, radiotherapy and chemotherapy. A promising target for new therapies are tyrosine kinases, because they regulate a large range of proteins involved in growth, metabolism and differentiation. The receptor tyrosine kinases, epidermal growth factor receptor (EGFR), platelet derived growth factor receptor (PDGFR) and C-Kit, as well as the non-receptor tyrosine kinase C-Abl are often amplified, overexpressed, and/or mutated in gliomas and play an important role in glioma development. A number of tyrosine kinase inhibitors (TKIs) have been developed and tested in clinical trials with mixed results.

In collaboration with Beaumont hospital 31 glioma cell cultures were established to identify molecular markers indicative of responsiveness to EGFR and PDGFR blockade. Each culture was characterised with regard to their protein expression profile, their proliferative and invasive behaviour and their responsiveness to three TKIs, erlotinib, gefitinib and imatinib, and two chemotherapy drugs, docetaxel and temozolomide.

All data of 26 high-grade gliomas (20 primary glioblastomas, 2 secondary glioblastomas, and 4 grade III astrocytomas including medical history of the patients were analysed using hierarchical clustering analysis (HCA) and principal component analysis (PCA) employing multivariate statistics.

Two distinct clusters of samples were found, which separated by the expression of PTEN and PDGFR-α in cluster 1 and predominately PDGFR-β, EGFR, phosphorylated C-Kit (p-C-Kit) and phosphorylated C-Abl (p-C-Abl) expression in cluster 2. Principal components analysis of the culture data captured 55% of the variance in the dataset showing PTEN, PGDFR-α and PGDFR-β loading vectors in approximately the same direction.

Imatinib responsiveness was strongly correlated with high expression levels of PTEN and PDGFR-α. Responsiveness to erlotinib was correlated with the lack of expression of all proteins tested, while non-responders showed higher expression of PTEN and PDGFR-α. Responders to gefitinib fit into two groups, the majority (group 1) were influenced by the expression of the proteins tested, while the second smaller group correlated with the lack of protein expression. Non-responders to

erlotinib and gefitinib showed higher expression of PTEN and PDGFR-α; in contrast, these markers were highly expressed in imatinib responders. While influenced by the proteins; erlotinib response may be characterised by lack of expression of those markers.

In a panel of 2 glioma cell lines and 2 glioma cultures tested, the combination effect of imatinib and docetaxel was tested and a strongly synergistic inhibition of the drug combination on proliferation and invasion was seen.

According to their proliferative and invasion characteristics two pools of glioblastoma cultures were chosen and analysed for their microRNA expression. MiR-93 was upregulated in highly proliferative glioblastoma cultures, downregulation of miR-93 reduced proliferation by 13.2%. Validation of miR-93 expression profile in 12 primary glioma cultures, one established glioblastoma culture and normal human astrocytes suggested that miR-93 played a role in the regulation of glioma proliferation and invasion. MiR-23b was upregulated in slowly proliferating glioblastoma cultures. Increased expression of miR-23b in a glioma cell line decreased proliferation by up to 40% and resulted in a 65% knockdown of the X-linked inhibitor of apoptosis gene (XIAP), which has been identified as the most potent member of the inhibitor of apoptosis (IAP) gene family. XIAP protects cancer cells against irradiation and anti-cancer drugs by binding to and inhibiting caspase-3, 7 and 9, caspases are enzymes involved in apoptosis, this makes XIAP an ideal target in the battle against cancer.

Section 1.0 Introduction

1.1 Background

The majority of brain tumours occur in adults from the age of 35 and older. Each year in the United States about 180,000 adults are found to have a brain tumour. In Ireland there were 302 malignant and 39 begnin registered cases of brain tumours in 2007 .

High-grade gliomas are the most common primary central nervous system neoplasms in adults. They are considered to be among the deadliest of human cancers (Jemal *et al*. 2005). Glioblastoma is the most common and aggressive primary malignant cancer of the central nervous system. Despite current therapies the average survival rate of a patient with a glioblastoma is 14 months (Stupp *et al*. 2005). The lethality of a glioblastoma is due to characteristics such as high growth rate, extreme invasiveness, and intrinsic resistance to current therapies. Even novel treatments have not substantially improved the survival rate of glioblastoma patients so far. The use of personalized medicine, by targeting essential molecular mechanisms involved in the survival of the tumour, provides new hope. Glioblastomas commonly express molecular or genetic abnormalities that influence signal pathways which regulate cell proliferation. Overexpression of EGFR and/or mutations of tumour suppressor genes such as phosphatase and tensin homolog (PTEN) (Frederick *et al*. 2000) are the most common oncogenic alteration in glioblastomas. These gains or losses may promote cancerous behaviour but also may be targets for new treatments.

The increasing knowledge of cell-growth signalling pathways and the role of oncogenes and tumour suppressor genes in tumorigenesis are critical for the development of new molecular-based approaches for the treatment of brain tumours. These new therapies may lead to improved prognosis for patients with brain tumours.

MicroRNAs (miRs), although known for several years, are lately gaining increasing importance in cancer research. Every type of tumour analysed has shown significantly different miR profiles, compared to normal cells from the same tissue. MiRs are small non-coding regulatory RNA fragments of 20-22 nucleotides. They regulate a variety of cellular pathways through the control of target gene expression. They bind mRNA through partial homology and, in doing so, can potentially regulate the expression of multiple targets (Zhu *et al*. 2007), most of which are still largely unknown. There are indications that miRs might regulate the expression of

up to 30% of the genome (Lewis *et al*. 2005). MiRs are now emerging as master regulators, which can act as oncogenes or tumour suppressors.

1.2 Glial Cells and Gliomas

There are over 100 different types of brain tumour. Primary brain tumours are classified by histology and location. Primary brain tumours arise from the brain itself, in contrast to metastases, which are derived from tumours developed in other organs and parts of the body. Primary brain tumours can be benign or malignant. Benign brain tumours (e.g. meningiomas, acoustic neuromas, pituitary gland tumours) usually grow slowly and can often be removed by surgery depending upon their specific location in the brain. Malignant brain tumours tend to grow rapidly spreading into the surrounding brain tissue and often cannot be entirely removed surgically. Any cell type in the central nervous system (CNS) has the potential to become neoplastic, often resulting in mixed cell types within a single tumour. Brain tumours are named after their cell type of origin. A schematic drawing of glial cell types present in the CNS is seen in figure 1.1. Astrocytes are stellate cells with numerous processes contacting several cell types in the CNS. These star-shaped cells provide structural and physiological support for neurons in the CNS. Astrocytes are named after the greek word "astro" meaning "star". Oligodendrocytes form the myelin sheets around axons and have an insulating function; they can myelinate up to 50 axonal segments. A number of interactions between glial cells, particularly between astrocytes in the mature CNS, are regulated by gap junctions, forming a glial network (Baumann and Pham-Dinh 2001).

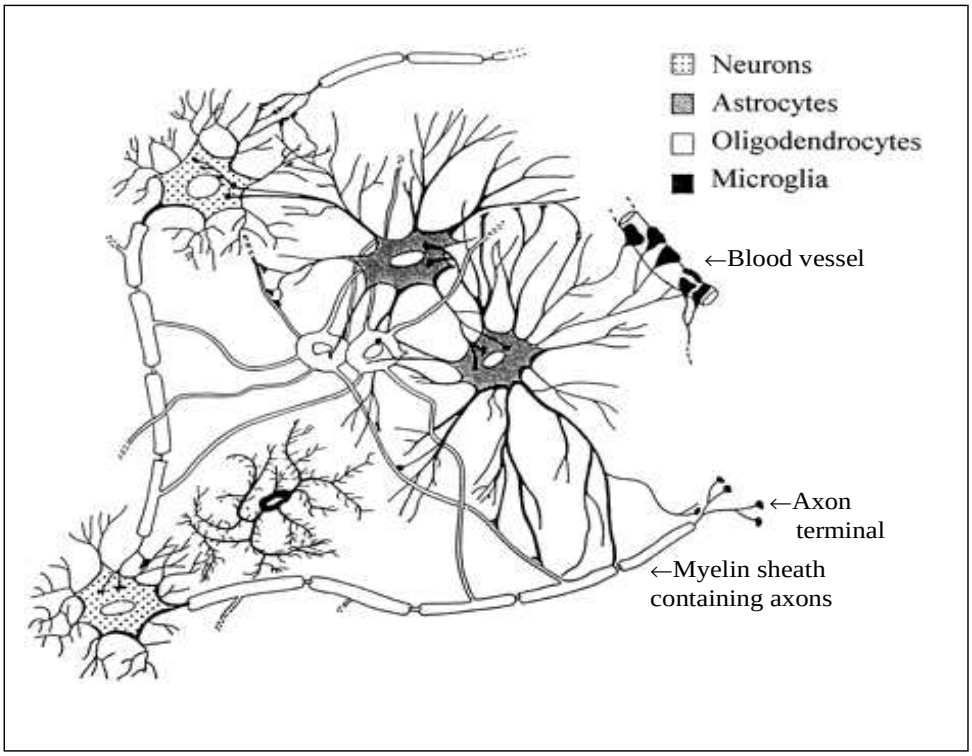

Fig. 1.1 Different types of glial cells in the CNS and their interactions (Baumann and Pham-Dinh 2001). Neurons conduct electrical impulses in the brain, astrocytes provide structural support, oligodendrocytes form myelin sheaths around axons, microglia are involved in the immune response in the brain.

1.2.1 Gliomas

Gliomas are formed from the glial component of the nervous system. These are the most common primary brain tumours. Gliomas are very heterogenous with an infiltrative growth pattern with the majority being resistant to both radiotherapy and chemotherapy. It is thought that a small population of cancer stem-like cells is responsible for resistance to therapy in gliomas (Auger *et al.* 2006; Kolenda *et al.* 2010). Brain tumours have been classified by the World Health Organisation (WHO) according to their cell type and malignancy. Gliomas are comprised of astrocytomas, oligodendrogliomas, oligoastrocytomas, and ependymomas. These tumours are graded according to their malignancy: astrocytomas I-IV, the latter also being known as glioblastoma; oligodendrogliomas and oligoastrocytomas grade II (low-grade) and grade III (anaplastic) lesions (Francis Ali-Osman 2005).

1.2.2 Astrocytomas

Astrocytomas usually occur in the cerebral hemispheres, however they can be found in any location in the CNS. They are derived from astrocytes, show diffuse

infiltration of brain structures, and low-grades tend to progress to more malignant phenotypes. Malignant astrocytomas are the most frequent intracranial neoplasms, and comprise more than 60% of all primary brain tumours. Table 1.1 gives the WHO classification of astrocytomas, based on histological criteria and molecular changes. The mean age of occurrence for low grade astrocytomas is 34, whereas higher grade astrocytomas typically occur within the age range of 40-70 years. Some low-grade astrocytomas progress rapidly to higher grades (1-2 years), while some may show no change in histological grade over more than 10 years. Grade II astrocytomas and higher grades exhibit diffuse invasion and a high rate of transformation, in addition primary glioblastomas are angiogenic, with a higher proliferation rate and increased cellular necrosis than lower grade gliomas (Fig. 1.2). Progression to a higher grade astrocytoma is associated with an increase in multiple genetic alterations. Tumour p53 mutations and overexpression of platelet derived growth factor (PDGFR) are associated with low-grade diffuse astrocytomas. Loss of heterozygosity (LOH) on chromosome 19q is associated with anaplastic astrocytomas. LOH on chromosome 10/MMAC1/PTEN, PDGFR amplification, and loss of DCC (deleted in colorectal cancer) are characteristic of glioblastoma (Table 1.1). Most gene amplification events in high-grade astrocytomas involve the gene for the receptor tyrosine kinase, EGFR. Half of all glioblastoma cases have receptor amplification associated with gene rearrangement. The most common mutation is EGFRvIII. The DCC gene encodes a protein involved in neural cell adhesion. Loss of DCC expression is increased during transformation from low-grade astrocytoma to glioblastoma. Primary glioblastomas usually occur in older patients who do not have a prior history of lower-grade astrocytoma, typically affecting older patients with an average age of 55 years (Paul Kleihues 1997). These primary glioblastomas generally overexpress EGFR, a tyrosine kinase receptor with downstream effects resulting in cell proliferation and invasion. Secondary glioblastomas are thought to arise from lower-grade astrocytomas and usually occur in younger age groups (Nagane *et al*. 2001). These glioblastomas generally do not overexpress EGFR; instead, they commonly have mutations in tumour suppressor gene p53 (Frederick *et al.* 2000), which is responsible for cell-cycle control, DNA repair after radiation damage, and induction of apoptosis, p53 is mutated in approximately 50% of cancers and in 30% of gliomas (Frankel *et al*. 1992) resulting in decreased apoptosis, and predisposition towards neoplastic transformation. There is an

increased risk of developing an astrocytoma when exposed to irradiation of the CNS. There is also a genetic susceptibility including Li-Fraumeni syndrome, p53 germline mutations, Turcot syndrome and the NF1 syndrome (Paul Kleihues 1997).

Table 1.1 WHO classification of diffuse astrocytomas (Paul Kleihues 1997).

WHO Grade	WHO Designation	Histological Criteria	Molecular Characteristics
II	Astrocytoma (low-grade diffuse)	Zero criterion nuclear atypia	P53 mutations Overexpression of PDGFR
III	Anaplastic astrocytoma	Nuclear atypia and mitotic activity	LOH on chromosome 19
IV	Primary Glioblastoma	Nuclear atypia, mitoses, endothelial proliferation and/or necrosis	EGFR overexpression LOH on chromosome 19/MMAC1/PTEN Loss of DCC
IV	Secondary Glioblastoma	Nuclear atypia, mitoses, endothelial proliferation and/or necrosis	P53 mutations LOH on chromosome 19/MMAC1/PTEN Loss of DCC

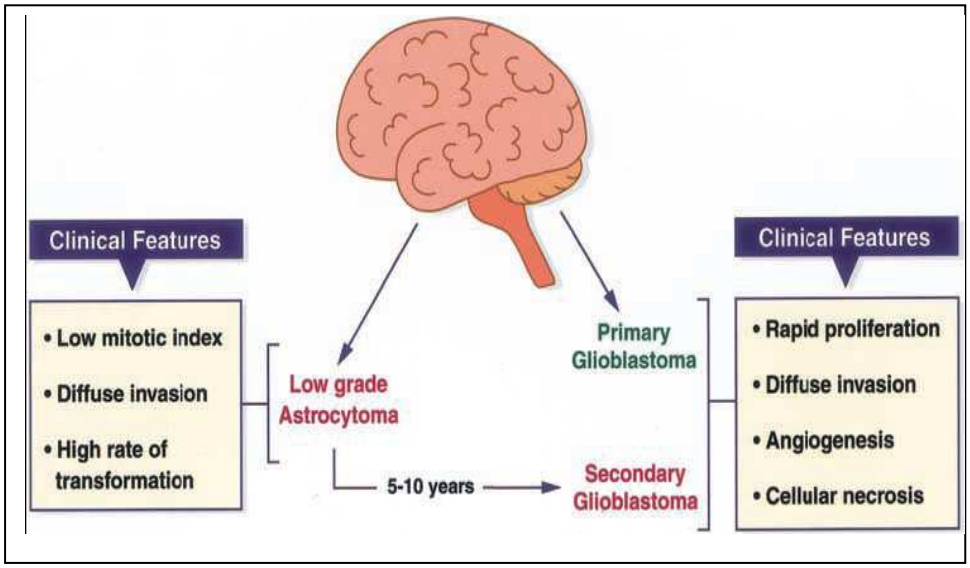

Fig. 1.2 Pathways to glioblastoma formation (Maher *et al*. 2001). There are two types of glioblastoma, (1) a secondary glioblastoma which is derived from a low grade astrocytoma and progresses to a glioblastoma over a number of years; (2) a primary glioblastoma occurs spontaneously. There are large differences in clinical features between primary and secondary glioblastomas.

1.2.3 Oligodendrogliomas

Oligodendrogliomas are derived from oligodendrocytes and account for 5-12% of all glial tumours. They are usually found in the cerebrum, especially in the frontal or temporal lobes, and at the optic nerve. They are more common in adults than in children, with a mean occurrence age of 40-49 years. Survival rates range from 3-10 years. They appear as grade II and III (anaplastic). Oligodendrogliomas with 1p19q respond well to treatment with a combination of procarbazine, CCNU, and vincristine (PCV) (Paul Kleihues 1997). Loss of 1p19q are associated with sensitivity of brain tumours to chemotherapy and radiotherapy, improved outcome with temozolomide treatment has been associated with promoter methylation of MGMT and loss of heterozygosity (LOH) of 1p and 19q in glioma patients (Rivera *et al.* 2010). Oligodendrogliomas are clinically less aggressive than astrocytomas, and tend to have a better prognosis than other gliomas. EGFR amplification and LOH on chromosomal region 19q are predictors of shorter progression-free survival giving a more aggressive form of tumour, and LOH on chromosomal region 1p is associated with longer survival. Mutations in p53 are found in about 10-15% of cases. Half of all oligodendrogliomas have EGFR overexpression (Paul Kleihues 1997).

1.2.4 Mixed Gliomas

Mixed gliomas are made up of two or more neoplastic cell types. The most common mixed gliomas are oligoastrocytomas (Paul Kleihues 1997) which consist of oligodendrocytes and astrocytes; the cell types may be mixed or found in two separate areas, resembling oligodendroglioma or an astrocytoma. Oligoastrocytomas appear as WHO grade II and III. The mean age of occurrence is 45 years. Oligoastrocytomas are usually found in the cerebral hemisphere, the frontal lobes are typically more affected, than the temporal lobes. Some oligoastrocytomas respond well to treatment with PCV. 30-50% of oligoastrocytomas have LOH of 1p and 19q, 30% also have mutations of the p53 gene and/or LOH on 17p. The survival ranges from 5 to 10 years (Paul Kleihues 1997).

Table 1.2 Mutations found in gliomas (Paul Kleihues 1997).

Tumour grade	Mutations
Oligoastrocytomas	Loss of genetic information on 1p and 19q (30-50%) TP53 and/or LOH 17p (~30%)
Oligodendrogliomas	EGFR amplification, overexpression (~50%) LOH 19q and 1p TP53 (10-15%)
Anaplastic Oligodendroglioma	Deletions 9p/or 10p LOH 19q and 1p EGFR overexpression and amplification
Anaplastic Astrocytoma	LOH 19q (~50%)

1.3 Tyrosine Kinases in High-Grade Astrocytic Tumours

The protein tyrosine kinases (PTKs) regulate a large range of proteins involved in processes including growth, metabolism and differentiation. They are divided into receptor and non-receptor tyrosine kinases, which initiate signalling processes by phosphorylation (activation) and dephosphorylation (deactivation) of a variety of downstream proteins including PI3K/Akt and members of the RAS/RAF/MAPK pathway (Schlessinger 2000). As previously mentioned progression to a higher grade astrocytoma is associated with an increase in multiple genetic alterations. The identification of genetic mutations in high-grade astrocytic tumours opened a whole field for possible new therapies, shifting away from the deregulated cell cycle control as the only target. The most prevalent mutations in high grade astrocytomas include the receptor tyrosine kinases (RTKs) EGFR, PDGFR, and the vascular endothelial growth factor receptor (VEGFR). Overexpression or gene loss results in increased downstream neoplastic signalling, and may promote neoplastic cell behaviour. Recent advances in our understanding of the signalling pathways of these growth factor receptors involving their downstream effectors, e.g. phosphoinositol3 kinase (PI3K)-AKT, RAS-mitogen-activated protein kinase (MAPK), made these available as targets and novel treatments have been developed, which resulted in some improvements, particularly in quality of life (Haas-Kogan *et al*. 2005).

1.3.1 Epidermal Growth Factor and its Receptor

EGFR is a receptor tyrosine kinase which plays an important role in normal tissue development and carcinogenesis. EGFR signalling promotes proliferation, migration, and invasion, and inhibits glioma cell apoptosis (Hynes and Lane 2005). EGFR is abnormally activated in 70% of solid cancers, and is amplified or overexpressed in up to 60% of primary glioblastomas (Omuro *et al*. 2007). EGFR amplification is the most common genetic abnormality in high-grade gliomas (Ziegler *et al*. 2008). EGFR is a type I cell surface receptor kinase and a member of the ErbB family which has 4 receptor members: EGFR/ERBB1, ERBB2, ERBB3 and ERBB4. EGFR is a highly glycosylated 170 kDa membrane spanning protein, with a single polypeptide chain of 1186 amino acids. The extracellular domain of EGFR has four subdomains designated I, II, III and IV. The domains I, II and III form the ligand-binding pocket (Fig. 1.3) (Ogiso *et al*. 2002). ERBB2 is the

heterodimerization partner of the other ligand-bound family members. Without the presence of a ligand EGFR exists as monomers on the cell surface. All have an extracellular ligand binding region, a single membrane spanning region and a cytoplasmic tyrosine kinase containing domain. The receptors are expressed in epithelial, mesenchymal and neuronal tissue. The EGF ligands are specific for each receptor (Fig. 1.4). Ligand binding to EGFR results in the formation of receptor homo- and heterodimers, depending on dimerization with itself or with another ErbB family member, and to phosphorylation of specific tyrosine residues in the cytoplasmic tail. These phosphorylated residues serve as docking sites for a number of proteins, resulting in the activation of intracellular signalling pathways (Fig. 1.5). The main pathways activated in response to EGFR and ERBB2 phosphorylation include MAPK, PI3K-AKT, signal transducer and activator of transcription (STAT) and SRC tyrosine kinase (Fig. 1.8) (Hynes and Lane 2005).

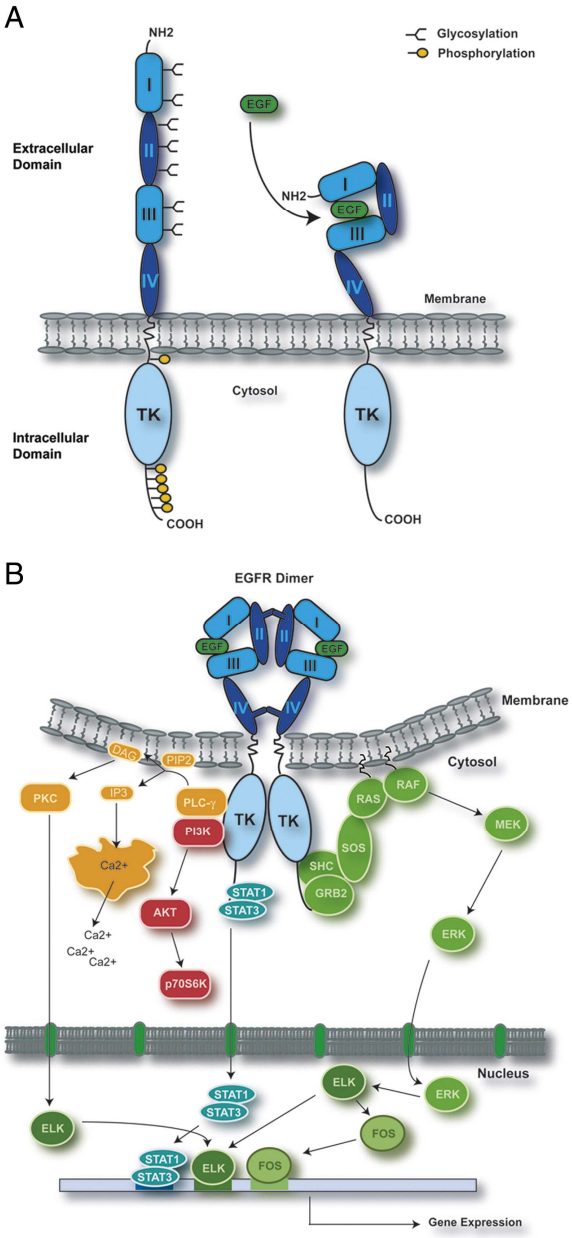

Fig. 1.3 EGFR structure and ligand binding (Zandi *et al*. 2007). The extracellular domain of EGFR has 4 subdomains I, II, III and IV, the domains I, II and III form the ligand binding pocket (A). Ligand binding to EGFR results in the formation of receptor homo- and heterodimers and to phosphorylation of specific tyrosine residues in the cytoplasmic tail; these phosphorylated residues serve as docking sites for a number of proteins, resulting in the activation of intracellular signalling pathways (B).

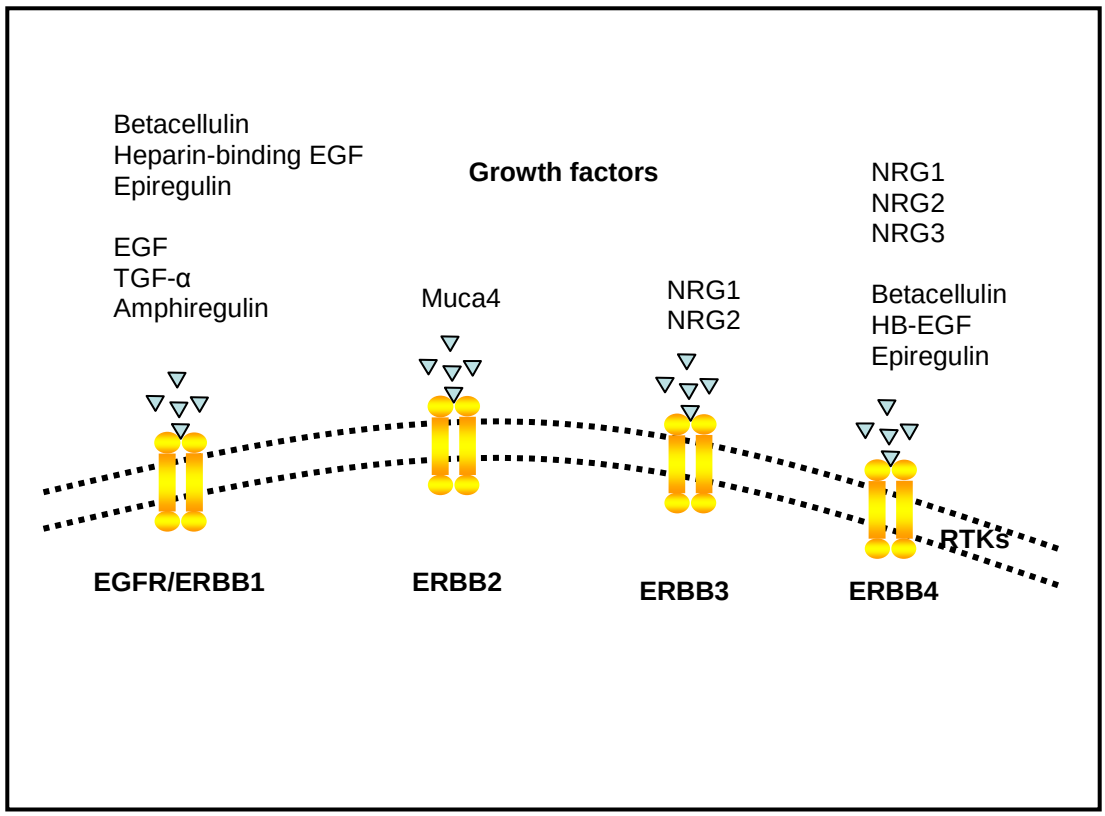

Fig. 1.4 Schematic diagram of EGFR receptors and their ligands. There are four types of EGFR receptors, ERBB1, ERBB2, ERBB3 and ERBB4. Each receptor has specific ligands.

1.3.1.1 EGFR and Cancer

Gene amplification causing EGFR overexpression is commonly found in cancers. Many EGF-related growth factors are produced by the tumour cells or the surrounding stromal cells giving rise to constitutive EGFR activation. EGFR amplification can be caused by structural rearrangements resulting in in-frame deletions in the extracellular domain of the receptor, e.g. EGFRVIII variant. The resulting mutant protein is ligand independent and constitutively phosphorylated. This variant has been found in glioma, breast, lung and ovarian carcinomas. Mutant EGFR activates the pro-survival pathways PI3K-AKT and STAT (Hynes and Lane 2005). Mammalian target of rapamycin (MTOR), a serine/threoine kinase, a downstream activator of the PI3K-AKT pathway, plays a very important role in tumour cell growth and proliferation, by sensing the availability of nutrients/energy. MTOR can also be activated by stimuli other than RTKs (Hynes and Lane 2005).

Mechanisms by which EGFR signalling becomes oncogenic include: (1) overexpression of EGFR, (2) autocrine and/or paracrine growth factor loops, (3)

heterodimerization with other EGFR family members and cross-talk with heterologous receptor systems, (4) failure in receptor downregulation and (5) activating EGFR mutations (Fig. 1.5).

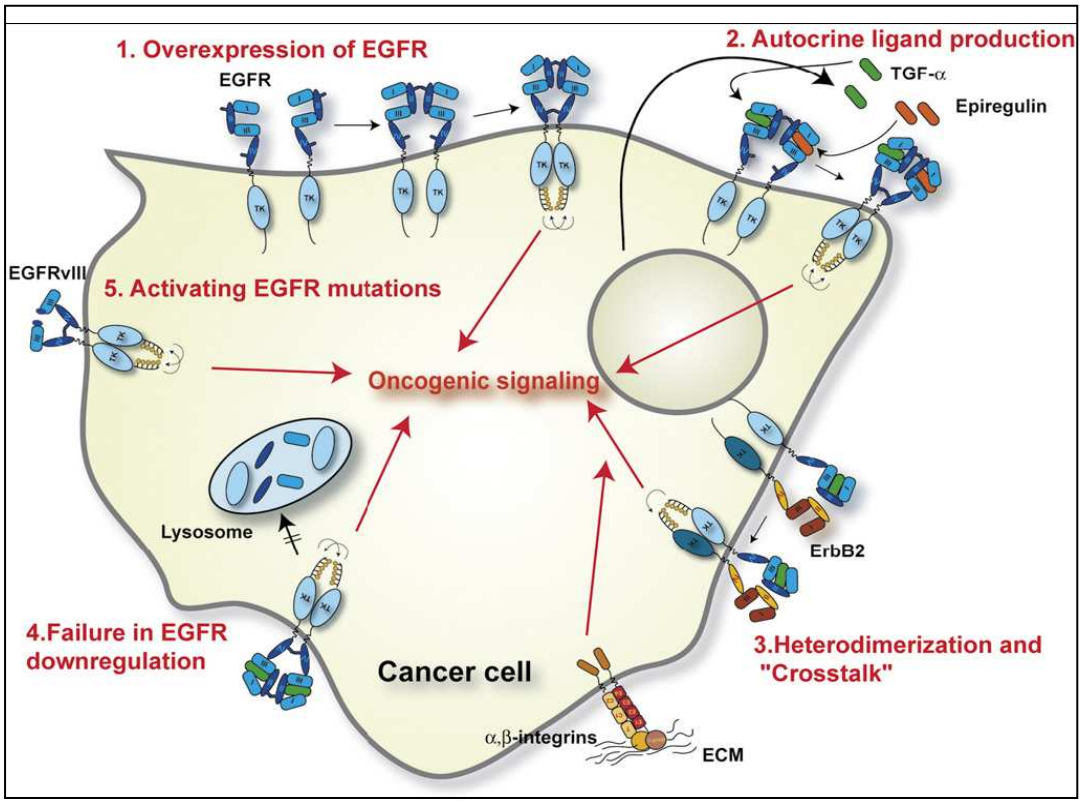

Fig. 1.5 Mechanisms leading to EGFR oncogenic signalling: (1) overexpression of EGFR, (2) autocrine and/or paracrine growth factor loops, (3) heterodimerization with other EGFR family members and cross-talk with heterologous receptor systems, (4) failure in receptor downregulation and (5) activating EGFR mutations (Zandi *et al.* 2007).

1.3.1.2 EGFR as a Target for Cancer Therapy

EGFR receptor overexpression has been found in many human tumours, providing an ideal candidate for selective therapy. Many monoclonal antibodies targeting EGFRs, are already in clinical trials e.g.: Trastuzumab (Herceptin), Pertuzumab (Omnitarg), Cetuximab (Erbitux), Matuzumab, and Panitumumab. However, monoclonal antibodies are of limited use in glioma therapy, because of the restricted passage through the blood brain barrier (BBB). An alternative treatment option is the use of tyrosine kinase inhibitors. They are small molecules preventing phosphorylation of tyrosine kinases, which results in the inhibition of downstream signalling pathways. Examples of TKIs are Gefitinib (Iressa), Erlotinib (Tarceva), Lapatinib,AEE788,CI-

1033, EKB-569 and EXEL 7647/EXEL 0999, some of which are multifunctional inhibitors targeting several TKs.

It is important to consider that by targeting multiple EGFR receptors this may also increase toxicity. Clinical trials have shown that patients with amplified EGFR gene and/or elevated EGFR mRNA expression, have a higher response rate to TKIs and improved survival, than those with low EGFR copy number and/or mRNA expression level (Hirsch *et al*. 2005; Dziadziuszko *et al*. 2006). Tumour cells containing mutated EGFR have constitutively activated pro-survival pathways PI3K-AKT and STAT, and are responsive to TKI treatment resulting in cell apoptosis. A subgroup of non small cell lung cancer patients with mutated EGFR showed tumour regression to treatment with gefitinib (Paez *et al*. 2004).

Another treatment option is a recombinant toxin, TP-38, which consists of the EGFR ligand TGF-α. This has been tested in a phase I toxicity trial for the treatment of glioblastoma patients with promising results: one patient showed a complete response and 3 out of 15 had a partial response, while no toxicity was seen (Sampson *et al.* 2003).

During development cancer cells typically have acquired multiple mutations, causing malignancy; therefore it is unlikely that targeting one specific mutation will kill these cells. The benefit of targeting EGFR as a treatment is still under discussion; it is not known whether treatment failure is due to ineffective agents, or inefficient drug delivery. Resistance to TKIs has become a clinical problem, e.g. chronic myelogenous leukemia (CML) patients expressing the oncoprotein BCR-ABL, usually have complete recovery with imatinib treatment; however, resistance to imatinib has been seen more and more, which is due to acquired mutations in the BCR-ABL kinase domain (Hynes and Lane 2005).

Another possibility for the ineffectiveness of TKI treatment could be the involvement of compensatory growth pathways. Activation of other RTKs has been found, e.g. insulin like growth factor-1 receptor (IGF1R), fibroblast growth factor receptor (Adnane *et al*. 1991; Laban *et al*. 2003). Therefore, a combination treatment targeting ERBB2 and IGF1R has shown reduced cell growth in MCF-7 breast cancer cells (Hynes and Lane 2005).

1.3.1.4 EGFR in Gliomas

EGFR is overexpressed in 50-60% of glioblastomas and EGFRvIII is present in 24-67% (Heimberger *et al*. 2005). Amplification and overexpression of EGFR is a characteristic of glioblastomas. EGFRvIII overexpression in the presence of EGFR amplification is a strong indicator of poor survival in glioblastoma patients (Shinojima *et al*. 2003). The role of EGFR is to mediate cell growth and proliferation signals via the PI3K-AKT pathway, which is negatively regulated by PTEN (Hesselager and Holland 2003). Mutations in the PTEN gene can further predispose the cells toward cancerous proliferation, and are found in 45% of glioblastomas (Pan E 2004).

Following promising results in patients with lung cancer, EGFR blockade was tested in recurrent glioblastomas and was successful in a sub-group. About 20% of patients responded to erlotinib and gefitinib, as determined by a reduction in tumour size measured by MRI. Response was correlated with co-expression of the mutated form EGFRvIII and PTEN; however, the detailed mechanism of action is still unknown (Mellinghoff *et al*. 2005). Sordella *et al*. have shown in lung cancer cells that EGFRvIII activates PI3K/AKT signalling and can sensitise cells to the EGFR inhibitor, gefitinib (Sordella *et al*. 2004). It has not been established whether this is true for glioblastomas. The loss of PTEN might promote resistance to EGFR kinase inhibitors (Bianco *et al*. 2003).

1.3.2 Platelet Derived Growth Factor and its Receptor

The overexpression of PDGF and its receptor PDGFR plays an important role in the development of cancer through an autocrine stimulation of cancer cells and angiogenesis. The PDGF family consists of 4 ligands, PDGF-A, -B, -C, and –D and 2 receptor tyrosine kinases, PDGFR-α and PDGFR-β (Fig. 1.6). The ligands form disulfide-linked homodimers, PDGF-AA, -BB, -CC, -DD, and the heterodimer PDGF-AB. PDGFR-α and PDGFR-β, are transmembrane glycoproteins and have tyrosine kinase activity (Kanakaraj *et al*. 1991). PDGFR-α binds A, B and C chains with high affinity, while PDGFR-β only binds the B and D chains (Lokker *et al*. 2002; Zhuo *et al*. 2004) (Fig. 1.6). Ligand binding leads to receptor homo- or heterodimerization and autophosphorylation of the tyrosine kinase residues which

initiates intracellular signalling cascades (Kanakaraj *et al.* 1991). Two most significant PDGFR signalling pathways are the RAS/MAPK pathway, which mediates an increase in proliferation, migration and differentiation (Schlessinger 1993), and the PI3K-AKT pathway promoting cell survival (Franke *et al*. 1995). PDGF-BB had a more important role than PDGF-AA in normal and tumour angiogenesis (Risau *et al.* 1992). The α–granules of platelets are the main site of PDGF formation; other cell types producing PDGF include macrophages, epithelial and endothelial cells (Lindroos *et al*. 1997; Mondy *et al.* 1997; Demayo *et al*. 2002). Expression of PDGF initiates organ development (Pinzani *et al*. 1996; Ponten *et al*. 2003), and diseases such as fibrosis and atherosclerosis (Wilcox *et al*. 1988).

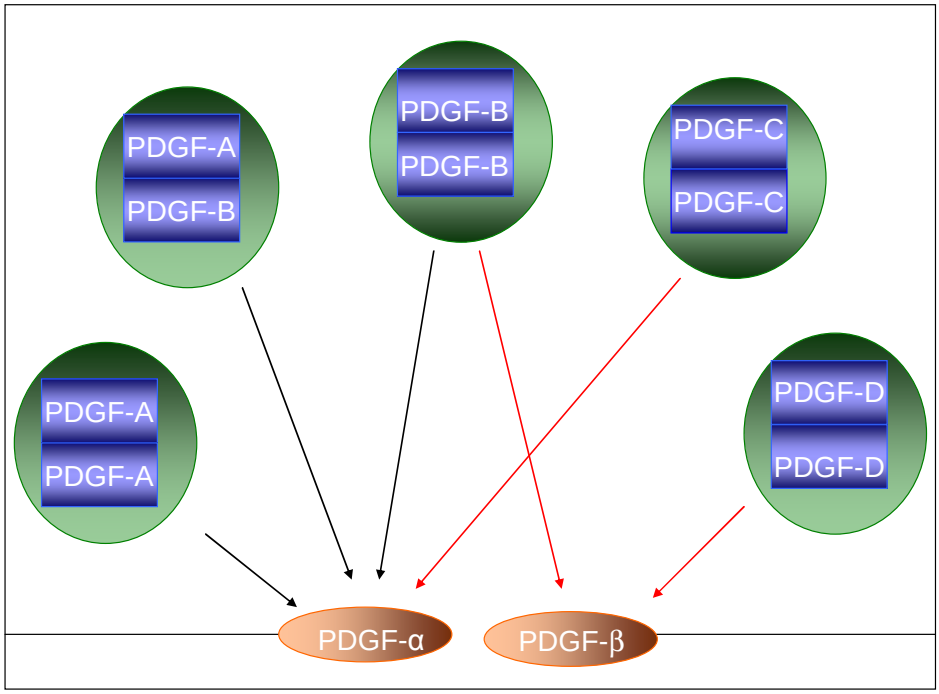

Fig. 1.6 A schematic diagram of PDGF receptors and actions. The ligands form disulfide-linked homodimers, PDGF-AA, -BB, -CC, -DD, and the heterodimer PDGF-AB. PDGFR-α and PDGFR-β, are transmembrane glycoproteins and have tyrosine kinase activity PDGFR-α binds A, B and C chains with high affinity, while PDGFR-β only binds the B and D chains.

1.3.2.1 PDGFR in Glioma

PDGFR and PDGF are commonly overexpressed in glioma, especially in secondary glioblastoma. The overexpression is associated with p53 tumour suppressor gene

loss (Omuro *et al.* 2007). One of the most common cellular signalling defects found in brain tumours, is the presence of a PDGF/PDGFR autocrine loop. The activation of the PDGF/PDGFR autocrine loop is thought to be an early event in the pathogenesis of malignant astrocytomas, and continues to play a role in late stage tumour maintenance (Guha *et al.* 1995). This occurs in all brain tumour grades, including low-grade and anaplastic astrocytomas, and glioblastomas (Maher *et al.* 2001). In addition to PDGF-A and –B, Lokker *et al*. identified the ligands –C and –D. They also found that PDGF-C was ubiquitously expressed in glioblastoma cells and tissue, but its expression was low or absent in normal adult and foetal brain. PDGF-D was expressed in 10 of 11 glioblastoma cell lines and in 3 of 5 primary brain tumour samples (Lokker *et al.* 2002). Looking for PDGFR expression in a series of 101 glioblastoma tissue samples Haberler *et al*, found 25.8% expressed the α form and 24.8% expressed the β form (Haberler *et al.* 2006). Nister *et al*, 1991 found three different phenotypes in 12 out of 13 glioma cell lines, those that expressed PDGFR-α or PDGFR-β only, and those that expressed both receptors (Nister *et al.* 1991).

1.3.3 C-Kit

KIT, a receptor tyrosine kinase, and its ligand stem cell factor (SCF), are highly expressed in embryonic and adult mouse brain, and play an important role in proliferation, differentiation, as well as in cancer cell metastasis, and glioma development (Stanulla *et al.* 1995). SCF induces angiogenesis in the normal brain, and probably in brain tumours since it is found in human gliomas. Expression of C-Kit protein was found only in a small number of tissue samples of low and high-grade gliomas (Blom et al. 2008) and in 4 out of 101 glioblastomas (Haberler *et al.* 2006). While in cell lines, C-Kit mRNA or protein was detected in about 50% (Hamel *et al*. 1992) to 100% (Stanulla *et al.* 1995). The coexpression of the receptor kinase C-kit and its ligand SCF was found in the cytoplasm of glioma cell lines, suggesting its involvement in the autocrine growth regulation of glioma cells (Stanulla *et al.* 1995).

SCF signalling includes the PI3-kinase-AKT, the phospholipase C, the STAT and the RAS/MAPK pathways leading to proliferation, differentiation, cell cycle regulation and apoptosis. It is suggested that KIT plays a role in altering cell

growth and size, and might be responsible for the transformation of astrocytes to gliomas (Blom *et al.* 2008).

1.3.4 C-Abl

C-Abl is a ubiquitously expressed non-receptor tyrosine kinase, which is activated by a number of signals including DNA damage and cell adhesion interactions. Expression of C-Abl is found in the nucleus and the cytoplasm and is involved in two cell responses, cell cycle arrest and apoptosis. C-Abl activates p53 (a cellular tumour suppressor). Under cellular stress p53 is negatively regulated by Mdm2, upon C-Abl phosphorylation p53 is dissociated from Mdm2 resulting in active p53, on recovery from damage p53 reassociates with Mdm2 to form a stable complex (Fig 1.7) (Levav-Cohen *et al.* 2005). Haberler *et al*, found C-Abl expression in just 7 out of 101 glioblastoma tissue samples (Haberler *et al.* 2006). Using tissue samples on a protein lysate array, Jiang *et al*. found overexpression of C-Abl in glioblastomas compared to lower grade gliomas, and suggested an association with poor survival (Jiang *et al*. 2006).

The oncogenic form of C-Abl occurs when the N-terminal portion of C-Abl is replaced with fragments of genes such as bcr, tel or the viral gag, forming the fusion tyrosine kinases Bcr-Abl, Tel-abl, and v-Abl (Shteper and Ben-Yehuda 2001; Wong and Witte 2004). The most important oncogenic form is Bcr-Abl; it is a cytoplasmic protein that triggers mitogenic and anti-apoptotic signals. Bcr-Abl promotes cell proliferation and counteracts p53-mediated apoptosis, by causing constitutive anti-apoptotic signals. Bcr-Abl is present in over 95% of CML patients (Levav-Cohen *et al.* 2005).

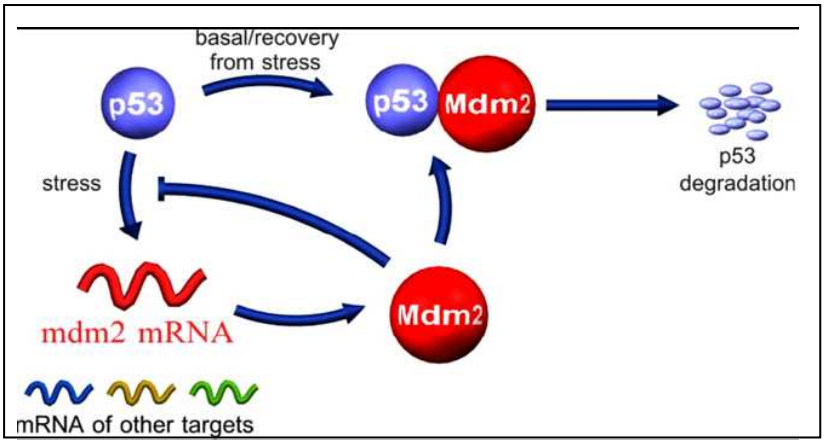

Fig. 1.7 The p53/ Mdm2 negative auto-regulatory loop (Levav-Cohen *et al.* 2005). With cellular stress p53 is negatively regulated by Mdm2, upon C-Abl phosphorylation p53 is dissociated from Mdm2 resulting in active p53, on recovery from damage p53 reassociates with Mdm2 to form a stable complex.

1.4 Signal Transduction Pathways

There are a number of different signal transduction pathways associated with the various receptors mentioned above. In the following paragraphs two of the pathways will be discussed in detail: the RAS/MAPK pathway, and the PI3K/AKT/MTOR pathway. These cellular signalling pathways are required for normal cell physiology (Schlessinger 2000). In gliomas, however, these pathways are overactive due to the overexpression and constitutively activated RTKs (Ali *et al.* 1999). The RAS/MAPK and the PI3K/AKT/MTOR pathway, in particular, are involved in tumour resistance to radiotherapy and chemotherapy.

1.4.1 RAS/MAPK Pathway

In normal cellular proliferation RAS proteins control signalling pathways which are key regulators of cell growth. Overactivation of the RAS/MAPK pathway can increase cellular proliferation, migration and differentiation in several types of cancers including gliomas (Schlessinger 1993). RAS is a membrane-bound G-protein; it exists in an inactive GDP-bound form and an active GTP-bound form. RAS is activated by RTKs, including EGFR, PDGFR, other growth factor receptors and cytokines (Gullick 2008). Activated RAS recruits Raf to the cell membrane. Raf activation requires phosphorylation of a tyrosine residue by a SRC kinase, and/ or phosphorylation of serine/threonine residues by PKC. Activated Raf

activates/phosphorylates mek kinases and subsequently MAPK and ERK, causing ERK translocation to the nucleus. ERK-2 activates nuclear targets such as topoisomerase II-α, a cell cycle progression mediator, and transcription factors including cyclic AMP response element binding protein (CREB), oestrogen receptor-α (ER-α), Iκ-B/NF-κB, and C-Fos. Activation of these transcription factors results in the expression of oncogenes involved in cell cycle progression, cell growth, neoangiogenesis, and anti-apoptosis (Fig. 1.8) (Wong *et al*. 2007). MAPK activation is partially influenced by the level of EGFR expression. MAPK activity is involved in cell migration by interacting with the cytoskeletal machinery; phosphorylation of the myosin light chain kinase results in the phosphorylation of myosin light chains which generate the force to move the cell forward (Wong *et al.* 2007).

Increased activity of RAS-GTP has been found in high-grade astrocytomas. Ras mutations in gliomas are rare in comparison with other cancers (Woods *et al.* 2002). It is thought that activation of Ras in malignant gliomas may be due to the overactivity of membrane tyrosine kinase receptors (Newton 2003). Ras inhibitors such as R111577 (tipifarnib) and SCH66336 (lonafarnib) are being tested in clinical trials (Brunner *et al*. 2003). Both of these demonstrated positive results in preclinical studies (Glass *et al*. 2000).

1.4.2 PI3K/AKT/MTOR Pathway

The PI3K/AKT pathway promotes cell survival. Phosphoinositide 3-kinase (PI3K) regulates EGF-driven cell motility and invasion of glioma, breast, and bladder cancer cell lines (Schlessinger 2000). The activation of this pathway is stimulated by the growth factor receptors, EGFR, PDGFR, fibroblast growth factor receptor (FGFR) and insulin-like growth factor receptor (IGFR). PI3Ks are a family of kinase heterodimers with separate p85 regulatory subunits which are phosphoprotein substrates for RTKs, such as VEGFR, EGFR and PDGFR and p110 catalytic subunits. This pathway is activated either directly through the p85-p110 complex or indirectly through RAS. Accumulation of phosphoinositol 3,4,5-triphosphate (PIP_3), a product of PI3K, is involved in directional movement. This is involved in the role of p85-p110α PI3K isoform in localising actin polymerization and lamellipodia extension in response to EGF. The accumulation of PIP_3 is recognised by Akt which

stimulates cell cycle progression and inhibits apoptosis. Akt promotes cell growth via the mammalian target of rapamycin (MTOR) signalling. MTOR is a central growth regulator. MTOR plays an important role in regulating protein translation through phosphorylation of p70 S6 kinase 1 (S6K1), a protein involved in ribosome biogenesis, and 4E-BP1 (eIF-4E binding protein), a translation repressor. It has been shown that MTOR has a direct linkage to the phosphatidylinositol-3'-kinase (PI3K)/PTEN-Akt survival pathway (Endersby and Baker 2008). Phosphatase and tension homolog (PTEN) is a major tumour suppressor gene which inhibits cell growth. PTEN inhibits PI3K by depleting levels of PIP_3. PTEN loss is correlated with aggressive phenotypes, indicating it plays a role in tumour cell invasion (Schlessinger 2000). PTEN mutations are found in up to 65% of high-grade gliomas, and 15% to 40% of primary glioblastomas (Omuro *et al.* 2007). In glioblastoma, the reduced level of PTEN and increased Akt activity has been correlated with more aggressive tumour behaviour and reduced survival time in patients (Wong *et al.* 2007).

PTEN mutations are found in 20-40% of malignant gliomas (Cai *et al.* 2005). The loss of function of the PTEN is more commonly found in high-grade gliomas, which are extremely invasive. Furukawa *et al*. introduced the wild-type PTEN gene into malignant glioma cell lines, which inactivated Rac and cdc42 (two Rho-family GTP-binding proteins), inhibited MMP-2 and 9 enzyme activity and decreased MMP-2 mRNA expression. This resulted in a significant reduction of migration and invasion activities of the transfected cells (Furukawa *et al.* 2006).

Direct inhibitors of Akt have been difficult to develop, and have not been tested in glioma clinical trials. As an alternative agents have been developed that are directed at the mammalian target of rapamycin (MTOR) pathway (Schmelzle and Hall 2000). The classic MTOR inhibitor is rapamycin, initially developed as an immunosuppressant for patients undergoing transplantation. This agent works by forming a complex that binds to MTOR and inhibits its kinase activity, resulting in G1 cell-cycle arrest (Neshat *et al*. 2001). Preclinical studies have shown that rapamycin is cytostatic against xenografts of glioblastoma and medulloblastoma (Geoerger *et al*. 2001). Compared with PTEN-positive tumours, PTEN-negative tumours appear to be more sensitive to inhibition by rapamycin (Neshat *et al.* 2001). Rapamycin is unstable in solution and has not been used in many clinical trials. Instead, more soluble ester analogs of rapamycin (e.g., CCI-779) have been studied.

CCI-779 has been shown to inhibit glioblastoma proliferation *in vitro* and is currently being tested in several clinical trials (Geoerger *et al.* 2001).

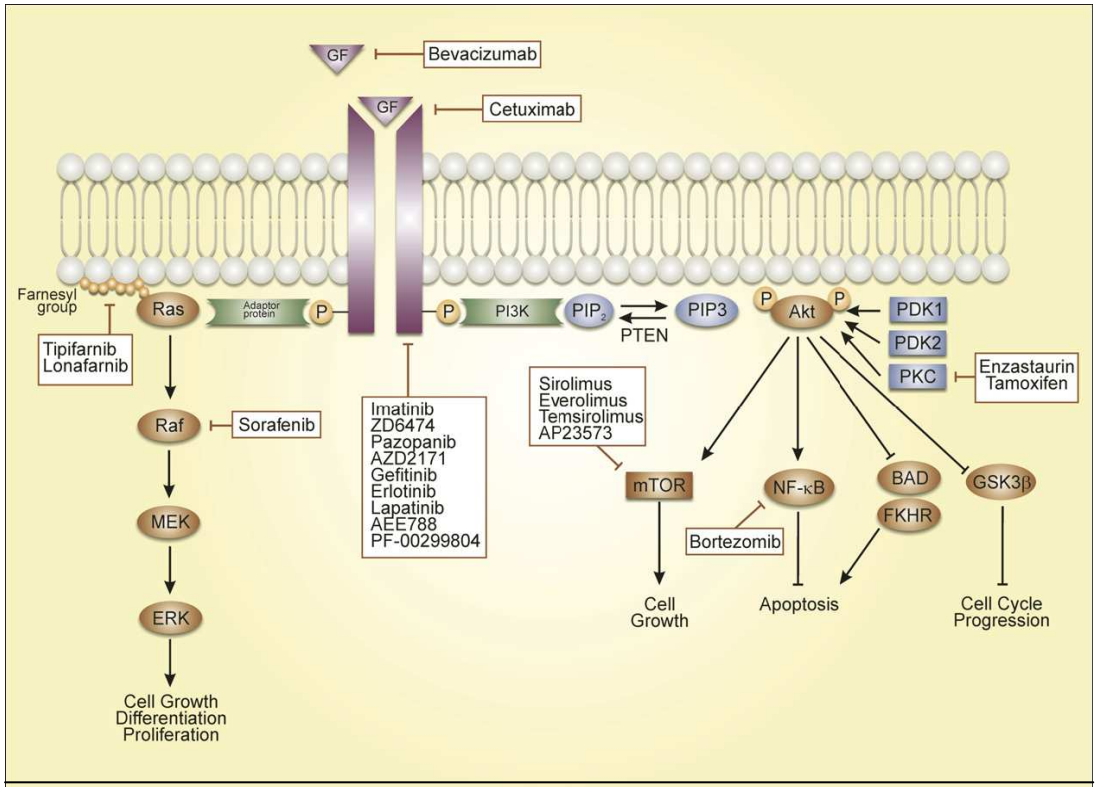

Fig. 1.8 Signalling pathways in malignant glioma. The activation of receptor tyrosine kinase by growth factors (GF) leads to the activation of PI3K/Akt and RAS/MAPK pathways downstream. Various functions are then activated such as growth, differentiation, and apoptosis. A number of targeted therapies are also listed at their site of action (Wong *et al.* 2007).

1.5 Tyrosine Kinase Inhibitors

Tyrosine kinase inhibitors inhibit the phosphorylation and dephosphorylation of a variety of downstream proteins. In addition to the primary effect on growth factor signalling, TKIs seem to reduce matrix metalloproteinase (MMP) expression and activity, which has a negative effect on the invasion and infiltration abilities of tumour cells (Newton 2004).

Clinical trials using TKI as monotherapy on high-grade astrocytic tumours have revealed only modest response rates, confirming *in vitro* studies, which have shown that e.g. effective siRNA silencing of EGFR in receptor-positive cell lines did not inhibit proliferation, migration and activation status of EGFR-coupled signalling cascades in these cells; suggesting single agent treatment not being sufficient (Vollmann *et al*. 2006). Glioblastoma, as with most epithelial cancers, has multiple interactive and dysregulated cell signalling pathways, that will require a multipotent combination of targeted therapies for effective invasion blockage and tumour cell killing.

Although there are several combination therapies currently in clinical trial phase, very little data are available on the interaction between TKIs directed at EGFR and PDGFR/C-Kit/C-Abl, and conventional, cytotoxic drugs.

1.5.1 Imatinib

A promising TKI is Imatinib (GLEEVEC^{TM}, STI1571, Novartis), it was specifically developed to treat chronic myeloid leukaemia (CML), many CML patients have shown a full recovery with imatinib treatment. It specifically inhibits BCR-ABL, created as a consequence of a (9:22) chromosomal translocation: known as the Philadelphia chromosome and used as a diagnostic marker for CML (Druker 2001). The chromosomal translocation causes the fusion of two broken genes, the *BCR* gene on chromosome 9, and the *ABL* gene on chromosome 22, to give a new gene called *BCR-ABL*. The ABL gene produces a tyrosine kinase, which controls growth and division. The fusion protein BCR-ABL contains unregulated tyrosine kinase activity, and is the target for imatinib (le Coutre *et al.* 2004). The development of imatinib began in the late 1980s, when several pharmaceutical companies initiated screens, to identify compounds that would interact with the BCR-ABL tyrosine kinase. The drug was approved in 2001.

Imatinib is a small molecule belonging to the group of phenylaminopyrimidines which have been shown to interact with and inhibit tyrosine kinases. Its main metabolite is N-desmethyl-imatinib. Imatinib itself specifically targets the BCR-ABL tyrosine kinase, blocks any growth signals, which the abnormal protein generates and prevents cell proliferation (le Coutre *et al.* 2004).

Imatinib also inhibits the tyrosine kinases PDGFR-α, PDGFR-β, the stem cell factor receptor C-Kit, the non-receptor protein tyrosine kinase C-Abl, and BCRP expression. PDGFR expression status is directly correlated with imatinib sensitivity (Kilic *et al*. 2000; Hagerstrand *et al*. 2006). However, Haberler *et al.* showed no correlation between the expression of these proteins and the response to imatinib in glioblastoma patients (Haberler *et al.* 2006). Imatinib inhibits growth by cell cycle arrest by selectively disrupting the PDGF receptor autocrine loop (Kilic *et al.* 2000). Clinical trials using imatinib as a single agent resulted in increased progression free survival after 6 months for a small number of patients with recurrent glioblastoma (Katz *et al.* 2004; Raymond *et al*. 2008). The low treatment response could be due to the limited permeability of imatinib into the brain. In mice only 20% of imatinib was shown to cross the BBB, as the other 80% is effluxed by BCRP and Pgp (Bihorel *et al*. 2007). Le Coutre *et al*. have reported a mean peak plasma concentration (PPC) for imatinib of 4-5 µg/ml of a 600 mg dose, and 2-3 µg/ml for a 400 mg dose, 4 hours after oral administration and for the metabolite N-desmethyl-imatinib 531 ng/ml. The average cerebrospinal fluid (CSF) concentration for imatinib was 38 ng/ml, and for N-desmethyl-imatinib it was less than 10 ng/ml showing that only a small amount of drug crosses the BBB (le Coutre *et al.* 2004). High-grade glioma patients have a disrupted BBB, which would allow a higher concentration of imatinib in the CNS; however, it still might not reach an effective concentration. Inhibition of PDGFR alone seems not to be sufficient to stop glioma growth, since other pathways might compensate (Wen *et al*. 2006).

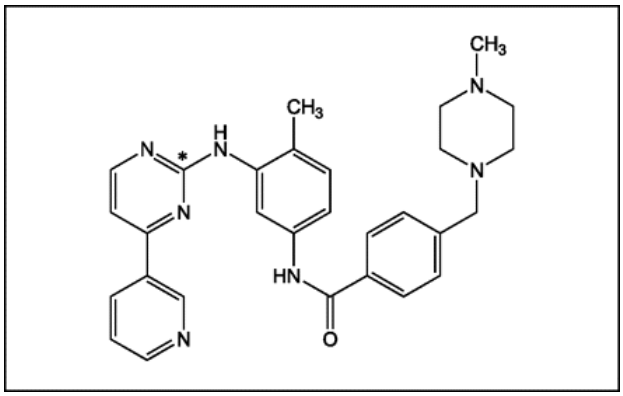

Fig. 1.9 Structure of imatinib, molecular formula $C_{29}H_{31}N_7O \cdot CH_4SO_3$, molecular weight 589.7 (Boddy *et al*. 2007).

1.5.2 Erlotinib

Erlotinib (TARCEVA®, OSI-774, OSI Pharmaceuticals) is an EGFR-specific TKI. It inhibits autophosphorylation of EGFR, resulting in inhibition of EGFR-dependent cell proliferation. In combination with temozolomide it has shown antitumour activity, in a small group of patients with glioblastoma, resulting in an increased survival time (Prados *et al*. 2009). Responsiveness to erlotinib in patients with glioblastomas seemed to be dependent on the co-expression of mutated EGFR (EGFRvIII) and the tumour suppressor gene PTEN (Mellinghoff *et al.* 2005).

The average PPC of 67 ng/ml erlotinib has been seen in patients who received escalating doses ranging from 50 mg/ml to 150 mg/ml of erlotinib (Yamamoto *et al*. 2008). A 75 mg erlotinib dose resulted in an average peak plasma concentration for erlotinib and its active metabolite OSI-420 of 30.3 µg/ml and 2.5 µg/ml, respectively, and in the CSF of 2.1 µg/ml and 0.2 µg/ml, respectively (Broniscer *et al*. 2007).

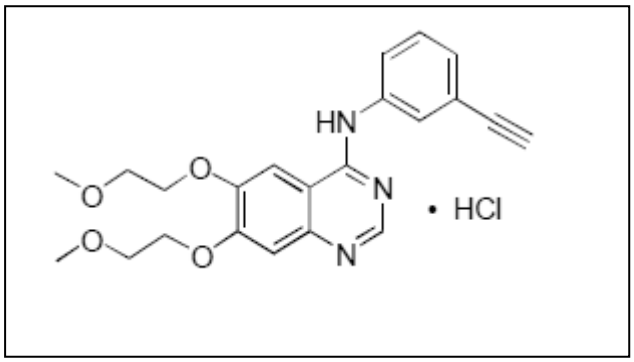

Fig. 1.10 Structure of erlotinib, chemical formula $C_{22}H_{23}N_3O_4 \cdot HCL$, molecular weight 429.90 (rxlist).

1.5.3 Gefitinib

Gefitinib (IRESSA®, ZD1839, AstraZeneca) is a specific inhibitor of EGFR; it inhibits the intracellular phosphorylation of Akt and PI3K. This results in inhibition of proliferation, angiogenesis and induction of apoptosis. Patients with phosphorylated Akt have been shown to be better responders to gefitinib; suggesting patients with Akt activation may be more sensitive to gefitinib (Cappuzzo *et al*. 2004). An average PPC of a 250 mg oral dose of gefitinib measured 5 hours after administration was 85 ng/ml (Swaisland *et al*. 2005).

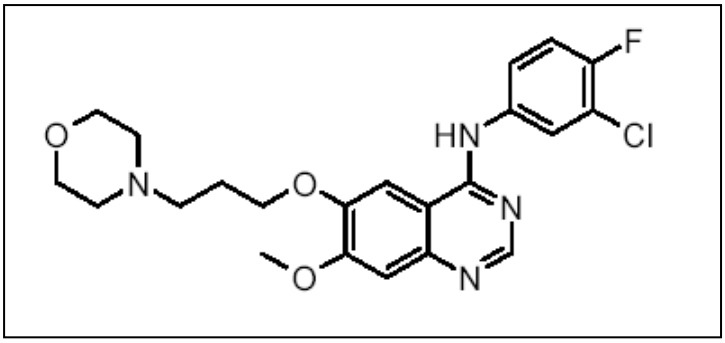

Fig. 1.11 Structure of gefitinib, chemical formula $C_{22}H_{24}ClFN_4O_3$, molecular weight 446.9 (rxlist).

1.5.4 Elacridar

Elacridar (GF120918) N-[4-[2-(6,7-Dimethoxy-3,4-dihydro-1H-isoquinolin-2-yl)ethyl] phenyl]-5-methoxy-9-oxo-10H-acridine-4-carboxamide], a second generation Pgp antagonist is a potent and selective inhibitor of P-gp and BCRP which affect drug efflux at nanomolar concentration (Stokvis *et al*. 2004).

It has been shown in mice that blockade of both Pgp and BCRP by elacridar produced significantly greater brain penetration of imatinib and docetaxel (Kemper *et al*. 2004; Bihorel *et al*. 2007); this effect has also been seen in glioma cell lines with imatinib (Decleves *et al*. 2008), and with docetaxel in lung cancer cell lines (Myer *et al*. 1999).

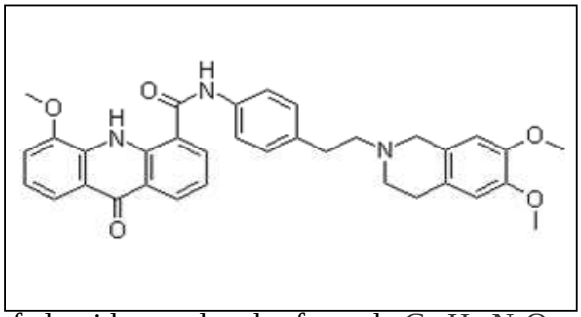

Fig. 1.12 Structure of elacridar, molecular formula $C_{34}H_{33}N_3O_5$, molecular weight 563.64 (www.chemblink.com).

1.6 Mechanisms of Drug Resistance

Multidrug resistance in tumour cells is due to an ATP-dependent decrease in drug accumulation, caused by the overexpression of specific ATP-binding cassette (ABC) transporter proteins. Some of the most significant ABC proteins involved in this process include P-glycoprotein (MDR1/Multidrug resistance 1/Pgp/*ABCB1*), the multidrug resistance protein 1 (MRP1/*ABCC1*), MRP2 (*ABCC2*), and the breast cancer resistance protein (BCRP/MXR/ABCP/*ABCG2*). As well as being involved in drug resistance, these proteins also play a role in tissue defence by forming an essential barrier in specific tissues (e.g. BBB, blood-CSF barrier, blood-testis barrier and maternal-fetal barrier or placenta) and are found in tissues involved in absorption (e.g. lung and gut), metabolism and elimination (e.g. liver and kidney) (Leslie *et al*. 2005).

1.6.1 The ATP-binding Cassette Transporter Superfamily

The ABC protein superfamily is very large and widely expressed throughout the body and in tumours. Most of its members actively transport a large range of compounds including phospholipids, ions, peptides, steroids, polysaccharides, amino acids, organic anions, bile acids, drugs and other xenobiotics. There are 48 ABC genes with 7 superfamilies (A-G) that have been identified in humans. Many of the ABC transporters require ATP binding and hydrolysis at their nuclear binding domain (NBD), to give them the energy to move their substrates across membranes. In each NBD three sequences Walker A, Walker B, and a sequence located between A and B called the ABC signature motif (or C motif), are conserved among all ABC transporter family members and other ATP binding proteins (Leslie *et al.* 2005).

Pgp was the first drug transporter to be associated with multiple drug resistance, followed by the detection of MRP1, MRP2, MRP3, MRP4, and MRP5. BCRP, another important transporter was originally found in a breast cancer cell line. BCRP is highly expressed in placenta, and is possibly regulated by sex hormones (Allikmets *et al*. 1998). The role of BCRP and MRP2-5 in drug resistance is not fully understood. All of the ABC proteins mentioned are also expressed in non-malignant tissue where they protect against xenobiotic accumulation. MRP1 is usually located in the basolateral cellular surface, and high levels are found in the lung, testis, kidneys, skeletal muscle and peripheral blood mononuclear cells.

MRP1, in certain tissues effluxes substrates into the blood. MRP2, BCRP, and Pgp are found in the apical surface of epithelial cells and are highly expressed in areas that need protection from xenobiotics, including the BBB, the placenta, liver, gut and kidneys (Leslie *et al.* 2005).

BCRP is activated by hypoxia-inducible transcription factor (HIF-1α), which is over-expressed in many primary and metastatic cancers, due to hypoxia or loss of Hif-1α-inactivating tumour suppressor genes such as VHL or PTEN (Semenza 2003). BCRP expression has been correlated with drug resistance in several studies about acute myeloid leukaemia (Nakanishi *et al*. 2003), and a subpopulation of tumour cells called a side population. This side population shows high expression levels of BCRP; it was hypothesised that this side population represents cells with stem-like characteristics (Hirschmann-Jax *et al*. 2004). Cancer stem cells are undifferentiated and have the potential for self-renewal and long term proliferation, they can differentiate into many different cell types. This side population has been found in a number of human solid cancers, e.g. ovarian carcinoma, small-cell lung carcinoma, Ewing sarcoma, and prostate cancer. BCRP has a significant role to play in clinical drug resistance and may also have prognostic value. Yoh *et al*. have shown that BCRP -negative non small-cell lung carcinomas had a better rate of response to therapy (44%) than BCRP-positive tumours (24%) (Yoh *et al*. 2004).

1.6.1.1 Specificity for Anticancer Drugs

Pgp is a primary active transporter of bulky amphipathic natural product type drugs e.g. taxanes, vinca alkaloids, anthracyclines, camptothecans, epipodophyllatoxins and TKIs. Besides the common substrates transported by Pgp, MRP1 and MRP2, they also transport uncharged drugs, like methotrexate, cisplatin, and anthracyclins Overexpression of MRP2 is associated with cisplatin resistance. MRP1 and MRP2 also transport metabolites of alkylating anticancer agents including chlorambucil and cyclophosphamide. BCRP causes resistance to a smaller range of anticancer agents, including anthracyclines, mitoxantrone, toptotecan, and the topoisomerase I inhibitor camptothecin, but does not transport vinca alkaloids, epipodophyllatoxins, paclitaxel or cisplatin. BCRP gives resistance to anthracyclines. The MRPs cause resistance to methotrexate after short-term exposure, whereas BCRP causes

resistance to methotrexate after long-term exposure to methotrexate (Leslie *et al.* 2005).

1.6.1.2 Expression of ABC Transporters in the BBB/CSF Barrier/ Brain Parenchyma

The BBB and the blood cerebro spinal fluid barrier (BCB) act as an interface between the circulatory systems. The BBB is made up of a monolayer of brain capillary cells, fused together by *zonulae occulents* and tight junctions to give a continuous cellular barrier, which is impermeable to almost everything except the smallest lipid soluble compounds. BBB capillaries are covered with a continuous basement membrane enclosing pericytes and a cell layer. An astrocytic foot is in contact with the basement membrane and plays a role in the establishment and maintenance of the brain endothelial cell phenotype. Drug metabolising enzymes including cytochrome P450 haemoproteins and UDP-glucoronosyltransferases provide an enzymatic barrier (Fig 1.12) (Leslie *et al.* 2005).

The BCB forms a barrier between the ventricular and the blood systems. It is located in the *choroid plexus* and is formed by highly vascularised cells located in the ventricular system of the brain, which produce cerebrospinal fluid. While the capillaries in the *choroid plexus* do not have tight junctions and are leakier than in the BBB, the choroid epithelial cells do have tight junctions and prevent the passage of compounds from the blood to the CSF. The brain parenchymal cells (glial cells and neurons) give additional protection to the brain by preventing toxin permeability. Pgp expression is found in many cell types in the brain including the choroid plexus, astrocytes, microglia and capillary endothelium. Most importantly Pgp is found in the luminal plasma membrane of the capillary endothelium, where it inhibits drugs and toxins from crossing the capillary membrane into the brain. Pgp is also present in the apical membrane of the *choroid plexus*, where it probably facilitates the transport of compounds from the blood into the CSF (Fig. 1.12(b)) (Leslie *et al.* 2005).

BCRP is mainly expressed at the luminal surface of brain capillaries. MRP1 is expressed at high levels in the choroid plexus, where it regulates the drug concentration in the CSF. MRP1 also functions in brain glial cells. MRP1 is found in the apical side of brain microvessel endothelial cells and in brain capillaries. MRP4

is located in the basolateral surface of the choroid plexus and the apical side of brain microvessel endothelial cells, where it protects against topotecan and other xenobiotics. MRP2 is located in the apical membranes of brain capillary endothelium where it effluxes xenobiotics (Leslie *et al.* 2005).

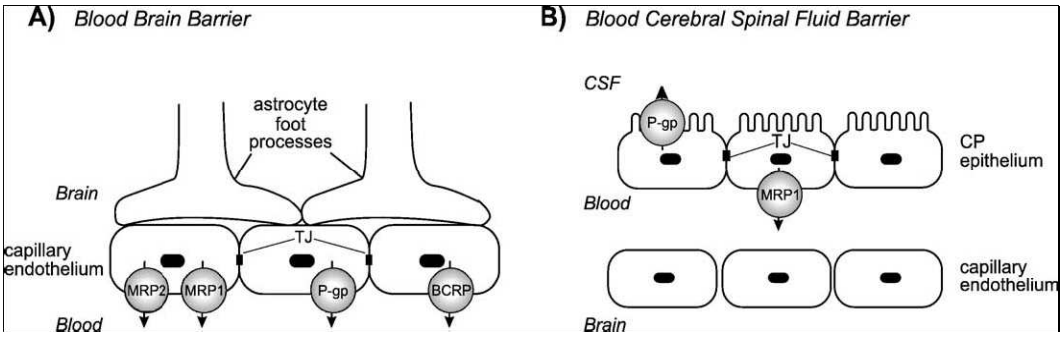

Fig. 1.13 A Schematic diagram showing the membrane localization of MRP1, MRP2, Pgp and BCRP in (A) blood–brain barrier and (B) blood–cerebral spinal fluid barrier. CP, choroid plexus; TJ, tight junctions (Leslie *et al.* 2005).

1.6.1.3 Drug Resistance in Gliomas

Increased expression of resistance genes was not correlated with overall survival of patients with medulloblastomas/PNET and high grade gliomas (Valera *et al.* 2007). Pgp is expressed in newly formed capillaries in human gliomas and might contribute to the resistant behaviour of these tumours (Toth et al. 1996). Pgp expression is upregulated in gliomas (Calatozzolo *et al.* 2005; Valera *et al.* 2007; Nakagawa *et al.* 2009). BCRP expression is upregulated in gliomas (Valera *et al.* 2007; Gilg *et al.* 2008). Pgp possibly inhibits the delivery of anticancer drugs to brain tumours. MRP1 and MRP3 are present in glioma capillaries; MRP1 is also present in glioma cells. MRP4 is present in astrocytes, glioma cells of astrocytic tumours and tumour capillaries. MRP4 may be the sole transporter for astrocytic glutathione release: glutathione is an intracellular reductant which protects cells from free radicals and other compounds. MRP5 is present in astrocytes, glioma capillaries and tumour cells. BCRP expression has not been detected in astrocytes or neurons, but has been found in glioma tumour capillaries, though not in the tumour cells (Nies 2007).

Pgp inhibitors are known as chemosensitizers or reversal agents. They inhibit Pgp drug transport and increase cellular concentrations of therapeutic agents, therefore they are co-administered. Reversal agents include calcium channel blockers like verapamil, calmodulin antagonists such as phenothiazines, quinolines,

immunosuppressive agents such as cyclosporin A, antibiotics such as cefoperazone, and rifampicin, steroid and hormonal analogs, reserpine, and surfactants. Unfortunately some of these agents have severe side effects. Verapamil and cyclosporin A cause cardiotoxicity and increase hepatic, renal, myeloid and neurotoxicity. Second generation analogs to verapamil and cyclosporin A have reduced the side effects (Leslie *et al.* 2005).

Alternative methods of overcoming Pgp mediated drug resistance are monoclonal antibodies against Pgp, anticancer drug containing liposomes which can bypass the Pgp in the lipid bilayer. MDR-1-specific antisense oligonucleotides have also been used to decrease the expression of Pgp mRNA l. As Pgp is expressed in other tissues such as the liver and kidneys, Pgp inhibitors co-administered with anticancer drugs could, however, lead to altered drug metabolism and excretion, and to unwanted side effects (Leslie *et al.* 2005).

1.7 Current Chemotherapy Drugs for Malignant Gliomas

1.7.1 Temozolomide

The first line drug for treatment of high-grade astrocytomas and recurrent glioblastomas is temozolomide (Temodar®, Temodal® – Shering Plough), an alkylating drug, which causes DNA methylation at the O^6 position of guanine and crosslinks between strands of DNA, which results in cell death. Temozolomide induces autophagy, or programmed cell death type II in glioma cells (Aoki *et al.* 2007). The active metabolite of temozolomide is 5-(3-methyltriazeno)-imidazole-4-carboxamide (MTIC) (Rudek *et al*. 2004). The DNA repair protein O^6-methylguanine-DNA methyltransferase (MGMT) reverses the alkylating effect of temozolomide, giving increased resistance to temozolomide. The allelic losses of 1p and 19q are associated with sensitivity of brain tumours to radiotherapy and chemotherapy. Improved outcome after treatment with temozolomide has been associated with promoter methylation of MGMT (or loss of MGMT) and Loss of heterozygosity (LOH) of 1p and 19q in patients with glioblastoma, anaplastic astrocytoma, oligoastrocytomas and, in particular, oligodendrogliomas. In particular, LOH in 1p and promoter methylation of MGMT was associated with longer progression free survival (Ishii *et al*. 2007). In malignant glioma patients temozolomide concentrations range between 0.10 µg/ml and 13.99 µg/ml in the plasma and between 0.16 µg/ml to 1.93 µg/ml in the CSF (Ostermann *et al*. 2004). Up to only 6 months progression free survival is reported for glioblastoma patients (Perry *et al.* 2010). A subcutaneous human xenograft glioma model gel matrix-temozolomide was placed directly at the tumour site, resulting in minimal cytotoxicity toward normal brain tissue, and high levels of oncolytic activity toward glioma cells were seen, this may offer an alternative treatment method (Akbar *et al.* 2009).

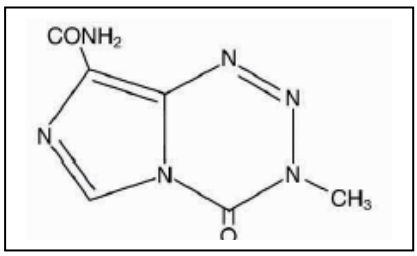

Fig. 1.14 Structural formula of temozolomide molecular formula of $C_6H_6N_6O_2$ and a molecular weight of 194.15 .

1.7.2 Docetaxel

Docetaxel (Taxotere®, Aventis) is a cytotoxic taxane that inhibits depolymerisation of microtubules, thereby interrupting cell proliferation and inhibiting cell motility (Bissery *et al.* 1995). Docetaxel is a hemisynthetic product derived from the European yew tree; it is used to treat various forms of cancer and is one of the most active chemotherapeutic agents for non-small cell lung cancer (Burris *et al.* 1995). As second line treatment in phase II trials for recurrent glioblastoma, docetaxel showed very little response in glioblastoma, which is probably due to the poor penetration of docetaxel through the BBB (Forsyth *et al.* 1996; Kemper *et al.* 2003; Kemper *et al.* 2004). This problem can be addressed by convection-enhanced delivery (CED), which is been used with paclitaxol in an ongoing clinical trial to patients with recurrent gliomas and is showing promising results. CED is a drug application method in which the drug is injected directly into the tumour avoiding the blockage through the BBB (Chamberlain 2006). PPCs for docetaxel have been reported to be 0.5 nM and 0.050 nM for CSF (Fracasso *et al*. 2004).

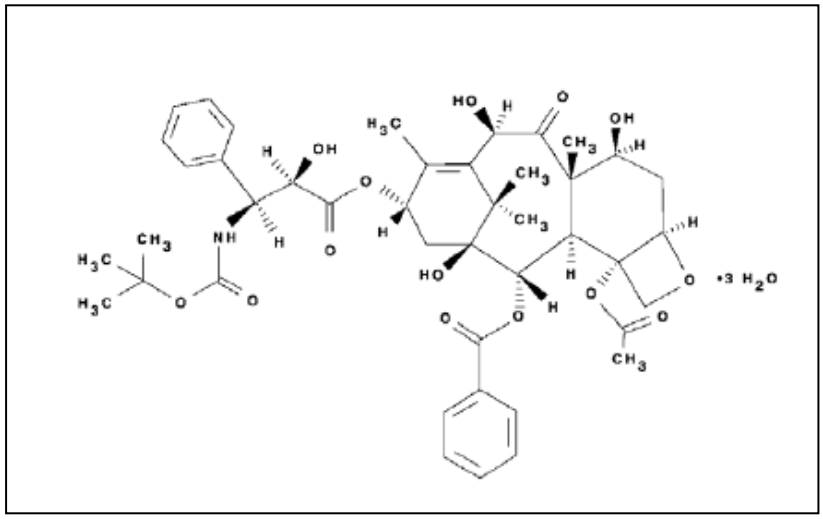

Fig. 1.15 structure of docetaxel, molecular formula of $C_{43}H_{53}NO_{14}•3H_2O$ and a molecular weight of 861.9 (rxlist).

1.8 MicroRNA

1.8.1 Introduction

Micro (mi) RNAs are highly conserved noncoding RNAs that control gene expression post-transcriptionally, by degradation of target mRNAs or the inhibition of protein translation. The discovery of Let-7 in *Caenorhabditis elegans* as a regulator of developmental cellular fate (Reinhart *et al.* 2000) and discovery of let-7-related genes in multiple species indicated the importance of these miRNAs (Pasquinelli *et al.* 2000). This led to the understanding that miRNAs act as key participants in cellular differentiation. MiRNAs have also been found to play a key role in neuronal patterning (Johnston and Hobert 2003), tissue homeostasis (Cui *et al.* 2006), and apoptosis (Baehrecke 2003). There are currently 678 mature human miRNA sequences listed in the miRNA registry (Sanger) with about 1000 predicted miRNAs, each possibly targeting 200 genes (Lewis *et al.* 2003). Lewis *et al*. also identified miRNA target sites in 5300 of 17850 genes in their data set, indicating that >30% of the human genome may be under the translational regulation of miRNAs (Lewis *et al.* 2005).

MiRNAs are now emerging as master regulators which either act as an oncogene or a tumour suppressor, or even affect both phases of tumourigenesis, e.g. the loss of let-7 causes tumour progression by modulating both apoptotic and cell cycle pathways. Each miRNA is thought to control the expression of multiple mRNA targets and have been shown to be involved in the initiation and progression of human cancer. As they control important processes such as differentiation, cell growth and cell death, miRNAs hold great promise for targeted cancer therapy. As miRNA biology evolves we will need to understand miRNA function more on a systems level, where relationships between miRNAs and target genes are less important, than changes in overall gene expression pattern induced by altered miRNA levels (Pasquinelli *et al.* 2000).

1.8.2 MicroRNA Transcription and Function

1. Transcription

These small non-coding RNAs are generated *in vivo* within the chromosome regions once called "junk DNA", which are the introns within protein coding genes. MiRNAs are encoded by specific genes (Nelson *et al.* 2003). MiRNAs are small molecules consisting of about 21 nucleotides; they mediate expression of the target genes by base pairing with complementary regions within target messenger RNA (mRNA). A perfect match causes destruction in a similar way to small interfering RNAs (siRNAs), and mismatches cause inhibition of translation (Nelson *et al.* 2003; Krol *et al.* 2004).

2. Hairpin Release in the Nucleus

MiRNAs are similar in size to siRNAs, but have distinct transcription units in the genome. MiRNAs expressed within introns are expressed with their host mRNA which is derived from introns within the same precursor mRNA (pre-mRNA) transcript. Whereas siRNAs, which are used therapeutically, have exogenous origins and are either directly introduced into cells as ~21-bp double stranded RNA molecules, or are generated *in vivo* from introduced expression vector systems.

All miRNA gene products originate in the nucleus. A primary precursor miRNA (pri-miRNA) is transcribed from noncoding transcription units, or spliced off from introns of pre-mRNA. MiRNAs are expressed as part of pri-miRNAs (Lee *et al.* 2002) and transcribed by RNA Polymerase II, that include 5' caps and 3' poly(A) tails (Smalheiser 2003). The miRNA portion of the pri-miRNA transcript forms a hairpin which signals for double stranded RNA-specific nuclease cleavage.

3. Export to the Cytoplasm

The double stranded RNA-specific ribonuclease Drosha digests the pri-miRNA in the nucleus to release hairpin, pre-miRNA (Lee *et al.* 2003). This Pri-miRNA is processed by Drosha-type endonucleases following the so called pre-miRNA, which is exported from the nucleus by the receptor exportin-5. Exportin-5 binds directly to correctly processed pre-miRNAs, which is a requirement for miRNA biogenesis and a probable role in coordination of nuclear and cytoplasmic processing steps (Yi *et al.* 2003; Lund *et al.* 2004). Pre-miRNAs are 70 nucleotide RNAs with 1–4 nucleotide

3' overhangs, 25–30 base pair stems, and relatively small loops. Drosha also generates either the 5' or 3' end of the mature miRNA, depending on which strand of the pre-miRNA is selected by RNA induced silencing complex (RISC) (Lee *et al.* 2003; Yi *et al.* 2003).

4. Dicer Processing

When the pre-miRNA reaches the cytoplasm it is cleaved by Dicer-type nucleases to form mature, fully processed miRNA. Dicer is a member of the RNase III superfamily of bidentate nucleases, and is involved in RNA interference in nematodes, insects, and plants (Lee *et al.* 2003; Yi *et al.* 2003). The resulting double-stranded RNA has 1–4 nucleotide 3' overhangs at either end (Lund *et al.* 2004). Only one of the two strands is the mature miRNA; some mature miRNAs derive from the leading strand of the pri-miRNA transcript, and with other miRNAs the lagging strand is the mature miRNA.

5. Strand Selection by RISC

Selection of the active strand from the double stranded RNA is based on the stability of the termini of the two ends of the double stranded RNA (Khvorova *et al*. 2003; Schwarz *et al.* 2003). The strand with lower stability base pairing of the 2–4 nucleotide at the 5' end of the duplex associates with the RNA-induced silencing complex (RISC) and thus becomes the active miRNA (Schwarz *et al.* 2003) (Fig. 1.15).

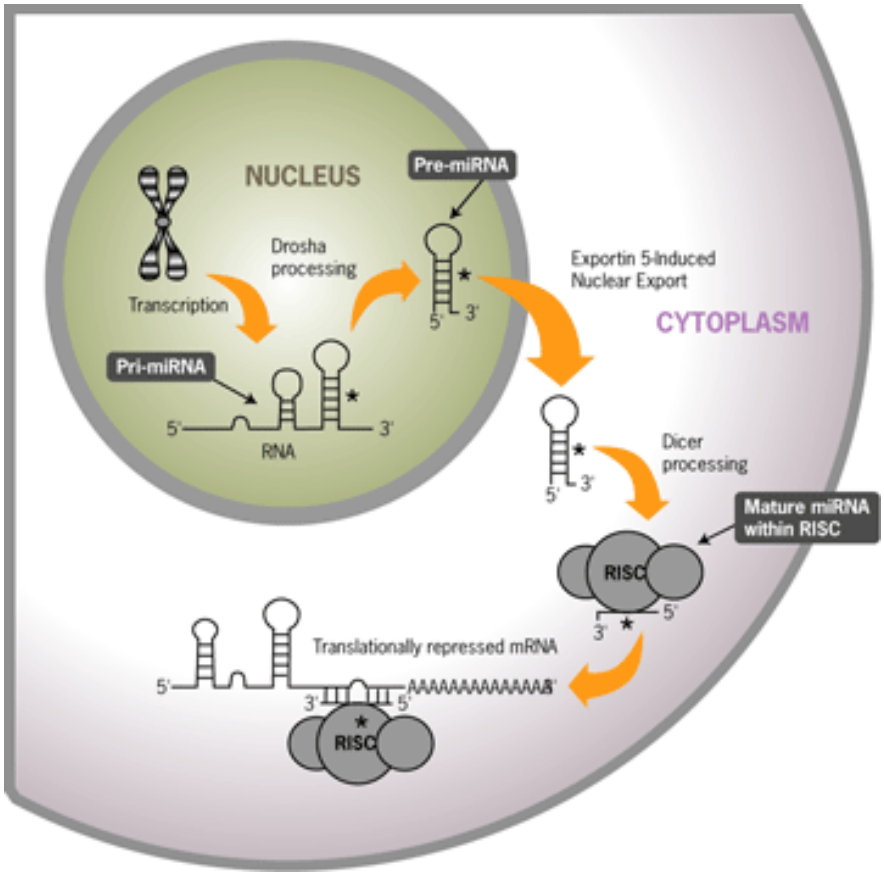

Fig. 1.15 MiRNA transcription. The excision and activation of active single-stranded miRNAs from precursor transcripts occurs through a multi-step process. A primary precursor miRNA (pri-miRNA) is transcribed from noncoding transcription units, or spliced off from introns of pre-mRNA. MiRNAs are expressed as part of pri-miRNAs and transcribed by RNA Polymerase II, that include 5' caps and 3' poly(A) tails. The miRNA portion of the pri-miRNA transcript forms a hairpin which signals for double stranded RNA-specific nuclease cleavage. The double stranded RNA-specific ribonuclease Drosha digests the pri-miRNA in the nucleus to release hairpin, pre-miRNA. This Pri-miRNA is processed by Drosha-type endonucleases following the so called pre-miRNA, which is exported from the nucleus by the receptor exportin-5. Exportin-5 binds directly to correctly processed pre-miRNAs, which is a requirement for miRNA biogenesis and a probable role in coordination of nuclear and cytoplasmic processing steps. The strand with lower stability base pairing of the 2–4 nucleotide at the 5' end of the duplex associates with the RNA-induced silencing complex (RISC) and thus becomes the active miRNA (Ambion).

1.8.3 MiRNA Expression in Gliomas

Oncogenic signalling is central to the development of most cancers, including the most common class of primary brain tumour, glioma. MicroRNAs are small non-coding RNA molecules that regulate protein expression by targeting the mRNA of protein-coding genes, for either cleavage or repression of translation. MiRNAs are

effective post-transcriptional regulators of gene expression and are important in many biological processes. Although the oncogenic and tumour suppressive functions of several miRNAs have been characterized, the involvement of miRNAs in tumour invasion and migration remains largely unexplored. Increased understanding of the molecular and cellular mechanisms that drive glioblastoma formation are required to improve patient outcome.

1.8.3.1 miRNAs Involved in the Proliferation and Invasion of Gliomas

Several miRNAs have been implicated in regulating the development of gliomas through their targeting of mRNA involved in processes including growth and invasion. Knockdown of miR-221/222 in glioma cells and xenograft tumours reduced growth, invasion ability, cell cycle was blocked at G(0)/G(1) phase of the cell cycle, and apoptotic cell number increased (Zhang *et al*. 2009), which resulted in the downregulation of the anti-apoptotic gene bcl-2 and the upregulation of negative regulators of the cell cycle including connexin43, p27, p57, PUMA, caspase-3, PTEN, TIMP3 and Bax (Gillies and Lorimer 2007; Medina *et al.* 2008; Zhang *et al.* 2009; Zhang *et al.* 2009). It is known that P27 is expressed at low levels in high-grade astrocytomas (Piva *et al*. 1997). It seems likely that miR-221/222 play a crucial role in enhancing proliferation in gliomas.

Very little is known about miRNA interactions with cellular pathways. MiRNAs have been associated with the Notch pathway, which plays key roles in nervous system development and in brain tumours (Kefas *et al.* 2009). Neuronally expressed miR-326 was upregulated following Notch-1 knockdown, and was not only suppressed by Notch but also inhibited Notch proteins and activity, indicating a feedback loop (Kefas *et al.* 2009). Transfection of miR-326 into both established and stem cell-like glioma lines and *in vivo* was cytotoxic, and rescue was obtained with Notch restoration (Kefas *et al.* 2009). MiR-326 partially mediated the toxic effects of Notch knockdown (Kefas *et al.* 2009).

MiR-34a is a transcriptional target of p53, and is down-regulated in some cancer cell lines (Li *et al*. 2009). Transfection of miR-34a down-regulated c-Met in human glioma and medulloblastoma cells and Notch-1, Notch-2, and CDK6 protein expressions in glioma cells and stem cells, and strongly inhibited *in vivo* glioma xenograft growth (Li *et al.* 2009). MiR-34a expression is down-regulated in

glioblastoma tissues in comparison to normal brain and in mutant p53 gliomas as compared with wild-type p53 gliomas. MiR-34a in glioma and medulloblastoma cell lines strongly inhibited cell proliferation, cell cycle progression, survival, and invasion (Li *et al.* 2009). In human astrocytes transfection with miR-34a did not affect cell survival or cell cycle status (Li *et al.* 2009). MiR-34a suppresses brain tumour growth by targeting c-Met and Notch in glioma cells and stem cells (Li *et al.* 2009).

Overexpression of miR-125b promotes human glioma cell proliferation and inhibits all-trans retinoic acid (ATRA)-induced cell apoptosis and low expression of miR-125b sensitizes cells to ATRA-induced apoptosis (Xia *et al*. 2009). Bcl-2 modifying factor (BMF) may play an important role in the process of miR-125b influencing cell apoptosis (Xia *et al.* 2009).

MiR-21 up-regulation has been reported for the majority of cancers profiled to date; the mechanism of action of miR-21 is poorly understood, although it is known to contribute to proliferation and apoptosis (Chen *et al*. 2008). MiR-21 expression plays a key role in regulating cellular processes in glioblastomas, and appears to function as an anti-apoptosis factor in glioblastomas (Chan *et al.* 2005; Chen *et al.* 2008; Ohno *et al.* 2009); however the functional target genes of miR-21 are largely unknown. Increased miR-21 levels have been found in human glioblastoma tumour tissues, early-passage glioblastoma cultures, and in established glioblastoma cell lines in comparison with non-neoplastic fetal and adult brain tissues, and in comparison with cultured nonneoplastic glial cells (Chan *et al.* 2005). In addition to increasing apoptosis, inhibiting miR-21 expression has also led to glioma cell growth suppression, invasion reduction, caspase-3 activity elevation and caspase-9 activation, but has not affected PTEN and caspase-8 expression (Shi *et al*. 2008). Inhibiting miR-21 expression could induce glioma cell apoptosis via caspase-9 and 3 activation, but not PTEN activation (Shi *et al.* 2008). MiR-21 is an important oncogene that targets a network of p53, TGF-beta, and tumour suppressor genes in glioblastoma cells (Zhu *et al.* 2007; Papagiannakopoulos *et al.* 2008). Downregulation of miR-21 contributes to the antitumour effects of IFN-beta and miR-21 expression is negatively regulated by STAT3 activation (Ohno *et al.* 2009), it also inhibits the EGFR pathway independently of PTEN status (Zhou *et al.*).

Over-expression of miR-15b resulted in cell cycle arrest at G0/G1 phase while suppression of miR-15b expression resulted in a decrease of cell populations

in G0/G1 phase, and a corresponding increase of cell populations in S phase (Xia *et al.* 2009). MiR-15b regulates cell cycle progression in glioma cells by targeting cell cycle-related molecules including CCNE1 (encoding cyclin E1) (Xia *et al.* 2009).

MiR-181a and miR-181b function as tumour suppressors leading to growth inhibition, apoptosis and inhibited invasion in glioma cells (Shi *et al.* 2008). Down-regulated miR-181a and miR-181b may be critical factors that contribute to malignancy in human gliomas (Ciafre *et al.* 2005; Shi *et al.* 2008).

Control of cell proliferation by Polycomb group proteins (PcG) is important in cellular homeostasis, and its disruption can promote tumorigenesis (Chao *et al.* 2008). Chromobox protein homologue 7 protein (CBX7) is a novel PcG protein controlling the growth of normal cells (Chao *et al.* 2008). The protein level of CBX7 was reduced in glioma tissues and cell lines in comparison to normal brain tissue and the up-regulation of miR-9 in glioma tissues and cell lines, was associated with down-regulation of CBX7 (Chao *et al.* 2008).

MiRNA-128 is significantly down-regulated in glioblastoma cell lines in comparison to normal brain tissue (Ciafre *et al.* 2005; Godlewski *et al.* 2008); increased expression of miR-128 in glioblastoma cells reduced proliferation (Godlewski *et al.* 2008; Zhang *et al.* 2009). MiR-128 targets angiopoietin-related growth factor protein 5 (ARP5/ANGPTL6), Bmi-1 and E2F-3a, key regulators of brain cell proliferation. ARP5/ ANGPTL6 is a transcription suppressor that promotes stem cell renewal, and inhibits the expression of known tumour suppressor genes involved in senescence and differentiation; Bmi-1, a transcription factor critical for the control of cell-cycle progression, and E2F-3a, were found to be up-regulated in glioblastoma (Cui *et al.* 2009; Zhang *et al.* 2009). Addition of miRNA-128 into glioblastoma cell lines restored ARP5 (ANGPTL6), Bmi-1 and E2F-3a expression, and significantly decreased proliferation. Down-regulation of miR-128 may contribute to glioma proliferation by up-regulating ARP5 (ANGPTL6), Bmi-1 and E2F-3a (Cui *et al.* 2009; Zhang *et al.* 2009).

The most common genetic alterations found in glioblastoma include EGFR activation and AKT pathways (Wong *et al.* 1987; Haas-Kogan *et al.* 1998). Low expression levels of miR-7 were found in glioblastoma in comparison to normal brain (Kefas *et al.* 2008). In glioblastoma cells transfection of miR-7 decreased the level of EGFR and upstream regulators of the AKT pathway, insulin receptor substrate 1 (IRS1) and insulin receptor substrate 2 (IRS2); these cells had increased

apoptosis and reduced invasion (Kefas *et al.* 2008). This would suggest that miR-7 regulates the EGFR and AKT pathways. MiR-7 is a potential tumour suppressor in glioblastoma targeting critical cancer pathways. MiR-7 decreased viability and invasiveness of primary glioblastoma lines and is a regulator of major cancer pathways and suggests that it has therapeutic potential for glioblastoma (Kefas *et al.* 2008).

MiR-10b was initially identified as a miRNA highly expressed in metastatic breast cancer, promoting cell migration and invasion (Sasayama *et al*. 2009). MiR-10b expression was found to be upregulated in glioma in comparison to normal brain tissue (Sasayama *et al.* 2009). The expression levels of miR-10b were associated with higher grade glioma. mRNA expressions of Ras homolog gene family, member C (RhoC) and urokinase-type plasminogen activator receptor (uPAR) were significantly correlated with the expression of miR-10b. MiR-10b might play some role in the invasion of glioma cells (Sasayama *et al.* 2009).

MiR-146b significantly reduced the migration and invasion of glioma cells, by targeting a matrix metalloproteinase gene, MMP16. This implicates miR-146b as a metastasis-inhibiting miRNA in glioma (Xia *et al.* 2009).

The Akt pathway, which is regulated by the tumour suppressor gene PTEN (phosphatase and tensin homolog), plays a crucial role in the process of gliomagenesis (Huse *et al.* 2009). MiR-26a is a direct regulator of PTEN expression. miR-26a is frequently amplified in human glioma, most often in association with monoallelic PTEN loss (Huse *et al.* 2009). MiR-26a-mediated PTEN repression in a murine glioma model enhanced *de novo* tumour formation (Huse *et al.* 2009).

1.9 Plan of Investigation

Characterisation of a Panel of Newly Developed Glioma Cultures

- To establish new glioma low passage cultures, derived from brain tumour biopsy samples.
- To compare these low passage cultures with established glioma cell lines and early passage cultures from other laboratories; to identify potential cellular or molecular therapeutic targets.
- To examine invasion, migration, proliferation and apoptosis in the presence of tyrosine kinase inhibitors imatinib, erlotinib, and gefitinib and chemotherapeutic drugs docetaxel and temozolomide, as single agents and in various combinations.
- To examine the expression of EGFR in the glioma cultures in relation to the responsiveness to tyrosine kinase inhibitors, as erlotinib and gefitinib are tyrosine kinase inhibitors which specifically target EGFR, to determine if EGFR expression is indicative of a responder or non-responder to TKIs which target EGFR in glioma.
- To compare the expression of specific targets of imatinib including PDGFR-β, C-Kit and C-Abl in relation to responsiveness to imatinib in the cultures, to see if these targets are indicative of responsiveness to imatinib in glioma.
- To see if the expression levels of ABC transporter proteins, Pgp and BCRP indicated sensitivity or responsiveness to TKIs or chemotherapeutic drugs.
- To correlate responsiveness to TKIs with their target expression including PDGFR-α, PDGFR-β, C-Abl, C-Kit, (specific targets of imatinib); EGFR and EGFRvIII (specific targets of erlotinib and gefitinib), and downstream targets of the EGFR and PDGFR signalling pathway, e.g. phosphorylated Akt, PTEN and p70S6K in the cultures.
- To measure the accumulation of tyrosine kinase inhibitor gefitinib in a panel of these cultures, to determine if the amount of drug within the cell is related to responsiveness to gefitinib in glioma cells.

Identification of Key MiRNAs

- Identification of key miRNAs, which are correlated with tumour proliferation and invasion, in fully characterized primary cell cultures developed from brain tumour tissue, in order to identify novel markers and increase our understanding on the pathways involved in glioblastoma proliferation and invasion.
- Validation of identified key miRNAs in selected established cell lines and primary glioma cultures and in normal human astrocytes. To identify miRNAs associated with proliferation/ invasion in malignant glioma.
- Functional validation of identified key miRNAs in selected glioma cultures, to demonstrate that these miRNAs have a significant role to play in the progression of malignant glioma.

1.10 Overall Thesis Hypothesis

To develop a cohort of early passage glioma cultures from tumour biopsy samples and determine their response to the TKIs, erlotinib, gefitinib and imatinib and correlate this with expression of specific targeted proteins of the TKIs, EGFR, PDGFR, C-Abl, C-Kit and downstream targets of the EGFR and PDGFR signalling pathway, PTEN, Akt and p70S6K to see if expression of these proteins is indicative of TKI response in glioma.

To characterise the glioma cultures in relation to their invasion and proliferation rate, and look at the effect of TKIs and chemotherapeutic drugs on these characteristics. To examine the expression of drug efflux pumps in these cultures, and to correlate this with drug sensitivity.

To identify key miRNAs which play a role in the malignant progression of glioma, i.e. that are directly involved in the regulation of proliferation and/ or invasion in glioma.

Section 2.0 Materials and Methods

2.1 Cell Culture

All cells were cultured in Dulbecco's Modified Eagle's Medium (DMEM) with 10% fetal calf serum (Harlan 5-0001AE), and 4% non-essential amino acids (NEAA) 100x (GIBCO 11140).

Normal human cerebral and foetal astrocytes were purchased from Lonza (CC-2565) and cultured in an astrocyte bullet kit (CC-3186) containing 500 mls of Astrocyte Basal Medium (no growth factors) and Supplements for a complete growth medium, developed especially for NHA.

2.1.1 Origin of Cell Cultures

Primary cell cultures were established from brain tumour biopsy samples from Beaumont Hospital, Dublin. Approved by the Ethics (Medical Research) (ERC/IRB) Committee in Beaumount Hospital, Dublin9, investigator: Professor Michael Farrell, protocol number: 04/05, title: Cellular Investigation of Drug Effect on the Invasive Behaviour of Malignant Astrocytoma, final approval date 31st August 2005.

All newly established glioma cultures were below passage 10. The passage numbers of other cell cultures used during this study are listed in table 2.1.

Table 2.1 Passage numbers of cell cultures used in this study.

Cell Culture	Passage Numbers
CLOM002	11 to 40
UPHHJA	9 to 25
SNB-19*	+9 to +31
IPSB-18	52 to 72
NHA	Below 6
SNB-19- Tem	+40

*: SNB-19 has the same origin as the cell line U251 and there is a possibility that they are the same cell line (Lorenzi *et al.* 2009).

Table 2.2 Origin of cell cultures

Cell Culture	Origin	Source
CLOM002	Primary Glioblastoma	1
UPHHJA	Primary Glioblastoma	1
SNB-19	Primary Glioblastoma	2
IPSB-18	Grade III Astrocytoma	1
NHA	Cerebral & Foetal Astrocytes	3
SNB-19-Tem	Primary Glioblastoma	4
N070055	Grade III Oligoastrocytoma	4
N070126	Primary Glioblastoma (later res)	4
N070152	Primary Glioblastoma	4
N070201	Grade III Astrocytoma	4
N070219	Grade II Oligodendroglioma	4
N070314	Grade II Oligodendroglioma	4
N070788	Grade III Astrocutoma (prev res)	4
N070859	Primary Glioblastoma	4
N070865	Primary Glioblastoma	4
N080501	Primary Glioblastoma	4
N080533	Primary Glioblastoma	4
N080540	Primary Glioblastoma	4
N080869	Primary Glioblastoma	4
N080923	Primary Glioblastoma	4
N080943	Primary Glioblastoma	4
N070229	Grade III Astrocytoma	4
N070237	Grade III Astrocytoma (prev res)	4
N070440	Secondary Glioblastoma (prev res)	4
N070450	Grade II Astrocytoma	4
N070780	Secondary Glioblastoma (prev res)	4
N070934	Primary Glioblastoma	4
N071155	Grade III Oligodendroglioma	4
N060893	Secondary Glioblastoma (prev res)	4
N060913	Primary Glioblastoma	4
N060950	Grade III Oligoastrocytoma	4
N060978	Primary Glioblastoma	4
N061007	Primary Glioblastoma	4
N061092	Primary Glioblastoma	4
N070454*	Primary Glioblastoma	4
N070701	Secondary Glioblastoma (prev res)	4
N070293	Primary Glioblastoma	4
N071026	Primary Glioblastoma	4
N071057	Primary Glioblastoma	4
N071060	Primary Glioblastoma	4
N071144	Primary Glioblastoma	4
N071271	Primary Glioblastoma	4
N080558	Primary Glioblastoma	4
N080749	Primary Glioblastoma	4
N080805	Primary Glioblastoma	4
N081185	Secondary Glioblastoma prev res)	4
N070215	Grade III Astrocytoma (prev res)	4
N070950	Grade III Oligoastrocytoma	4
N070311	Secondary Glioblastoma	4

Tem:temozolomide. Prev res: previous resection. Later res: later resection.
1: Geoff Pilkington's laboratory, University of Portsmouth, UK.
2: The German cell bank Deutsche Sammlung von Mikroorganismen und Zellkulturen GmbH (DSMZ), Germany (German Collection of Microorganisms and Cell Cultures).
3: Lonza biologics, Cambridge, UK (CC-2565).
4: The National Institute for Cellular Biotechnology, Dublin City University, Ireland.

Table 2.3 Preparation of Drugs

Drug	Dilution	Source
Erlotinib (Tarceva®)	10 mg/ml	Sequoia Research Products Ltd
Gefitinib (Iressa®)	10 mg/ml	Sequoia Research Products Ltd
Elacridar (GF120918)	10 mg/ml	Sequoia Research Products Ltd
Imatinib (Glivec®)	10 mg/ml	Novartis
Docetaxel (Taxotere®)	10 mg/ml	Sanofi Aventis
Temozolomide (Temodal®)	20 mg/ml	Donated from the National Cancer Institute, USA

Drugs were diluted in DMSO, Docetaxel was in liquid form.

2.2 Generation of Cultures from Biopsy Samples

The tissue sample was placed into a petri dish, with cold DMEM media containing 10% fetal calf serum and 4% NEAA. Each tissue sample was dissected into very small pieces using a scalpel and tweezers (to hold the tissue in place). The dissected tissue sample was pipetted up and down 3-4 times to further break up the sample. The media containing the dissected tissue sample was then pipetted into vented $25cm^2$ flasks. After 2 days the media was removed and placed into fresh vented $25cm^2$ flasks. Fresh media was placed onto the original vented $25cm^2$ flasks, where attached cells were left to proliferate. All flasks were continuously given media changes to generate primary cultures. Generation of each primary culture ranged from one to four months.

2.3 Proliferation Assays

Cells in the exponential phase of growth were harvested by trypsinisation. Cell suspensions containing $2x10^4$ cells/ml were prepared in cell culture medium. 100 µl/well of the cell suspension was added to 96-well plates (Costar, 3599). Plates were agitated gently in order to ensure even dispersion of cells over the surface of the wells. Cells were then incubated overnight. Drug dilutions were prepared at 2X their final concentration in cell culture medium, as 100 µl of cells was already on the plate this allowed for a 1 in 2 dilution of the drug. 100 µl of the drug dilutions were then added to each well. Plates were then mixed gently as above. Cells were incubated for a further 7 days until the control wells had reached approximately 80-90% confluency.

2.3.1 Assessment of Cell Number - Acid Phosphatase Assay

A. Acid Phosphatase in 96-well plate format.

Following an incubation period of 6-7 days, media was removed from the plates. Each well on the plate was washed with 100 µl PBS. This was removed and 100 µl of freshly prepared phosphatase substrate (10 mM p-nitrophenol phosphate (Sigma 104-0) in 0.1 M sodium acetate (Sigma, S8625), 0.1% triton X-100 (BDH, 30632), pH 5.5) was added to each well. The plates were wrapped in tinfoil and incubated in the dark at 37°C for 1.5 hours. The enzymatic reaction was stopped by the addition of 50 µl of 1 M NaOH to each well.

B. Acid Phosphatase in 6-well plate format.

Following an incubation period of 72 hours, media was removed from the plates. Each well on the plate was washed with 1 ml PBS. This was removed and 2ml of freshly prepared phosphatase substrate in 0.1 M sodium acetate, 0.1% triton X-100 (BDH, 30632), pH 5.5) was added to each well. The plates were wrapped in tinfoil and incubated in the dark at 37°C for 2 hours. The enzymatic reaction was stopped by the addition of 1 ml of 1 M NaOH to each well. Plates were read in a dual beam plate reader at 405 nm with a reference wavelength of 620 nm. Assessment of cell survival in the presence of drug was determined by the acid phosphatase assay. Results were graphed as percentage survival (relative to the control cells) versus drug concentration, using excel software.

2.3.2 Measurement of Doubling Time

Cells were seeded in two 6 well plates at a concentration of 5000 cells/2ml/well and incubated approximately 72 hours before the first cell count. For each cell count cells of two wells were trypsinized, centrifuged and resuspended in 100 µl culture medium. Cells were counted using a haemocytometer. Cells were counted every 48 or 72 hours and 6 times in total. The doubling time was calculated in three steps: The counted cell number was divided by the previous count resulting in a multiplication factor. Then the time period between two counts was divided by the multiplication factor and the resulting number was multiplied by 2. A series of doubling times was obtained for each cell line, which were then averaged. Trypan blue staining was used to check for viable cells.

2.4 Drug Scheduling for Proliferation Assays

Cells were exposed to each drug/drug combination for 24 hrs in a consecutive way. For the proliferation assay each treatment schedule was performed with three different drug concentrations (IC_{10}, IC_{25} and IC_{50}) per drug, representing high, medium and low concentrations. The assay was done twice in triplicates. In the invasion assay we tested 4 different drug schedules individually with one set of drug concentrations. After the last incubation drug/drug combination containing medium was replaced with fresh medium and the cells were incubated for a further 3 days.

2.5 Analysis of Drug Combination Effects

The effect of the drug combination on cell kill was performed and analysed according to a protocol by Chou and Talalay (Chou and Talalay 1984). For each cell line the IC_{10}, IC_{20}, and IC_{30} of imatinib was combined with the IC_{10}, IC_{20}, and IC_{30} of docetaxel, resulting in a total of nine value points per combination index (CI) plot. A range of IC values were tested to examine the combination effect at low and high toxicity. A CI value smaller than 1 indicates a synergistic action of the two drugs; a CI value equal 1 an additive effect and a CI value greater than 1 indicates an antagonistic effect.

2.6 Apoptosis Assay

On day 0 cells were set up at $1x10^4$ cells/well in a 24-well plate. On day 3 the media was removed and drug was added. After 24 or 48 hrs cells were trypsinized and counted. After incubation, the supernatant was removed to eppendorfs, rinsed with 300 µl sterile PBS, this PBS was added to the same eppendorf. During trypsinisation this was spun at 1000rpm for 5 minutes at RT. 300 µl trypsin was added to each well, the plate was covered with parafilm and incubated at 37^oC and 5% CO_2 with monitoring until the cells had detached. 600 µl of serum-supplemented medium was added to each well and this was added to the initial eppendorf, with previously removed supernatant containing centrifuged cells. Each well was washed with 300 µl sterile PBS and this was also added to the same eppendorf. This was also spun at 1000rpm for 5 minutes at RT. The supernatant was gently removed and resuspended in 150 µl serum-supplemented medium. 75 µl of sample was added to a well in a 96-well round bottomed plate. A 75 µl sample of a positive control (cells exposed to drug) was included, and also a 75 µl sample that is a negative control (cells not

exposed to anything). These were used to adjust the settings on the Guava. 75 µl of nexin reagent was added; this was mixed and incubated for 20 minutes with gentle mixing in the dark (i.e. covered with tin foil). Cells were assessed for early and total apoptosis using the Guava Nexin® Assay and the Guava® EasyCyte™ Flow Cytometer according to manufacturer's recommendations. At least 3 biological replicates in duplicate for each condition was used.

The Guava Nexin® Annexin V Assay

The Guava Nexin® Annexin V Assay offers detected early apoptosis. The assay relies on the translocation of phosphatidyl serine (PS) to the outer surface of the cell membrane, an event often associated with the onset of apoptosis. A mix-and-read assay for monitoring externalization of PS through the binding of Annexin V to the exposed PS, the automated single-cell analysis assay is the choice for monitoring apoptosis due to its sensitivity and reproducibility. Annexin V is a calcium-dependent phospholipid binding protein with high affinity for phosphatidylserine (PS), a membrane component normally localized to the internal face of the cell membrane. Early in the apoptotic pathway, molecules of PS are translocated to the outer surface of the cell membrane where Annexin V can readily bind to them. The assay relies on a two-dye stategy: 1) Annexin V-PE to detect PS on the external membrane of apoptotic cells and 2) 7-AAD, a cell impermeant dye, as an indicator of membrane structural integrity. 7-AAD is excluded from live, healthy cells and early apoptotic cells, but permeates late-stage apoptotic and dead cells.

2.7 3D Collagen Invasion Assay

Cell spheroids were formed using the hanging drop method described by Del Duca (Del Duca et al. 2004). Briefly, after trypsinisation the cells were diluted with conditioned medium (CM) reaching a concentration of $1x10^6$cells/ml. Drops (20 µl) of cell suspensions were placed onto the lids of 100 mm Petri dishes, which were inverted over dishes containing 10 ml sterile water. Hanging drop cultures were incubated for 24-48 hrs until cell aggregates were formed, which were transferred to a 100 mm dish coated with 4% agar and filled with 10 ml CM. The aggregates/spheroids were incubated for another 2 days, while they rounded up, and then implanted into collagen gel. Cold PureCol™ (INAMED, USA) was mixed with cold 10-fold concentrated minimal essential medium (Sigma) and cold 0.1 M

sodium hydroxide at a ratio of 8:1:1 reaching a final concentration of 2.4 mg/ml collagen type I. The pH was neutralised by adding 1 M NaOH (Sigma). The collagen solution was distributed into 24-well plates (0.5 ml/well) and one spheroid was placed into each well. The plates were kept at 37°C for about 30-60 min. After solidification the gels were overlaid with 0.5 ml CM and kept at 37°C under 5% CO_2. On day 4, the medium was replaced with fresh CM (control) or drug-containing CM. Cell migration out of the spheroid was measured before drug addition (day 0) to 12 after drug addition.

2.7.1 Spheroid Measurement

Spheroid measurements were taken at 4X magnification using a graticule eye piece, with 10 mm line in 100 parts, each part = 0.1 mm. A spheroid measurement was taken from a central point in the spheroid. Each spheroid had 4 measurements per timepoint. Day 0 (post 4 day spheroid invasion) measurements were subtracted from the overall measurements. Each condition was done in duplicate per experiment, with 3 biological repeats, in some cases 2 biological repeats.

2.8 *In vitro* Invasion Assay

Invasion assays were performed using the method of Albini *et al*.(Albini *et al.* 1997). 100 µl of matrigel were placed into each insert (Falcon 3097) (8.0 µm pore size, 24 well format) and kept at 4 ^{o}C for 24 hours. 4 inserts per 24 well plate was used per assay, with 3 separate assays. The insert and the plate were then incubated for one hour at 37 ^{o}C to allow the proteins to polymerise. Cells were harvested and resuspended in culture media containing 5% FCS at 1 × 10_6 cells/ml. Excess media/PBS was removed from the inserts, and they were rinsed with culture media. 100 µl of the cell suspension was added to each insert. A further 100 µl of culture media was added to each insert and 500 µl of culture media containing 5% FCS was added to the well underneath the insert. Cells were incubated for 24 hours. After this time period, the inside of the insert was wiped with a cotton swab dampened with PBS, while the outer side of the insert was stained with 0.25% crystal violet for 10 minutes and then rinsed in distilled water (dH_2O) and allowed to dry. The inserts were then viewed and photographed under the upright brightfield microscope. The invasion assays were quantified by counting cells in 10 random fields within a grid

at 20x objective and graphed as the total number of cells invading at 200x magnification.

2.9 Drug Accumulation Assay

On day 0 Cells were seeded at 5 x 10^4 cells/ml in T25 flasks (3 flasks per cell line per drug) and 3 control flasks also with no drug. On day 1 the medium was removed and 5mls of medium with drug was added. The flasks were incubated for 2 hours; the drug containing medium was then removed. The flasks were than washed with 4 mls of cold PBS. The cells were than trypsinised with 2 mls of trypsin; this was stopped with 2mls of medium. The suspensions were transferred into extraction tubes, centrifuged at 1000rpm and the supernatant then removed leaving the pellet intact. The pellet was resuspended in 1ml of PBS. A small aliquot was removed for counting. This was then spun down, and the PBS was removed, the pellet was then frozen at -20^{o}C. The samples were then analysed by mass spectrometry by a postgraduate student, Sandra Roche, in the National Institue for Cellular Biotechnology.

2.10 Western Blotting

2.10.1 Whole Cell Extract Preparation

Cells were grown to 80-90% confluency in cell culture grade petri dishes. Media was removed and cells were washed twice with 10 mls ice cold PBS. All procedures from this point forward were performed on ice. Cells were lysed with 150 µl of NP-40 lysis buffer (425 ml dH_2O water, 25 ml 1 M Tris-HCl (pH 7.5) 50 mM Tris-HCl (pH 7.5), 15 ml 5 M NaCl 150 mM NaCl, 2.5 ml NP-40 0.5% NP-40) 15 µl of the 10X protease (100X Protease inhibitors 2.5 mg/ml leupeptin, 2.5 mg/ml aprotinin, 15 mg/ml benzamidine and 1 mg/ml trypsin inhibitor in dH_2O) and 1.5 µl phosphatase inhibitors (100 mM DTT 154 mg in 10 ml dH_2O, 100 mM PMSF 174 mg in 10 ml 100% ethanol) were also added to each petri dish and incubated on ice for 20 minutes. Cells were then removed with a cell scraper and further homogenised by passing through a 21 guage syringe. Sample lysates were centrifuged at 14,000 rpm for 10 minutes at 4 ^{o}C. Supernatant containing extracted protein was transferred to a fresh chilled eppendorf tube. Protein concentration was quantified using the Biorad assay. Samples were then stored in aliquots at -80°C.

2.10.2 Protein Quantification

Protein levels were determined using the Bio-Rad protein assay kit (Bio-Rad, 500-0006) according to maufacturers guidelines, with a 2 mg/ml bovine serum albumin (BSA) solution (Sigma, A9543).

2.10.3 Gel Electrophoresis

Proteins for analysis by Western blotting were resolved using SDS-polyacrylamide gel electrophoresis (SDS-PAGE). PAGEr®duramide®Precast Gels with 7.5% Tris-Glycine gels (Lonza, 59601) were used. The gels were run at 250V and 20mA until the bromophenol blue dye front was found to have reached the end of the gel, at which time sufficient resolution of the molecular weight markers was achieved. In advance of samples being loaded in to the relevant sample wells, 20 µg of protein was diluted in 5x loading buffer. Molecular weight markers (Sigma, C1992) were loaded alongside samples. Western Blotting was performed by the method of

Towbin *et al*, 1979. Once electrophoresis was complete, the SDS-PAGE gel was equilibrated in transfer buffer (25 mM Tris (Sigma, T8404), 192 mM glycine (Sigma, G7126), pH 8.3-8.5) for approximately 15 minutes. Five sheets of Whatman 3 mm filter paper were soaked in freshly prepared transfer buffer. These were then placed on the cathode plate of a semidry blotting apparatus (Bio-rad). Air pockets were then removed from between the filter paper. Nitrocellulose membrane (GE Healthcare, RPN 3032D), which had been equilibrated in the same transfer buffer, was placed over the filter paper on the cathode plate. Air pockets were once again removed. The gels were then aligned onto the membrane. Five additional sheets of transfer buffer soaked filter paper were placed on top of the gel and all air pockets removed. The anode was carefully laid on top of the stack and the proteins were transferred from the gel to the membrane at a current of 275mA at 25 V for 30-40 minutes, until all colour markers had transferred. Following protein transfer, membranes were stained using PonceauS (Sigma, P7170) to ensure efficient protein transfer. The membranes were then blocked for 2 hours at room temperature using 5% blotting grade blocker (Bio-Rad 170-6404) in PBS with 0.1% tween 20 (Sigma P1379) at 4 °C. Membranes were incubated with primary antibody overnight at 4 °C. Antibodies were prepared in 5% blotting grade blocker in PBS with 0.1% tween. Primary antibody was removed after this period and the membranes rinsed 3 times with PBS containing 0.5% Tween 20 for a total of 15-30 minutes. Secondary antibody (1 in 1,000 dilution of anti-mouse IgG peroxidase conjugate (Sigma, A4914)) in PBS, was added for 1.5 hours at room temperature. The membranes were washed thoroughly in PBS containing 0.5% Tween for 15 minutes.

Table 2.4 Western Blot antibodies.

Primary Antibody	Dilution	Source
Pgp	1:200	Sc-13131, Santa Cruz
EGFR	1:100	Ab-15, Lab Vision
PDGFR-β	1:50	PR7212, Calbiochem
PDGFR-α	1:500	Ab35765, Abcam
BCRP	1:40	Ab3380, Abcam
C-Abl	1:500	Tyr245, Cell signalling
BCR-Abl	1:1000	3902, Cell Signalling
C-Kit	1:1000	Ab32363, Abcam
β-actin	1:10,000	A5441, Sigma
Secondary Antibody	**Dilution**	**Source**
Anti-mouse	1:1000	A6782, Sigma
Anti-rabbit	1:500	18772, Sigma

2.10.4 Enhanced Chemiluminescence (ECL) Detection

Immunoblots were developed using Luminol (Sc-2048, Santa Cruz) and ECL Advance™ (Amersham, RPN2135) which facilitated the detection of bound peroxidase-conjugated secondary antibody.

2.11 Immunocytochemistry

2.11.1 Primary Culture Preparation for Immunocytochemistry

To ensure the cells were screened in their natural state, they were plated on chamber slides (Menzel Glaeser) at a concentration of $6.25x10^4$ cells/ml in 80 µl culture medium per well. Cells were incubated for 24hrs at 37^{o}C, 5% CO_2, and were then fixed with ice cold acetone, air dried and stored at -20^{o}C. This work was carried out with my supervisor Dr. Verena Amberger Murphy. The slides were transported to Beaumont Hospital for staining by immunohistochemistry. The following 3 sections describe ICC carried out by Rachel Howley in Beaumont hospital.

2.11.2 Automated Immunocytochemistry (ICC)

To ensure all tissue microarrays (TMAs) and chamber slides were treated under the same conditions, where possible, antibodies were optimised for use on the automated Bond™maX system (Vision Biosystems™, Leica Microsystems, Milton Keynes, UK.) The procedure for automated immunocytochemistry on Bond™maX was set up as described in the user manual (Table 2.5).

2.11.3 Manual Immunocytochemistry

Both cultured chamber slides and formalin fixed paraffin embedded (FFPE) TMAs were immunohistochemically manually stained for phospho-AKT and phospho-P70S6K. Culture chamber slides were treated with 3% hydrogen peroxide for 5 mins to block endogenous peroxidases. They were then washed for 5 mins (x2) in TBS-T, circled with the pap pen. All slides were blocked with 100-200 µl per slide of blocking buffer (5% Normal Goat Serum (Vector)) in TBST for 1 hour at room temperature, followed by an incubation with primary antibody overnight at 4^{o}C. Both primary antibodies were diluted in blocking buffer; 1/60 and 1/30 for phospho-AKT and phospho-P70S6K.

The following day all unbound primary antibody was removed using 5 min (x3) washes with TBS-T. The biotinylated anti-rabbit secondary antibody (Vector) was diluted 1/200 in blocking buffer and applied to each slide for 30 mins at room temperature. Again, all unbound antibody was removed by washing with TBS-T (5

min x3). The ABC complex (ABC vectastain kit, Vector) diluted 1/100 in TBS-T was applied to the slides for 30 mins at room temperature. (Note: the ABC complex was prepared 30 mins prior to use to allow the Avidin-Biotin Complex to form.) All unbound Avidin complex was removed by washing with TBS-T for 5 mins (x3) after which the chromagen Novared (Vector) was applied for 5-10 mins. This peroxidase labelled chromagen reacts with the Horseradish Peroxidase (HRP) labelled Avidin resulting in a red stain located wherever the primary antibody is bound. The reaction was stopped by immersing in a trough of running tap water before being Haematoxylin stained for 1 min. Excess Haematoxylin was rinsed in running tap water and the slides were dipped in acid alcohol once before allowing the haematoxylin to darken in running tap water for 5 mins. Finally, the slides were dehydrated by dipping once in three alcohol dips (95%, 100%, 100% ethanol) before being submerged in two xylene washes. Finally the slides were mounted with DPX (Fisher) and viewed under the microscope for manual scoring or image analysis (Table 2.5).

2.11.4 Manual Scoring of Immunocytochemistry

In order to quantify the amount of each protein present in ICC stained slides a manual scoring system was established. This scoring system took into consideration both the staining intensity and the percentage of cells that were stained as previously described by Riemenschneider (Riemenschneider *et al*. 2006). The staining intensity was recorded on a scale of 0-3 for each protein. The percentage of cells stained was divided into the four quartiles; 0, 1-25%, 26-50%, 51-75% and 76-100% which were assigned values of 0, 1, 2, 3 and 4 respectively. An overall score was determined by multiplying the score for staining intensity (0-3) by the score for the percentage of cells stained (0-4) for an overall score between 0-12. Manual scoring was carried out by a Ph.D student, Rachel Howley from Beaumont Hospital, Dublin and a neuropathologist, Professor Michael Farrell.

Table 2.5 Immunocytochemistry methods.

Antibody	Cat. No.	Company	Working Dilution	IHC Method	Technology	Chromagen (staining)
EGFR tot	4267S	CST	1:50	Automated	BPDS	DAB
EGFR vIII	Donated by Darell D. Bigner, Duke University		1:50	Automated	BPDS	DAB
PTEN (Clone 6H2.1)	ABM-2052	Cascade Biosciences	1:300	Automated	BPDS	DAB
Phos-AKT (Pan) (Thr308)	9266L	CST	1:60	Manual	Vecastain ABC Biotin / Avidin	Novared
Phos-P70S6K (Thr389)	Ab32359	Abcam	1:30	Manual	Vecastain ABC Biotin / Avidin	Novared
PDGFR α	3164	CST	1:100	Automated	BPDS	DAB
PDGFR β	3169	CST	1:50	Automated	BPDS	DAB
Phos-C-Abl (Thr245)	Ab4479	Abcam	1:50	Automated	BPDS	DAB
Phos-C-KIT (Tyr 721)	Ab5632	Abcam	1:/65	Automated	BPDS	DAB
GFAP	Z0334	Dako	1:7000	Automated	BPDS	DAB
NESTIN (Clone 10C2)	MAB 5326	Millipore	1:500	Automated	BPDS	DAB

CST: Cell Signalling Technologies, BPDS: Bond Polymer Detection System.

2.12 Statistical Methods

Statistical methods were used to analyse our immunocytochemistry (section 3.5) results in comparison to responsiveness to TKIs of the cell cultures; to test the dependency of the cultures with the PI3K/Akt pathway. The cohort included 26 high-grade glioma cell cultures, this dataset was too small for supervised analysis, therefore unsupervised analysis was used, hierarchial clustering analysis and principal components analysis were chosen for multivariate statistics.

2.12.1 Hierarchical Clustering Analysis

Cluster analysis is the assignment of a set of observations into subsets (called clusters) so that observations in the same cluster are similar in some sense. This is an unsupervised analysis which is commonly used. Hierarchical clustering creates a hierarchy of clusters which can be depicted in a tree structure called a dendrogram. The root of the tree consists of a single cluster containing all observations, and the leaves correspond to individual observations. Any valid metric may be used as a measure of similarity between pairs of observations. The choice of which clusters to merge or split is determined by a linkage criterion, which is a function of the pairwise distances between observations. The results are in a dendrogram signifying a hierarchical clustering algorithm using Ward's linkages in Euclidian space (Lomo *et al*. 2008).

2.12.2 Principal Components Analysis

Principal component analysis (PCA) involves a mathematical procedure that transforms a number of possibly correlated variables into a smaller number of uncorrelated variables called principal components. The first principal component accounts for as much of the variability in the data as possible, and each succeeding component accounts for as much of the remaining variability as possible. It is a popular technique in pattern recognition. It can be used to extract relevant information from confusing data sets. It can transform a complex data set to a lower dimension to reveal the sometimes hidden, simplified structures that often underlie it (Shlens 2009).

2.12.2 One Way Anova

One-way analysis of variance is a technique used to compare means of two or more samples (using the F distribution). This generates a p value; a p value less than or equal to 0.05 is classified as statistically significant.

2.13 MicroRNA

2.13.1 Taqman Low Density Array (TLDA)

The TaqMan® Custom Array is a 384-well micro fluidic card that allows you to perform 384 simultaneous real-time PCR reactions without the need to use multi-channel pipettors to fill the card. This card allows for 1-8 samples to be run in parallel against 12-384 TaqMan® Gene Expression Assay targets that are pre-loaded into each of the wells on the card.

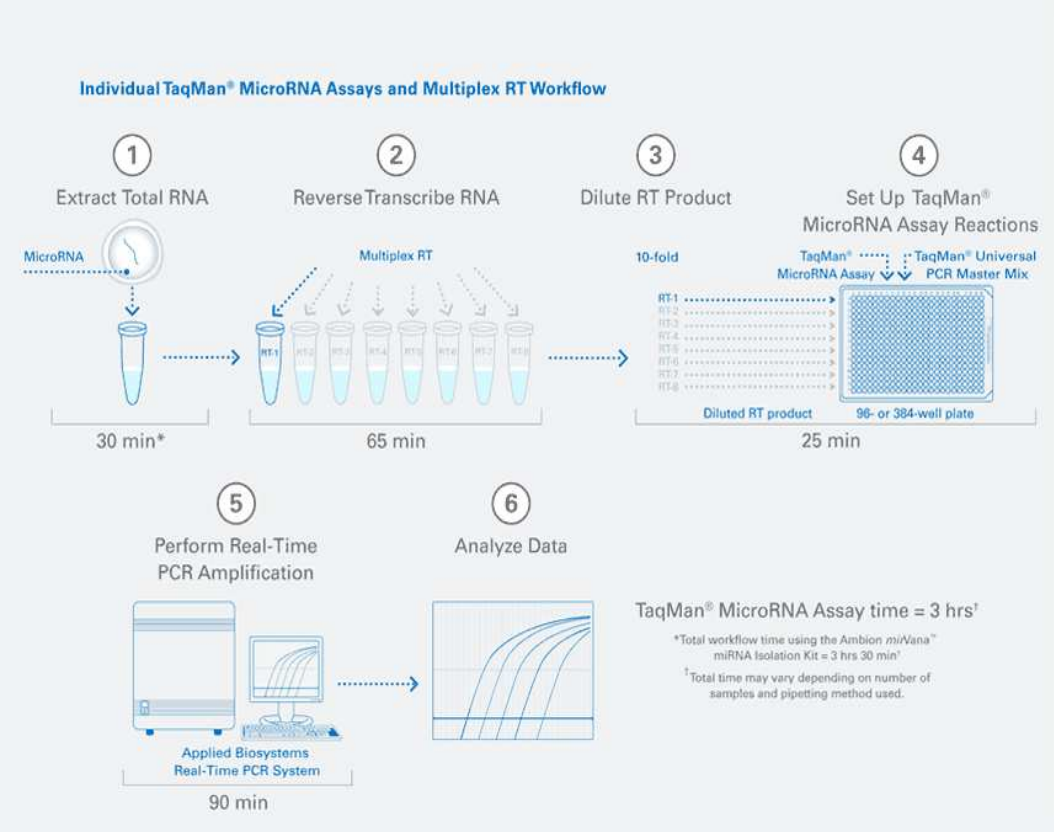

(www.appliedbiosystems.com)

Fig 2.1 TaqMan low density array workflow. 1:Isolate total RNA that contains small RNAs such as miRNA, siRNA, and snRNA. 2: convert miRNA to cDNA prior to real-time PCR quantitation.3: dilute RT product. 4: TaqMan® Universal Master Mix II is added to each sample and pipetted into the sample loading ports of a TaqMan® Array Card. 5: The Taqman arr card in run, performing real-time PCR.6: data analyzed.

Materials for TLDA anaylsis

Human Multiplex RT set (Pools 1-8) (P/N 4384791, Applied Biosystems)

TaqMan® MicroRNA Reverse Transcription Kit (200 reactions) (Applied Biosystems P/N 4366596)

TaqMan® 2X Universal PCR Master Mix, No AmpErase® UNG (Applied Biosystems P/N 4324018)

TaqMan® Array Human MicroRNA Panel V 1.0 (4 Arrays) (Applied Biosystems P/N 4384792)

MirVana™ miRNA isolation kit (Applied Biosystems AM1560)

Multiplex reverse transcription

1. **Prepare the RT master mix**

   The taqman microRNA reverse transcription kit components were thawed on ice. The directions and volumes listed below were for a single sample and were scaled appropriately.

   a. The RT master mix for a total of eight multiplex RT reactions was prepared in a polypropylene tube (12.5% excess volume was allowed for pipetting losses).

   b. This was mixed gently and centrifuged at 1000 rpm for 30 seconds, then placed on ice.

Table 2.6 Preparation of RT master mix

Component	Volume for one RT reaction (µl)	Volume for one sample (8 RT reactions) with 25% excess (µl)
100 mM dNTPs	0.2	2
MultiScribe™ reverse transcriptase, 50 U/µl	2	20
10x reverse transcription buffer	1	10
RNase inhibitor, 20U/µl	0.125	1.25
Nuclease-free water	2.675	26.75
Total	6	60

Add the RNA template

a. 2 µl of the 50 ng/µl total RNA template was dispensed into each well of the MicroAmp™ optical reaction plate.

b. The MicroAmp™ optical reaction plate was placed on ice.

2. Prepare the multiplex RT reaction

a. 6 µl of RT master mix was dispensed into each well of the MicroAmp™ optical reaction plate.

b. 1 µl of each multiplex RT human primer pool (5x) was transferred into the appropriate wells. A total of eight independent RT reactions were run per sample. The plate was sealed using MicroAmp™ optical adhesive film.

c. This was mixed gently. The plate was placed on ice for 5 minutes before loading it into the thermal cycler.

3. Perform multiplex reverse transcription

a. The thermal cycler was set to the 9600 emulation mode as follows

Table 2.7 Thermal cycle for RT reaction

Step Type	Time (min)	Temperature (°C)
HOLD	30	16
HOLD	30	42
HOLD	5	85
HOLD	∞	4

The volume was set to 10 µl, the plate was put into the thermal cycler and the run was started.

Taqman array

1. Preparing the RT reaction-specific PCR mix

a. The RT reaction was diluted 62.5-fold by adding 615 µl of nuclease free water to each of the eight 10 µl RT reactions. For each RT reaction a 1.5 ml microcentrifuge tube was labelled.

b. The Taqman Universal PCR Master Mix was thawed on ice.

c. The following components were added to each 1.5 ml microcentrifuge tube

Table 2.8 Preparation of PCR master mix

Component	Volume (µl) per fill reservoir
Diluted RT reaction	50.0
TaqMan 2x Universal PCR Master Mix (No AmpErase® UNG)	50.0
Total volume	100.0

d. The microcentrifuge tubes were capped and mixed gently.

e. The tubes were centrifuged to eliminate air bubbles from the mixture, and placed on ice.

2. Loading the RT reaction-specific PCR reaction mix into fill reservoirs

a. When the TaqMan array had equilibrated to room temperature, the card was carefully removed from the packaging, and placed foil side down on the lab bench.

b. 100 µl of the RT reaction-specific PCR reaction mix was loaded into the corresponding ports. This was dispensed so that it went in and around the fill reservoir toward the vent port; the entire 100 µl was pipetted into the fill reservoir.

3. Centrifuge the TaqMan Array

a. The TaqMan Arrays were centrifuged according to the user bulletin: Applied Biosystems TaqMan® Low Density Array (P/N 4371129).

b. Centrifugation was repeated so that the arrays were centrifuged for a total of two consecutive, 1 minute spins to ensure complete distribution of the PCR reaction mix.

c. When complete each array was examined to determine if filling was complete.

4. Seal the TaqMan Array

a. The array was sealed according to the user bulletin: Applied Biosystems TaqMan® Low Density Array (P/N 4371129).

b. By using a scissors we trimmed the fill reservoirs from the array.

5. Set up and run the plate document

Referred to the user bulletin: Applied Biosystems TaqMan® Low Density Array (P/N 4371129) and Applied Biosystems 7900HT Fast Real-Time PCR System and SDS Enterprise Database User Guide (P/N 4351684).

6. Analyze the PCR reactions

Referred to the SDS online help, 7900HT system user guide.

2.13.2 Relative quantity of miRs by qRT-PCR

Total RNA was extracted as per section (2.14.2.1) and cDNA synthesised and experiments were performed in triplicate, according to the manufacturer's instructions. Reverse transcriptase (RT) reactions were performed using micropipettes which were specifically allocated to this work. To form cDNA, a high-capacity cDNA reverse transcription kit (Applied Biosystems) was used.

The number of copies of a mRNA transcript of a gene in a cell or tissue is determined by the rates of its expression and degradation. The Real-Time PCR system is based on the detection and quantitation of a fluorescent reporter (Livak *et al*. 1995). There are two conventional real time PCR methods SYBR® Green and TaqMan probe based. The former was the first to be used in real-time PCR. It is a fluorescent dye that binds to double-stranded DNA and emits light when excited. Unfortunately, it binds to any double-stranded DNA which could result in a non-specific signal, especially compared with the specificity found with TaqMan probe based method. This uses a fluorogenic probe which is a single stranded oligonuleotide of 20-26 nucleotides and is designed to bind only the DNA sequence between the two PCR primers. Cycle threshold is defined as Cycle number (in qPCR) at which the fluorescence generated within a reaction well exceeds a defined threshold. The threshold is defined by the software or user to reflect the point during the reaction at which the number of amplicons is doubling with each PCR cycle (Fig. 2.14.2).

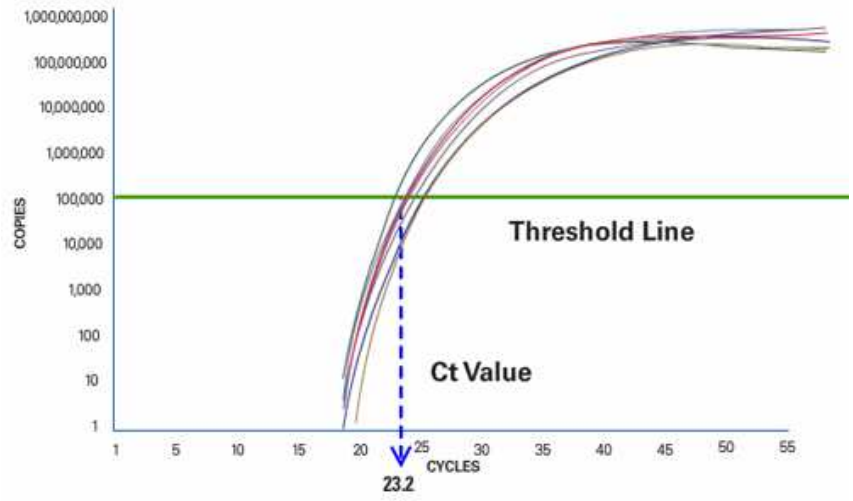

www.appliedbiosystems.com)

Fig 2.2 The PCR cycle at which the sample reaches a fluorescent intensity above background is the Cycle Threshold or Ct.

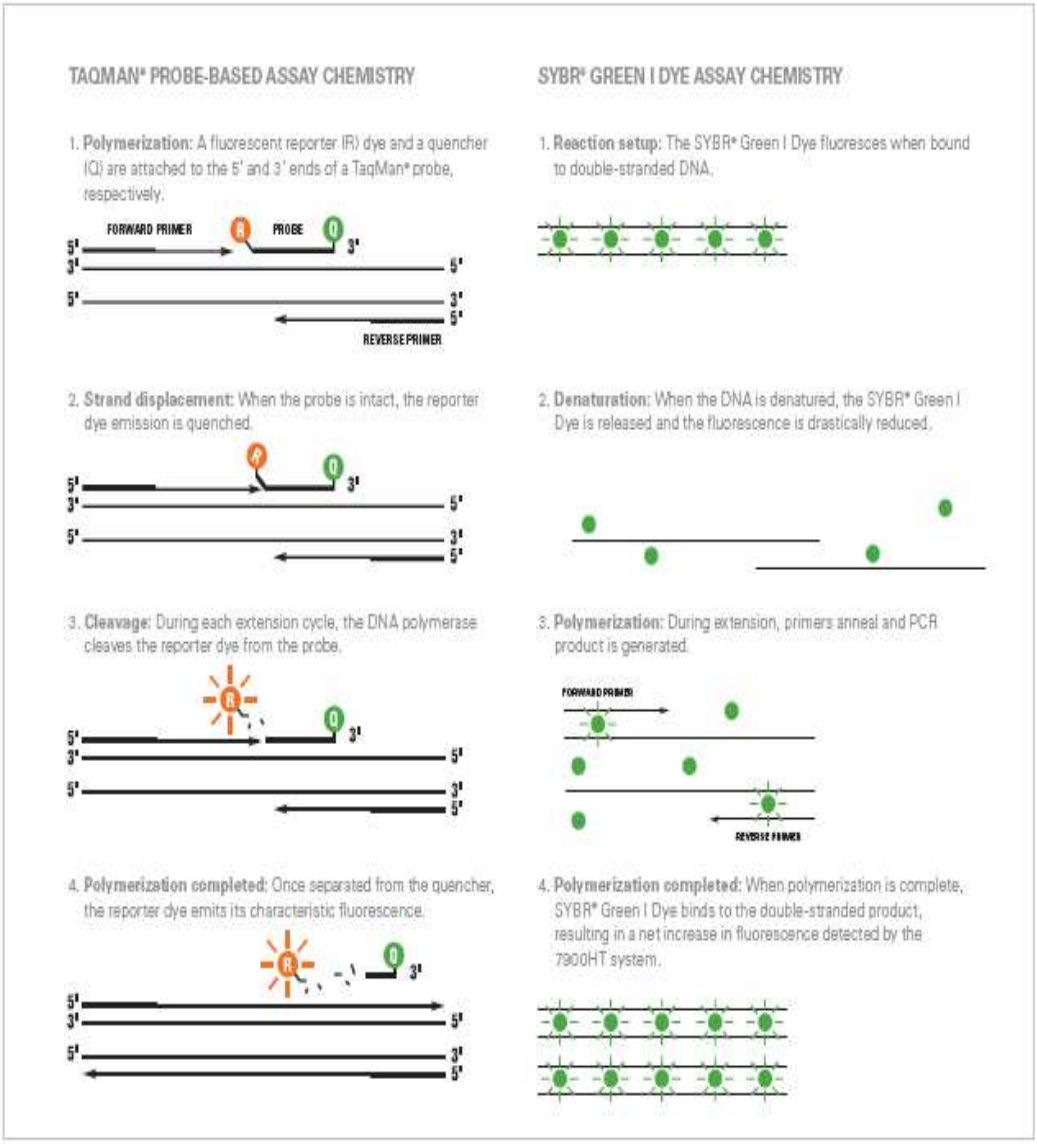

(www.appliedbiosystems.com)

Fig 2.3 Gene expression analysis with Taqman® probe-based assay chemistry, and SYBR® GREEN I assay chemistry.

Materials for qRT-PCR

TaqMan® MicroRNA Reverse Transcription Kit (200 reactions) (Applied Biosystems, P/N 4366596)

TaqMan® 2X Universal PCR Master Mix, No AmpErase® UNG (Applied Biosystems, P/N 4324018)

Fast SyBr® Green master mix (Applied Biosystems, P/N 4385612)
MirVana^{TM} miRNA isolation kit (Applied Biosystems, AM1560)

MicroAmpTm Fast 96-well Reaction Plate with barcode (Applied Biosystems, PN 4346906)

MicroAmp^{Tm} optical adhesive film (100 covers) (Applied Biosystems, PN 4311971)

Nuclease free water (Applied Biosystems, AM9930)

RNU44 control (Applied Biosystems, PN4373384)

MiR-93 TaqMan® MicroRNA Assay (Applied Biosystems, PN4427975, ID2139)

MiR-155 TaqMan® MicroRNA Assay (Applied Biosystems, PN4427975, ID2623)

MiR-23b TaqMan® MicroRNA Assay (Applied Biosystems, PN4427975, ID400)

2.13.2.1 Organic RNA Extraction using MirVana miRNA Isolation Kit

Cells were cultured in vented 75cm2 flasks until they reached 80% confluency. The cells were then lysed and RNA was extracted from them using the MirVana^{TM} miRNA isolation kit (catalogue number 1560, 1561).

Cell Lysis Prior to RNA Extraction

Trypsinised cells were washed by gently re-suspending in 10 mls of 1X PBS and pelleted at low speed. The PBS was removed and the cells were resuspended in 600 µl lysis/binding solution (from the MirVanaTM miRNA isolation kit). The sample was then vortexed vigorously to ensure complete lysis of the cells and to obtain a homogenous lysate.

The **MirVana^{TM} miRNA isolation kit** designed for purification of RNA is suitable for studies of both siRNA and miRNA. The kit employs organic extraction followed by immobilization of RNA on glass-fibre filters to purify either total RNA, or RNA enriched for small species, from cells or tissue samples. The total RNA from cell

samples was isolated as per the manufacturer's protocol a recommended 10^2-10^7 cells were used for RNA extraction.

2.13.2.2 Using the Nanodrop to Measure Nucleic Acids

The NanoDrop is a cuvette free spectrophotometer. It uses just 1 µl to measure from 5 ng/µl to 3000 ng/µl of nucleic acids in solution. Before applying the RNA sample the pedestal was wiped down using a lint free tissue dampened with UHP. 1 µl of UHP was then loaded onto the lower measurement pedestal. The upper sample arm was then brought down so as to be in contact with the solution. "Nucleic acid" was selected on the NanoDrop software to read the samples. After the equipment was initialised the "blank" option was chosen, and after a straight line appeared on the screen the "measure" option was selected. All sample readings were automatically saved as text files which could be viewed using Microsoft Excel. The upper and lower pedestals were cleaned with a clean dry wipe between samples. When finished, the pedestal was cleaned with a wipe dampened with UHP followed by drying with a dry wipe. The purity of the RNA extraction was determined by calculating the A_{260}:A_{280} ratio. An A_{260}:A_{280} ration of 2 is indicative of pure RNA. Only those samples with ratios between 1.7 and 2.1 were used in this study.

2.13.2.3 Two step RT-PCR

In the reverse transcription (RT) step, cDNA (complemetary DNA) was reverse transcribed from total RNA samples using specific miRNA primers from the TaqMan MicroRNA Assays and reagents from the TaqMan® MicroRNA Reverse Transcription Kit and the TaqMan® 2x Universal PCR Master Mix, No AmpErase® UNG. PCR was carried out using the TaqMan® MicroRNA Assays, with the control RNU44. The following products were also used for PCR nuclease free water, MicroAmp^{Tm} fast optical 96-well reaction plate with barcode, 0.1ml E94 20 plates, and MicroAmp^{Tm} optical adhesive film 100 covers E215. RT-PCR was carried out according to TaqMan® microRNA Assay Protocol. The following reagents were thawed and mixed on ice in a 0.5 ml eppendorf (Eppendorf, 0030 121.023).

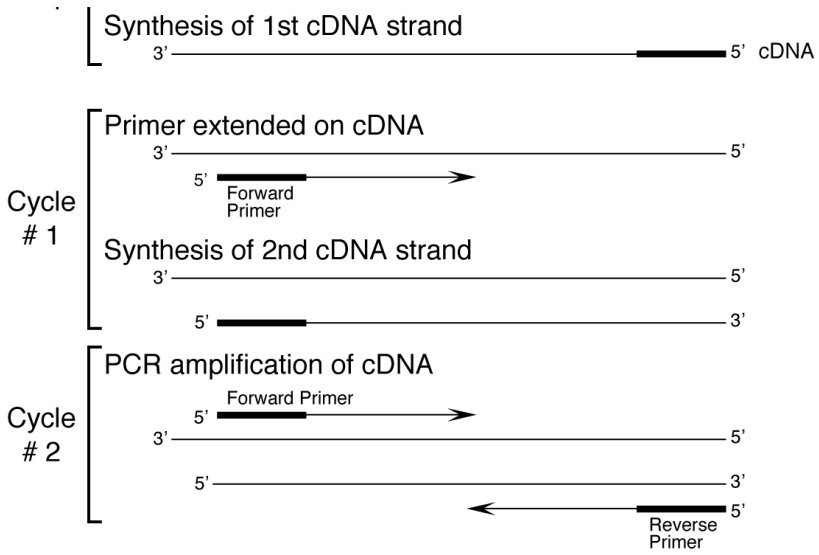

(www.appliedbiosystems.com)

Fig. 2.4 Two step RT-PCR The first step is reverse transcription (RT), in which RNA is reverse transcribed to cDNA using reverse transcriptase. This step is very important in order to perform PCR since DNA polymerase can act only on DNA templates. The RT step can be performed either in the same tube with PCR (one-step PCR) or in a separate one (two-step PCR) using a temperature between 40°C and 50°C, depending on the properties of the reverse transcriptase used

Table 2.9 Preparation of RT master mix per 15 µl reaction.

Components	In 15 µl reaction
dNTP mix (100mM)	0.15 µl
MultiscribeTM RT enzyme (50 U/ µl)	1.00 µl
10 x RT Buffer	1.50 µl
RNase Inhibitor (20 U/ µl)	0.19 µl
Nuclease free water	4.16 µl
Primer	3.00 µl

The master mix was placed on ice and mixed gently, cDNA reverse transcription reaction was prepared by adding 10 µl of the RT master mix into an individual tube, 5 µl (10ng/ µl) of RNA was pipetted into master mix containing tubes, sealed, centrifuged briefly and loaded into the thermal cycler (Hybaid). The reaction volume was set to 15 µl.

Table 2.10 Thermal cycle for RT reaction.

Temperature Hold (^{o}C)	Duration (minutes)
16	30
42	30
85	5
4	∞

After completion of the reaction cDNA was ready for quantitative PCR.

Table 2.11 Preparation of PCR master mix per 20 µl reaction

Components	Per reaction (20 µl)
2X PCR master mix	10.00 µl
Nuclease free water	7.67 µl
Primer	1.00 µl
cDNA	1.33 µl

The PCR reaction was carried out the Applied Biosystems 7900HT Fast Real-Time PCR system.

Table 2.12 Thermal cycle for qRT-PCR

Step	Temperature Hold (°C)	Duration	Cycle
Denature	95	10 minutes	1
Denature	95	15 seconds	2
Annealing & Extending	60	60 seconds	X40

2.13.2.4 High-Capacity cDNA Reverse Transcription with SyBr Green

Table 2.13 Preparation of 2X RT master mix per 20 µl reaction.

Components	In 20 µl reaction
10 x RT Buffer	2.0 µl
dNTP mix (100mM)	0.8 µl
10x RT Random Primers	2.0 µl
MultiscribeTM RT enzyme (50 U/ µl)	1.0 µl
RNase Inhibitor (20 U/ µl)	1.0 µl
Nuclease free water	3.2 µl
Total per Reaction	10.0 µl

The master mix was placed on ice and mixed gently, cDNA reverse transcription reaction was prepared by adding 10 µl of the RT master mix into an individual tube, 10 µl (100ng/ µl) of RNA was pipetted into master mix containing tubes, sealed, centrifuged briefly and loaded into the thermal cycler (G-Storm). The reaction volume was set to 15 µl.

Table 2.14 Thermal cycle for High-Capacity RT reaction.

Temperature Hold (°C)	Duration (minutes)
25	10
37	120
85	5 sec
4	∞

Table 2.15 Preparation of SyBr Green PCR master mix per 20 µl reaction.

Components	Per reaction (20 µl)
2X PCR master mix	10.0 µl
Nuclease free water	7.0 µl
Primer (10 µM F & R)	1.0 µl
cDNA	2.0 µl

F: forward, R: reverse.

Table 2.16 Thermal cycle for SyBr Green qRT-PCR

Step	Temperature Hold (^{o}C)	Duration (seconds)	Cycle
Denature	95	20 secs	1
Denature	95	3 secs	2
Annealing & Extending	60	30 secs	X40

Table 2.17 PCR Primers.

Primer Name	Sequence 5' – 3' Direction	Tm (^{0}C)
SEMA6D.s	TGCTTTCCATAACCACAGTGCTGAA	61.3
SEMA6D.a.s	TCGTACACCATGGCAGTCCCCT	64
XIAP.s	TGTCCTGGCGCGAAAAGGTGG	63.7
XIAP.s	ACCCTGCTCGTGCCAGTGTTG	63.7
SMAD5.s	AGCCGGCTCGCGAAAAGGAA	61.4
SMAD5.a.s	TGCTTCTTTCATTGGGTCAAGTCCTGT	63.2
MAP4K4.s	CGAGGTGCCTCCAAGGGTTCC	65.7
MAP4K4.a.s	TTCTGCTGCCCACTGCCCTG	63.5
BCL2.s	TGAACCGGCACCTGCACACC	63.5
BCL2.a.s	CAAAGGCATCCCAGCCTCCGT	63.7
MET.s	TGCTTTGCCAGTGGTGGGAGC	63.7
MET.a.s	AGAGCGATGTTGACATGCCACTG	62.4
PDGFA.s	AGAGGACACGGATGTGAGGTGAGG	66.1
PDGFA.a.s	CCATGTCCCAGGAAAGGGCTGC	65.8
Actin.s	CAATGGCTCCGGCCTGGTGA	63.5
Actin.a.s	CCATGACGCCCTGGTGTCGG	65.5

Tm: annealing temperature
s: sense, a.s: anti-sense

2.13.3 Transient Transfections with anti-miR and pre-miR

Anti-miR was used to inhibit miRNA activity in the cells, and pre-miR was used to increase the copy number of miRNA in the cells. Anti-miR and pri-miR used were chemically synthesised (Ambion Inc). These miRNAs were 21-23 bps in length and were introduced to the cells via reverse transfection with the transfection agent siPORT™ *Neo*FX™ (Ambion Inc., 4511), or lipofectamine™ 2000 (Invitrogen, 11668-019).

Table 2.18 Synthetic miRNA Oligonucleotides

miRNA	Catalogue No.	Product ID
Pre-hsa-miR-93	AM17100	PM10951
Anti-hsa-miR-93	AM17000	AM10951
Pre-hsa-miR-23b	AM17100	PM10711
Pre-miR-control	AM17110	-
Anti-miR-control	AM17010	-

2.13.3.1 Transfection Optimisation

In order to determine the optimal conditions for miRNA transfection, optimisation with kinesin siRNA (Ambion Inc., Am4639) was carried out for each cell line. A protocol was optimised for the miRNA transfection of an established glioblastoma cell line, SNB-19. Cell suspensions were prepared at $2x10^4$, $1x10^5$, $3x10^5$ and $5x10^5$ cells per ml. Solutions of negative control (Ambion Inc., 4390843) and kinesin (Ambion Inc., 4392420) siRNAs at a final concentration of 30 nM/ 50 nM were prepared in optiMEM (Gibco™, 31985). Transfection reagent solutions at a range of concentrations were prepared in optiMEM in duplicate and incubated at room temperature for 10 minutes. After incubation, either negative control or kinesin siRNA solution was added to each neoFX concentration. These solutions were mixed well and incubated for a further 10 minutes at room temperature. 100 µl of the siRNA/transfection reagent solutions were added to each well of a 6-well plate. 1 ml of the relevant cell concentrations were added to each well. The plates were mixed gently and incubated at 37°C for 24 hours. After 24 hours, the transfection mixture was removed from the cells and the plates were fed with fresh medium. The

plates were assayed for changes in proliferation at 72 hours using the acid phosphatase assay. Optimal conditions for transfection were determined as the combination of conditions which gave the greatest reduction in cell number, after kinesin siRNA transfection, and the least cell kill in the presence of transfection reagent.

2.13.3.2 Proliferation Assays on miRNA Transfected Cells

Cells were seeded using 2 µl Neofx/lipofectamine 2000 to transfect 30 nM/ 50 nM miRNA in a cell density of $1x10^5$ per well of a 6-well plate. After 24 hrs, transfection medium was replaced with fresh media and cells were allowed to grow until they reached 80-90% confluency, a total of 72 hours. Cell number was assessed using the acid phosphatase assay. All experiments were carried out independently at least three times. In the miRNA experiments, siRNA scrambled transfected cells were used as control compared to miRNA treated samples. This was to ensure no 'off-target' effects of the transfection procedure. Non-treated controls were used to ensure scrambled siRNA was having no effects and to normalise data. Pre-miR negative control (AM17110) was used to ensure no 'off-target' effects of pri-miR-93 with the transfection procedure. Cell number was assessed using the acid phosphatase assay described in section 2.4.1 B. Analysis of the difference of comparisons, as well as untreated versus miRNA treated mean percentage survival was calculated on Microsoft Excel.

2.13.4 Agarose Gel Preparation

5 g of agarose was weighed and added to 200 ml of TAE buffer (1X), this was placed in the microwave for 3 minutes at power 70. This was then left to stand for 10-15 minutes to come to room temperature. 4 µl of ethidium bromide were added to the mixture in a fumehood. This was then poured into a mould (containing combs) to set, the gel was left to set for 1 hour.

Section 3.0 Results

3.1 Imatinib and Docetaxel in Combination can Effectively Inhibit Glioma Invasion in an *in vitro* 3D Invasion Assay

The effect of the combination of imatinib and docetaxel was examined on 4 established glioma cell cultures, with respect to proliferation and invasion.

3.1.1 The Effect of Imatinib and Docetaxel on Glioma Proliferation

The IC_{50} values were established for imatinib and docetaxel on four different glioma cell lines; CLOM002 and UPHHJA are primary cell lines, which were used at low passage numbers, and SNB-19 and IPSB-18 are established cell lines. The IC_{50} for imatinib was similar for all four cell lines, ranging between 15.7 µM and 18.7 µM (Table 3.1). Docetaxel inhibited cell proliferation at much lower concentrations. SNB-19 was the most sensitive cell line with an IC_{50} of 0.7 nM docetaxel, and UPHHJA was the least sensitive cell line with a 28-times higher IC_{50} value of 19.8 nM. In addition, normal human astrocytes (NHAs) were tested, where an IC_{50} with imatinib of 17 µM was found, which is very similar to the value found with the glioma cell lines; with docetaxel the graph plateaued and 50 % inhibition could not be reached with a concentration up to 124 nM.

Table 3.1 IC_{50} values for imatinib and docetaxel on cell proliferation of four different glioma cell cultures and normal human astrocytes. Data represents 3 individual biological assays. Standard deviations were generated using Microsoft Excel software.

Drug	CLOM002	UPHHJA	IPSB-18	SNB-19	NHA
Imatinib (µM)	15.7 ± 1.3	17.7 ± 1.3	17.4 ± 2	18.7 ± 2	17 ± 0.2
Docetaxel (nM)	11.8 ± 0.6	19.8 ± 2.5	8.2 ± 0.7	0.7 ± 0.02	>124

3.1.2 Combined Treatment with Imatinib and Docetaxel Synergistically Inhibited Cell Proliferation in 3 out of 4 Cell Cultures

To investigate the drug combination effect three low kill concentrations of docetaxel and one low kill concentration for imatinib were chosen, which reduced cell proliferation of CLOM002, UPHHJA and IPSB-18 cells only up to 37% (Fig. 3.1.1). The combination of both drugs at low concentration resulted in up to 87% inhibition in these three cell lines compared to imatinib or docetaxel alone. On the other hand, the combined treatment of imatinib and docetaxel had no significant effect on SNB-19 (Fig. 3.1.1).

For each cell culture the combined effect of the IC_{10}, IC_{20} and IC_{30} of imatinib and docetaxel revealed a synergistic effect for 3 out of 4 tested cultures analysed/, using the combination plot according to Chou and Talalay (Chou and Talalay 1984). An effect is synergistic when the combination of two drugs results in a higher toxicity than expected, based on pre-determined toxicity levels of either drug alone, an effect is additive when the combination of two drugs gives the expected toxicity. Highest synergism was seen in IPSB-18 cells with a combination index (CI) between 0.05 and 0.25; in UPHHJA the CI was between 0.1 and 0.4 and the weakest synergy was in CLOM002 cells with a CI between 0.1 and 0.7. The CI in SNB-19 cells was between 0.7 and 1.0 representing an additive effect.

1: imatinib (Im), 2: docetaxel (Do1), 3: Im&Do1, 4: Do2, 5: Im&Do2, 6: Do3, 7: Im&Do3

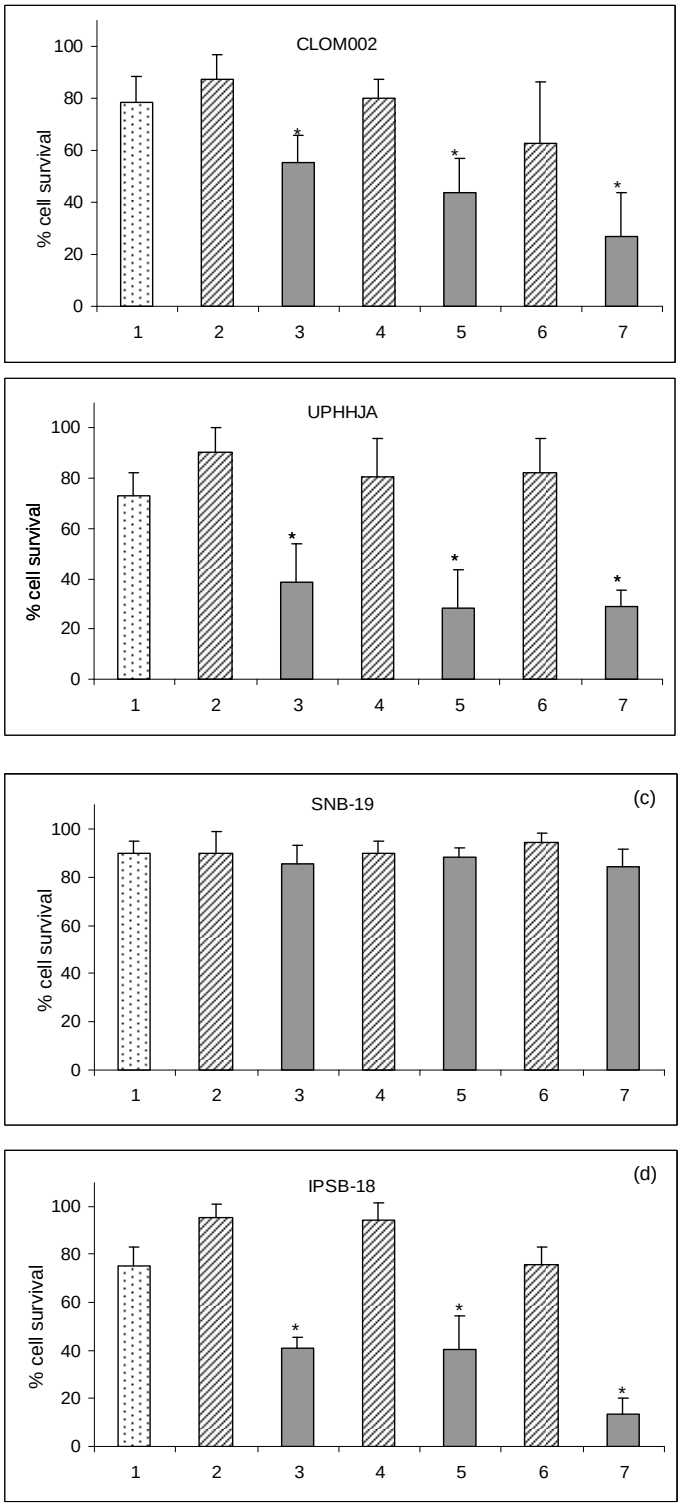

Table 3.1.2 The concentrations of docetaxel and imatinib used in the proliferation assay in figure 3.1.1.

Cell Culture	Docetaxel (nM)		
	Do1	Do2	Do3
CLOM002	0.5	0.9	1.2
UPHHJA	1.2	2.5	3.7
SNB-19	0.1	0.2	0.3
IPSB-18	1.2	2.5	3.7
	Imatinib (μM)		
CLOM002	3.4		
UPHHJA	3.4		
SNB-19	1.7		
IPSB-18	3.4		

Do: Docetaxel, Im: Imatinib.

Fig. 3.1.1 Combination effect of imatinib (Im) and docetaxel (Do) on cell proliferation. *: $p < 0.05$. Data represents 3 individual biological assays. Standard deviations were generated using Microsoft Excel software.

3.1.3 Imatinib Combined with Docetaxel Induces Apoptosis in Glioma Cultures

Total apoptosis was analysed in the presence of single drug and drug combinations. Over 24 to 48 hours between 2 and 3.4% apoptotic cells were measured in the controls (no drug) (Fig. 3.1.2(a)). Drug effects were low after 24 hours, but much more pronounced after 48 hours: imatinib alone induced apoptosis in 4.7-7% cells and docetaxel alone in 4.3-10% cells, while the combination of imatinib and docetaxel caused apoptosis in 13.8-40.1% cells, with CLOM002 cells being the most sensitive. In SNB-19, however, docetaxel alone caused 10% apoptotic cells and the drug combination increased this effect to 13.8% apoptotic cells (Fig. 3.1.2(a)). There was no major difference in early and late apoptosis (not shown). Neither drug alone had a significant effect on cell viability of CLOM002, IPSB-18, and UPHHJA cells; however, the combination significantly reduced cell viability by over 30% in all three cell lines (Fig. 3.1.2(b)). In SNB-19 cells, docetaxel alone caused 10% reduction in cell viability, which was similar to the effect of the combination (Fig. 3.1.2(b)).

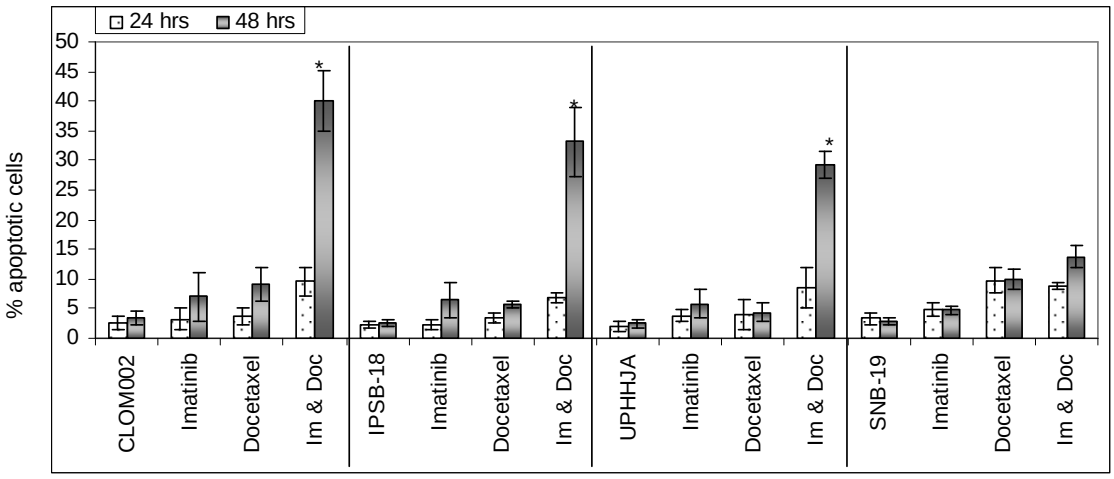

Fig. 3.1.2 (a) Percentage of total apoptotic cells measured after 24 and 48 hrs in the absence and presence of drug; imatinib 13.5 µM; docetaxel 14.9 nM. Im & Doc: imatinib and docetaxel. The first two bars in each set represent the controls for each cell culture, i.e. no drug added. *: P < 5E-3. Data represents 3 individual biological assays. Standard deviations were generated from Microsoft Excel software.

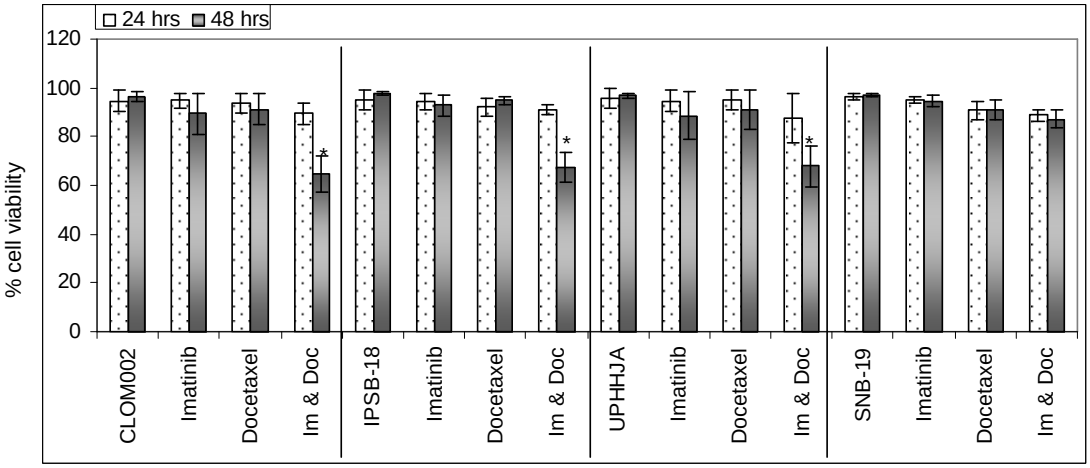

Fig. 3.1.2 (b) Percentage cell viability after 24 and 48 hrs in the absence and presence of drug; imatinib 13.5 µM; docetaxel 14.9 nM. Im & Doc: imatinib and docetaxel. The first two bars in each set represent the controls for each cell culture, i.e. no drug added. *: P < 5E-3. Data represents 3 individual biological assays. Standard deviations were generated from Microsoft Excel software.

3.1.4 Drug Scheduling Effect with Imatinib and Docetaxel on Cell Proliferation

In order to increase the inhibitory effect on proliferation five different drug schedules were tested (Table 3.1.3). Each treatment was performed with three different drug concentrations; high, medium and low. The high drug concentrations were chosen just under the IC_{50} values, medium was the IC_{25} and the lowest was the IC_{10}. Treatment 5 involving a combination of imatinib and docetaxel on day 1 and 2, followed by imatinib alone on day 3 and 4 was the most effective treatment (Fig. 3.1.3). With treatment 5 survival of CLOM002, UPHHJA and IPSB-18 cells was less than 10% in the presence of both high and medium drug concentrations with all three cell lines showing similar sensitivity. SNB-19, however, was less responsive to the drug scheduling treatment, with 23% survival with the highest concentration, and 50% survival with the medium concentration with schedule 5 (Fig. 3.1.3).

Table 3.1.3 Drug treatment schedules: Cells were treated with each drug/drug combination for 24 hrs. On day 5 medium was replaced with fresh medium without drugs. Cell proliferation was determined at day 8.

Schedule	Day 1	Day 2	Day 3	Day 4
1	Imatinib	Imatinib & Docetaxel	Imatinib	Imatinib
2	Imatinib	Docetaxel	Imatinib	Imatinib
3	Docetaxel	Imatinib	Imatinib	Imatinib
4	Docetaxel	Imatinib & Docetaxel	Imatinib	Imatinib
5	Imatinib & Docetaxel	Imatinib & Docetaxel	Imatinib	Imatinib

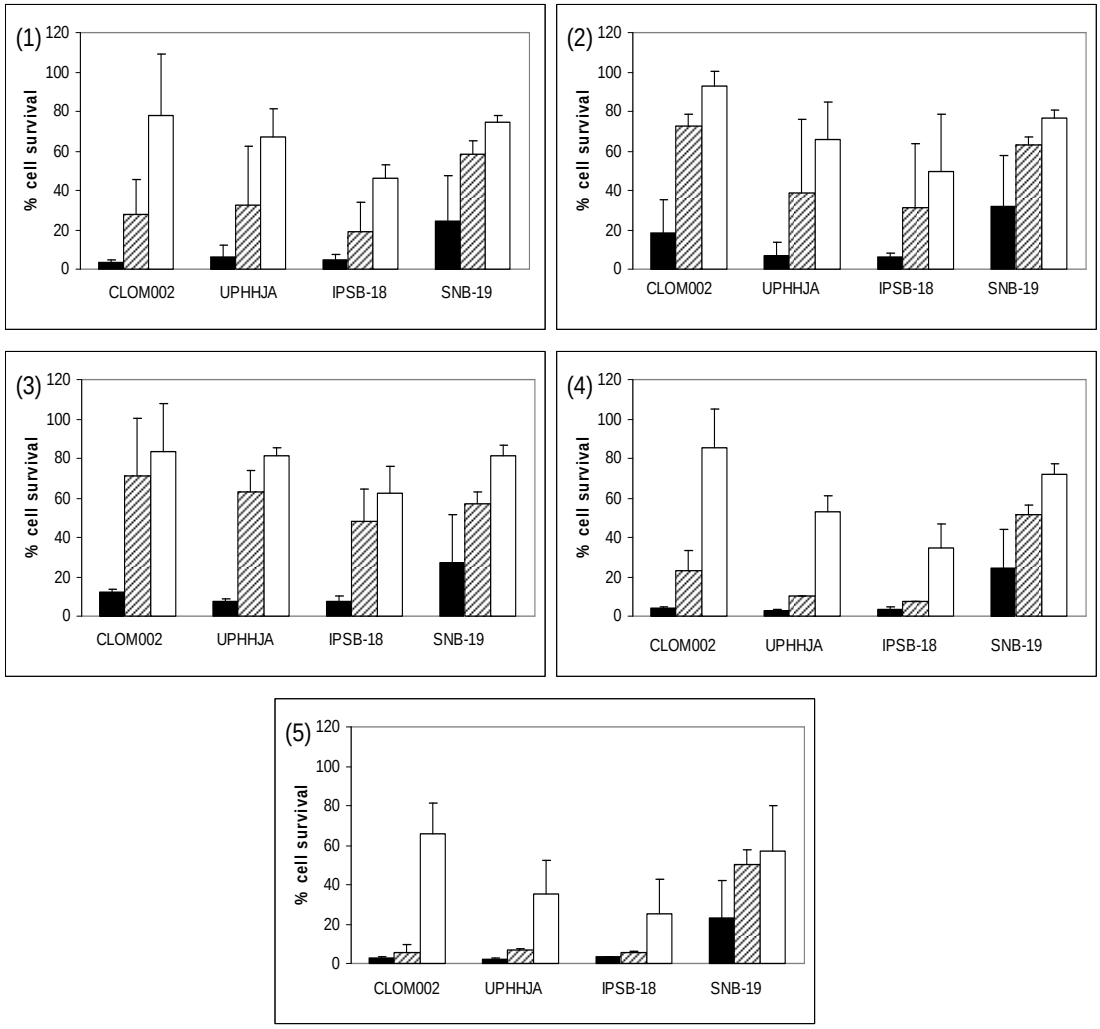

Fig. 3.1.3 Cell survival (%) after 5 different drug schedules using three different drug concentrations; high = closed bars, medium = hatched bars, low = open bars. Each drug treatment was measured against 100% cell survival of cells in the absence of drug. Data represents 2 individual biological assays. Standard deviations were generated from Microsoft Excel software.

Table 3.1.4 Concentrations of docetaxel and imatinib for drug scheduling with CLOM002, UPHHJA, IPSB-18, and SNB-19.

Cell Line	Docetaxel (nM)			Imatinib (μM)		
	Do1	Do2	Do3	Im1	Im2	Im3
CLOM002	12.4	6.2	2.5	13.5	6.8	0.2
UPHHJA	12.4	6.2	2.5	13.5	6.8	1.7
IPSB-18	12.4	6.2	2.5	13.5	6.8	1.7
SNB-19	0.6	0.4	0.008	13.5	6.8	3.4

Do: Docetaxel, Im: Imatinib.

3.1.5 Effect of Imatinib and Docetaxel on Glioma Invasion

In the absence of drug the cell lines UPHHJA, IPSB-18 and CLOM002 showed similar invasion activity reaching a distance between 1700 μm and 2000 μm from the spheroid within 11/12 days; SNB-19 cells invaded much less and reached only a distance of 760 μm within the specified time (Fig. 3.1.4). To investigate the effect of imatinib and docetaxel on actively invading cells, the drug was added 4 days after implanting the spheroids, when invasion had already started. Imatinib alone had little inhibitory effect (CLOM002, UPHHJA, and IPSB-18) or even a slightly increasing effect on invasion activity (SNB-19) compared to invasion in the absence of drug (Fig. 3.1.5). Docetaxel alone reduced the invasion distance reached after 11/12 days up to 40% in CLOM002, IPSB-18 and UPHHJA and 50% in SNB-19. The combination of imatinib and docetaxel did not increase the inhibitory effect on SNB-19 invasion, in comparison to docetaxel alone; however, the combination of imatinib and docetaxel substantially decreased the invasion of IPSB-18 (87.7%), CLOM002 (63%), and UPHHJA (59%) in comparison to either single drug treatment and controls (Fig. 3.1.5 and 3.1.7). NHAs showed significant invasion activity, which was only inhibited up to 60% although treated with much higher concentrations of drug than glioma cell lines (imatinib 40.7 μM, docetaxel 29 nM). The combination of imatinib and docetaxel did not significantly increase the effect of docetaxel alone, a similar result to that obtained with SNB-19 (Fig. 3.1.6).

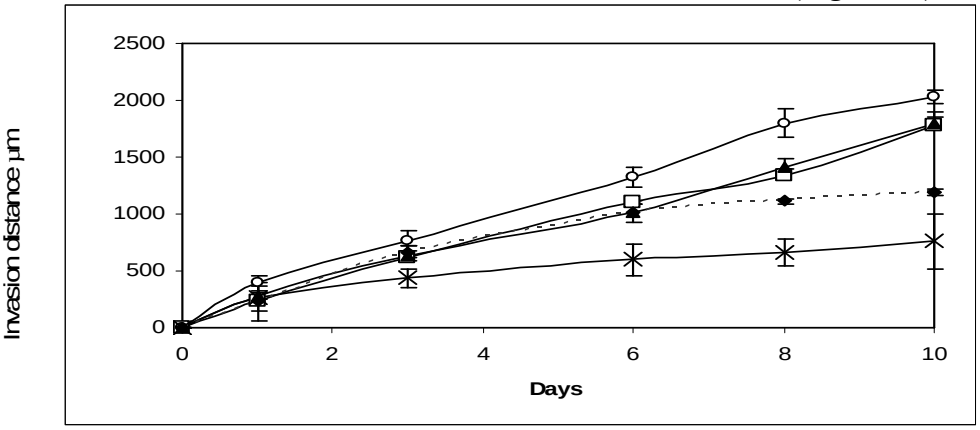

Fig. 3.1.4 Invasion activity of four cell lines and NHAs in the absence of drug; UPHHJA (○), IPSB-18 (□), CLOM002 (▲), SNB-19 (×), cells were tested in biological triplicate assays. NHA (---♦---) NHAs were tested in duplicate in one experiment. Standard deviations were derived using Microsoft Excel software.

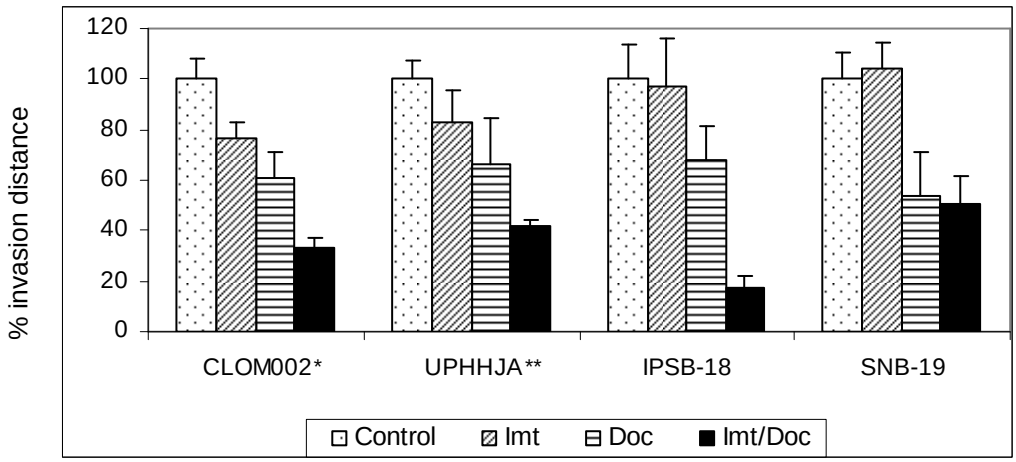

* 10 days ** 11 days

Fig. 3.1.5 Average invasion distance over 10-12 days in the absence (control) and presence of imatinib 13.5 µM and docetaxel 14.9 nM alone and in combination. Cells were tested in biologically triplicate assays. Standard deviations were derived using Microsoft Excel software.

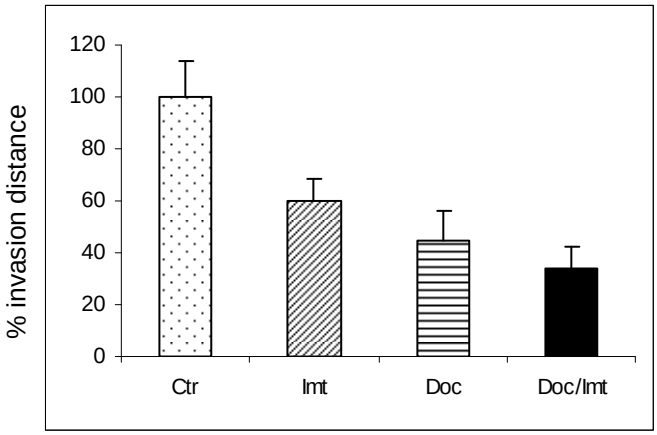

Fig. 3.1.6 Percentage of average invasion over 13 days with normal human astrocytes with imatinib (Imt) 40.7 µM and docetaxel (Doc) 29 nM in comparison to the control (Ctr). Cells were tested in duplicate of one experiment. Standard deviations were derived using Microsoft Excel software.

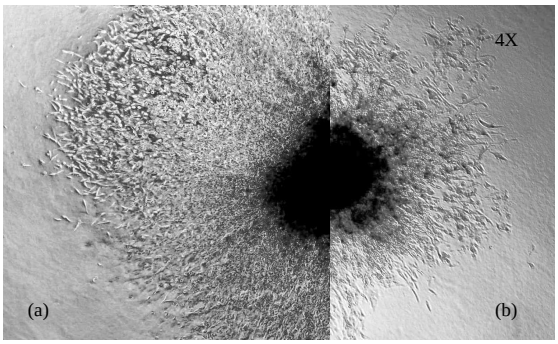

Fig. 3.1.7 CLOM002 cell invasion on day 24 in the absence (a) and presence of the combination of imatinib 13.5 µM and docetaxel 14.9 nM (b).

3.1.6 Protein Expression Profile of Glioma Cell Cultures

Using western blotting the protein expression of tyrosine kinases (PDGFR-β, PDGFR-α, C-Kit, C-Abl) of multidrug resistance pumps (Pgp, BCRP) and of glial fibrillary acidic protein (GFAP) were analysed. All four cultures were positive for GFAP proving their glial origin (Fig. 3.1.8). Low expression of PDGFR-β was seen in CLOM002, UPHHJA, and SNB-19, and higher expression was found in IPSB-18 (Fig. 3.1.8). In addition low expression of PDGFR-β in NHAs was found (Fig. 3.1.10). All cell cultures expressed low levels of PDGFR-α, but no C-Kit. C-Abl was expressed in cell cultures (Fig. 3.1.8) and in NHAs (Fig. 3.1.10). In SNB-19 cells the C-Abl antibody recognized an additional band around 210 KDa which is similar to the pattern expressed in the positive control K562, a chronic myelogenous leukaemia cell line expressing both C-Abl and the mutated form Bcr-Abl (Fig. 3.1.8). A Bcr-Abl-specific antibody recognized the same band in SNB-19 cells suggesting the expression of a mutated form of C-Abl in these cells (Fig. 3.1.9).

The multidrug resistance protein BCRP (ABCG2, MXP) was found in all four cell cultures (Fig. 3.1.8); however, SNB-19 and IPSB-18 expressed much higher levels compared to CLOM002 and UPHHJA cells. Pgp (MDR-1, ABCB1) was only expressed in SNB-19 cells (Fig. 3.1.8). Higher expression of Pgp was found in the NHAs and low expression of BCRP (Fig. 3.1.10). In summary, SNB-19 protein expression differed from the other cell cultures in a strong BCRP expression, the presence of Pgp, and a protein similar to the mutated tyrosine kinase Bcr-Abl.

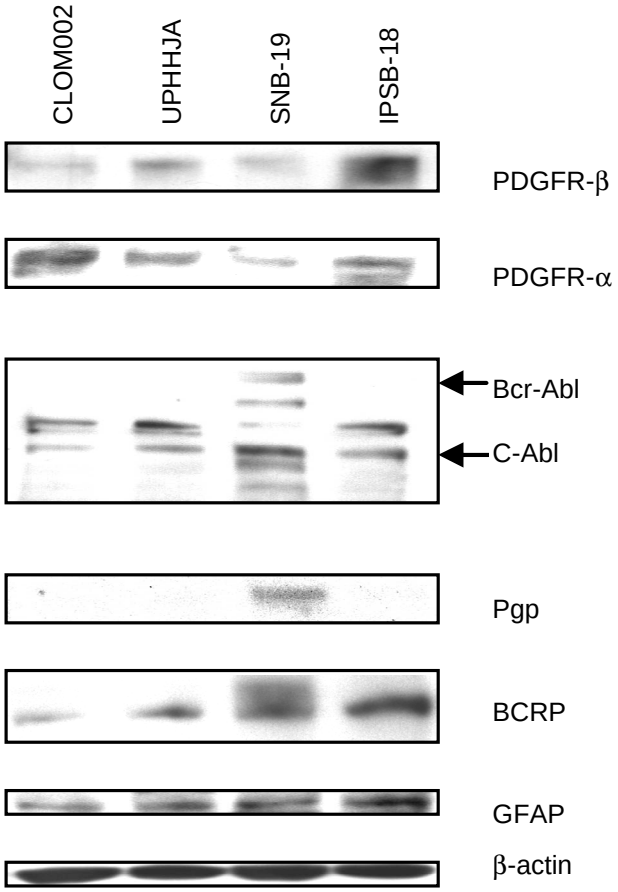

Fig. 3.1.8 Western blot analysis of tyrosine kinases PDGFR-β, PDGFR-α, Bcr-Abl, and C-Abl, multidrug resistance pumps BCRP, Pgp and the astrocyte marker GFAP. CLOM002 (1), UPHHJA (2), SNB-19 (3) IPSB-18 (4).

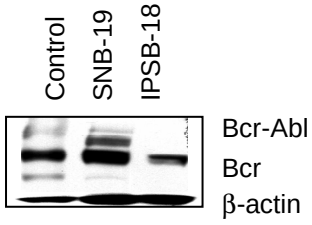

Fig. 3.1.9 Western blot analysis with Bcr-Abl specific antibody. Positive control (K562) (1), SNB-19 (2), IPSB-18 (3).

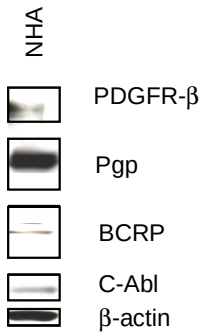

Fig. 3.1.10 Western blot analysis of PDGFR-β, C-Abl, multidrug resistance pumps Pgp and BCRP expression in normal human astrocytes.

3.1.7 Effect of Elacridar in Combination with Imatinib and Docetaxel on Proliferation of Glioma Cell Lines

SNB-19 was the only cell line expressing Pgp, and had the highest BCRP expression. Imatinib is a substrate for both Pgp and BCRP (Leslie *et al.* 2005), which has possibly led to a higher efflux of imatinib in SNB-19 cells. Docetaxel is also a substrate of Pgp. To test the functionality of Pgp and BCRP, a specific inhibitor of both pumps, elacridar, was added which should prevent the efflux of the substrates imatinib and docetaxel resulting in stronger inhibition of proliferation. Elacridar was tested on CLOM002 and SNB-19 using an IC_{10} of imatinib, an IC_{20} of docetaxel, and an IC_{20} of elacridar, a concentration which has been optimised previously in lung cancer cell lines. In CLOM002 the inhibition of Pgp did not result in inhibition of proliferation in the presence of imatinib and docetaxel (Fig. 3.1.11); however in SNB-19 the addition of elacridar resulted in a 17% increase in inhibition of proliferation in the presence of the drug combination (Fig. 3.1.12). This indicated that the efflux pumps Pgp and BCRP were active in SNB-19 cells and were responsible for effluxing imatinib and docetaxel.

1: Imatinib (Imt), **2**: Docetaxel (Doc), **3** Elacridar (El), **4**: Imt & Doc, **5**: Imt & El, **6**: Doc & El, **7**: Imt & Doc & El

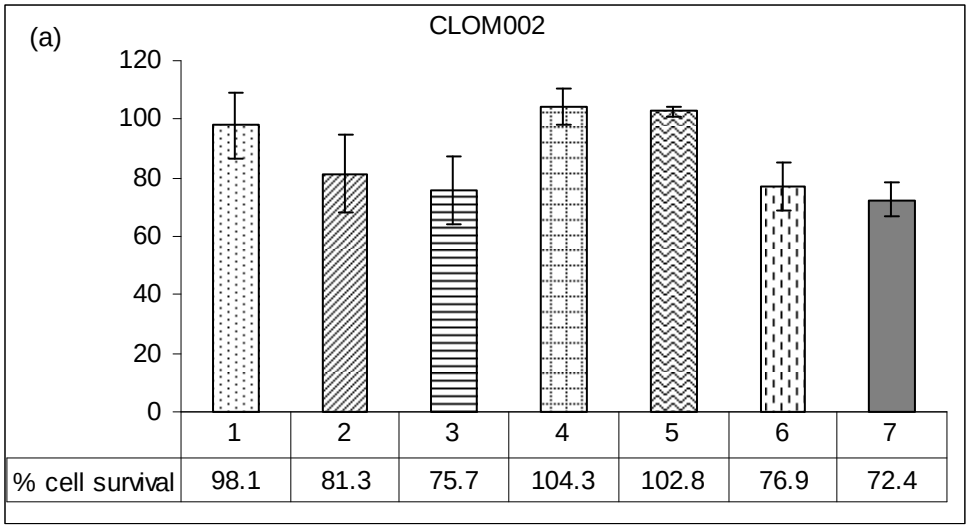

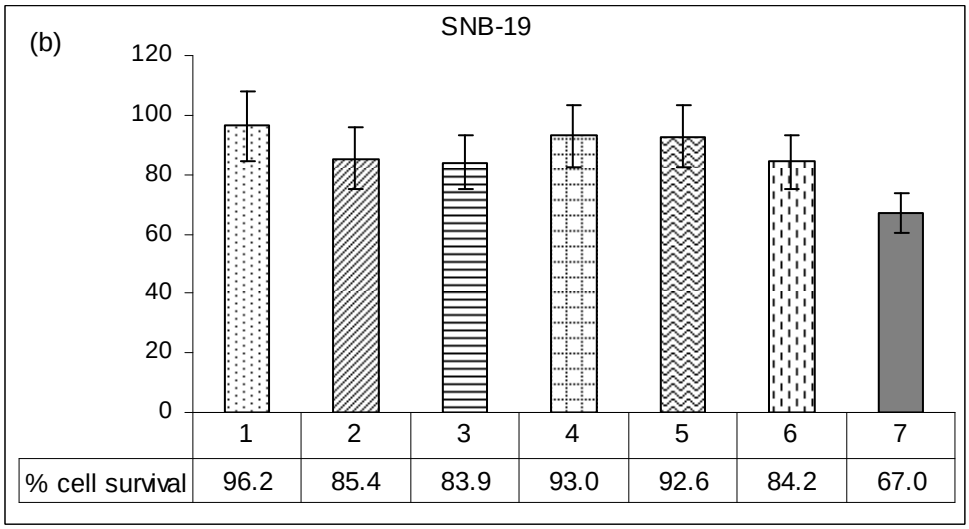

Fig. 3.1.11 The combined effect of imatinib 1.7 µM, docetaxel 0.12 nM and elacridar 0.25 µM on proliferation. 1: Elacridar (El), 2: Imatinib (Imt), 3: Imt and El, 4: Docetaxel (Doc), 5: Doc and El, 6: Imt and Doc, 7: Imt and Doc and El. Data represents 3 individual biological assays. Standard deviations were generated from Microsoft Excel software.

3.1 Discussion

Imatinib and Docetaxel can Effectively Inhibit Invasion and Proliferation in Glioma

Introduction

In the present study the inhibitory effect of the TKI imatinib singly and in combination with the chemotherapeutic drug docetaxel has been examined in glioma cell cultures. Clinical trials using imatinib as a single agent for the treatment of recurrent glioblastoma resulted in increased progression free survival after 6 months for only a small number of patients (Katz *et al.* 2004; Raymond *et al.* 2008). A similar result was seen in primary cultures of glioma specimen; out of 15 specimens Hägerstrand *et al*, 2006 identified a small subgroup of high-grade human glioma cultures, which were imatinib-sensitive (Hagerstrand *et al.* 2006). In this subgroup the PDGFR expression and phosphorylation status was significantly correlated with imatinib sensitivity, indicating a dependency on the PDGFR signalling (Hagerstrand *et al.* 2006).

TKs regulate a large range of proteins involved in processes including growth, metabolism and differentiation. A number of small molecule inhibitors were developed to target tyrosine kinases; some of these inhibitors are highly effective in the treatment of specific types of cancer, e.g. imatinib. Imatinib for example had been designed to target Bcr-Abl, a mutated form of the non-receptor kinase C-Abl found in Philadelphia chromosome positive chronic myeloid leukaemia (CML) (Sherbenou and Druker 2007). The success of this compound in the treatment of CML triggered the hope that imatinib could also be effective against other tumour types. Besides BCR-Abl imatinib targets PDGFR, stem cell factor C-Kit and C-Abl, causing cell cycle arrest and/or apoptosis (Kilic *et al.* 2000; Nagar 2007).

There are various possible reasons for the ineffectiveness of imatinib monotherapy on the majority of gliomas: inhibition of C-Kit and PDGFR by imatinib may lead to induction of vascular epithelial growth factor (VEGF) resulting in angiogenesis; inhibition of a single tyrosine kinase might be insufficient to impact downstream signalling cascades, and the molecular targets of imatinib may not play a key role in glioma growth and spread. Higher levels of VEGF are found in high-grade glioma, making this an ideal therapeutic target (Takano *et al.* 2010); an antibody targeting VEGF, bevacizumab, showed promising results in glioma,

initially, however the development of resistance emerged (Norden *et al*. 2008; Narayana *et al*. 2009). A more promising treatment in glioma is currently being examined by combining temozolomide with radiotherapy and bevacizumab (Narayana *et al*. 2008).

The main problem in the treatment of malignant gliomas is their invasive behaviour. Successful resection of the main tumour mass cannot prevent recurrence due to single cells invading the surrounding brain parenchyma at the time of diagnosis. The clinical effectiveness of combination therapy PCV (Procarbazine, CCNU and Vincristine), which was used for over 30 years in the treatment of malignant astrocytomas and glioblastomas, is still doubtful. The development of new treatment strategies is urgently needed.

Another possibility for increasing the response and effectiveness of TKIs could be a combination treatment consisting of a TKI and a cytotoxic drug, e.g. docetaxel. Docetaxel is a hemisynthetic product derived from the European yew tree, which promotes the assembly and inhibits the depolymerisation of microtubules in the cells (Bissery *et al.* 1995). This drug is widely used as chemotherapeutics and is particularly effective in the treatment of non-small cell lung cancer (Plosker and Hurst 2001). The use of docetaxel alone for the treatment of glioblastomas has shown little or no significant response possibly due to the BBB limiting drug flow into the brain (Forsyth *et al.* 1996; Sanson *et al.* 2000). However, docetaxel combined with radiotherapy resulted in a partial response (Koukourakis *et al*. 1999), and local delivery of docetaxel *in vivo* in an animal model significantly improved survival (Sampath *et al*. 2006).

The combined treatment of imatinib and docetaxel was tested on four glioma cell cultures. Two of the cell cultures (CLOM002 and UPHHJA) derived from primary glioblastomas were used at low passage numbers (CLOM002 passage 11 to 40, UPHHJA passage 9 to 25) and were developed in Professor Geoffrey Pilkington's laboratory in Portsmouth, UK. A cell line IPSB-18 also from Professor Geoffrey Pilkington's laboratory was derived from a grade III astrocytoma, was used at passages 57 to 72. A second cell line SNB-19 is an established and commercially available cell line and was used between passages +9 to +31 (after purchase). The cell lines IPSB-18 and SNB-19 appeared as homogeneous populations possibly due to higher passage number; while the primary glioblastoma cell cultures CLOM002 and UPHHJA presented as heterogeneous cell populations.

All cell cultures had fast proliferation rates and were highly invasive. The effect of imatinib and docetaxel singly and in combination on proliferation, invasion and apoptosis was examined.

Effect of Imatinib and Docetaxel on Proliferation and Invasion of Glioma Cell Cultures CLOM002, UPHHJA and IPSB-18

To examine if the combination of the TKI imatinib and the chemotherapeutic drug docetaxel decreases proliferation activity of glioma cells the IC_{50} concentration for each drug was determined in a monolayer proliferation assay (Table 3.1). The IC_{50} values for imatinib were in the micromolar range (15.7 µM to 17.4 µM), which is consistent with published data where Servidei *et al*, 2006 showed IC_{50} values ranging from 18.6 µM to 32.6 µM in U87 glioma cells (Servidei *et al*. 2006). IC_{50} values for docetaxel ranged from 8.2 nM (IPSB-18) to 19.8 nM (UPHHJA) (Table 3.1).

The combination of both drugs at low concentration (Fig. 3.1.1) (Table 3.1.2) resulted in up to 87% inhibition of proliferation in CLOM002, UPHHJA and IPSB-18. For each cell culture the combined effect of the IC_{10}, IC_{20} and IC_{30} of imatinib and docetaxel was analysed using the Chou and Talalay plot (Chou and Talalay 1984). This revealed a synergistic effect of imatinib together with docetaxel in these 3 glioma cell cultures. The highest synergism was seen in IPSB-18 cells followed by UPHHJA and CLOM002 cells. Gucluler and Baran *et al*, have shown that the combined treatment of imatinib and docetaxel decreased cellular proliferation in chronic myeloid leukaemia cell lines (Gucluler and Baran 2009). They increased the chemosensitivity of human K562 cells to imatinib in combination with docetaxel, and showed that the combination of both drugs decreased cellular proliferation and increased apoptosis as compared to any drug alone. Apoptosis was reduced through caspase-3 enzyme activity (Gucluler and Baran 2009).

It has been reported that small amounts of imatinib in the plasma can cross the blood–brain barrier (BBB). Bihorel *et al*, have shown that in mice only 20% of imatinib is crossing the BBB, while 80% is effluxed by BCRP and Pgp (Bihorel *et al.* 2007). Le Coutre *et al*, found a mean plasma concentration with imatinib in leukaemia patients of 2–5 µg/ml and 531 ng/ml for the metabolite N-desmethyl-imatinib (le Coutre *et al.* 2004). They also found that the average CSF concentration for imatinib was 38 ng/ml, and less than 10 ng/ml for N-desmethyl-imatinib (le

Coutre *et al.* 2004). High-grade glioma patients have a disrupted BBB in the tumour centre, which would allow a higher concentration of imatinib in the CNS; however, it is not clear if an effective concentration can be reached.

A similar problem exists with docetaxel. Docetaxel as a substrate of Pgp probably does not reach a sufficient concentration in the brain, which might explain the poor response seen in recurrent glioblastoma treated with docetaxel systemicallypo (Forsyth *et al.* 1996; Kemper *et al.* 2003; Kemper *et al.* 2004). Plasma concentrations for docetaxel are around 0.5 nM, while concentrations in the cerebrospinal fluid (CSF) are ten times lower (0.05 nM) (Fracasso *et al.* 2004). This issue has been addressed recently by using convection-enhanced delivery (CED), for the treatment of recurrent gliomas with some promising results, where direct regional administration of protein toxins is achieved through stereotactically implanted catheters by using CED (Chen *et al.* 1999; Debinski 2002). The concentrations of docetaxel in the proliferation assays with SNB-19 and CLOM002 (0.1 nM to 0.5 nM) (Table 3.1.2), were within the reported plasma concentration reported by Fracasso *et al*, for docetaxel (Fracasso *et al.* 2004), and over 4 times higher for UPHHJA and IPSB-18 (1.2 nM) (Table 3.1.2); and the concentrations for imatinib are lower than the plasma concentrations reportedly found by Le Coutre *et al*, for imatinib (up to 8 µM) (le Coutre *et al.* 2004). It is possible that the concentrations of imatinib and docetaxel currently achievable in the CSF are inactive concentrations and have no toxic effect on glioma.

The synergistic effect of imatinib and docetaxel in combination was caused by apoptosis, while single drugs had little apoptotic effect (Fig. 3.1.2). Docetaxel causes G2/M cell cycle arrest (Gucluler and Baran 2009) and imatinib induces cell cycle arrest at the G0-G1 or G2/M phase in glioma cells (Ren *et al*. 2009). Increased apoptosis through combination of imatinib and docetaxel has also been found in human K562 chronic myeloid leukaemia cells, and this effect was induced by caspase-3 enzyme activity (Gucluler and Baran 2009).

A variety of drug scheduling assays were carried out to increase the combination effect of imatinib and docetaxel (Fig. 3.1.3). A combination of imatinib and docetaxel on day 1 and 2, followed by imatinib alone on day 3 and 4 was the most effective treatment, resulting in 90% cell kill in CLOM002, UPHHJA and IPSB-18 cells (Fig. 3.1.3).

UPHHJA, IPSB-18 and CLOM002 show similar invasion activity reaching a distance between 1700 and 2000 µm from the spheroid within 11/12 days (Fig. 3.1.4). Imatinib alone had little or no effect on glioma invasion activity while docetaxel slightly inhibited invasion in these 3 cell cultures (Fig. 3.1.5). The drug combination, however, reduced invasion activity between 63% in CLOM002, 59% in UPHHJA and 87.7% in IPSB-18, and was much more effective compared to single drugs. It is also possible that the 3D invasion assay allowed some cells to invade and some to proliferate, therefore the drugs may have had an effect on both invasion and proliferation. In figure 3.1.7 the image of the invasion assay with CLOM002 after 24 days invasion shows cells with an elongated structure, these may have been invasive, and cells with a round structure, which may have been involved in proliferation, possibly indicating a difference in function for each cell type (Fig. 3.1.7). Golembieski *et al*, have shown migrating U87MG glioma cells maintain an elongated morphology on a fibronectin substrate, migration was correlated with decreased proliferation, they found an increase in the number of rounded cells with proliferative function (Golembieski *et al*. 2008). It is possible that docetaxel inhibited both proliferation and invasion, as it specifically targets microtubules, which are involved in cell division and motility.

All cell cultures expressed GFAP proving their glial origin (Fig. 3.1.8). C-Abl, PDGFR-α and PDGFR-β were expressed at low levels in all cell cultures, while C-Kit expression was absent. Low expression or absence of these imatinib targets could explain the low sensitivity to imatinib. C-Kit and C-Abl are frequently mutated or overexpressed in glioblastomas (Haberler *et al.* 2006), and are associated with glioma progression (Stanulla *et al.* 1995; Jiang *et al.* 2006), Overexpression of C-Kit and C-Abl was not found in the tested glioma cells. Other growth factors such as EGFR, tumour growth factor (TGF), insulin growth factor (IGF) may play a more significant role in proliferation of these cell lines. EGFR which signals through the PI3K/Akt pathway (Hynes and Lane 2005) is commonly overexpressed in gliomas (Heimberger *et al.* 2005).

IPSB-18 had the highest expression of PDGFR-β, which is not surprising as the activation of the PDGF autocrine loop is thought to be an early event in the pathogenesis of malignant astrocytomas (Guha *et al*. 1995) and IPSB-18 is derived from a grade 3 astrocytoma. Secondary glioblastomas are usually associated with

overexpression of platelet derived growth factor (PDGF) and its receptor tyrosine kinase PDGFR forming an autocrine loop, which contributes to tumour growth, and the transformation process to a more malignant phenotype (Hermanson *et al.* 1992; Westermark *et al.* 1995).

Effect of Imatinib and Docetaxel on Proliferation and Invasion of Normal Human Astrocytes

As a control cell line normal human astrocytes (NHAs) were included. Their IC_{50} for imatinib was 17 µM, which is similar to the value found in glioma cell cultures, suggesting the possibility of side effects on normal cells. Bartolovic *et al*, found a reversible effect with normal hematologic (CD34 positive) progenitor cells at IC_{50s} ranging from 0.3 µM to 1.8 µM (Bartolovic et al. 2004). This effect was independent of C-Kit signalling and could not be seen with stem cells (Bartolovic *et al.* 2004).

With the NHAs an IC_{50} concentration with docetaxel could not be achieved, the highest concentration tested was 124 nM (Table 3.1), which resulted in an $IC_{20;}$ this is a very low toxicity in comparison to that seen with the glioma cells. It appears from this result that docetaxel is more toxic to cancerous cells, making docetaxel an ideal therapy for glioma, with low-toxicity to normal astrocytes. Docetaxel is a known substrate of Pgp, the NHAs had very high expression of Pgp (Fig. 3.1.10) in comparison to the glioma cells (Fig. 3.1.8). Pgp expression is known to be expressed in the BBB (Leslie *et al.* 2005) and in human astrocytes (Marroni *et al*. 2003). It is possible that Pgp effluxes docetaxel in NHAs and that there is a loss of function of Pgp in glioma cells.

Rabi and Bishayee *et al*, have shown that *d* –limonene, a non-nutrient dietary component, enhanced the antitumor effect of docetaxel against human prostate cancer cells without being toxic to normal prostate epithelial cells (Rabi and Bishayee 2009). Cells have a complex defence system for protection against free radical-induced damage resulting in the generation of glutathione (GSH), cysteine and antioxidant enzymes, including GSH peroxidase, superoxide dismutase and catalase (www.benbest.com/nutrceut/AntiOxidants.html). Hydrogen peroxide (H_2O_2) has been identified as a major cytotoxic molecule of reactive oxygen species (ROS) in docetaxel-induced cell death (Bauer 2000; Bohler *et al.* 2000; Komatsu *et al.* 2001). Rabi and Bishayee *et al*, 2009 have shown that docetaxel induced certain

amounts of ROS with cell death and suggested that the different effects of docetaxel on the prostate cancer cells in comparison to the normal prostate epithelial cells, may be due to the presence of more effective endogenous antioxidant mechanisms in the normal cells than in the malignant ones (Rabi and Bishayee 2009).

To our surprise, NHAs invaded collagen gel from the spheroid up to a distance of 1193 µm within 10 days (Fig. 3.1.4). NHAs used in this project are of cerebral and foetal origin suggesting the presence of a mixture of astrocytes and oligodendrocyte-type 2 astrocyte progenitor cells (O2A). Rat O2A cells have been shown to spread and migrate on myelin coated dishes, and on spinal cord sections (Amberger *et al.* 1997).

NHA invasion activity was only inhibited up to 60% although treated with much higher drug concentrations than the glioma cultures, mainly due to the docetaxel effect (imatinib 40.7 µM, docetaxel 29 nM) (Fig. 3.1.6). As NHAs had high Pgp expression and both imatinib and docetaxel are substrates for Pgp, it is possible that they were effluxed, which could explain why high concentrations were necessary to show an effect on invasion. The combination of imatinib and docetaxel did not significantly increase the effect of docetaxel alone, a similar result to that obtained with SNB-19 (Fig. 3.1.6).

NHAs also had low expression of PDGFR-β, BCRP and C-Abl (Fig 3.1.10). The 2 low passage primary cultures CLOM002 and UPHHJA had similar expression of BCRP to the NHAs, again possibly indicating that BCRP expression is correlated with increased passage number (Figs 3.1.8 and 3.1.10).

Effect of Imatinib and Docetaxel on Proliferation and Invasion with the Established Glioma Cell Line SNB-19

The established cell line SNB-19, derived from a glioblastoma, had an IC_{50} for imatinib of 18.7 µM, and for docetaxel an IC_{50} of 0.7 nM was found (Table. 3.1). The combination of both drugs resulted in an additive effect in contrast to the results obtained with the other glioma cells (Fig. 3.1.1). With drug scheduling a cell kill of 77% could be reached in SNB-19 (Fig. 3.1.3), showing their lower responsiveness to the drug combination.

SNB-19 appear as a homogeneous population and seem to have the potential to revert to a cancer stem cell-like genotype when exposed to chemotherapeutic drug (Auger *et al*. 2006). Stem cells seem to be responsible for resistance to chemotherapy, which might explain the lower cell kill effect of drug combination on SNB-19. Auger *et al*, developed temozolomide resistant variants of SNB-19 which did not show increased MGMT expression (Auger *et al.* 2006). Ma *et al*, also found MGMT expression not to be correlated with resistance in glioma; but some loss of chromosome 2p no amplification of chromosome 4 and 16q (Ma *et al*. 2002). Drug resistance in glioma is due to chromosome recombination (Duesberg *et al*. 2001); however, Auger *et al*, found that SNB-19 temozolomide-resistant variants had less rearranged chromosomes than the parental population, these cells were possibly derived form a pre-existent population in the parental cell line (Auger *et al.* 2006). They used microarray analysis to compare gene expression profiles of SNB-19-temozolomide resistant variants in comparison to the parental cell line. They found a number of genes known to be involved in developmental pathways to be overexpressed in the resistant variants, including frizzled-2 (FZD2) (Galceran *et al*. 2004) which is involved in the Wnt pathway or in stem cell self-renewal, and genes involved in proliferation such as leukaemia inhibitory factor (LIF) (Pitman *et al*. 2004), RNA polymerase II elongation factor (ELL) (Kanda *et al*. 1998), and Co-purified with NNF1 protein 1 (CNN1) (Xie *et al*. 2004). If following temozolomide treatment gliomas have the ability to revert back to senescent drug resistant stem cell-like cells it could explain why tumours relapse over time.

Invasion activity of SNB-19 cells was slow and the cells reached a distance of only 760 µm within 10 days (Fig. 3.1.4). Invasion was strongly inhibited in the presence of docetaxel alone, and the drug combination did not significantly increase this effect (Fig. 3.1.5). Western blot analysis revealed an additional band similar to that found in K562, a CML cell line, representing the fusion protein Bcr-Abl at 210 kDa (Fig. 3.1.8 and 3.1.9). Bcr-Abl is a specific target for imatinib; however SNB-19 did not show higher sensitivity to imatinib suggesting that the band does not represent Bcr-Abl. Several BCR-Abl kinase domain point mutations have been identified, in CML tumour cells after imatinib treatment, it is more common to find these mutations in patients with acquired resistance to imatinib, than patients with primary resistance (Qin *et al.* 2010; Sherbenou *et al.* 2010). It is possible that SNB-

19 has a mutated form of Bcr-Abl, which can be examined by specifically looking at single nucleotide polymorphisms using PCR.

SNB-19 cells expressed both efflux pumps, Pgp and BCRP which might explain why the drug combination was not as effective as it was on the other tested cultures. Using elacridar, a specific Pgp and BCRP inhibitor (Evers *et al.* 2000), suggested the functionality of these pumps in SNB-19 cells (Fig. 3.1.11). It has been shown in mice that blockade of both Pgp and BCRP by elacridar produced significantly greater brain penetration of imatinib and docetaxel (Kemper *et al.* 2004; Bihorel *et al.* 2007); this effect has also been seen in glioma cell lines with imatinib (Decleves *et al.* 2008), and in lung cancer cell lines with docetaxel (Myer *et al.* 1999).

Co-expression of Pgp and BCRP has also been found in an imatinib resistant subgroup of acute myeloid leukaemia patients (van den Heuvel-Eibrink *et al.* 2007).

It is also possible that the more established cell lines SNB-19 and IPSB-18, have developed into more resistant cell lines over time, as they have undergone more passages, possibly allowing for clonal selection, resulting in higher expression of BCRP and Pgp expression in SNB-19 in comparison to the two cell cultures which have less passages, CLOM002 and UPHHJA.

3.1 Summary and Conclusion

The Effect of Imatinib and Docetaxel on Glioma

The combined effect of the TKI, imatinib and the chemotherapeutic drug, docetaxel had a synergistic antitumourigenic effect on glioma cells. The drug combination strongly inhibited both proliferation and invasion, and had a pro-apoptotic effect in 3 out of 4 glioma cell cultures. The combined treatment of imatinib and docetaxel is a promising treatment for glioma patients.

SNB-19 cells express a mutation of the Abl protein, which might prevent imatinib binding. Out of 4 cell cultures only SNB-19 expressed both BCRP and Pgp, which might lead to higher efflux of imatinib explaining the low sensitivity of SNB-19 cells to the drug combination.

3.2 Development of Drug Resistant Cell Lines

To study drug resistance in glioma it was necessary to develop drug resistant glioma cells. Two glioma cultures were chosen to develop resistant variants, SNB-19 an established glioma cell line bought in from DSMZ, and CLOM002 cells which originated from a glioblastoma and was developed in Professor Geoffrey Pilkington's laboratory in University House, Winston Churchill Avenue, Portsmouth, Hampshire, PO1 2UP, UK. Both cell cultures were exposed for 4 hours once a week over 10 weeks, separately to imatinib (169 µM), docetaxel (4.96 nM and 1.24 nM), and temozolomide (257.5 µM). Neither SNB-19 nor CLOM002 developed resistance to imatinib or docetaxel, only CLOM002 did not develop resistance to temozolomide. However, SNB-19 became strongly resistant (15 fold) to temozolomide in comparison to the parental population (temozolomide IC_{50} 561.4 µM ± 45.8 µM versus 37 µM ± 4.1 µM). The parental cell line was used at passage P+16, and were temozolimide resistant at passage P+40. Figure 3.2.1 shows cell morphology at 10 and 20 times magnification of the parental cell line ((a) and (c)), and the temozolomide resistant variant ((b) and (d)). The latter appeared rounder and with a more flattened structure.

Table 3.2.1 Temozolomide IC_{50} values SNB-19 and SNB-19 temozolomide resistant cell line.

Cell Line	IC_{50}
Parental SNB-19 P+16	37 µM ± 4.1 µM
Temozolomide resistant SNB-19 P+40	561.4 µM ± 45.8 µM

Standard deviations represent the result of 3 biologically individual assays.

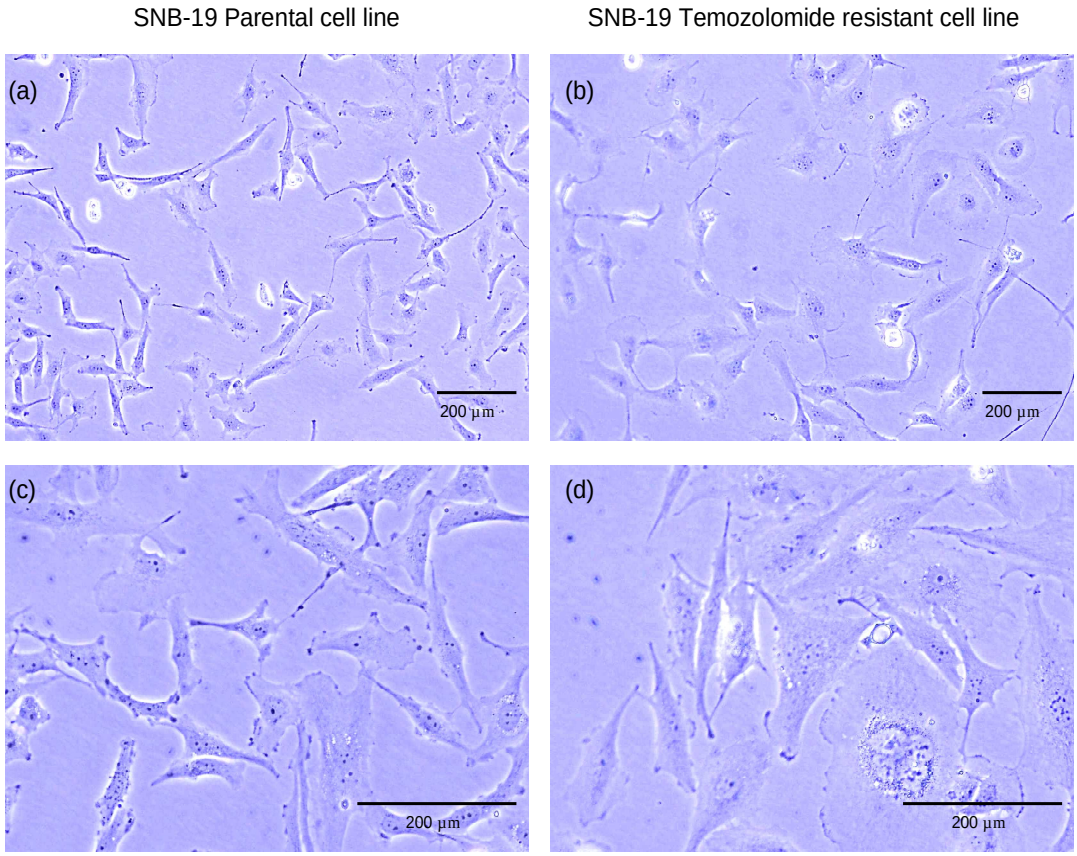

Fig. 3.2.1 (a) and (c) show the parental cell line SNB-19 without drug exposure; (b) and (d) show the SNB-19 after 10 weeks exposure to temozolomide.

3.2 Discussion

Development of Drug Resistant Cell Lines

Introduction

Development of resistance in glioma to current therapies over time ultimately results in treatment failure in glioma patients. Exploration of resistance mechanisms in glioma cells should increase our understanding of resistance in glioma, and enable identification of new targets for treatment. In order to study resistance in glioma it was necessary to firstly make a resistance model; an established glioma cell line SNB-19, and the glioma culture CLOM002 were chosen, both were derived from glioblastomas.

Both cultures were separatley pulse selected with imatinib, docetaxel and temozolomide four 4 hours once a week over 10 weeks. Toxic concentrations of drug were chosen; the concentrations used were 169 µM imatinib, 4.96 nM and 1.24 nM of docetaxel, and 257.5 µM of temozolomide. With either culture there was no change in resistance to imatinib and docetaxel in comparison to the parental cells, when the IC_{50} values were tested. CLOM002 did not develop resistance to temozolomide; however SNB-19 developed strong resistance to temozolomide (15-fold). The parental cell line SNB-19 had an IC_{50} with temozolomide of 37 µM, while the SNB-19 temozolomide resistant cell line had a much higher IC_{50} of 561.4 µM (Table 3.2.1). Auger *et al.* used an incremental concentration of 3-150 µM of temozolomide with SNB-19 and created two resistant variants, SNB-19A4 and SNB-19C1 which had a 100-fold and 55-fold resistance to temozolomide in comparison to the parental SNB-19 cell line (Auger *et al.* 2006). They initially used a low concentration of temozolomide (3 µM) and selected out the more resistant clones, then they incremented the concentration of temozolomide over time, this appears to be a more effective way of developing resistant variants (Auger *et al.* 2006).

The parental cell line had a homogeneous population, with elongated cells, while the SNB-19 temozolomide resistant cell line had a mixed population of elongated, flattened and rounded cell types (Fig. 3.2.1). There were much larger nuclei present in the resistant cell line, possibly indicating the presence of a stem cell-like population, as stem cells tend to have larger nuclei with less defined

structures (Li and Xie 2005). Strong staining for stem cell markers such as CD133 in these temozolomide resistant cells and the parental cells would be interesting to see if there are stem cells present and if there is a higher population of stem cells in the resistant cells. If there are stem cells in the resistant cells they could be isolated by fluorescently activated cell sorting (FACS) analysis, and further testing of temozlomide resistance could be examined to see if these cells are more resitant than the original mixed population.

The induction of O^6-G-methylation by temozolomide is reversed by the DNA repair gene MGMT. Increased levels of MGMT leads to resistance to temozolomide in some glioblatomas, however Auger *et al*, found that the levels of temozolomide resistance did not correlate with MGMT expression levels (Auger *et al.* 2006). Very few gliomas actually overexpress O^6-G-methylation-DNA methyltransferase, suggesting dependence on other resistance mechanisms. Some tumours develop resistance independently to MGMT status, with mechanisms such as loss of p53 function, which causes cell cycle arrest and apoptosis (Auger *et al.* 2006); or the Akt pathway which prevents senescence and mitosis (van den Bent *et al.* 2009). Ulasov *et al*, found that glioma CD133 positive stem cells which were resistant to temozlomide treatment had more active Notch and Sonic hedgehog (SHH) pathways, the pathway activity was further enhanced after exposure to temozolomide (Ulasov *et al.* 2010). The SHH pathway is involved in prenatal brain development where it regulates proliferation (Dahmane *et al.* 2001). The Notch pathway is associated with proliferation differentiation and apoptosis (Miele and Osborne 1999). The activationof these pathways in the temozolomide resistant cells from the present study could be examined by using westrn blotting and looking at phosphorylated proteins of these pathways.

Kitange *et al*, have identified CD74 as a potential modulator of temozolomide responsiveness; CD74 is a membrane receptor for the proinflammatory cytokine macrophage migratory inhibitory factor (MIF) on immune cells, which promotes cell proliferation through the MAPK and Akt pathways (Kitange *et al.* 2010). They found overexpression of CD74 in glioblastoma (Kitange *et al.* 2010). The levels of CD74 in the SNB-19 temozolomide resistant cells from the present study could be examined to see if CD74 expression correlates with resistance in these cells.

Schaich *et al*, examined MDR1 nucleotide polymorhisms of glioblastoma patients treated with temozolomide (Schaich *et al.* 2009). They found that response to temozolomide treatment was dependent on MDR1 expression, analysis of MDR1 genotypes showed that the C/C variant of the exon12 C1236T SNP was associated with higher survival for patients treated with temozolomide, the effect was independent of MGMT methylation status (Schaich *et al.* 2009). The overexpression of MDR1 has been found in most brain tumours (Demeule *et al.* 2001). It has been suggested temozolomide resistant clones of SNB-19 develop resistance due to less differentiated pre-existent cells possibly of stem cell origin (Auger *et al.* 2006). Tumour stem cells are thought to be naturally resistant to chemotherapy due to their quiescence, their ability to repair DNA, and their increased ABC transporter expression (Auger *et al.* 2006). In a previous section it was shown that SNB-19 have high expression of Pgp and express BCRP (Kinsella *et al.* 2011), BCRP is known to be a stem cell marker (Wang *et al.* 2008). It would be interesting to check the levels of Pgp and BCRP expression in the temozolomide resistant cell line developed to see if the levels have increased in comparison to the parental population.

3.2 Summary and Conclusion

A temozolomide resistant variant (15-fold) was developed from exposure of SNB-19 cells to temozolomide. There was a change in morphology, resistant cells were larger with a flattend elongated structure.

3.3 Glioma Cell Cultures Generated from Biopsy Samples from Beaumont Hospital

31 cell cultures were generated from biopsy samples from 44 glioma patients. 15 of the cultures had good growth. The cultures were grown in DMEM with 20% fetal calf serum, and 4% non-essential amino acids. Reasons for unsuccessful development were non-adherence to the bottom of the flask, bacterial contamination, and cell division arrest. The age range of the patient cohort was 22 to 78 years, 35.5% of the patients were between 24-49 years, and 64.5% of the patients were 50-78 years. The cohort included 31 male and 12 female patients. Malignant gliomas are more frequently found in older male patients (Paul Kleihues 1997), which is consistent with our findings. The survival time was determined in months from the point of enrollement. 26 of these patients passed away during the course of this study, patient survival did not correlate with cell growth rate (Table 3.3.3); this is not surprising as benign meningioma cultures usually grow rapidly for ten passages and then senesce (Rooprai *et al.* 2003; Ragel *et al.* 2008). Patients with a glioblastoma had an average age of 58 years and an average survival time of 16.5 months, in comparison to the lower grade tumours where the average age was lower at 40 years with more than a 2-fold increase in an averge survival time of 34 months (Fig 3.3.1).

Of the 39 biopsy samples which formed cell cultures, 25 originated from glioblastomas, 5 secondary glioblastomas, other samples included 4 grade III astrocytomas, 1 grade II astrocytoma, 1 grade III oligoastrocytoma, 1 grade III oliogodendroglioma and 2 grade II oliogodendrogliomas II (Table 3.3.2). Fig. 3.3.2 shows representative morphologies of the different cell lines. Figures 3.3.3 to 3.3.8 are images of each cell culture, showing the vast range of differences in morphology with each culture. The cultures with fast growth had a more elongated structure (Figs 3.3.3 and 3.3.4), the slow growing cell lines had more of a mixture of elongated and rounded cells (Figs 3.3.5, 3.3.6 and 3.3.7).

In total 15 cultures were established with fast growth rates; 7 with slow growth, and 18 samples were slow initially and slowed down even further after less than 10 passages (Table 3.3.2). One grade III astrocytoma sample (N070215) stopped growing completely (Table 3.3.2). A grade III oligoastrocytoma and a secondary glioblastoma (N070950 and N070311) failed to attach to the bottom of

the flask (Table 3.3.2), and one glioblastoma sample (N070948) became contaminated with bacteria (Table 3.3.2).

Figure 3.3.3 contains images of the glioma cultures with a fast growth rate N070055 has a typical oligoastrocytoma structure, with clusters of cells forming networks with each other typical of an oligodendroglioma, with a typical star shaped astrocytic cell to the right hand side of the image, these cell types had large nuclei and represent a mixed cell population of oligodendrocytes and astrocytes. The glioblastoma images (N070126, N070152, and N070859) showed mixed cell types of mostly elongated cells and some rounded cells, with small nuclei; N070126 shows a low confluency population of cells. The grade III astrocytomas (N070201 and N070788) shows typical astrocytic cellular networks between clusters of cells. Both grade II oligodendrogliomas (N070219 and N070314) have elongated cells typical of oligodendrocytes, in addition there are a few smaller more rounded shaped cells.

In figure 3.3.4 all of the images are of glioblastoma cell cultures with a fast growth rate, and show mixed cell type populations, of mostly elongated cells and rounded cells, typical of the heterogeneity of a glioblastoma. However there are differences in cell size between samples, N080501 has much larger cells with larger nuclei, while N080923 has smaller cells and small nuclei in comparison. There is also a difference in confluency beween the images, N080533 and N080869 have low confluency, while N080943 is the most confluent.

Figure 3.3.5 shows images of glioma cultures with a slow growth rate. The astrocytomas (N070229, N070237, and N070450) have a typical star-like structure of an astrocyte, however N070229 has larger cells and N070237 has a higher confluency. The secondary glioblastoma N070440 has a very low confluency in this image, showing small rounded cells, the other secondary glioblastoma N070780, has larger flattened cells, these are very different in cell types of the glioblastomas with fast growth rates from figures 3.3.3 and 3.3.4. The glioblastoma N070934 has very small cells which are a mixture of thin elongated and rounded cells, again they are very different in structure to the glioblastoma cells with fast growth in figures 3.3.3 and 3.3.4. N071155 represents a typical oligodendroglioma structure, flattened and elongated with a rounded center.

Figure 3.3.6 shows images of glioma cultures whose growth rate slowed down in culture below passage 10. The secondary glioblastoma N060893 had a

typical mixed cell type population of elongated and rounded cells, however in comparison to glioblastomas, there is a higher population of small rounded cells. The other secondary glioblastoma shown here N070701, has large flattened cells. Figure 3.3.7 also shows glioma cultures which slowed down in culture with fewer than 10 passages. These were all derived from a glioblastoma and all slowed down in culture. Figure 3.3.8 shows a glioblastoma with large flattened cells with a rounded centre, more typical of an oligodendroglioma, it also shows a secondary glioblastoma with large flattened cells. Figure 3.3.9 is an image of a grade III astrocytoma culture which stopped growing, it mainly has small rounded cells with one cell containing thin elongated processes.

Fast growing cultures originated from patients with an average survival time of 22 months, the cultures with slow growth originated from patients with an average survival time of 25 months, while the cultures which slowed down in growth (with the exception of the outlier N06893 with greater than 138 months survival) had a much lower average patient survival time of 13 months (Table 3.3.3 (a)). All biopsy samples were taken prior to treatment (Table 3.3.3 (b)).

Table 3.3.1 Brain tumour types of glioma cell cultures.

Tumour Type	Number of samples which formed cultures
Primary Glioblastoma	25 out of 26
Secondary Glioblastoma	5 out of 6
Grade III Astrocytoma	4 out of 5
Grade II Astrocytoma	1 out of 1
Grade III Oligoastrocytoma	1 out of 3
Grade III Oliogodendroglioma	1 out of 1
Grade II Oliogodendroglioma II	2 out of 2

Table 3.3.2 The take rate of glioma cultures.

Tumour Type	Fast Growth	Slow Growth	Slowed Down	Stopped Growing	Never Attached	Cont
Primary Glioblastoma (26 samples)	10	1	14	-	-	1
Secondary Glioblastoma (6 samples)	-	2	3	-	1	-
Grade III Astrocytoma (5 samples)	2	2	-	1	-	-
Grade II Astrocytoma (1 sample)	-	1	-	-	-	-
Grade III Oligoastrocytoma (3 samples)	1	-	1	-	1	-
Grade III Oligodendroglioma (1 sample)	-	1	-	-	-	-
Grade II Oligodendroglioma (2 samples)	2	-	-	-	-	-

Never attached: never attached to the bottom of the flask. Cont: contaminated.

Table 3.3.3 (a) Establishment of glioma cell cultures.

Cell Culture	Tumour Type	Growth Rate	Age	Survival Time (months)
N070055	Grade III Oligoastrocytoma	Fast	32	>38
N070126	Primary Glioblastoma (LR)	Fast	56	28
N070152	Primary Glioblastoma	Fast	52	5
N070201	Grade III Astrocytoma	Fast	42	>36
N070219	Grade II Oligodendroglioma	Fast	66	>36
N070314	Grade II Oligodendroglioma	Fast	33	>36
N070788	Grade III Astrocytoma (PR)	Fast	38	>31
N070859	Primary Glioblastoma	Fast	55	12
N070865	Primary Glioblastoma	Fast	70	5
N080501	Primary Glioblastoma	Fast	60	18
N080533	Primary Glioblastoma	Fast	55	15
N080540	Primary Glioblastoma	Fast	51	?>12
N080869	Primary Glioblastoma	Fast	54	>20
N080923	Primary Glioblastoma	Fast	61	15
N080943	Primary Glioblastoma	Fast	62	>19
N070229	Grade III Astrocytoma	Slow	22	>36
N070237	Grade III Astrocytoma (PR)	Slow	33	55
N070440	Secondary Glioblastoma (PR)	Slow	45	7
N070450	Grade II Astrocytoma	Slow	35	>34
N070780	Secondary Glioblastoma (PR)	Slow	60	4
N070934	Primary Glioblastoma	Slow	52	10
N071155	Grade III Oligodendroglioma	Slow	36	>28
N060893	Secondary Glioblastoma (PR)	Slowed down	40	>138
N060913	Primary Glioblastoma	Slowed down	67	10
N060950	Grade III Oligoastrocytoma	Slowed down	50	>30
N060978	Primary Glioblastoma	Slowed down	54	3
N061007	Primary Glioblastoma	Slowed down	75	1
N061092	Primary Glioblastoma	Slowed down	78	6
N070454*	Primary Glioblastoma	Slowed down	73	3
N070701	Secondary Glioblastoma (PR)	Slowed down	39	>56
N070293	Primary Glioblastoma	Slowed down	38	>36
N071026	Primary Glioblastoma	Slowed down	46	10
N071057	Primary Glioblastoma	Slowed down	73	7
N071060	Primary Glioblastoma	Slowed down	58	>29
N071144	Primary Glioblastoma	Slowed down	53	8
N071271	Primary Glioblastoma	Slowed down	59	11
N080558	Primary Glioblastoma	Slowed down	64	5
N080749	Primary Glioblastoma	Slowed down	74	4
N080805	Primary Glioblastoma	Slowed down	75	6
N081185	Secondary Glioblastoma (PR)	Slowed down	55	4
N070215	Grade III Astrocytoma (PR)	Stopped growing	58	>36
N070950	Grade III Oligoastrocytoma	Cells failed to attach to flask	52	14
N070311	Secondary Glioblastoma	Cells failed to attach to flask	57	6
N070948	Primary Glioblastoma	Bacterial contamination	51	5

* Only cell line which initially had fast growth and then slowed down.

PR: Previous resection. LR: Later resection. ?: patient emigrated and contact details were lost

Table 3.3.3 (b) Patient treatment during the course of the study.

Sample Number	Tumour Type	Radiation Treatment	Temozolomide	Gliadel	PCV
N070126	Primary Glioblastoma	60Gy (30fr)	Yes	Yes	No
N070152	Primary Glioblastoma	56Gy (28fr)	Yes	No	No
N070201	Grade III Astrocytoma	55Gy (30fr)	No	No	Yes
N070788	Grade III Astrocytoma	Yes amt?	No	No	No
N070859	Primary Glioblastoma	45Gy (20fr)	Yes	No	No
N070865	Primary Glioblastoma	60Gy (30fr)	Yes	No	No
N080501	Primary Glioblastoma	Unknown	Unknown	No	No
N080533	Primary Glioblastoma	Yes amt?	Yes	No	No
N080540	Primary Glioblastoma	58Gy (28fr)	Yes	No	No
N080869	Primary Glioblastoma	60Gy (30fr)	Yes	No	No
N080923	Primary Glioblastoma	60Gy (30fr)	Yes	No	No
N080943	Primary Glioblastoma	58Gy (29fr)	Yes	No	No
N070229	Grade III Astrocytoma	Unknown	Unknown	No	No
N070237	Grade III Astrocytoma	55Gy (30fr)	No	No	No
N070440	Secondary Glioblastoma	No	No	yes	No
N070780	Glioblastoma	No	No	No	No
N070934	Primary Glioblastoma	56Gy (28fr)	Yes	Yes	No
N060893	Secondary Glioblastoma	60Gy (30fr)	Yes	No	No
N060913	Primary Glioblastoma	66Gy (30fr)	No	No	No
N060978	Primary Glioblastoma	20 Gy (5fr)	No	No	No
N061007	Primary Glioblastoma	No	No	No	No
N061092	Primary Glioblastoma	45Gy (20Fr)	No	No	No
N070454	Primary Glioblastoma	40Gy (60fr)	No	No	No
N070701	Secondary Glioblastoma	60Gy (30fr)	Yes	No	No
N070293	Primary Glioblastoma	60Gy (30fr)	Yes	No	No
N071026	Primary Glioblastoma	Unknown	Unknown	No	No
N071057	Primary Glioblastoma	Unknown	Unknown	No	No
N071060	Primary Glioblastoma	30Gy (60Fr)	Yes	No	No
N071144	Primary Glioblastoma	Unknown	Unknown	No	No
N07-1271	Primary Glioblastoma	60Gy (30fr)	Yes	No	No
N080558	Primary Glioblastoma	30Gy (30Fr)	Yes	No	No
N080749	Primary Glioblastoma	Unknown	Unknown	No	No
N080805	Primary Glioblastoma	Unknown	Unknown	No	No
N081185	Secondary Glioblastoma	No	No	No	No
N070215	Grade III Astrocytoma	No	Yes	No	No
N070311	Secondary Glioblastoma	55Gy (30fr)	Yes	No	No

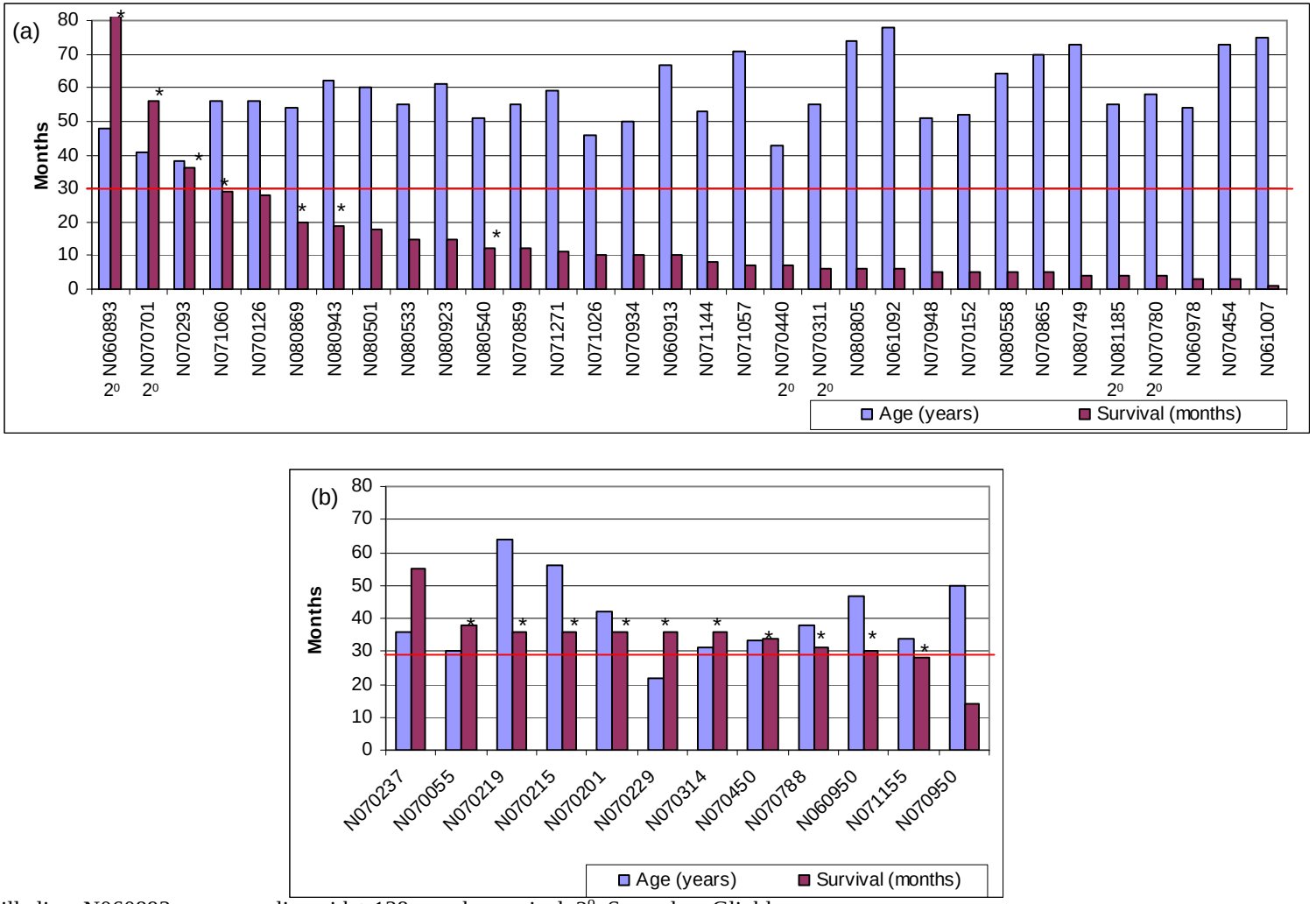

*: Patient still alive. N060893 was an outlier with >138 months survival. 2^{o}: Secondary Glioblastoma.

Fig 3.3.1 (a) Survival and age of patients with a glioblastoma (b) survival and age of patients with a lower grade glioma

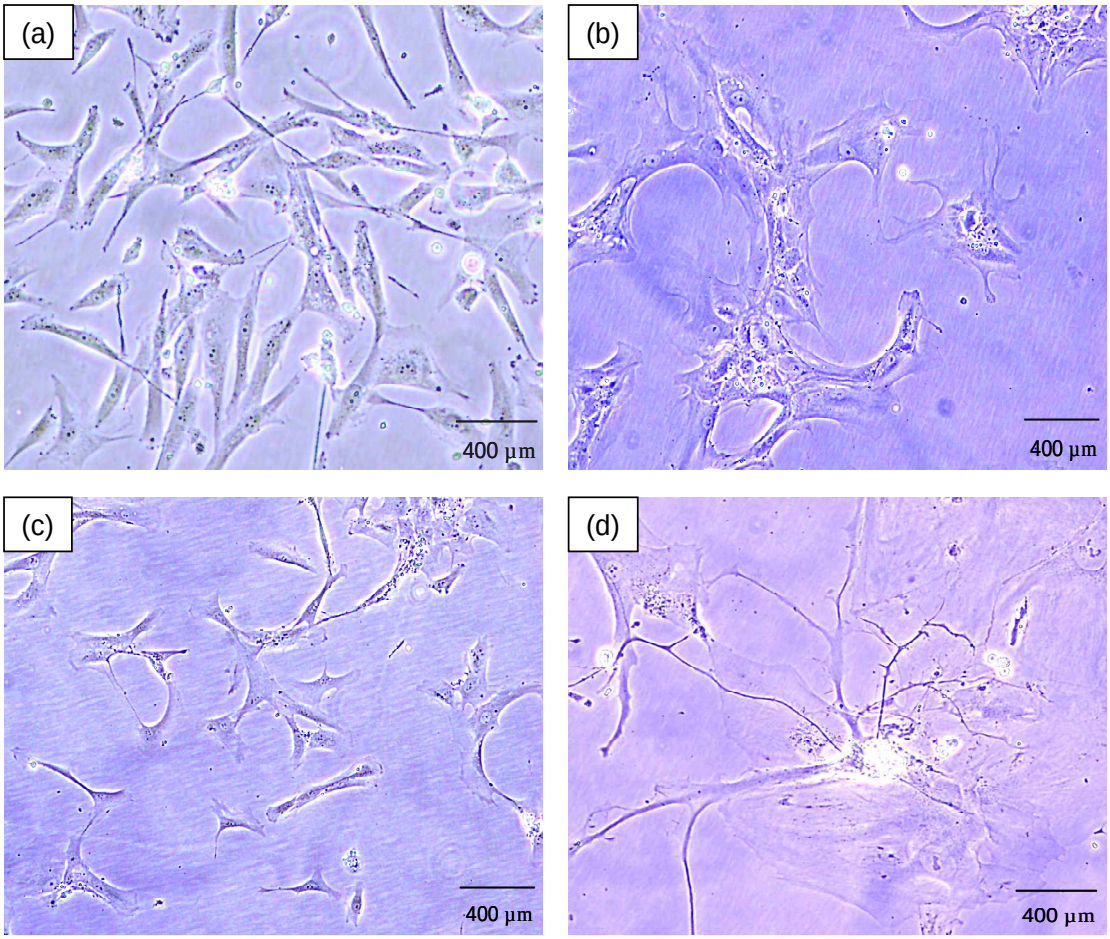

Fig. 3.3.2 Images of glioma cell cultures. (a) Glioblastoma, (b) Grade III Oligoastrocytoma (c) Grade III Astrocytoma (d) Grade III Oligodendroglioma.

N070055 (Grade III Oligoastrocytoma)

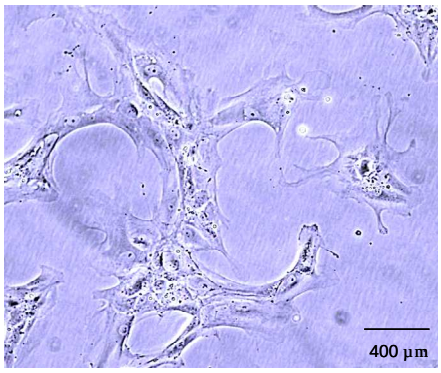

N070126 (Primary Glioblastoma)

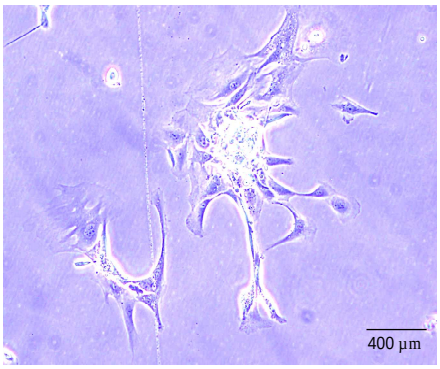

N070152 (Primary Glioblastoma)

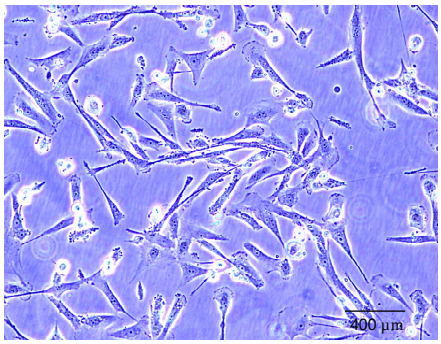

N070201 (Grade III Astrocytoma)

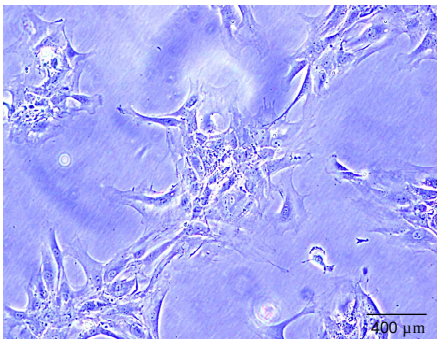

N070219 (Grade II Oligodendroglioma)

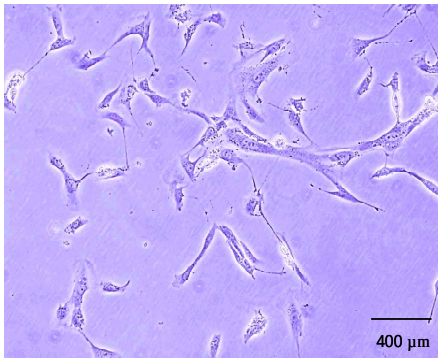

N070314 (Grade II Oligodendroglioma)

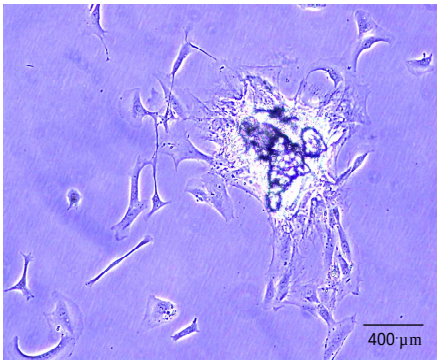

N070788 (Grade III Astrocytoma)

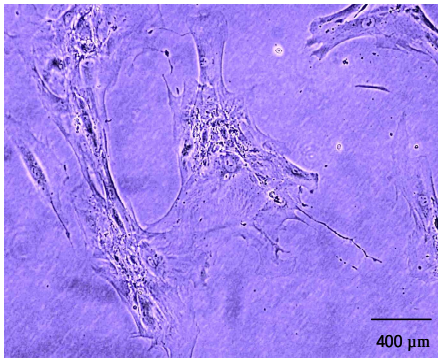

N070859 (Primary Glioblastoma)

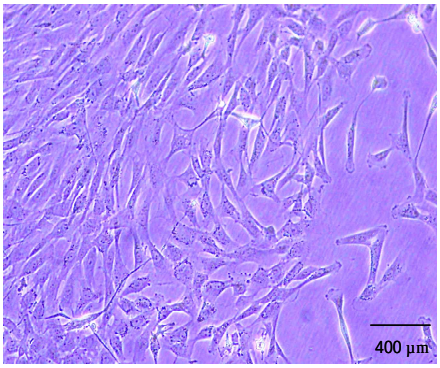

Fig. 3.3.3 Images (10x) of glioma cell cultures with fast growth rate.

N070865 (Primary Glioblastoma)

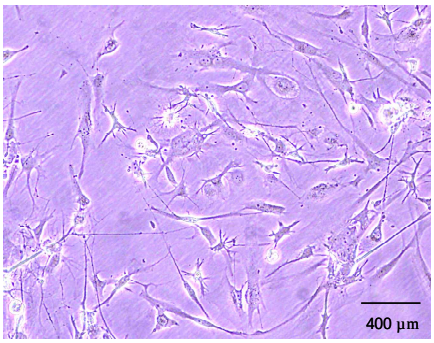

N080501 (Primary Glioblastoma)

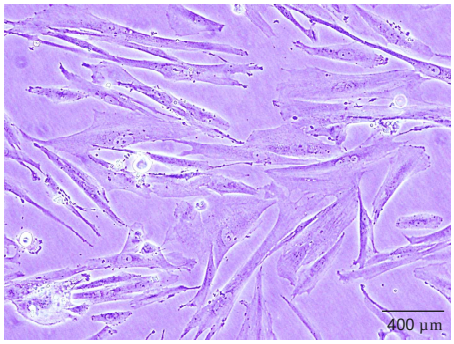

N080533 (Primary Glioblastoma)

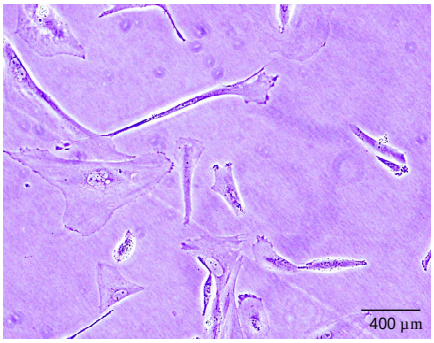

N080540 (Primary Glioblastoma)

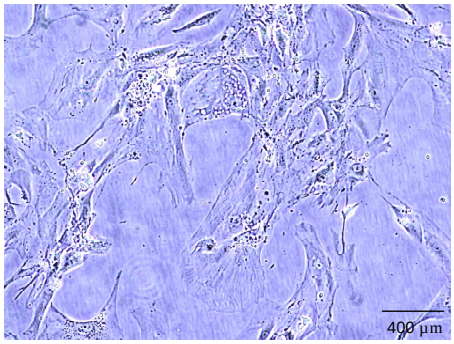

N080869 (Primary Glioblastoma)

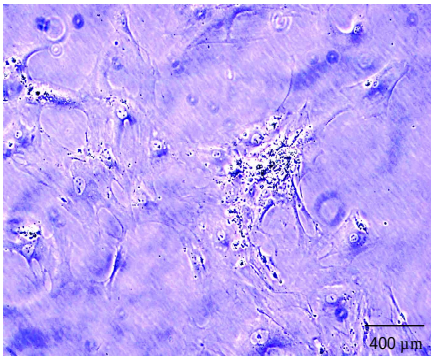

N080923 (Primary Glioblastoma)

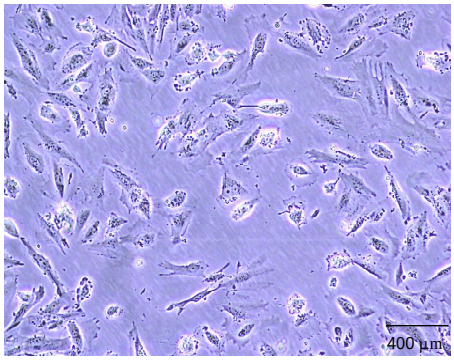

N080943 (Primary Glioblastoma)

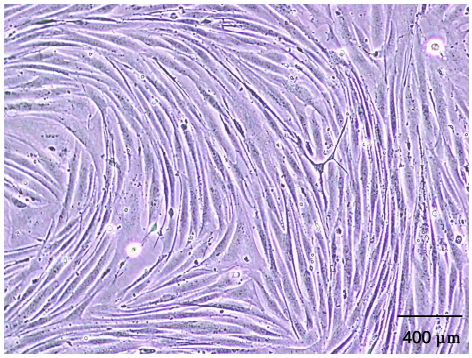

Fig. 3.3.4 Images (10x) of glioma cell cultures with fast growth rate.

N070229 (Grade III Astrocytoma)

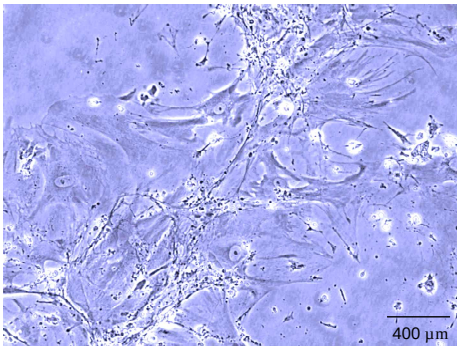

N070237 (Grade III Astrocytoma)

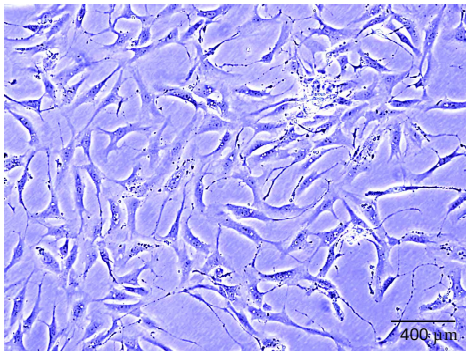

N070440 (Secondary Glioblastoma)

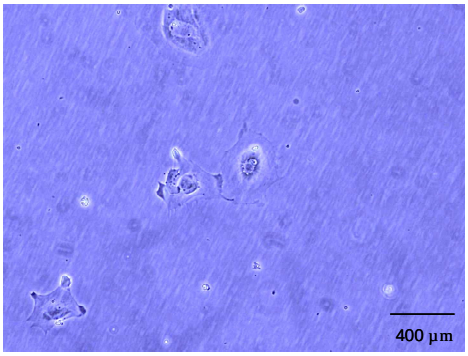

N070450 (Grade II Astrocytoma)

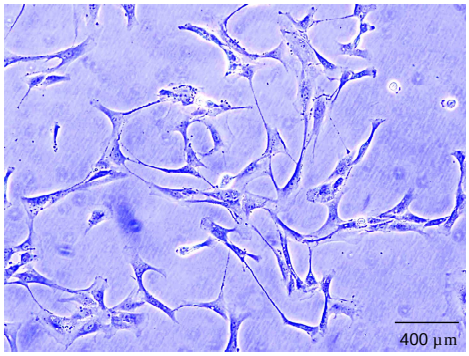

N070780 (Secondary Glioblastoma)

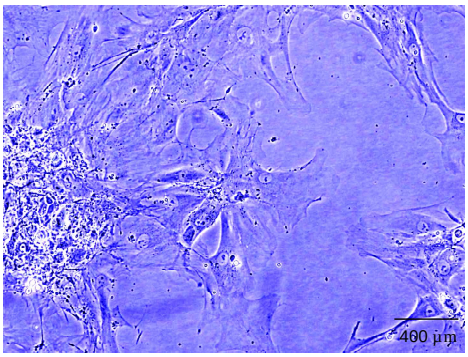

N070934 (Primary Glioblastoma)

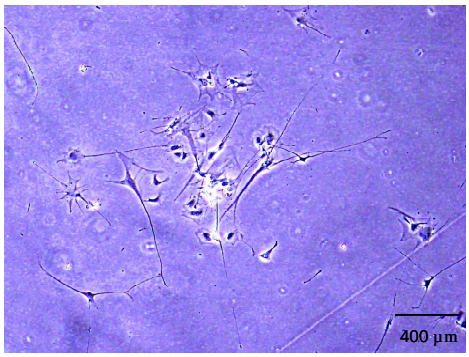

N071155 (Grade III Oligodendroglioma)

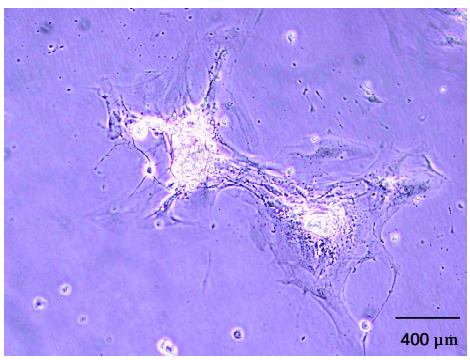

Fig. 3.3.5 Images (10x) of glioma cell cultures with slow growth rate.

N060893 (Secondary Glioblastoma)

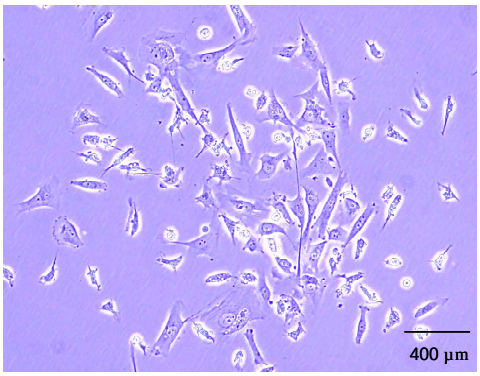

N060913 (Primary Glioblastoma)

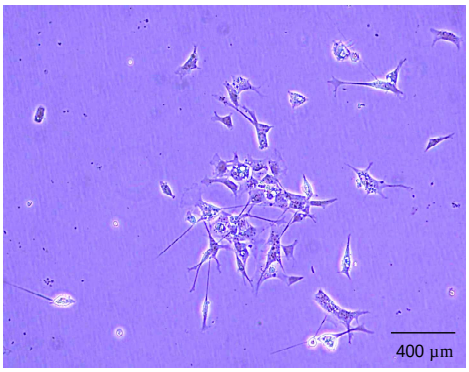

N060950 (Grade III Oligoastrocytoma)

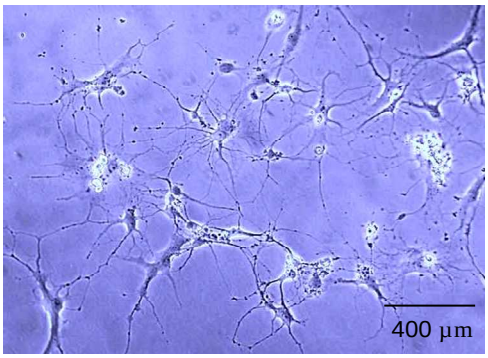

N060978 (Primary Glioblastoma)

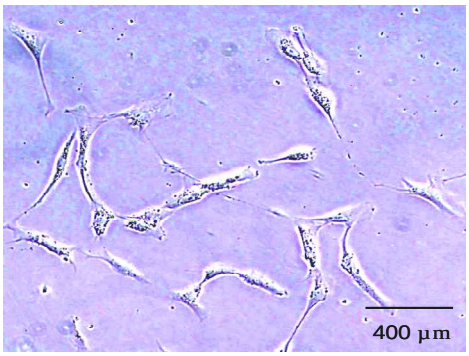

N061007 (Primary Glioblastoma)

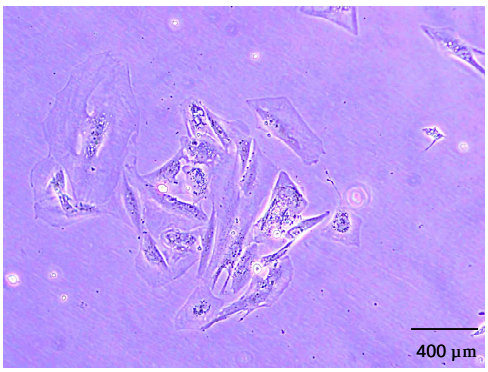

N061092 (Primary Glioblastoma)

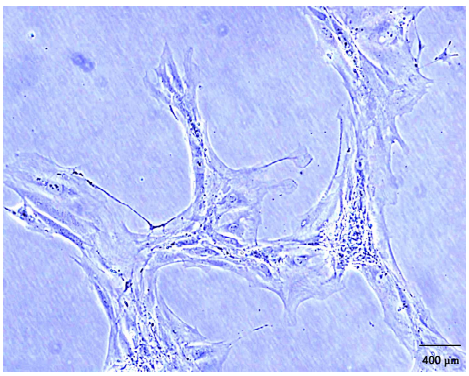

N060454 (Primary Glioblastoma)

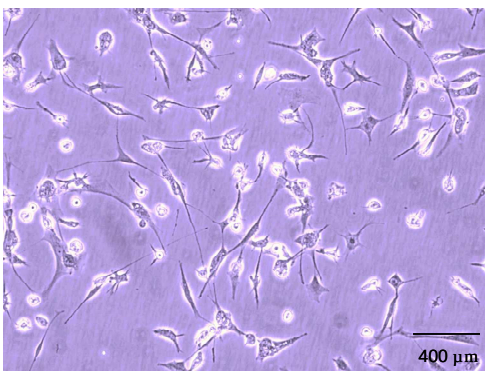

N070701 (Secondary Glioblastoma)

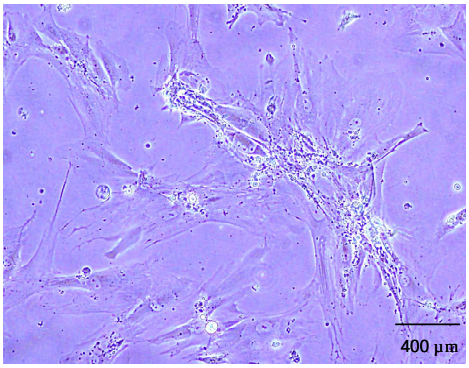

Fig. 3.3.6 Images (10x) of glioma cell cultures which slowed down in growth.

N060293 (Primary Glioblastoma)

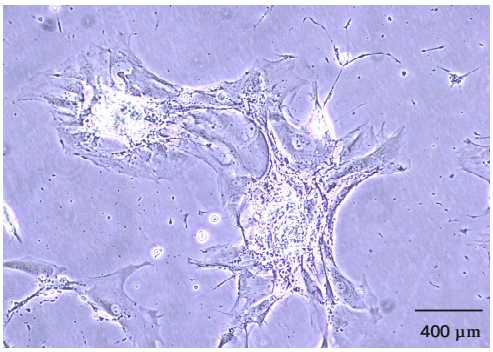

N061026 (Primary Glioblastoma)

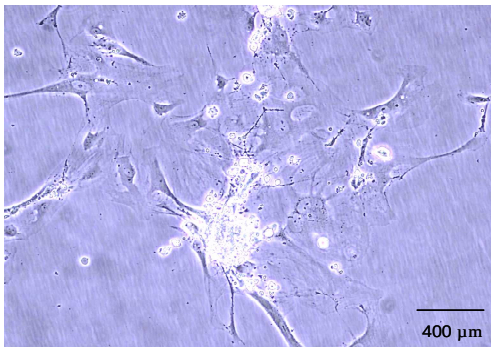

N061057 (Primary Glioblastoma)

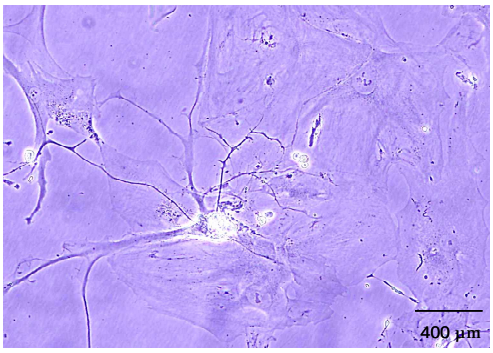

N061060 (Primary Glioblastoma)

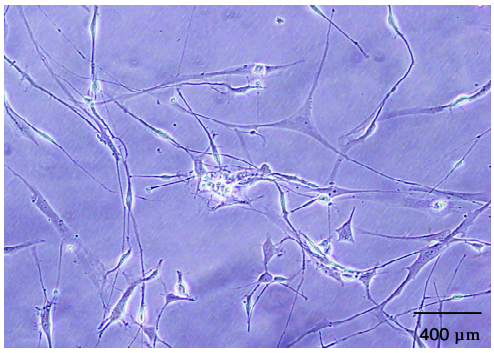

N071144 (Primary Glioblastoma)

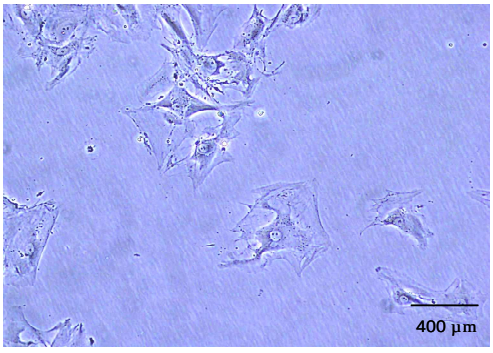

N071271 (Primary Glioblastoma)

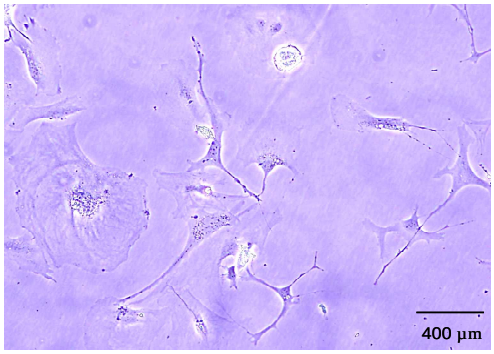

N080558 (Primary Glioblastoma)

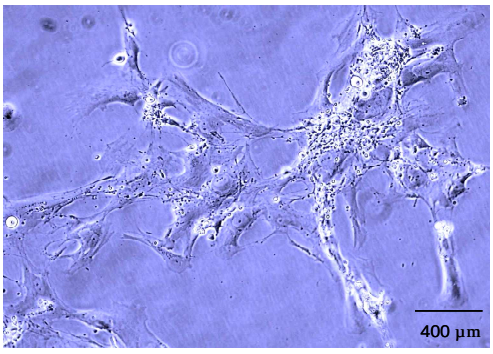

N080749 (Primary Glioblastoma)

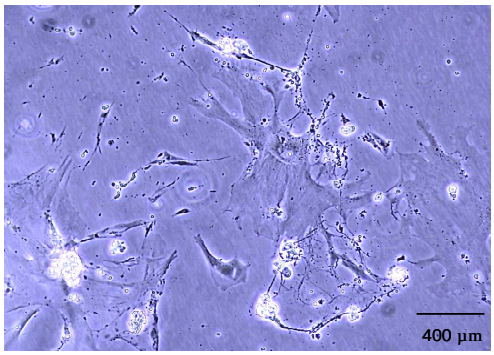

Fig. 3.3.7 Images (10x) of glioma cell cultures which slowed down in growth.

N080805 (Primary Glioblastoma)

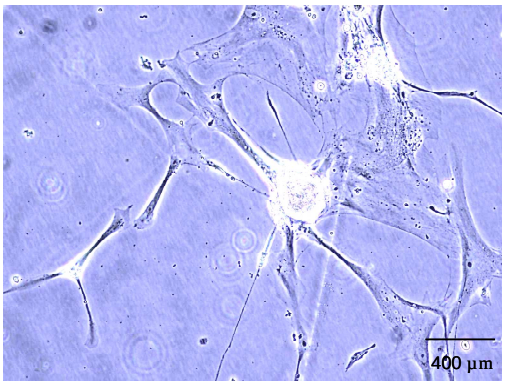

N081185 (Secondary Glioblastoma)

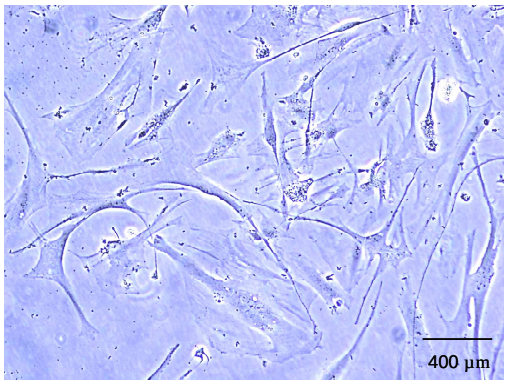

Fig. 3.3.8 Image (10x) of glioma cell cultures which slowed down in growth.

N070215 (Grade III Astrocytoma)

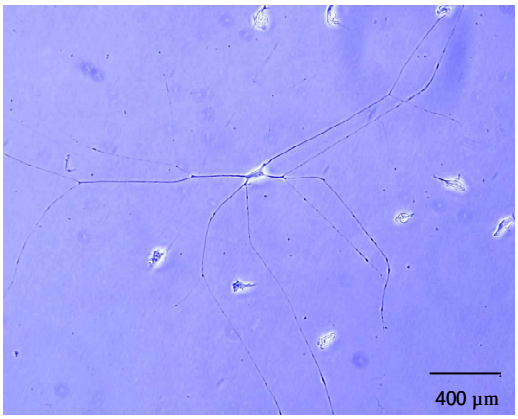

Fig. 3.3.9 Image (10x) of glioma cell culture which stopped growing.

3.3.1 Characterization of Newly Developed Glioma Cell Cultures

The newly developed glioma cell cultures were characterised in relation to invasion, proliferation, sensitivity to TKIs and chemotherapeutic drugs, and protein expression.

3.3.1.1 Invasion and Proliferation

Invasion and proliferation was tested with my supervisor, Dr. Verena Amberger-Murphy. The 3D spheroid collagen invasion assay was used because it is a better model for tumour invasion *in vivo*. One cell culture was additionally tested in the Boyden Chamber assay, which resulted in similar invasion activity. 65% of all cell cultures tested were invasive. Out of 19 glioblastomas, 4 were non-invasive, and 15 were invasive, 5 cell cultures showed invasive behaviour with biospheres produced from segments of the biopsy sample, the other cell cultures showed invasive behaviour from spheroids produced from the cell cultures (see section 2.8). Within the lower grade tumours invasive behaviour was independent of the tumour type and grade of malignancy. The overall invasion rate per day ranged from 5.23 µm to 50.69 µm (Fig. 3.3.10).

Proliferation activity was determined by measuring the doubling time, which ranged from 37.3 to more than 168 hours (Figs. 3.3.11 and 3.3.12). Again proliferation rate was independent of tumour type and grade. Invasion did not correlate with proliferation rate in glioblastomas or the lower grade tumours (Fig. 3.3.13). The ICC for GFAP and Nestin with 17 of the cultures was carried out a Ph.D student, Rachel Howley. ICC of GFAP and nestin was correlated with doubling time for the cultures, a low amount of GFAP was detected overall, there was an increase in nestin expression with slower proliferating cultures (Fig. 3.3.14).

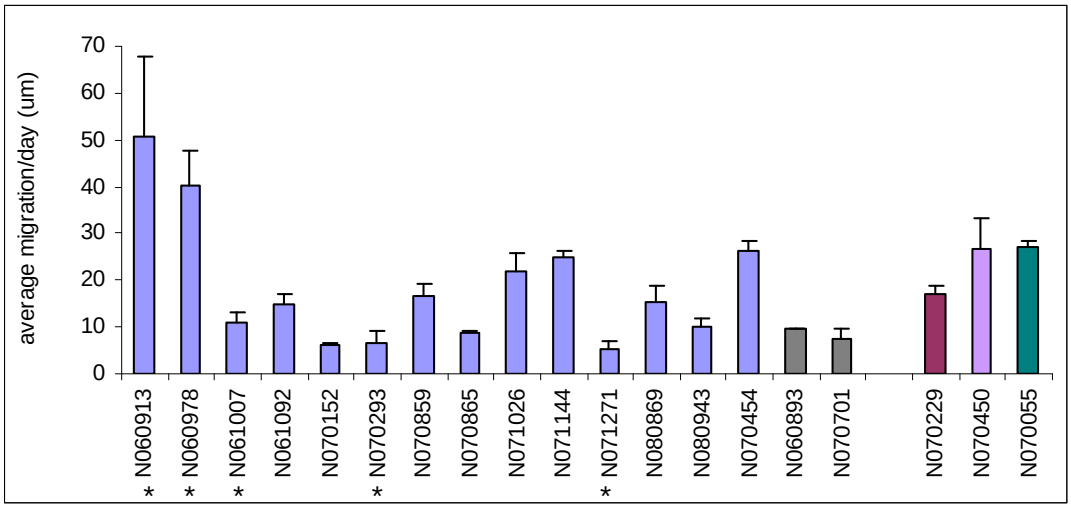

Glioblastomas, Secondary glioblastoma, Grade III Astrocytoma,

Grade II Astrocytoma, Grade III Oligoastrocytoma. * Biosphere

Fig. 3.3.10 Invasion rate per day for 19 invasive cultures. Data represents 3 individual biological assays. Standard deviations were generated from Microsoft excel software.

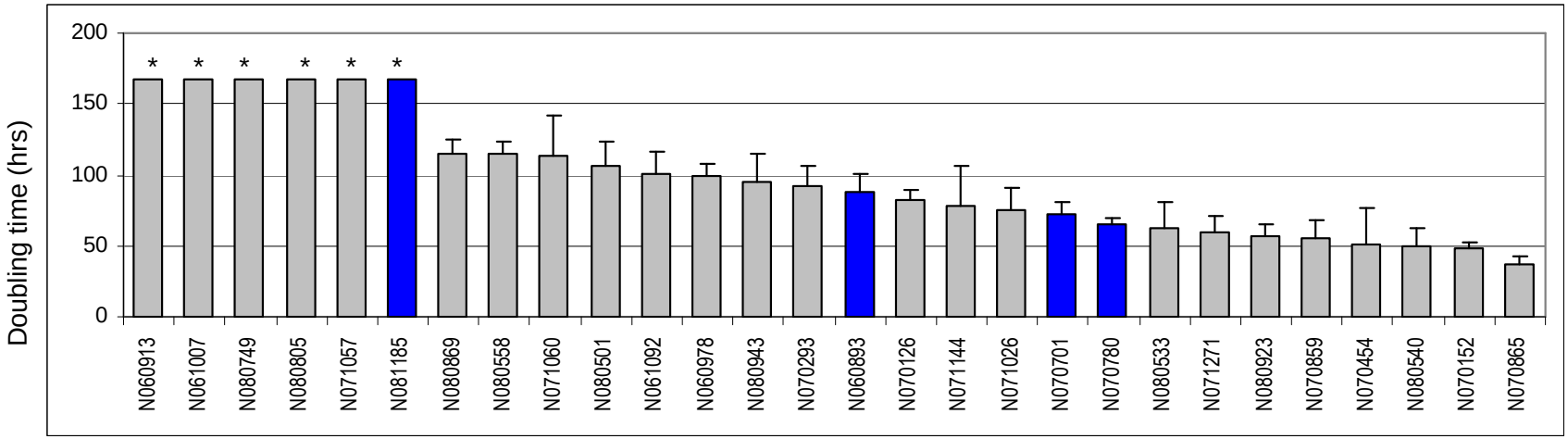

*: Doubling time greater than 168 hours. Blue bars represent secondary glioblastomas.

Fig. 3.3.11 Doubling time of glioblastoma cell cultures measured in hours. Data represents 3 individual biological assays. Standard deviations were generated from Microsoft excel software.

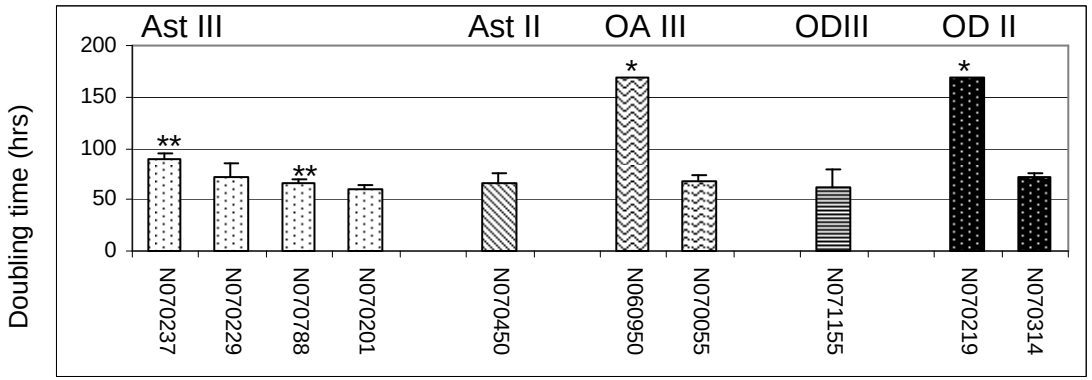

*: Doubling time greater than 168 hours. ** repeat astrocytoma III.

Fig. 3.3.12 Doubling time of cell cultures derived from other tumour types measured in hours. Data represents 3 individual biological assays. Standard deviations were generated from Microsoft excel software. A: astrocytoma, OA: grade II oligoastrocytoma, OD: oligodendroglioma

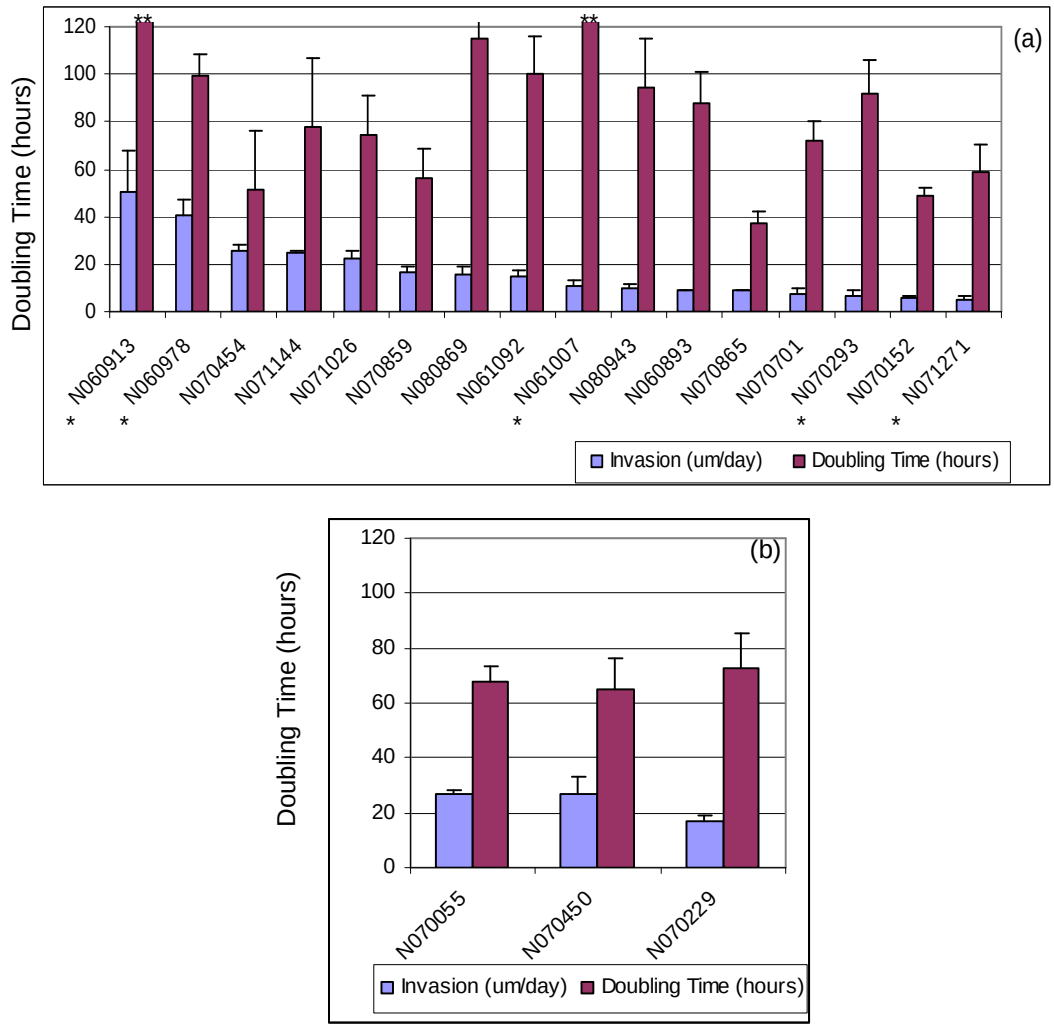

Biosphere, ** Doubling Time greater than 168 hours.

Figure 3.3.13 The invasion and proliferation rate of glioblastoma cultures (a) and the invasive lower grade cultures, a grade III oligoastrocytoma (N070055), a grade II astrocytoma (N070450), and a grade III astrocytoma (N070229) (b). Invasion was measured in micrometres per day, doubling time was measured in hours. Data represents 3 individual biological assays. Standard deviations were generated from Microsoft Excel software.

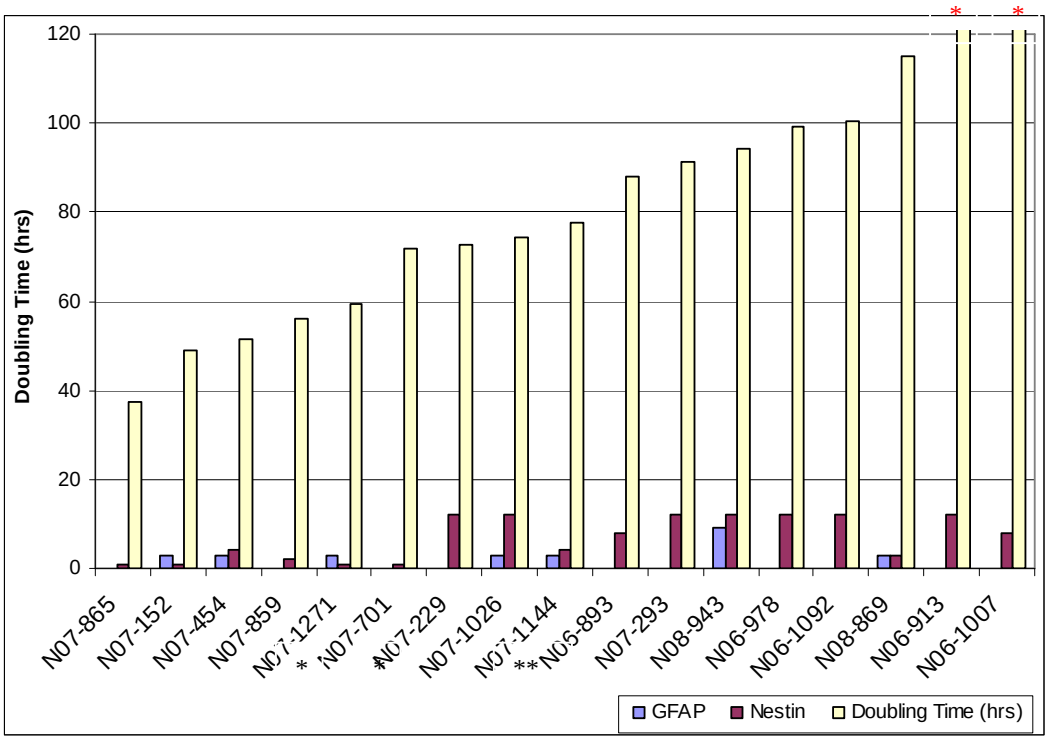

*: Grade III Astrocytoma. **: Secondary GLioblastoma. *: doubling time greater than 168 hours.

Figure 3.3.14 Doubling time of cultures tested for ICC of GFAP and nestin. GFAP and nestin were graded 1 to 12.

3.3.1.2 Sensitivity to Tyrosine Kinase Inhibitors

31 glioma cell cultures were tested for sensitivity to three TKIs, erlotinib, gefitinib, and imatinib. Using a cut-off concentration based on data published in the literature each cell culture was classified as a responder or non-responder to the TKIs (Table 3.3.4). The cut off concentration for Erlotinib was 10 µM based on Mellinghoff *et al*, (Mellinghoff *et al.* 2005) and Zerbe *et al*, who reported a concentration of erlotinib of up to 9 µM found in tumours of an animal model (Zerbe *et al.* 2008). The cut off concentration for gefitinib was 20 µM, based on Hofer and Frei, (Hofer and Frei 2007); they found gefitinib concentrations of up to 24 µM in human glioblastoma tissue. Cemeus *et al*, (Cemeus *et al.* 2008) classified glioblastoma cell lines as responsive, if they were inhibited by gefitinib at a concentration of 20 µM. The cut off concentration for imatinib was 20 µM which is consistent with data published by Servidei *et al*, (Servidei *et al.* 2006).

8 out of 23 glioblastomas, 1 out of 5 astrocytomas III, and 1 out of 2 oligoastrocytomas III were responsive to erlotinib (Table 3.3.5). Responders to gefitinib included 13 out of 23 glioblastomas (Table 3.3.6). 6 out of 23 glioblastomas, 2 out of 5 astrocytomas, and 1 out of 2 oligoastrocytomas III, and the only oligodendroglioma II responded to imatinib (Table 3.3.6). Overall there were more imatinib responders found in astrocytomas and mixed tumours than in glioblastoma.

Figure 3.4.4 represents the glioblastoma responder profile. 7 glioblastomas responded to 2 TKIs. One grade III astrocytoma responded to both erlotinib and imatinib (N070201), and one grade III oligoastrocytoma (N070055) responded to both erlotinib and imatinib (Tables 3.3.7 to 3.3.9). Only one secondary glioblastoma culture was sensitive to all three TKIs tested (N070701) (Tables 3.3.7 to 3.3.9).

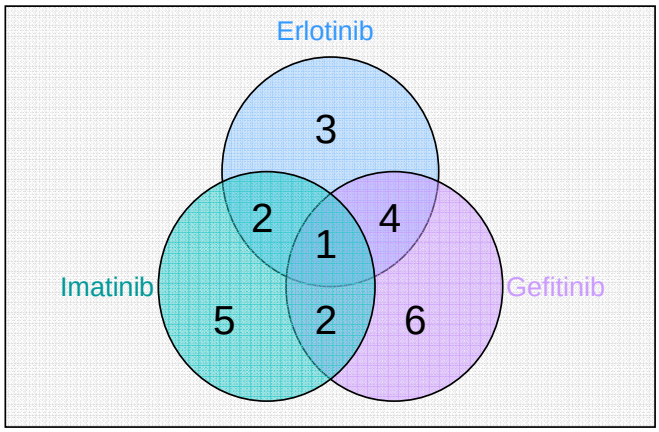

Fig. 3.3.15 Glioblastoma cultures which responded to the tyrosine kinase inhibitors, erlotinib, gefitinib and imatinib.

Table 3.3.4 Classification of glioma cultures as responders and non-responders to erlotinib, gefitinib and imatinib.

Cell Culture	Tumour Type	Erlotinib	Gefitinib	Imatinib
N070701	Secondary Glioblastoma	+	+	+
N060978	Primary Glioblastoma	+	+	-
N070152	Primary Glioblastoma	+	+	-
N071144	Primary Glioblastoma	+	+	-
N080923	Primary Glioblastoma	+	+	-
N080540	Primary Glioblastoma	-	+	+
N071057	Primary Glioblastoma	-	+	+
N070055	Grade III Oligoastrocytoma	+	-	+
N070201	Grade III Astrocytoma	+	-	+
N060913	Primary Glioblastoma	+	-	-
N061007	Primary Glioblastoma	+	-	-
N061092	Glioblastoma	+	-	-
N060893	Secondary Glioblastoma	-	+	-
N070126	Primary Glioblastoma	-	+	-
N070293	Primary Glioblastoma	-	+	-
N071271	Primary Glioblastoma	-	+	-
N080501	Primary Glioblastoma	-	+	-
N080533	Primary Glioblastoma	-	+	-
N070454	Primary Glioblastoma	-	-	+
N071026	Primary Glioblastoma	-	-	+
N080869	Primary Glioblastoma	-	-	+
N070450	Grade II Astrocytoma	-	-	+
N070314	Grade II Oligodendroglioma	-	-	+
N070788	Grade III Astrocytoma	-	-	-
N070859	Primary Glioblastoma	-	-	-
N070865	Primary Glioblastoma	-	-	-
N080558	Primary Glioblastoma	-	-	-
N080943	Primary Glioblastoma	-	-	-
N070229	Grade III Astrocytoma	-	-	-
N070237	Grade III Astrocytoma	-	-	-
N060950	Grade III Oligoastrocytoma	-	-	-

Responder: + Non-responder:-

Table 3.3.5 IC_{50} values of glioma cell cultures responsive to erlotinib.

Cell Culture	Tumour Type	Erlotinib (μM)
N070152	Glioblastoma	6.5 ± 0.9 *
N060913	Glioblastoma	7.2 ± 0.2 *
N080923	Glioblastoma	7.2 ± 0.5
N070701	Secondary Glioblastoma	7.9 ± 0.7
N061007	Glioblastoma	9.1 ± 1.2 *
N071144	Glioblastoma	9.3 ± 0.5
N060978	Glioblastoma	9.5 ± 1.4
N061092	Glioblastoma	9.3 ± 1.4
N070201	Grade III Astrocytoma	8.4 ± 0.1 *
N070055	Grade III Oligoastrocytoma	9.3 ± 0.7

Standard deviations are from 3 biologically individual assays. *: 2 biologically individual assays.

Table 3.3.6 IC_{50} values of glioma cell cultures responsive to gefitinib.

Cell Culture	Tumour Type	Gefitinib (μM)
N080923	Primary Glioblastoma	15.2 ± 0.7
N071271	Primary Glioblastoma	16.7 ± 1.3
N080533	Primary Glioblastoma	16.7 ± 1.1
N070701	Secondary Glioblastoma	16.7 ± 1.1
N060893	Secondary Glioblastoma	16.8 ± 1.6 *
N080501	Primary Glioblastoma	16.9 ± 0.9
N070152	Primary Glioblastoma	17.0 ± 0.9
N060978	Primary Glioblastoma	17.2 ± 2 *
N070293	Primary Glioblastoma	18.3 ± 2.2
N080540	Primary Glioblastoma	18.5 ± 1.8
N070126	Primary Glioblastoma	20.0 ± 1.1 *
N071144	Primary Glioblastoma	19.5 ± 2 *
N071057	Primary Glioblastoma	17.2 ± 0.9 *

Standard deviations are from 3 biologically individual assays. *: 2 biologically individual assays.

Table 3.3.7 IC_{50} values of glioma cell cultures responsive to imatinib.

Cell Culture	Tumour Type	Imatinib (μM)
N080869	Primary Glioblastoma	14.0 ± 4 *
N070701	Secondary Glioblastoma	14.4 ± 0.7
N080540	Primary Glioblastoma	15.8 ± 1.7
N070454	Primary Glioblastoma	16.7 ± 1.5 *
N071026	Primary Glioblastoma	19.6 ± 2.4 *
N071057	Primary Glioblastoma	14.0 ± 1.7 *
N070201	Grade III Astrocytoma	20.0 ± 0.7 *
N070450	Grade II Astrocytoma	15.8 ± 3.2 *
N070055	Grade III Oligoastrocytoma	18.0 ± 0.5
N070314	Grade II Oligodendroglioma	19.6 ± 1 *

Standard deviations are from 3 biologically individual assays. *: 2 biologically individual assays.

Overall, the IC_{50} values for each drug were relatively high and no cell culture showed particular sensitivity to any TKI.

3.3.1.3 Sensitivity to Chemotherapeutic Drugs

The same cell cohort was also tested for sensitivity to the chemotherapeutic drugs docetaxel and temozolomide. The IC_{50} values for docetaxel ranged in glioblastomas from 0.4 nM to 25.4 nM and the astrocytomas from 1.4 nM to 59.5 nM; both grade III oligoastrocytomas had an IC_{50} of 2.7 nM, and for grade II oligodendroglioma the IC_{50} for docetaxel was 24.8 nM. The IC_{50} values clearly demonstrate that sensitivity to docetaxel is not correlated with tumour type and grade. 11 out of 23 glioblastomas and 1 grade III astrocytoma had an IC_{50} <2 nM for docetaxel (Table 3.3.8, Fig. 3.3.15) and were responsive to one, two or three TKIs; this would indicate there might be a benefit from combing docetaxel and TKIs.

The IC_{50} values of temozolomide also did not correlate with tumour type and grade. They ranged in glioblastoma from 198.3 µM to 1146 µM, in astrocytoma from 437.8 µM to 1037.8 µM, in grade III oligoastrocytomas from 417.2 µM to 852.4 µM, and the IC_{50} value in the grade II oligodendroglioma was 939.9 µM (Table 3.3.9, Fig. 3.3.16).

Table 3.3.8 Docetaxel IC_{50} values of glioma Cultures.

Cell Culture	Tumour Type	Docetaxel (nM)
N080923	Primary Glioblastoma	0.4 ± 0.05 *
N070152	Primary Glioblastoma	0.5 ± 0.0
N071271	Primary Glioblastoma	0.6 ± 0.02 *
N080540	Primary Glioblastoma	0.7 ± 0.01 *
N070454	Primary Glioblastoma	0.9 ± 0.2
N060978	Primary Glioblastoma	1.0 ± 0.4
N070701	Secondary Glioblastoma	1.1 ± 0.4
N061007	Primary Glioblastoma	1.2 **
N060893	Secondary Glioblastoma	1.6 ± 0.7
N070201	Grade III Astrocytoma	1.4 ± 0.1
N061092	Primary Glioblastoma	1.5 ± 0.4
N070126	Primary Glioblastoma	1.4 ± 0.1
N070859	Primary Glioblastoma	2.1 ± 0.1
N060950	Grade III Oligoastrocytoma	2.7 ± 0.6
N080533	Primary Glioblastoma	2.6 ± 1.6
N070055	Grade III Oligoastrocytoma	2.7 ± 0.2
N070865	Primary Glioblastoma	5.0 ± 1.7
N060913	Primary Glioblastoma	5.6 ± 3.1
N080501	Primary Glioblastoma	5.8 ± 0.5 *
N071144	Primary Glioblastoma	6.4 ± 1.5
N070450	Grade II Astrocytoma	8.3 ± 2.2
N080943	Primary Glioblastoma	9.0 ± 1.2
N070229	Grade III Astrocytoma	9.4 ± 1 *
N070293	Primary Glioblastoma	13.0 ± 5.2
N070237	Grade III Astrocytoma	16.4 ± 1
N070314	Grade II Oligodendroglioma	24.8 *
N080869	Primary Glioblastoma	19.0 ± 5.2 *
N071026	Primary Glioblastoma	23.2 ± 4 *
N080558	Primary Glioblastoma	25.4 ± 4.3
N070788	Grade III Astrocytoma	**59.5 ± 3.5**

Standard deviations represent biological duplicate results calculated in Microsoft Excel.* Biologically triplicate results. ** Result of a single assay. **N070788 is an outlier not included in Fig. 3.3.16.**

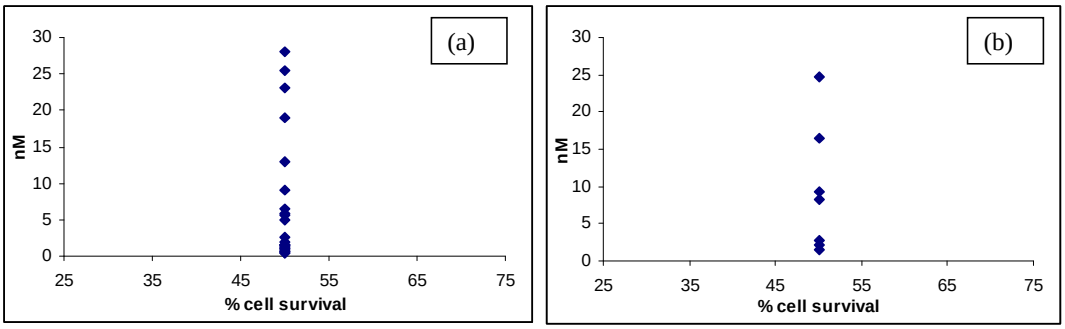

Fig. 3.3.16 The IC_{50} values of docetaxel in glioblastomas (a), and in other glioma cell cultures (b).

Table 3.3.9 Temozolomide IC_{50} values of glioma cell cultures.

Cell Culture	Tumour Type	Temozolomide (μM)
N070126	Primary Glioblastoma	198.3 ± 10.8 *
N080923	Primary Glioblastoma	322.9 ± 66.9
N071271	Primary Glioblastoma	372.4 ± 44.8
N070055	Grade III Oligoastrocytoma	417.2 ± 65.4 *
N070201	Grade III Astrocytoma	437.8 ± 22 *
N070152	Primary Glioblastoma	497.0 ± 98.4 *
N070859	Primary Glioblastoma	502.2 ± 91.2 *
N070788	Grade III Astrocytoma	515.0 ± 0 *
N080805	Primary Glioblastoma	515.0 **
N061007	Primary Glioblastoma	566.6 **
N080540	Primary Glioblastoma	609.3 ± 90.7
N061092	Primary Glioblastoma	618.0 ± 0 *
N070454	Primary Glioblastoma	638.7 ± 284.3 *
N071144	Primary Glioblastoma	638.7 ± 126.7
N070865	Primary Glioblastoma	643.8 ± 182.3 *
N080501	Primary Glioblastoma	700.5 ± 116.4
N070237	Grade III Astrocytoma	713.4 ± 114.3
N080533	Primary Glioblastoma	738.1 ± 136.5
N071026	Primary Glioblastoma	738.1 ± 59.2
N080869	Primary Glioblastoma	763.8 ± 147.8
N070701	Secondary Glioblastoma	772.6 ± 67
N071057	Primary Glioblastoma	793.2 ± 320.4 *
N060978	Primary Glioblastoma	810.2 ± 73.1
N060950	Grade III Oligoastrocytoma	852.4 ± 18 *
N080943	Primary Glioblastoma	877.3 ± 127.7
N070450	Grade II Astrocytoma	888.5 ± 346.1*
N070314	Grade II Oligodendroglioma	939.9 ± 127.2 *
N080558	Primary Glioblastoma	940.5 ± 95.8
N070293	Primary Glioblastoma	1004.4 ± 164.3
N070229	Grade III Astrocytoma	1037.8 ± 25.2 **
N060913	Primary Glioblastoma	1133.1 ± 145.8 *
N060893	Secondary Glioblastoma	1146.0 ± 91.2 *

Data represents biologically triplicate assays. * Standard deviations are from biologically duplicate assays. ** result of a single assay.

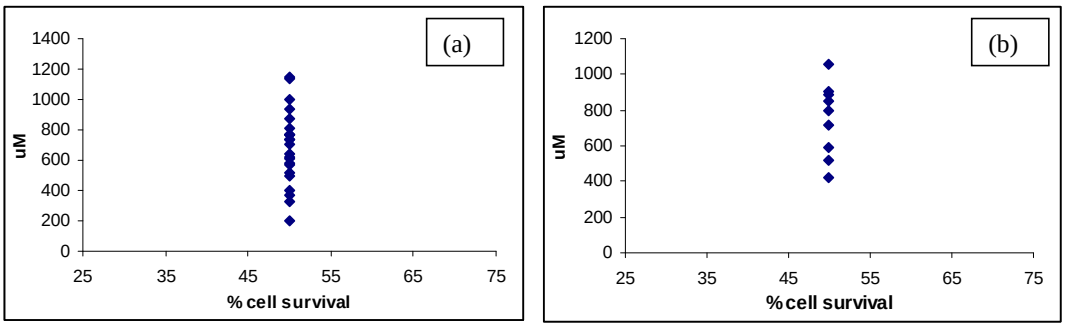

Fig. 3.3.17 The IC_{50} values of temozolomide in glioblastomas (a), and in other glioma cell cultures (b).

3.3.1.4 Normal Human Astrocytes

To evaluate the drug effects on normal cells, we tested cell proliferation of normal human astrocytes (NHAs) in the presence of TKIs and the chemotherapeutic drugs. NHAs were not responsive to erlotinib; however, they had IC_{50} values of 7.8 µM for gefitinib, and 16.9 µM for imatinib. We also found that the NHAs were not sensitive to chemotherapeutic drugs. IC_{50} values were 1228.4 µM for temozolomide and >124 nM for docetaxel. The NHAs had higher IC_{50} values for both chemotherapeutic compounds than any glioma cell culture.

3.3.1.5 Accumulation of Gefitinib in Glioma Cells

To test the accumulation of gefitinib in tumour cells we selected 4 glioma cell cultures according to their responsiveness to gefitinib: glioblastoma 1 and the oligoastrocytoma III as non-responders, and glioblastoma 2 and glioblastoma 3 as responders. The cell cultures were exposed to 2 µM gefitinib for 2 hours, followed by mass spectrometry analysis carried out by a Ph.D student in our centre, Sandra Roche. Glioblastoma 2 and glioblastoma 3 showed a 2 fold increased uptake of gefitinib in comparison to glioblastoma 1 (Fig. 3.3.17). Although the grade III oligoastrocytoma, was not a responder to gefitinib (IC_{50}>10 µM) it showed a much higher drug uptake (1125.1 ng/million cells) than all three glioblastomas (136.2-291.5 ng/million cells).

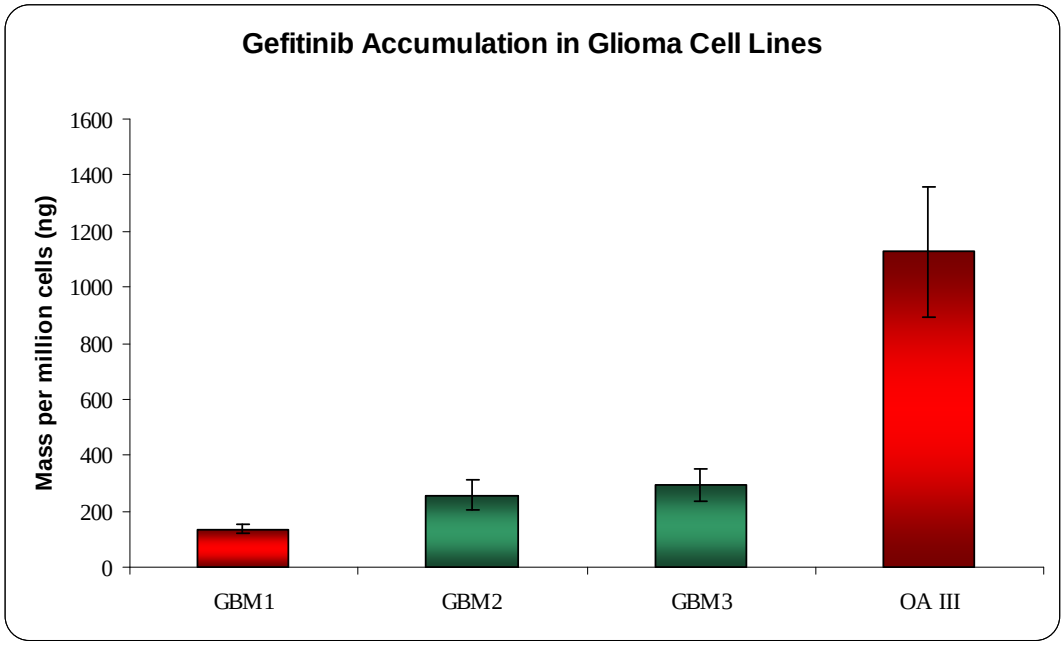

OA: oligoastrocytoma.

Fig. 3.3.18 Accumulation of gefitinib in three glioblastomas and one grade III oligoastrocytoma. Data represents triplicate samples. Standard deviations were generated from Microsoft excel software.

3.3.1.6 Expression at Protein Level of Growth Factor Receptors, ATP Transport Proteins, and Tyrosine Kinases

Western blotting analysis was carried out on 26 cell cultures and on NHAs (Fig. 3.3.18 (i) and (ii)), to analyse protein expression of Pgp and BCRP. The ATP-transporter Pgp was expressed in all cultures except two, the glioblastoma lines N070152 and N080943. However, N070152, has a very low IC_{50} value for docetaxel, which does not fit with the low levels of Pgp expression. BCRP expression varied greatly between the cultures. 8 cultures showed very low BCRP expression (Fig. 3.3.18 (ii)), these blots were developed with enhanced chemiluminescence confirming the presence of BCRP in these cultures (Fig. 3.3.18 (iii)).

Table 3.3.10 Cell cultures analysed by western blotting in figure 3.3.18 (i) and (iii).

Lane	Sample	Tumour Type
1	Positive control	-
2	N060893	Secondary Glioblastoma
3	N060978	Primary Glioblastoma
4	N070055	Grade III Oligoastrocytoma
5	N070152	Primary Glioblastoma
6	N070201	Grade III Astrocytoma
7	N061092	Primary Glioblastoma
8	N070126	Primary Glioblastoma
9	N070293	Primary Glioblastoma
10	N070314	Grade II Oligodendroglioma
11	N070229	Grade III Astrocytoma
12	N070701	Secondary Glioblastoma
13	N070788	Grade III Astrocytoma
14	N070859	Primary Glioblastoma
15	N070865	Primary Glioblastoma
16	N060913	Primary Glioblastoma
17	N071026	Primary Glioblastoma
18	N071271	Primary Glioblastoma
19	N080501	Primary Glioblastoma
20	N080533	Primary Glioblastoma
21	N080540	Primary Glioblastoma
22	N080869	Primary Glioblastoma
23	N080923	Primary Glioblastoma
24	N080943	Primary Glioblastoma
25	NHA	Normal Human Astrocytes
26	N070450	Grade II Astrocytoma
27	N061007	Primary Glioblastoma
28	N071144	Primary Glioblastoma

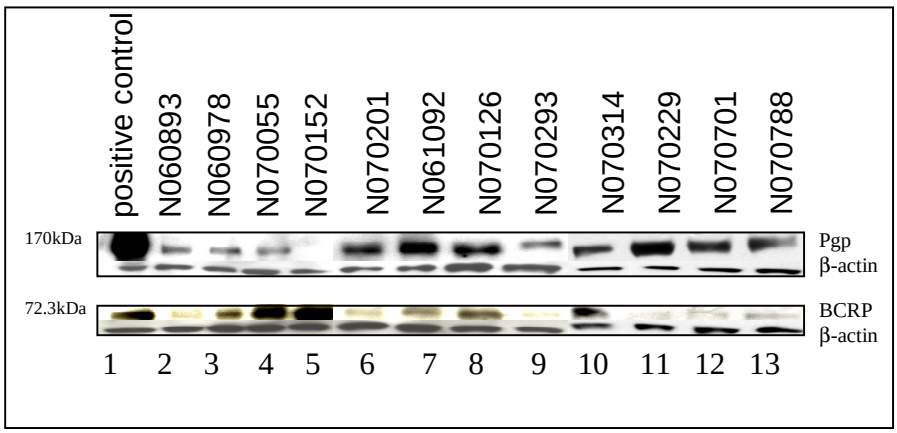

Fig. 3.3.19 (i): Western blot analysis of the tyrosine kinases multidrug resistance proteins Pgp, and BCRP.

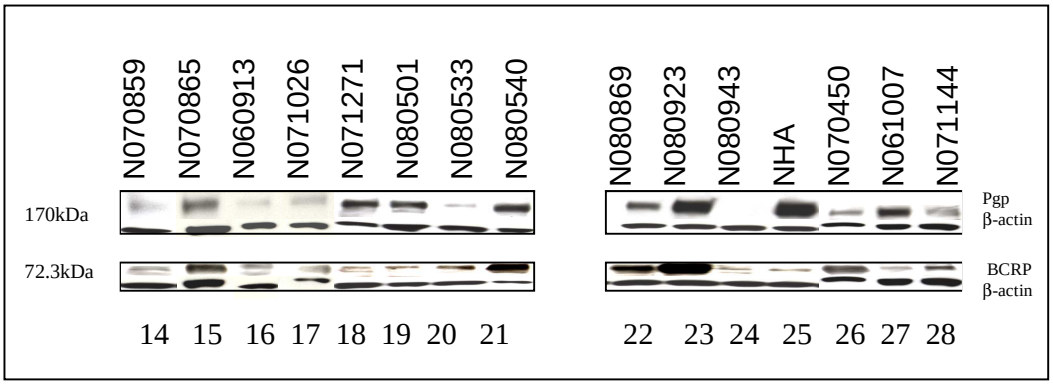

Fig. 3.3.19 (ii) Western blot analysis of the tyrosine kinases multidrug resistance proteins Pgp, and BCRP.

3.3.1.7 Specific Targets of Erlotinib and Gefitinib

Western blot analysis was carried out on 26 cell cultures and NHAs, to examine the expression of EGFR. Both erlotinib and gefitinib specifically target EGFR. All cell cultures expressed EGFR (Fig. 3.3.19). 3 cultures were responsive to erlotinib alone, 7 cultures were responsive to gefitinib alone, and 5 cultures were responsive to both erlotinib and gefitinib. One culture, N070152, expressed both EGFR and EGFRvIII, and was responsive to both erlotinib and gefitinib. 8 cultures did not respond to either drug.

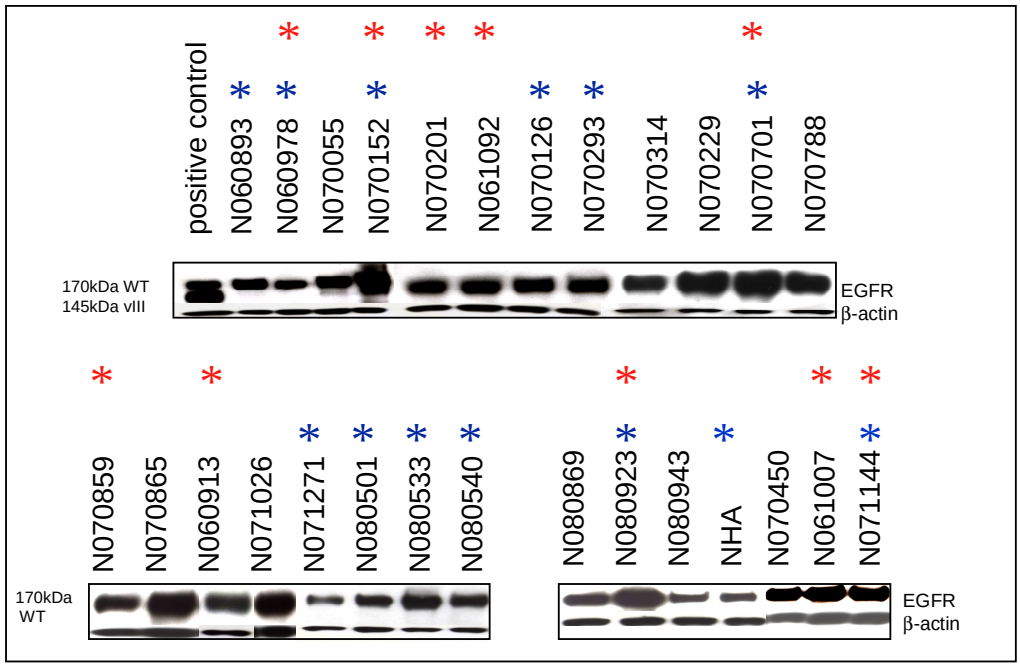

* Responsive to Erlotinib * Responsive to Gefitinib

Fig. 3.3.20 Expression of EGFR and EGFRvIII in the glioma cell cultures.

3.3.1.8 Specific Targets of Imatinib

The expression of the specific targets of imatinib in the cell cultures was examined, including PDGFR-β, C-Abl and C-Kit. All cultures expressed PDGFR-β, however, N070152 had much lower expression in comparison to the other cultures (Fig. 3.4.10 and 3.4.11). N070978 was the only culture not to express C-Abl and N070152 was the only culture not to express C-Kit (Fig. 3.4.11). Expression of these imatinib targets did not always correspond to responsiveness to imatinib.

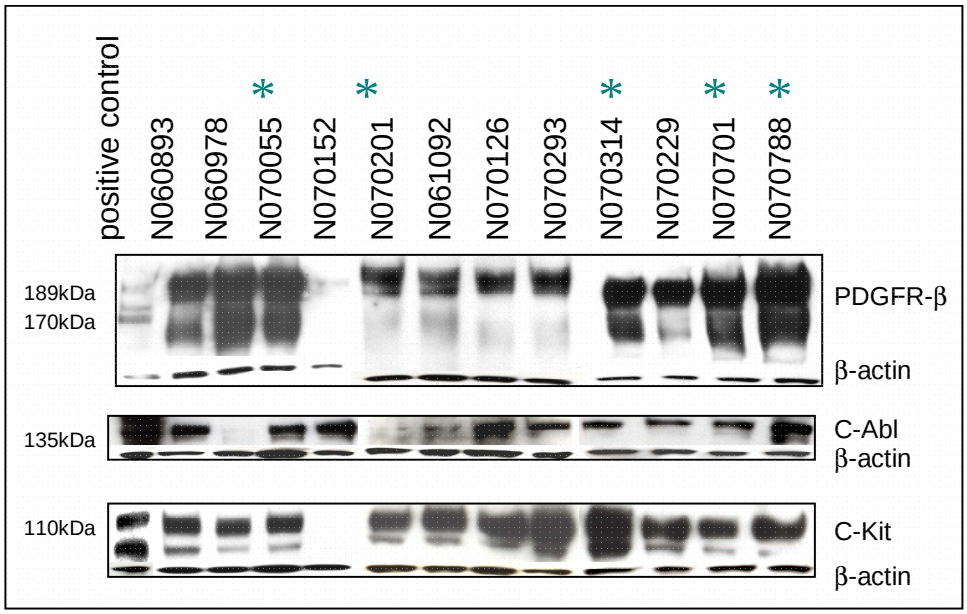

* Responsive to imatinib

Fig. 3.3.21 (a) Expression of PDGFR-β, C-Abl and C-Kit in the cell cultures. PDGFR-β has 2 bands, C-Kit also has 2.

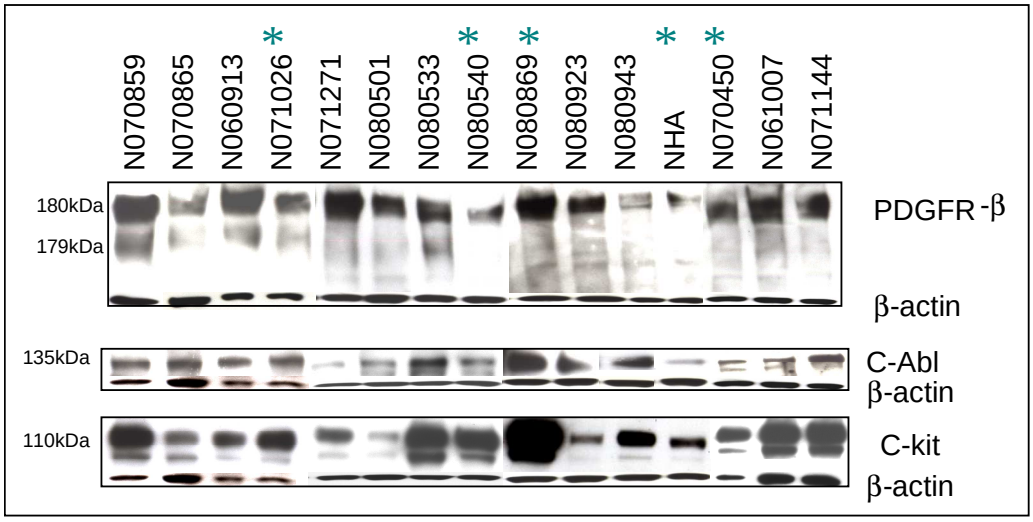

* Responsive to imatinib

Fig. 3.3.21 (b) Expression of PDGFR-β, C-Abl and C-Kit in the cell cultures. PDGFR-β has 2 bands, C-Kit also has 2.

3.3 Discussion

Characterization of newly Developed Glioma Cell Cultures

Introduction

Established immortalised glioma cell lines which have undergone several passages, involving clonal selection *in vitro* are homogeneous, their phenotype typically does not change, and may not represent the diversity of genetic abnormalities found in brain tumours (http://ehis.niehs.nih.gov/; Harry *et al.* 1998; Francis Ali-Osman 2005). The experimental results obtained with these cell lines may be quite different from those obtained from studies using biopsy specimens. To maintain the cell heterogeneity typically found in a brain tumour, glioma cell cultures were developed from brain tumour biopsy samples and characterized at early passages (below passage 10) with regard to protein expression, sensitivity to TKIs and chemotherapeutic drugs, proliferation and invasion activity. In parallel the corresponding tissue had undergone immunohistochemical and molecular characterisation, which is subject of a different thesis.

Out of 44 glioma biopsy samples 39 cell cultures were developed (Table 3.3.2). The age of the patient cohort ranged from 22-78 years, with the majority of patients being aged between 50-78 years (Table 3.3.3). The average survival of patients with a glioblastoma in our cohort was 16 months with an average age of occurrence of 58 years (Table. 3.3.3), this is consistent with published data (Van Meir EG 2010). The average survival for patients with a lower grade glioma was 34 months and the average age was 40 years (Table. 3.3.3), patients with lower grade gliomas tend to be younger and have a higher survival rate (Paul Kleihues 1997).

Glioblastoma cell cultures were characterized by both elongated and rounded cells, depicting the heterogeneity seen *in vivo*. The grade III oligoastrocytoma had clusters of cells forming networks with other clusters, and the grade III astrocytoma showed a typical star-shaped cell structure. The grade III oligodendroglioma showed the typical fried egg cell structure reported by others (Paul Kleihues 1997).

The dominating cell type found in the fast cultures was elongated, these are possibly the fast proliferating cells (Fig.3.3.3 to 3.3.4). The slow growing cultures

had more of a mixed and flattened cell type, while the cultures which slowed down in growth with less than 10 passages had more of a mixed cell type population, with larger flattened cells present (Fig.3.3.5 to 3.3.8). The cultures with fast growth originated from patients with an average survival time of 22 months, the slow growing cultures originated from patients with an average survival time of 25 months, while the cultures which slowed down in culture originated from patients with an average survival time of 13 months. The culture which stopped growing was derived from a patient with greater than 36 months survival. It is possible that the culture which slowed down in growth contained more of a mixed cell population than the fast or slow growth cultures, and possibly even contain stem cell-like cells, which would explain the large cell types with large nuclei. 17 cultures were examined by ICC for GFAP and nestin expression, a low amount of GFAP was expressed, and nestin expression was higher in the lower proliferating cultures (Fig. 3.3.14). This indicated that there was possibly undifferentiated stem cells present in the slower cultures, as nestin is a neuronal stem cell marker (Kawataki *et al.* 2010).

Invasion and Proliferation of Newly Developed Glioma Cell Cultures

The invasion and proliferation rate of each cell culture was examined. The majority of the glioblastomas were invasive, however the average invasion activity ranged from 6 µm/day to 50 µm/day (Fig. 3.3.10). Within the group of astroctyomas and mixed gliomas both invasive and non-invasive phenotypes were found. There was a large variation of proliferation rates in the cultures; there was no correlation between tumour grade and proliferation rate (Fig. 3.3.11 and. 3.4.12). There was no significant correlation between invasion and proliferation, i.e. a highly invasive culture was not necessarily a slow proliferating one, and a low amount of invasion did not always correlate with a fast proliferating culture (Fig. 3.3.13). Invasion and proliferation are dependent on substrate, no correlation may have been due to different substrates, proliferation assays were carried out with plastic and invasion with collagen. It would be possible to correlate invasion and proliferation if you used the MIB-1 antibody to the Ki-67 antigen, this antigen is expressed in cells in the proliferative phase of the cell cycle an is not expressed in cells at the resting

stage (Khoshyomn *et al.* 1999; Kogiku *et al.* 2008). Hagerstrand *et al*, established 20 high-grade glioma primary cultures and also found large variation in growth rates among the cultures, the fastest growing culture displayed an 18-fold increase in cell number, the slowest growing cultures only showed a 1.2-fold increase in cell number over the 4-day culture period (Hagerstrand *et al.* 2006). While low-grade astrocytomas *in vivo* tend to be highly invasive, but slow proliferating, the proliferation rate of glial tumour cells and mixed gliomas seems to increase with the grade of malignancy (Francis Ali-Osman 2005).

These characteristics were not fully reflected in their *in vitro* behaviour. It is possible that the *in vitro* 3D collagen invasion assay was not suitable for each cell culture, some cultures did not form hanging drops, instead they remained as loose cell aggregates, other invasion assays such as the Boyden Chamber assay could have been used. However it is also thought that different sections of the tumour contain cells with specific functions, some may be specifically involved in proliferation and others in invasion, the biopsy section of the tumour could have determined the characteristics of the cell culture, i.e. a highly proliferative section of a tumour could have given rise to a cell culture with high proliferation, and a highly invasive section of a tumour could have resulted in a highly invasive cell culture. As all invasion and proliferation assays were carried out below passage 10 with each culture, and large differences were seen with both characteristics this further supports the hypothesis that biopsy samples were taken from different sections of each tumour. With *in vitro* assays glioma spheroids have been shown to be organised adaptive biosystems, which carefully correlate the proliferative and invasive ratio within the spheroid to maximise cell number and spheroid expansion (Deisboeck *et al.* 2001; Huang *et al.* 2008), confirming that different sections of a tumour have different biological functions.

With cultures of glioma cells Giese *et al*, have shown have shown a relationship between migratory and proliferative behaviour (Giese *et al.* 2003). Highly motile glioma cells tend to have lower proliferation rates, i.e. cells proliferate only when they do not move this is known as the or ‘Go or Grow’ mechanism (Giese *et al.* 1996). Biological evidence indicates that migratory and proliferative processes

share common signalling pathways, suggesting a unique intracellular mechanism that regulates both behaviours (Giese *et al.* 2003; Godlewski *et al*. 2010; Hatzikirou *et al.* 2010).

Machesparan *et al*, established 12 glioblastoma and 1 astrocytoma culture from biopsy samples, and found a much more heterogeneous migratory response from these samples in comparison to their previous work with established glioma cell lines (Mahesparan *et al.* 1999). They found that the ability to migrate in response to extracellular matrix (ECM) was specific to each biopsy specimen as opposed to any individual ECM component; in addition with immunohistochemical analysis they found anti-glial fibrillary acidic protein (GFAP) staining revealed both GFAP-positive and -negative migrating cells, further supporting the presence of different cell types in these samples (Mahesparan *et al.* 1999). It is possible that by altering the ECM there could have been differences in invasion.

Poor prognosis in glioblastomas arises from invasive tumour cells which have escaped treatment. It has been shown that glioblastoma cells have the ability to switch between invasive and proliferative phenotypes (Godlewski *et al.* 2010; Molina *et al.* 2010). Molina *et al*, developed an *in vivo* model of human invasive glioblastoma in mouse brain from a human glioblastoma cell line, they showed an increase in tumourigenicity *in vivo* with increased invasion, and decreased proliferation *in vitro* for invasive cells (Molina *et al.* 2010). They also found Akt activation was directly related to increased tumourigenicity, stemness and invasiveness, and MAPK activation correlated with proliferation; cross-talk was found between these two pathways (Molina *et al.* 2010). If this cross-talk in glioblastomas is a key regulator of survival, inhibitors of the PI3K/Akt pathway may activate the MAPK pathway and *vice versa*, allowing an internal phenotype control switch between proliferation and invasion activation. Liu *et al*, have shown that activation of Notch1 signalling represses both, PI3K/Akt and MAPK in endothelial cells (Liu *et al.* 2006) increasing Notch1 signalling may have an antitumourigenic effect in glioma.

Response of Glioma Cell Cultures to Tyrosine Kinases

Specific tyrosine kinase inhibitors (TKI) of the epidermal growth factor receptor (EGFR) and the platelet derived growth factor receptor (PDGFR) have been used in the treatment of various cancer types where increased signalling is thought to contribute to tumour progression. Only subgroups of patients have been shown to response to each TKI. The molecular characteristics which determine a patients response to a TKI have yet to be fully defined. However EGFR kinase domain mutations were predictive of responsiveness of lung cancer patients to the EGFR TKIs erlotinib and gefitinib (Pao and Miller 2005).

Receptor tyrosine kinases, like EGFR and PDGFR, have been identified as therapeutic targets in glioblastoma; however, treatment success with inhibitors of these receptors is still debated since they are effective only in a limited number of patients (Omuro *et al.* 2007). It was thought that the expression of tyrosine kinases including EGFR, PDGFR, C-Abl, and C-Kit, which are specifically targeted by tyrosine kinase inhibitors, would be indicative of a responder or non-responder of each TKI in glioma. Each glioma cell culture was tested for sensitivity to three TKIs, erlotinib and gefitinib which target EGFR, and imatinib which targets PDGFR, C-Abl, and C-Kit. Using cut-off concentrations for IC_{50s}, based on published data (Mellinghoff *et al.* 2005; Servidei *et al.* 2006; Hofer and Frei 2007; Zerbe *et al.* 2008) each cell line was classified as a responder or non-responder to each TKI (Table 3.3.4 – 3.3.7).

35% of the glioblastomas were responsive to erlotinib (Table 3.3.5) and 56% to gefitinib (Table 3.4.6). 26% of glioblastomas responded to two TKIs and 1 responded to all 3 TKIs; the glioblastoma which responded to all 3 was a secondary glioblastoma, the other secondary glioblastoma tested was responsive to gefitinib, it is possible that secondary glioblastomas are more sensitive to TKIs; this would need to be further clarified with a larger number of secondary glioblastoma samples. Normal human astrocytes were not responsive to erlotinib, but were responsive to gefitinib and imatinib.

This response rate to EGFR-TKIs is high compared to the observations reported by Mellinghoff *et al*, (Mellinghoff *et al.* 2005). They found in their study

that only 10-20% of glioblastoma patients responded to erlotinib and gefitinib, with reduction of tumour size by 25%; however, a higher response is possible *in vitro* because of the absence of a BBB, allowing exposure to higher TKI concentrations. Mellinghoff *et al*, also analysed the tumour tissue of their patients and correlated co-expression of EGFRvIII and PTEN in tumour cells with responsiveness to these EGFR kinase inhibitors (Mellinghoff *et al.* 2005). In a phase II trial with 110 glioblastoma patients Van den Bent *et al*, found no correlation with EGFR, EGFRvIII expression and improved outcome with erlotinib; they also found insufficient single-agent activity in glioblastomas (van den Bent *et al.* 2009). Sarkaria *et al*, found 2 erlotinib sensitive glioblastoma tumours each with amplified EGFR and expressing wild-type PTEN, one of the tumours had truncated EGFRvIII, and the other had full length EGFR (Sarkaria *et al.* 2007). By western blot analysis only one cell culture N070152 had expression of EGFRvIII; therefore it was not possible to determine if expression of EGFRvIII was correlated with TKI response in the glioma cell cultures. It would have been necessary to examine the expression of PTEN in all cell cultures to identify its role in the response to these TKIs.

The majority of the cell cultures over-expressed wild-type EGFR in comparison to the NHAs regardless of tumour grade (Fig. 3.3.20); within this group 32% of the cell cultures were responsive to erlotinib and 42% to gefitinib. Suggesting that responsiveness to erlotinib and gefitinib *in vitro* seems not to be directly correlated with EGFR expression. In the literature it is reported that EGFR is overexpressed in 50-60% of glioblastoma patients and amplification is often coupled with gene rearrangement (Omuro *et al.* 2007). The most common mutated form is EGFRvIII which is present in 24-67% of glioblastoma patients (Heimberger *et al.* 2005). Hwang *et al*, found that overexpression of EGFR is correlated with the grade of malignancy in tumour tissue; 67% in low-grade astrocytomas, 87% in anaplastic astrocytomas, and 100% in glioblastomas (Hwang *et al.* 1997). Torp *et al*, 1991 also found that high-grade gliomas contain more EGFR positive tumour cells than low-grade gliomas, and that small neurons and normal glial cells did not express EGFR (Torp *et al.* 1991). Haas-Kogan *et al*, showed that the response to erlotinib treatment was higher in glioblastoma with high EGFR expression and low

phosphorylated protein kinase B (PKB)/Akt than those with low EGFR expression and high (PKB)/Akt levels (Haas-Kogan *et al.* 2005). Additionally, they found no correlation between EGFRvIII expression and response (Haas-Kogan *et al.* 2005).

Gefitinib has been shown to be effective in lung cancer patients carrying mutations in exons 19 and 21 of the EGFR tyrosine kinase domain. These mutations were not found in a study involving 95 gliomas including glioblastomas, anaplastic oligodendrogliomas, and low-grade gliomas, which might explain the limited success of gefitinib in glioma treatment (Marie *et al.* 2005). Using a multi-institutional study with glioblastoma tissue and cell lines Lee *et al*, have shown that EGFR missence mutations and amino acid substitutions have an important role in determining sensitivity to EGFR small molecule inhibitors (Lee *et al.* 2006). Different mutations of EGFR found in gliomas in comparison to mutations of EGFR found in other cancers, may be responsible for resistance to gefitinib in glioma. To determine if response to gefitinib is directly related to mutations of EGFR, it would be necessary to screen all of the glioma cultures for these mutations. A PCR based GeneTailorTM/ QuickChange II site-directed high-throughput mutagenesis system could be used for that.

It appears that EGFR amplification and mutations together with the expression of functional PTEN are involved in glioma sensitivity to EGFR inhibition; additional factors influencing glioma sensitivity to EGFR have yet to be identified, such as other key pathways or mutations of downstream proteins of these pathways.

Only 6 out of 23 glioblastomas responded to imatinib, whereas the response rate was higher within anaplastic astrocytomas and mixed gliomas. Haberler *et al*, found a 15.7% imatinib response rate in patients with glioblastoma (Haberler *et al.* 2006). Hagerstrand *et al*, found a positive correlation in gliomas between PDGFR expression and imatinib sensitivity (Hagerstrand *et al.* 2006). The use of imatinib as a single agent in patients with recurrent malignant gliomas was successful only in a small group of patients, and only 3% had 6 months progression free survival (Wen *et al.* 2006). Phase II trials with imatinib alone in gliomas had very little effect (Wen *et al.* 2006; Raymond *et al.* 2008). It is uncertain whether this was due to poor

penetration of imatinib through the BBB to the target site. In the present study strong expression of C-Kit in 25 out of 26 cell cultures was found. In the literature the amount of C-Kit mRNA or protein expression in glioma cell lines varies between 50% and 100% (Hamel *et al.* 1992; Stanulla *et al.* 1995). The co-expression of the receptor kinase C-Kit and its ligand SCF, was found in glioma cell lines, suggesting it is involved in intracellular mechanisms for autocrine growth regulation of glioma cells (Stanulla *et al.* 1995). In the present study C-Abl expression was found in all cell cultures, with the exception of one, which was a non-responder to imatinib (Fig. 3.3.21). Jiang *et al*, found C-Abl to be overexpressed in glioblastomas compared to lower grade gliomas, and they suggest it is associated with poor survival (Jiang *et al.* 2006).

One glioblastoma culture, N070152, a non-responder to imatinib showed very low expression of PDGFR-β and no C-Kit expression; on the other hand, EGFR and EGFRvIII were highly expressed (Fig. 3.3.20) and the cells did respond to both EGFR inhibitors erlotinib and gefitinib. Another culture, N070701, expressed EGFR, PDGFR-β, C-Kit, and C-Abl and was sensitive to all three TKIs tested (Fig. 3.3.20 and 3.3.21). However, TKI target proteins was not indicative of a responder in the majority of the cultures.

Various other growth factor receptors are also activated in glioma including the vascular endothelial growth factor receptor (VEGFR), and the insulin-like growth factor (IGF) receptor; their inhibition can prevent tumour growth (Ziegler *et al.* 2008). It has been suggested that inhibition of multiple tyrosine kinases is necessary to effectively inhibit downstream signalling, as many tyrosine kinases involved in the PI3K signalling pathway are activated at the same time (Shingu *et al.* 2009). Imatinib is an inhibitor of multiple tyrosine kinases including PDGFR and C-Kit, which are associated with the PI3K/Akt pathway, but its effect as a single drug is minimal in glioma.

To date molecular targeted therapy has not translated into phase III trials for malignant glioma. The mechanisms of resistance to receptor tyrosine kinase (RTK) inhibition are not fully understood. New trials for gliomas are likely to involve a multiple target approach and combination with chemotherapy and/ or radiotherapy

(Omuro *et al.* 2007). Many anti-apoptotic mechanisms are responsible for the resistance of glioblastoma cells to chemotherapy and radiotherapy, and it is suggested that these mechanisms are also responsible for resistance to RTK inhibition (Ziegler *et al.* 2008).

The oncogenetic process in gliomas is regulated by differentially activated or silenced signalling pathways; which include PI3K/AKT/PTEN/MTOR, Ras/Raf/MAPK and protein kinase C signalling. Due to the large amount of cell heterogeneity in malignant gliomas and low prevalence of each genetic abnormality, it has been difficult to identify targets that act as key promoters of oncogenesis, with many studies reporting conflicting results. Several drugs have been tested for glioma therapy, including tyrosine kinase inhibitors erlotinib and gefitinib, the PDGFR-TKI imatinib, the mTOR inhibitors temsirolimus and everolimus, VEFGR, protein kinase C-beta inhibitors, and other angiogenesis pathway inhibitors such as vatalanib, bevacizumab, and enzataurin (Omuro *et al.* 2007). A new approach is involving the inhibition of multiple targets simultaneously with less specific, multi-targeting drugs, which can be the use of two or more single-targeted drugs, in combination with cytotoxic chemotherapy and/or radiotherapy. It may be necessary to target other key proteins in the PI3K/AKT and Ras/MAPK growth and survival pathways, in addition to the proteins targeted in this study, to find an effective treatment for gliomas.

Sensitivity of Glioma Cell Cultures to Temozolomide

Temozolomide is currently the standard drug for the treatment of newly diagnosed and recurrent glioblastoma (Dresemann 2010). An IC_{50} range for the glioma cultures of 198.3 µM-1146 µM for temozolomide was found (Table 3.3.9) (Fig. 3.3.17), which is much higher than the plasma concentration of 72 µM reported for malignant glioma patients (Ostermann *et al.* 2004). A 100 µM concentration of temozolomide was found in the brain tumour of a xenograft model (Kato *et al.* 2010), which is still significantly lower than the IC_{50} range found with the cell cultures. A similar IC_{50} concentration range with melanoma cell lines was found in the NICB by Dr. Alex Eustace (between 223 µM and 791 µM). Normal human

astrocytes were found to have an IC_{50} of 1228.4 µM, showing that temozolomide has little toxicity to normal cells *in vitro*. Temozolomide is rapidly hydrolysed to its active metabolite 5-(3-methyltriazeno)-imidazole-4-carboxamide (MTIC) which can reach a plasma concentration of 276 ng/ml (Rudek *et al.* 2004). Under physiological conditions temozolomide has a short half life of 1.8 hours, which might explain the high concentrations needed in *in vitro* assays to see an effect. Another explanation could be that temozolomide is a substrate of the MDR pump Pgp, which is expressed in the majority of the cell cultures (Fig. 3.3.19) (Schaich *et al.* 2009). Akbar *et al*, have published a gel-matrix containing temozolomide which was placed directly at the tumour site in a rat intracranial resection model. This resulted in high levels of oncolytic activity towards glioma cells, and minimal cytotoxicity toward normal brain tissue, this could be a promising treatment for gliomas (Akbar *et al.* 2009).

Sensitivity of Glioma Cell Cultures to Docetaxel

Docetaxel is a very successful drug in the treatment of a variety of solid tumours particularly in lung cancer (Burris *et al.* 1995). All IC_{50s} for the glioma cell cultures were in the nanomolar range, (0.4 nM to 24.5 nM) 12 out of 22 glioblastomas had an IC_{50} < 2 nM (Table 3.3.8) (Fig. 3.3.16). There was no difference in sensitivity between glioblastomas and lower grade tumours (Fig. 3.3.16). One cell culture, a grade III astrocytoma, was not as sensitive to docetaxel (IC_{50} of 59.5 nM) (Table 3.3.8), normal human astrocytes were not as sensitive to docetaxel (IC_{50} of >124 nM) (Table 3.1). 24 out of 26 cell cultures expressed Pgp: with 2 glioblastomas being negative for Pgp expression. One of these was highly sensitive to docetaxel (IC_{50} of 0.5 nM) (Fig. 3.3.8). Fracasso *et al*, have found a plasma concentration of docetaxel of 0.5 nM in glioma patients and a CSF concentration of 0.05 nM (Fracasso *et al.* 2004), the two sensitive glioblastoma cultures had an IC_{50} for docetaxel (Table 3.3.8) within that found in plasma.

Expression of the MDR pump BCRP was found in all cell cultures tested: one glioblastoma and one grade II oligodendroglioma showed particularly high expression of BCRP compared to the positive control (Fig. 3.3.19). One grade III

astrocytoma culture showed IC_{50} of 59.5 nM for docetaxel but not particularly high expression of both ABC pumps Pgp and BCRP (Fig. 3.3.19). Therefore, the lack of sensitivity to docetaxel by MDR pump expression could not be explained.

Other ABC transporter pumps, such as MRP1 and MRP2 have been found in gliomas (Leslie *et al.* 2005), and might be involved in docetaxel resistance/ sensitivity in the cell cultures, this remains to be examined. Clinical trials using systemic docetaxel have not been effective in malignant gliomas probably due to poor penetration of drug through the BBB and into the tumour (Forsyth *et al.* 1996; Sanson *et al.* 2000; Kemper *et al.* 2003; Kemper *et al.* 2004). This can be addressed by convection-enhanced delivery (CED), a drug application method in which the drug is injected directly into the tumour avoiding the blockage through the BBB; this is being used in an ongoing clinical trial with paclitaxol with recurrent gliomas and is showing promising results (Chamberlain 2006). All glioblastomas with low docetaxel IC_{50} (< 2 nM) were also responsive to one, two, or three TKIs. These combinations could be useful in a clinical approach.

Accumulation of TKIs in 4 Glioma Cell Cultures

It was thought that response to TKIs may be directly related to the amount of drug accumulated in the cells. Therefore the accumulation of gefitinib in 4 glioma cell cultures was examined by mass spectrometry. The cultures were selected according to their responsiveness to gefitinib. The cells were exposed to 2 µM of gefitinib for 2 hours. Glioblastoma cells which were responsive to gefitinib had a 2 fold increase in uptake of gefitinib compared to the non-responsive glioblastomas. The grade III oligoastrocytoma, however had a significantly higher uptake of gefitinib than all 3 glioblastoma cultures although it was a non-responder to gefitinib. Therefore, the uptake of gefitinib seems not to predictive for responsiveness to the drug in the oligoastrocytoma cells.

The accumulation of gefitinib to the brain is limited by the expression of Pgp and BCRP (Agarwal *et al.*). However, seen in the cultures analysed. There may be other membrane efflux pumps present in these glioma cells such as MRP1 and MRP2 (Leslie *et al.* 2005). Bronger *et al*, have shown the membrane pumps ABCC4

and ABCC5, to be more strongly associated with oligoastrocytomas (Bronger *et al.* 2005).

3.3 Summary and Conclusion

Characterization of Newly Developed Glioma Cell Cultures

In collaboration with Beaumont hospital 31 glioma cell cultures were developed directly from tissue samples and characterized with regard to their invasion and proliferation rate. The majority of the glioblastoma cultures were invasive, however the average invasion activity varied between cultures. It was expected that all glioblastomas would be invasive, as is typically the case *in vivo*. Within the group of astroctyomas, and mixed gliomas both invasive and non-invasive phenotypes were found, while low-grade astrocytomas *in vivo* tend to be highly invasive. The proliferation rate of glial tumour cells and mixed gliomas seems to increase with the grade of malignancy *in vivo*. These invasive and proliferation characteristics are obviously not fully reflected in the *in vitro* behaviour.

Response of Glioma Cell Cultures to Tyrosine Kinases

Within the glioma cell culture cohort it was found that 35% of the glioblastomas were responsive to TKIs targeting EGFR, whereas anaplastic astrocytomas, mixed gliomas, and the oligodendroglioma responded better to imatinib, targeting PDGFR, C-Kit, and Bcr-Abl. However, in most cases the protein expression of the tyrosine kinases EGFR and PDGFR-β, C-Kit, and C-Abl, did not correlate with the responsiveness to the specific TKIs. Even though the cultures do express the target proteins of the TKIs, none of the cultures were sensitive to them; sensitivity to a TKI is usually seen with an IC_{50} of 1 µM or less, the lowest IC_{50} was 6.5 µM. The *in vitro* data indicated that individually the TKIs may not be a sufficient treatment for gliomas.

Expression of Drug Efflux Pumps and Sensitivity to Chemotherapeutic Drugs

The expression of Pgp and BCRP did not always correlate to sensitivity to docetaxel or temozolomide. Therefore the expression levels of these pumps are not indicative of response to chemotherapeutic drugs. High concentrations of temzolomide were necessary to achieve an IC_{50} in the cultures. All glioblastomas, which were sensitive to docetaxel (IC_{50} < 2 nM) were also responsive to one or more TKIs, the combination treatment with docetaxel and one or two of these TKIs is potentially a good treatment option for these cases.

Effect of TKIs and Chemotherapeutic Drugs on Invasion in Glioma

As single drug treatments only docetaxel and imatinib were effective in inhibiting invasion activity. Unfortunately, their penetration through the BBB is limited. In general response rates of glioblastoma patients to TKIs which specifically target EGFR has been low, however the present study showed docetaxel and imatinib to be promising treatments for glioma.

Accumulation of Gefitinib in Gliomas

The intracellular accumulation of gefitinib was higher in gefitinib responsive glioblastomas than in non-responsive ones; however, a mixed glioma sample showed much higher up-take of TKI despite the fact that it was non-responsive to gefitinib. Further experiments have to be performed to explain this result.

3.4 Drug Effects in a 3D Invasion Assay

The work in this section was carried out with my supervisor Dr Verena Amberger-Murphy. Due to the highly infiltrative and invasive behaviour of gliomas, finding an effective drug to treat gliomas has proved difficult. The effect of TKIs and 2 chemotherapy drugs on invasion in a 3D invasion assay was examind. The compounds tested included erlotinib (Erl), gefitinib (Gef) and imatinib (Imt), and the chemotherapeutic drugs temozolomide (Tmz) and docetaxel (Doc). The effect of each individual drug and the combination effect of TKIs with chemotherapy drugs was assessed. 16 invasive glioma cultures were examined, including: 11 primary glioblastomas, 2 secondary glioblastomas, 2 grade III astrocytomas and 1 oligoastrocytoma.

Spheroids of each culture were implanted into collagen type I gels and cells were left to invade for 4 days prior to drug treatment (Fig. 3.4.1) (see section 2.8). Invasion was then measured over 9-29 days in the presence and absence (Ctr) of drug. Drug concentrations were calculated as approximately twice the IC_{50} for each cell culture from the monolayer proliferation assay, as higher concentrations are typically required for spheroids; in some cases IC_{50} data were not available, and drug concentrations had to be estimated. The drug concentrations used for both proliferation and invasion are shown (Table 3.4.1 to 3.4.18). For each spheroid four measurements (in µm) were taken. Each condition was done in duplicate per experiment. Due to the slow proliferation rates of some cultures, repeated experiments were not always possible. Tables 3.4.12, 3.4.15 and 3.4.19 show the overall effect of drugs on the cultures.

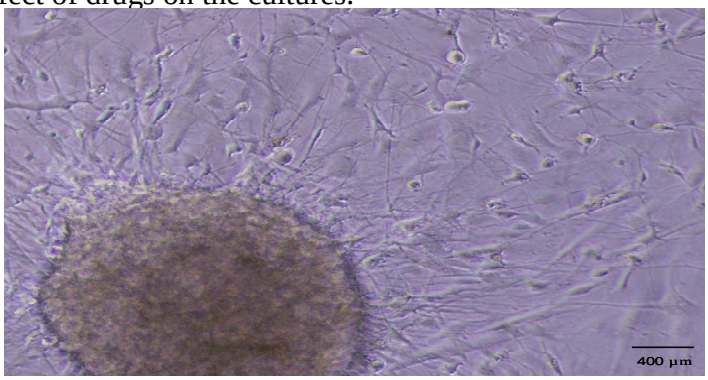

Fig. 3.4.1 A primary glioblastoma spheroid implanted into collagen gel, after 4 days invasion, 10x magnification.

3.4.1 Drug Effect on Invasion Activity of Primary Glioblastomas

Table 3.4.1 Drug concentrations N061007.

Drug	Invasion Assay Concentration	IC_{50} Concentration Proliferation Assay
Erlotinib	18.3 µM	9.1 µM
Gefitinib	20 µM	>20 µM
Imatinib	13.6 µM	>20 µM
Temozolomide	41.2 µM*	566.6 µM
Docetaxel	13.9 nM	1.2 nM

*: The invasion assay was carried out prior to the proliferation assay therefore the concentration used was too low. >: greater than the cut-off concentration (IC_{50} not determined).

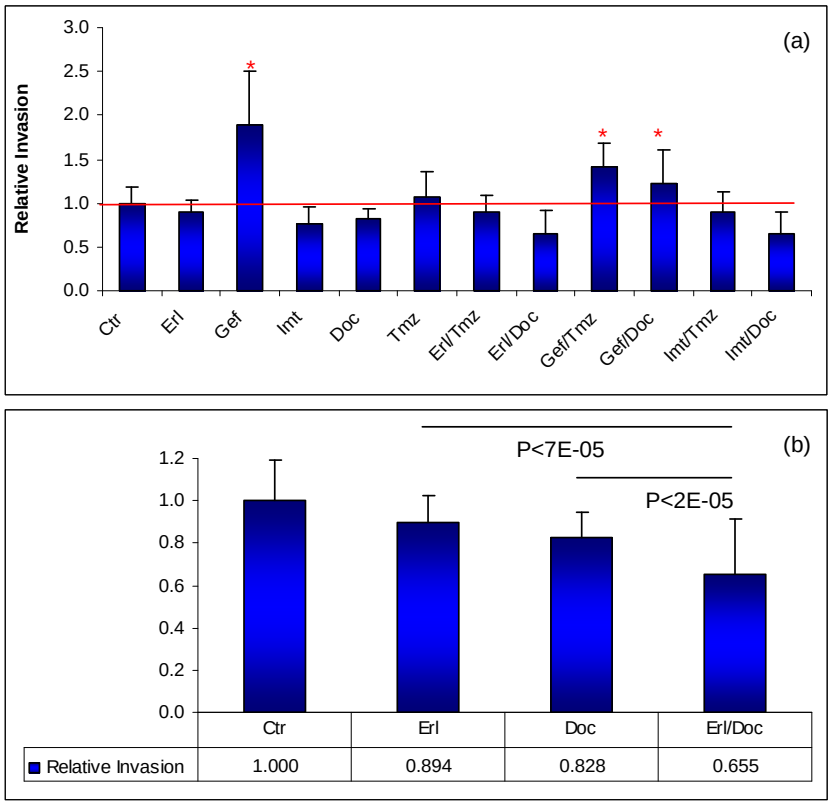

*: invasion increased.

Fig. 3.4.2 (a) Average invasion per day over 13 days for N061007, (b) significance of combination effect of erlotinib and docetaxel compared to single drug effect. The deviations represent measurements over 13 days. Standard deviations were generated from Microsoft Excel software.

Surprisingly gefitinib alone and in combination with temozolomide and docetaxel increased invasion with N061007, single treatment with imatinib and docetaxel had a small inhibitory effect on invasion (Fig. 3.4.2 (a)).The combination of erlotinib and docetaxel had the strongest inhibitory effect
(Fig. 3.4.2 (b)).

Table 3.4.2 Drug concentrations N061092.

Drug	Invasion Assay Concentration	IC_{50} Concentration Proliferation Assay
Erlotinib	11.6 μM	9.3 μM
Gefitinib	44.8 μM	>20 μM
Imatinib	67.8 μM	>20 μM
Temozolomide	1030 μM	618 μM
Docetaxel	4.6 nM	1.5 nM

>: greater than cut-off concentration (IC_{50} not determined).

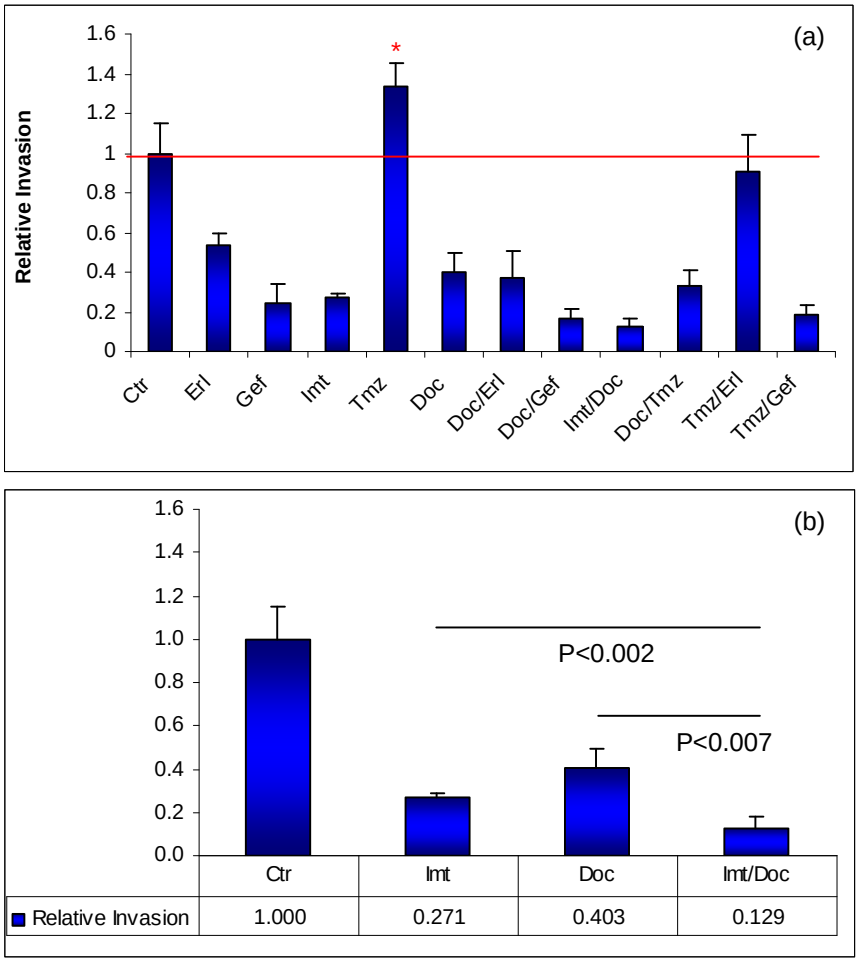

*: increased invasion.

Fig. 3.4.3 (a) Average invasion per day over 27 days for N061092, (b) significance of combination effect of imatinib and docetaxel compared to single drug effect. The deviations represent measurements over 27 days. Standard deviations were generated from Microsoft Excel software.

Erlotinib, gefitinib, imatinib and docetaxel had a very strong inhibitory effect on the invasion of N061092, however, temozolomide showed an increase in invasion even though a high concentration was used (Fig. 3.4.3 (a)). The strongest inhibitory effect was with the combination of imatinib and docetaxel (Fig. 3.4.3 (b).

Table 3.4.3 Drug concentrations N070152.

Drug	Invasion Assay Concentration	IC_{50} Concentration Proliferation Assay
Erlotinib	11.6 µM	6.5 µM
Gefitinib	44.8 µM	17 µM
Imatinib	67.8 µM	>20 µM
Temozolomide	1030 µM	497 µM
Docetaxel	4.6 nM	0.5 nM

>: greater than cut-off concentration (IC_{50} not determined).

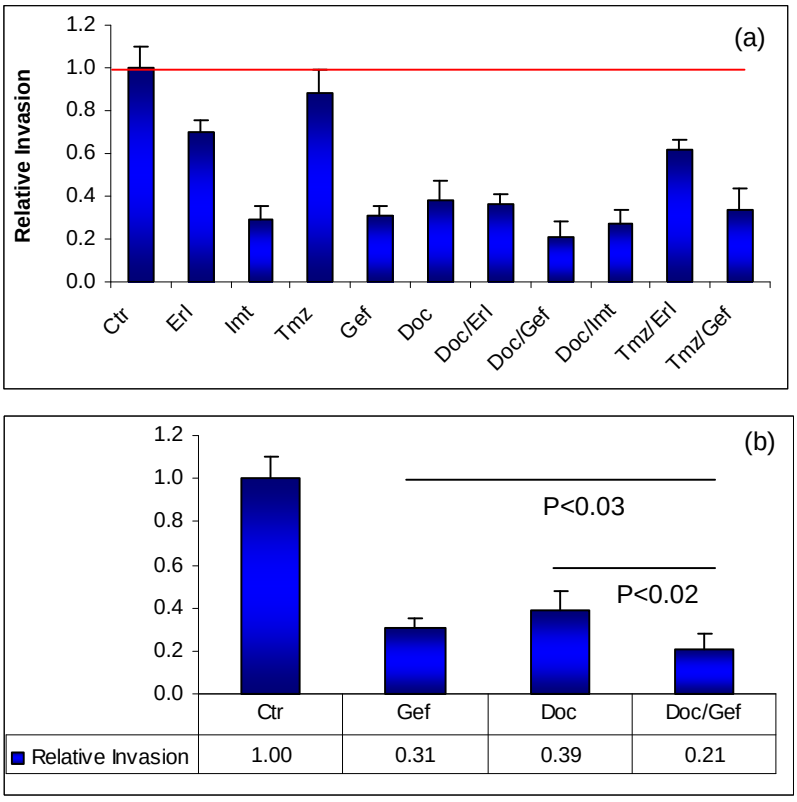

Fig. 3.4.4 (a) Average invasion per day over 27 days for N070152, (b) significance of combination effect gefitinib and docetaxel compared to single drug effect. The deviations represent measurements over 27 days. Standard deviations were generated from Microsoft Excel software.

Erlotinib had a strong inhibitory effect on the invasion of N070152, imatinib, gefitinib and docetaxel had an even stronger effect (Fig. 3.4.4 (a)). The strongest effect was with the combination of docetaxel and gefitinib (Fig. 3.4.4 (b)).

Table 3.4.4 Drug concentrations N070454.

Drug	Invasion Assay Concentration	IC_{50} Concentration Proliferation Assay
Erlotinib	46.5 µM	>10 µM
Gefitinib	44.8 µM	>20 µM
Imatinib	10.1 µM	16.7 µM
Temozolomide	2472.3 µM	638.7 µM
Docetaxel	11.6 nM	0.9 nM

>: greater than cut-off concentration (IC_{50} not determined).

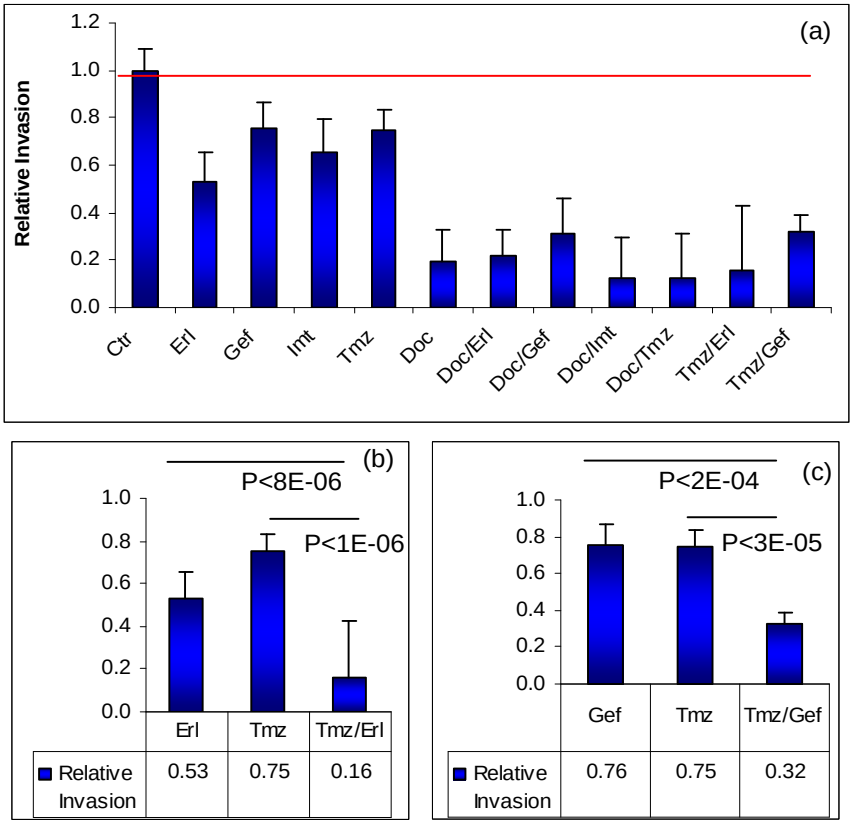

Fig. 3.4.5 (a) average invasion per day over 15 days in comparison to the control for the cell line N070454, (b) and (c) significance of combination effect compared to single drug effect. The deviations represent measurements over 15 days. Standard deviations were generated from Microsoft Excel software.

All of the single drug treatments had an inhibitory effect on invasion for N070454, docetaxel had a very strong effect (Fig. 3.4.5 (a)). When erlotinib or gefitinib were combined with temozolomide a stronger inhibitory effect was seen (Fig. 3.4.5 (b)).

Table 3.4.5 Drug concentrations N070859.

Drug	Invasion Assay Concentration	IC_{50} Concentration Proliferation Assay
Erlotinib	18.6 μM	>10 μM
Gefitinib	40.3 μM	>20 μM
Imatinib	67.8 μM	>20 μM
Temozolomide	1287.6 μM	502.2 μM
Docetaxel	11.6 nM	1.9 nM

>: greater than cut-off concentration (IC_{50} not determined).

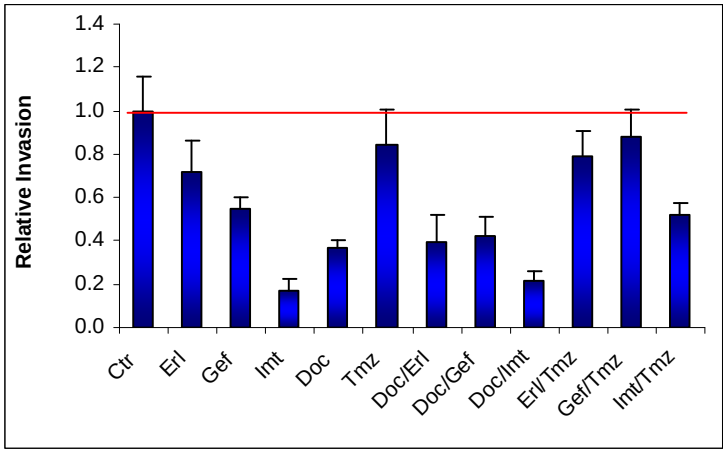

Fig. 3.4.6 Average invasion per day over 9 days for N070859. The deviations represent measurements over 9 days. Standard deviations were generated from Microsoft Excel software.

Temozolomide had a small inhibitory effect on the invasion of N070859, erlotinib, gefitinib had a stronger effect, imatinib and docetaxel had a very strong inhibitory effect (Fig. 3.4.6).

Table 3.4.6 Drug concentrations N070865.

Drug	Invasion Assay Concentration	IC_{50} Concentration Proliferation Assay
Erlotinib	18.6 μM	>10 μM
Gefitinib	40.3 μM	>20 μM
Imatinib	67.8 μM	>20 μM
Temozolomide	1287.6 μM	772.6 μM
Docetaxel	6.9 nM	5 nM

>: greater than cut-off concentration (IC_{50} not determined).

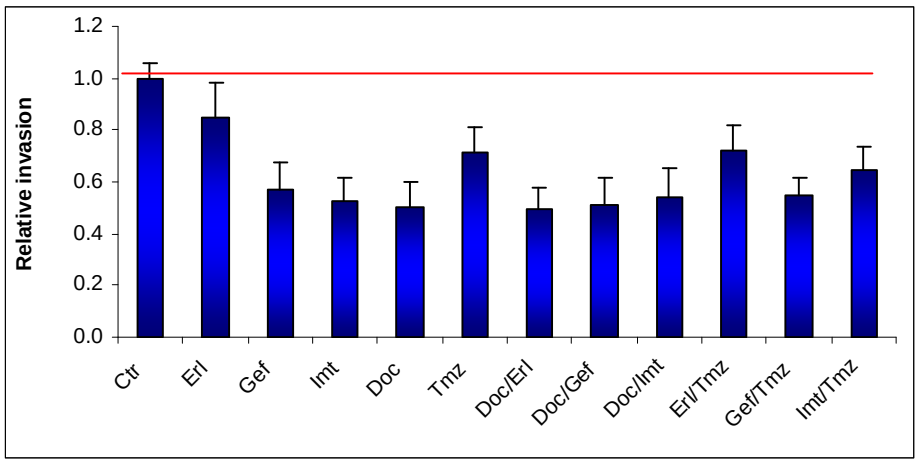

Fig. 3.4.7 Average invasion per day over 9 days for N070865. The deviations represent measurements over 9 days. Standard deviations were generated from Microsoft Excel software.

Erlotinib and temozolomide had a small inhibitory effect on the invasion of N070865, gefitinib, imatinib and docetaxel had a stronger effect; there was no increased effect with combination treatments (Fig. 3.4.7).

Table 3.4.7 Drug concentrations N071026.

Drug	Invasion Assay Concentration	IC_{50} Concentration Proliferation Assay
Erlotinib	23.2 μM	>10 μM
Gefitinib	40.3 μM	>20 μM
Imatinib	33.9 μM	19.6 μM
Temozolomide	1442.1 μM	738.1 μM
Docetaxel	46.1 nM	23.2 nM

>: greater than cut-off concentration (IC_{50} not determined).

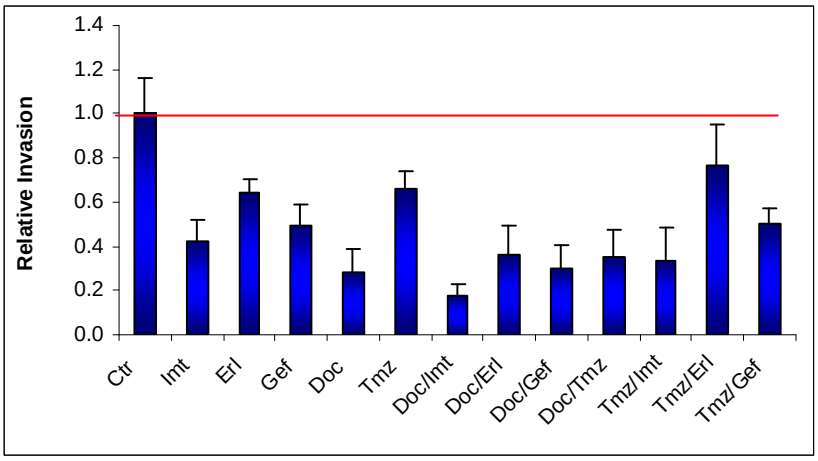

Fig. 3.4.8 Average invasion per day over 14 days for N071026. The deviations represent measurements over 14 days. Standard deviations were generated from Microsoft Excel software.

Erlotinib, gefitinib and temozolomide had a strong inhibitory effect on the invasion of N071026, docetaxel and imatinib had a very strong effect, the combination of imatinb and docetaxel had the strongest effect (Fig. 3.4.8).

Table 3.4.8 Drug concentrations N071144.

Drug	Invasion Assay Concentration	IC_{50} Concentration Proliferation Assay
Erlotinib	18.6 μM	9.3 μM
Gefitinib	44.8 μM	19.5 μM
Imatinib	50.8 μM	>20 μM
Temozolomide	1514.3 μM	401.7 μM
Docetaxel	8.3 nM	6.4 nM

>: greater than cut-off concentration (IC_{50} not determined).

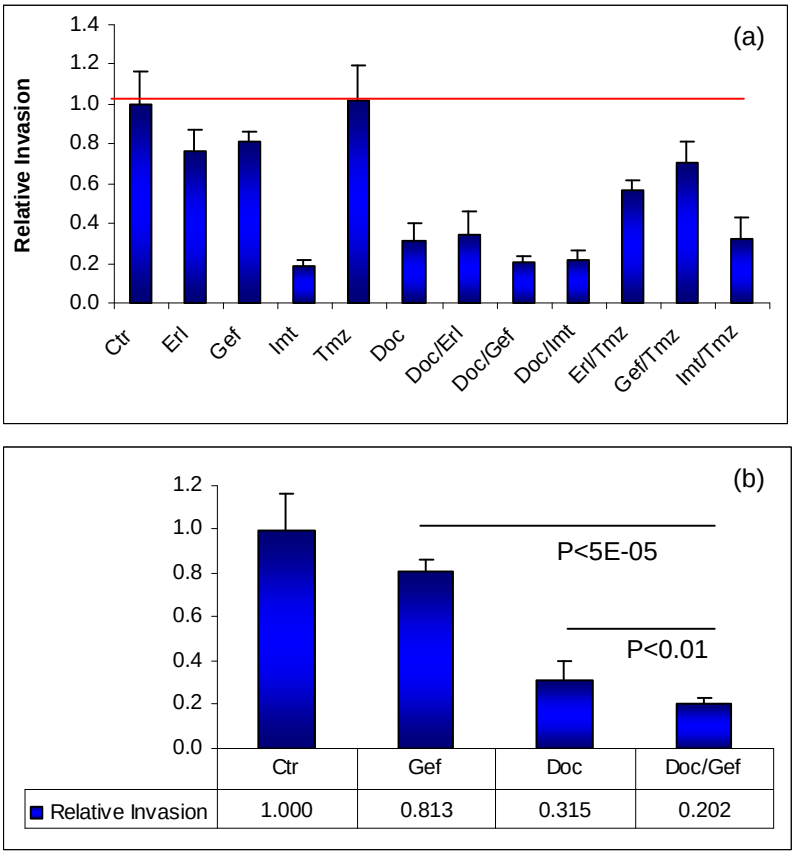

Fig. 3.4.9 (a) Average invasion per day over 16 days for N071144, (b) significance of combination effect of gefitinib and docetaxel compared to single drug effect. The deviations represent measurements over 16 days. Standard deviations were generated from Microsoft Excel software.

Erlotinib and gefitinib had a small inhibitory effect on the invasion of N071144, temozolomide had no effect, imatinib and docetaxel had a very strong effect (Fig. 3.4.9 (a)). A further significant inhibitory effect on invasion was seen with the combination of gefitinib and docetaxel with p-values of less than 0.05 (Fig. 3.4.9 (b)).

Table 3.4.9 Drug concentrations N071271.

Drug	Invasion Assay Concentration	IC_{50} Concentration Proliferation Assay
Erlotinib	23.2 μM	>10 μM
Gefitinib	35.8 μM	16.7 μM
Imatinib	47.4 μM	>20 μM
Temozolomide	669.6 μM	372.4 μM
Docetaxel	1.16 nM	0.6 nM

>: greater than cut-off concentration (IC_{50} not determined).

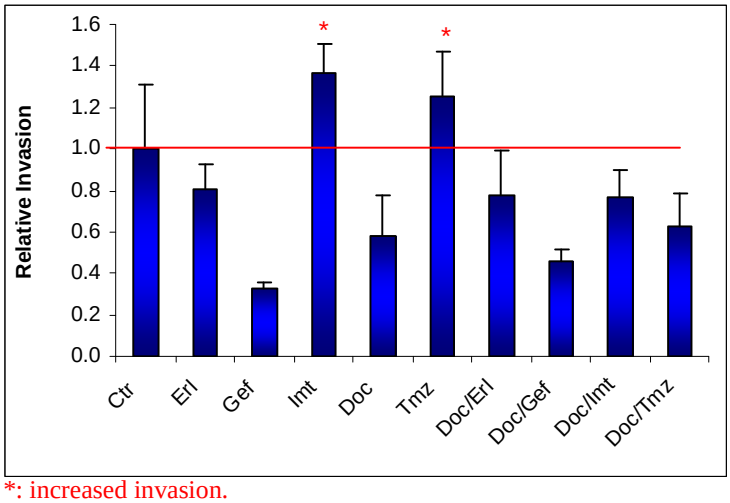

*: increased invasion.

Fig. 3.4.10 Average invasion per day over 15 days for N071271. The deviations represent measurements over 15 days. Standard deviations were generated from Microsoft Excel software.

Erlotinib had a small inhibitory effect on the invasion of N071271, docetaxel had a stronger effect, gefitinib had a very strong effect; both imatinib and temozolomide substantially increased invasion (Fig. 3.4.10).

Table 3.4.10 Drug concentrations N080869.

Drug	Invasion Assay Concentration	IC_{50} Concentration Proliferation Assay
Erlotinib	20 µM	>10 µM
Gefitinib	44.8 µM	>20 µM
Imatinib	40.7 µM	14 µM
Temozolomide	1236.1 µM	763.8 µM
Docetaxel	29 nM	19 nM

>: greater than cut-off concentration (IC_{50} not determined).

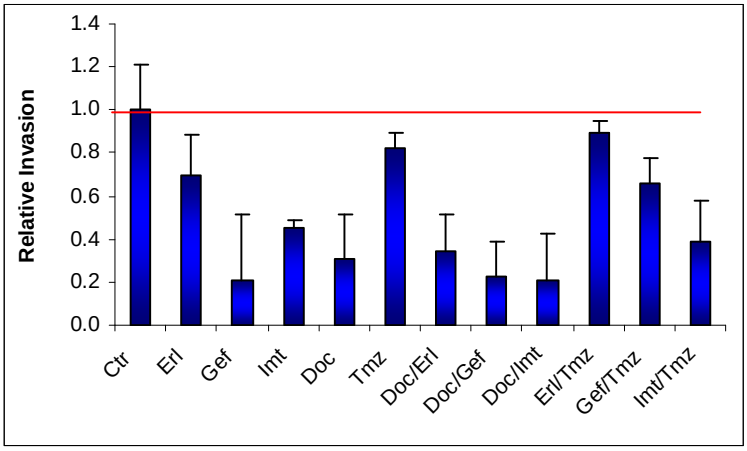

Fig. 3.4.11 Average invasion per day over 15 days for N080869. The deviations represent measurements over 15 days. Standard deviations were generated from Microsoft Excel software.

Gefitinib, imatinib and docetaxel had a strong inhibitory effect on the invasion of N080869, erlotinib and temozolomide had a small effect (Fig. 3.4.11).

Table 3.4.11 Drug concentrations N080943.

Drug	Invasion Assay Concentration	IC_{50} Concentration Proliferation Assay
Erlotinib	20 μM	>10 μM
Gefitinib	44.8 μM	>20 μM
Imatinib	40.7 μM	>20 μM
Temozolomide	1854.2 μM	877.3 μM
Docetaxel	13.9 nM	9 nM

>: greater than cut-off concentration (IC_{50} not determined).

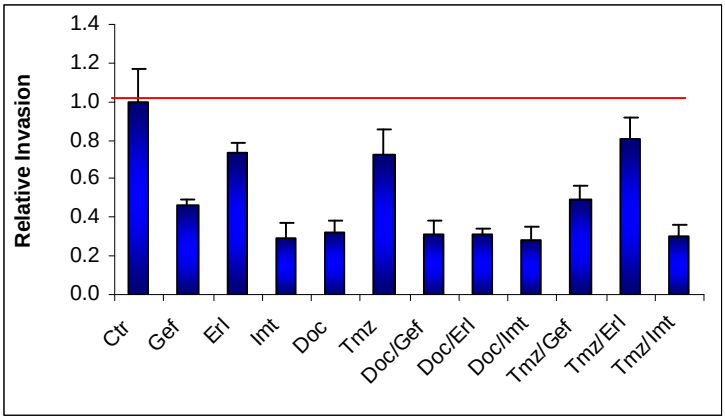

Fig. 3.4.12 Average invasion per day over 15 days for N080943. The deviations represent measurements over 15 days. Standard deviations were generated from Microsoft Excel software.

Single drug treatments of gefitinib, imatinib and docetaxel had the strongest inhibitory effect on the invasion of N080943, erlotinib and temozolomide had a small effect (Fig. 3.4.12).

Table 3.4.12 Summary of drug effects on invasion activity of primary glioblastomas.

Cell Culture	Erl	Gef	Imt	Tmz	Doc	Erl/ Tmz	Erl/ Doc	Gef/ Tmz	Gef/ Doc	Imt/ Tmz	Imt/ Doc
N061007	0.9	1.9	0.7	1.0	0.8	0.9	0.6	1.4	1.2	0.9	0.6
N061092	0.5	0.2	0.3	1.3	0.4	0.9	0.4	0.2	0.2	-	0.1
N070152	0.7	0.3	0.3	0.9	0.4	-	0.4	0.3	0.2	-	0.3
N070454	0.5	0.8	0.7	0.7	0.2	0.2	0.2	0.3	0.3	-	0.1
N070859	0.7	0.5	0.2	0.8	0.4	0.8	0.4	0.9	0.4	0.5	0.2
N070865	0.8	0.6	0.5	0.7	0.5	0.7	0.5	0.5	0.5	0.6	0.5
N071026	0.6	0.5	0.4	0.7	0.3	0.8	0.4	0.5	0.3	0.3	0.2
N071144	0.8	0.8	0.2	1.0	0.3	0.6	0.3	0.7	0.2	0.3	0.2
N071271	0.8	0.3	1.4	1.3	0.6	-	0.8	-	0.5	-	0.8
N080869	0.7	0.2	0.5	0.8	0.3	0.9	0.3	0.7	0.2	0.4	0.2
N080943	0.7	0.5	0.3	0.7	0.3	0.8	0.3	0.5	0.3	0.3	0.3

The effect of drug treatment on invasion activity was compared to the control (1.0). The most effective single drug treatments are highlighted in blue. The combination treatments which had an increased inhibitory effect on invasion in comparison to either drug alone are highlighted in red. Erl: erlotinib, Gef: gefitinb, Imt: imatinib, Tmz: temozolomide, Doc: docetaxel.

Overall the most effective single drug treatment with the primary glioblastomas was imatinib. The most effective drug combination treatment was with imatinib and docetaxel.

3.4.2 Drug Effect on Invasion Activity of Secondary Glioblastomas

Table 3.4.13 Drug concentrations N060893.

Drug	Invasion Assay Concentration	IC_{50} Concentration Proliferation Assay
Erlotinib	15.3 µM	>10 µM
Gefitinib	33.5 µM	16.8µM
Imatinib	49.4 µM	>20 µM
Temozolomide	2334.2 µM	1146 µM
Docetaxel	1.6 nM	1.6 nM

>: greater than cut-off concentration (IC_{50} not determined).

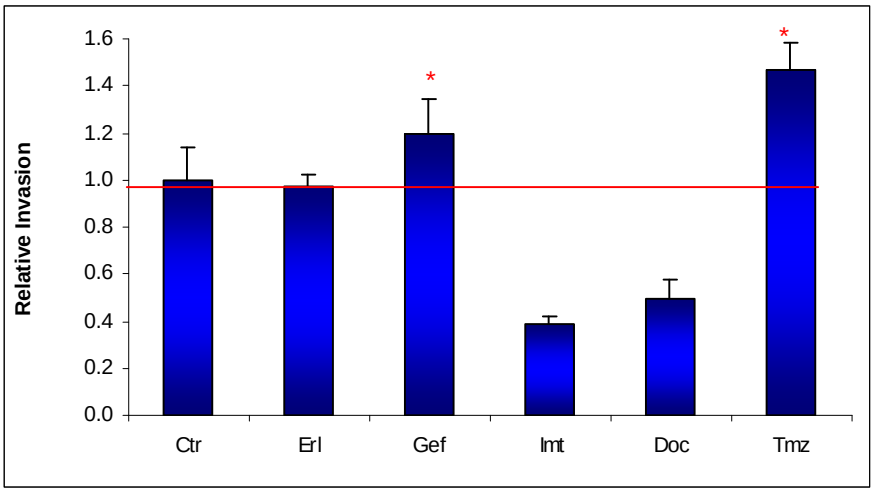

*: increased invasion.

Fig. 3.4.13 Average invasion per day over 26 days for N060893. The deviations represent measurements over 26 days. Standard deviations were generated from Microsoft Excel software.

Imatinib and docetaxel had a strong inhibitory effect on the invasion of N060893, erlotinib had no effect, gefitinib increased invasion and temozolomide strongly increased invasion (Fig. 3.4.13).

Table 3.4.14 Drug concentrations N070701.

Drug	Invasion Assay Concentration	IC_{50} Concentration Proliferation Assay
Erlotinib	23.2 μM	7.9 μM
Gefitinib	27.8 μM	16.7μM
Imatinib	50.8 μM	14.4 μM
Temozolomide	1545.2 μM	772.6 μM
Docetaxel	1.6 nM	1 nM

>: greater than cut-off concentration (IC_{50} not determined).

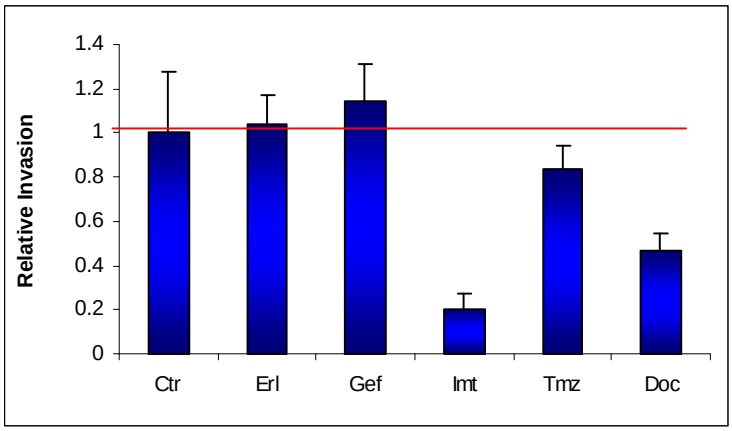

Fig. 3.4.14 Average invasion per day over 24 days for N070701. The deviations represent measurements over 24 days. Standard deviations were generated from Microsoft Excel software.

Imatinib and docetaxel had the strongest inhibitory effect on the invasion of N070701, temozolomide had a small effect, gefitinib increased invasion.

Table 3.4.15 Drug effects on invasion activity of secondary glioblastomas.

Cell Culture	Erl	Gef	Imt	Tmz	Doc
N060893	1.0	1.2	0.4	1.5	0.5
N070701	1.0	1.1	0.2	0.8	0.5

Drug treated spheroids were compared to the control (1.0), imatinib showed the most inhibition of invasion. The treatments which had the strongest inhibitory effect on invasion are highlighted in blue. Erl: erlotinib, Gef: gefitinb, Imt: imatinib, Tmz: temozolomide, Doc: docetaxel.

Erlotinib had no effect on the invasion of both secondary glioblastomas; gefitinib increased invasion. Imatinib had a strong inhibitory effect with both secondary glioblastomas.

3.4.3 Drugs Effect on Invasion Activity of Astrocytomas and an Oligoastrocytoma

Table 3.4.16 Drug concentrations N070229 (grade III astrocytoma).

Drug	Invasion Assay Concentration	IC_{50} Concentration Proliferation Assay
Erlotinib	79 μM	>10 μM
Gefitinib	58.3 μM	>20 μM
Imatinib	67.8 μM	>20 μM
Temozolomide	1030.1 μM	1055.9 μM
Docetaxel	4.6 nM	9.4 nM

>: greater than cut-off concentration (IC_{50} not determined).

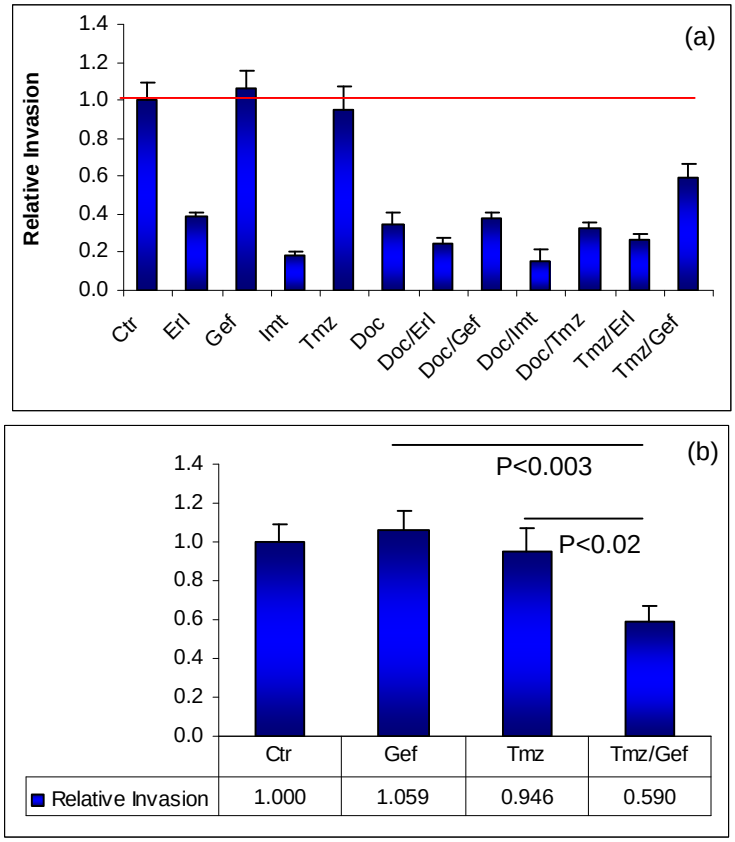

Fig. 3.4.15 (a) Average invasion per day over 15 days for N070229 (b) significance of combination effect of gefitinib and temozolomide compared to single drug effect. The deviations represent measurements over 15 days. Standard deviations were generated from Microsoft Excel software.

Erlotinib, imatinib and docetaxel had a very strong inhibitory effect on the invasion of N070229, temozolomide had very little effect and gefitinib had no effect (Fig. 3.4.15 (a)). The combination of gefitinib and temozolomide had increased inhibitory effect on invasion (Fig. 3.4.15 (b)).

Table 3.4.17 Drug concentrations N070450 (grade II astrocytoma).

Drug	Invasion Assay Concentration	IC_{50} Concentration Proliferation Assay
Erlotinib	23.2 µM	>10 µM
Gefitinib	44.8 µM	>20 µM
Imatinib	33.9 µM	15.8 µM
Temozolomide	1287.6 µM	888.5 µM
Docetaxel	11.6 nM	8.3 nM

>: greater than cut-off concentration (IC_{50} not determined).

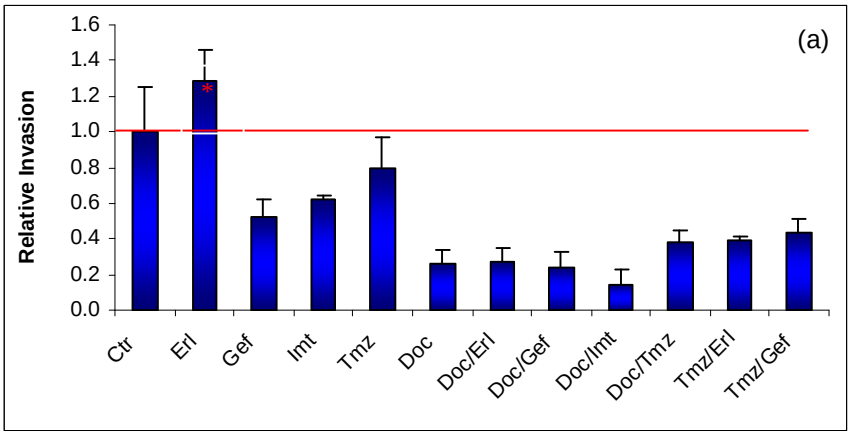

*: increased invasion.

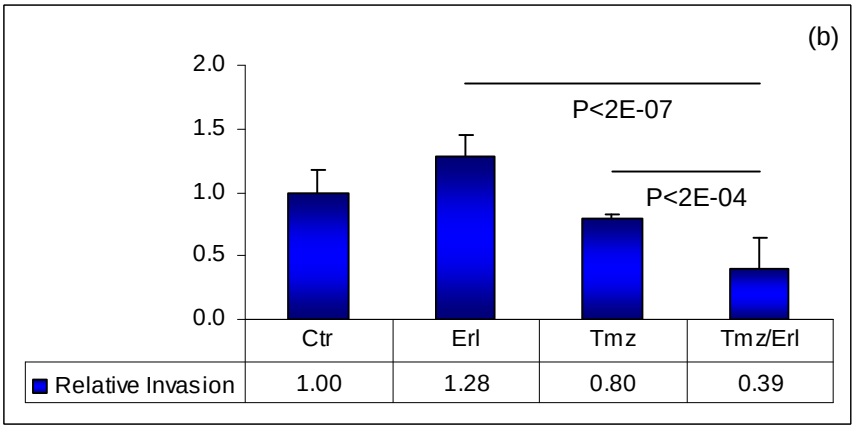

Fig. 3.4.16 (a) Average invasion per day over 15 for N070450, (b) significance of combination effect of erlotinib and temozolomide compared to single drug effect. The deviations represent measurements over 15 days. Standard deviations were generated from Microsoft Excel software.

Gefitinib and imatinib had a strong inhibitory effect on the invasion of N070450, docetaxel had a very strong effect (Fig. 3.4.16 (a)). The combination of erlotinib and temozolomide had an increased effect with significant p-values less than 0.05 (Fig. 3.4.16 (b)).

Table 3.4.18 Drug concentrations N070055 (grade III oligoastrocytoma).

Drug	Invasion Assay Concentration	IC_{50} Concentration Proliferation Assay
Erlotinib	18.6 μM	9.3 μM
Gefitinib	44.8 μM	>20 μM
Imatinib	33.9 μM	18 μM
Temozolomide	1030.1 μM	417.2 μM
Docetaxel	4.6 nM	2.7 nM

>: greater than cut-off concentration (IC_{50} not determined).

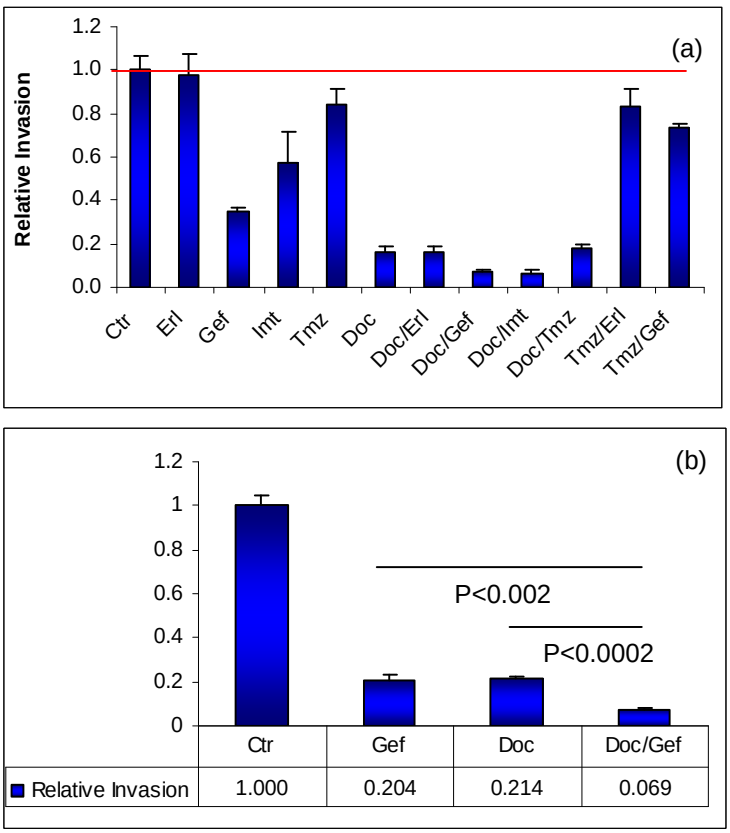

Fig. 3.4.17 (a) Average invasion per day over 29 days for N070055, (b) significance of combination effect of docetaxel and gefitinib compared to single drug effect. The deviations represent measurements over 29 days. Standard deviations were generated from Microsoft Excel software.

Gefitinib and imatinib had a strong inhibitory effect on the invasion of N070055, docetaxel had the strongest effect (Fig. 3.4.17 (a)). The combination of gefitinib and docetaxel had an increased inhibitory effect with significant p-values less than 0.05 (Fig. 3.4.17 (b)).

Table 3.4.19 Drug effects on invasion activity of astrocytomas and an oligoastrocytoma.

Cell Culture	Erl	Gef	Imt	Tmz	Doc	Erl/ Tmz	Erl/ Doc	Gef/ Tmz	Gef/ Doc	Imt/ Tmz	Imt/ Doc
N070229	0.4	1.1	0.2	0.9	0.3	0.3	0.2	0.6	0.4	-	0.2
N070450	1.3	0.5	0.6	0.8	0.3	0.4	0.3	0.4	0.2	-	0.1
N070055	1.0	0.3	0.6	0.8	0.2	0.8	0.2	0.7	0.1	-	0.1

N070229 and N070450: grade III astrocytoma. N070055: Oligoastrocytoma.
The inhibitory effect of each drug treatment on invasion was measured in comparison to the control (1.0), the most effective single drug treatments are highlighted in blue. The combination treatments which had an increased effect on invasion in comparison to either drug alone are highlighted in red. Erl: erlotinib, Gef: gefitinb, Imt: imatinib, Tmz: temozolomide, Doc: docetaxel.

Imatinib and docetaxel were the most effective single drug treatments with the astrocytomas and the oligoastrocytoma, while the most effective combination treatment was imatinib and docetaxel (Table 3.4.19).

3.4 Discussion

Effect of Tyrosine Kinase Inhibitors and Chemotherapeutic Drugs on Invasion in Glioma

Introduction

Very little information is available on the direct effect of TKIs and chemotherapeutic drugs on glioma invasion. Therefore the effect of these drugs individually and in combination on the newly established glioma cultures, was examined using a 3D collagen invasion assay. Some of the pathways known to be involved in glioma invasion include the RAS/MAPK pathway and the PI3K/Akt pathway. RAS is activated by receptor tyrosine kinases, including EGFR, PDGFR, other growth factor receptors and cytokines (Gullick 2008). Overactivation of the RAS/MAPK pathway can increase cellular proliferation, migration and differentiation in several types of cancers including gliomas (Schlessinger 1993). The PI3K/Akt pathway is also stimulated by the growth factor receptors, EGFR, PDGFR, fibroblast growth factor receptor (FGFR) and insulin-like growth factor receptor (IGFR) and promotes cell survival, regulates EGF-driven cell motility and invasion of glioma, breast, and bladder cancer cell lines (Schlessinger 2000). About 50% of glioblastomas overexpress EGFR (Omuro *et al.* 2007). A mutated form, EGFRvIII, has been found in 24 to 67% of glioblastomas. EGFRvIII is constitutively activated in and is involved in response to TKIs (Heimberger *et al.* 2005) PDGFR is overexpresed in about 25% of glioblastoma and 60% of astrocytomas (Haberler *et al.* 2006). Besides inhibing growth factor signalling, TKIs reduce matrix metalloproteinase (MMP) expression and activity, which has a negative effect on the invasive and infiltrative behaviour of tumour cells (Newton 2004). Tumour cell-secreted MMPs and serine proteinases degrade extracellular matrix (ECM) proteins and provide space for movement and infiltration. Which mediates invasion in glioma through the induction of membrane type 1-MMP (Van Meter *et al.* 2004).

To date single drug treatments with TKIs or chemotherapeutic drugs has shown little improvement in glioma treatment, therefore combinations of TKIs and

chemotherapeutic drugs were tested in this project expecting an increased inhibitory effect on glioma invasion. The effect of TKIs on invasion of newly developed glioma cultures was examined using erlotinib and gefitinib, which specifically target EGFR, and imatinib which targets PDGFR/C-Kit/ and C-Abl.

In a previous section it has been shown that imatinib and docetaxel acted synergistically on 3 out of 4 glioma cell cultures and significantly decreased invasion in a 3D spheroid invasion assay (Kinsella *et al.* 2010). This result, however, could not be reproduced in early passage glioma cultures using the same assay. This could be due to heterogeneity of early passage cultures, possibly including stem-like cells.

Response rates of glioblastoma patients to TKIs which specifically target EGFR has been low, with 10-20% of glioblastoma patients responding to erlotinib and gefitinib (Mellinghoff *et al.* 2005). Haberler *et al*, found a 15.7% imatinib response rate in patients with glioblastoma (Haberler *et al.* 2006). There are ongoing clinical trials in glioblastoma patients with erlotinib and chemotherapeutic drugs , however it may also be necessary to look at the effectiveness of some multiple targeting TKIs such as sunitinib which is showing promising results in glioma cells (Giannopoulou *et al.* 2010). Sunitinib specifically targets the growth factors PDGFR and VEGFR, it has shown strong antiangiogenic and antitumour activity in renal gastrointestinal and neuroendrocrine cancer cell lines (Abrams *et al.* 2003; Adams and Leggas 2007; Cuneo *et al.* 2008). Dasatinib is another TKI which specifically targets EGFR and SRC, SRC plays a key role in invasion through focal adhesion kinase (FAK) in glioblastoma, Milano *et al*, have shown dasatinib to be more effective in glioblastoma that were PTEN negative (Milano *et al.* 2009).

It is believed that by combining TKIs and chemotherapeutic drugs this might improve patient outcome in glioma. In a phase II study Prados *et al*, found that a combination of erlotinib and temozolomide together with radiotherapy in patients with glioblastoma and gliosarcoma; resulted in 19.3 months median survival in comparison to the control group with a median survival of 14.1 months (Prados *et al.* 2009). Longer survival was correlated with O^6-methylguanine-DNA methyltransfease (MGMT) promotor methylation and functional PTEN (Prados *et*

al. 2009). Van den Bent *et al*, examined a phase II trial in 110 recurrent glioblastoma patients who received prior radiotherapy, looking at erlotinib treatment in comparison to temozolomide or carmustine (BCNU) (van den Bent *et al.* 2009). There was no increase in survival, with erlotinib treatment they found an 11.4% 6 month progression free survival, and in the control arm it was 24%, only low phosphorylated Akt expression had a low correlation with improved outcome, and none of the patients with EGFRvIII mutant presence and PTEN expression had 6 month progression free survival (van den Bent *et al.* 2009). However Mellinghoff *et al*, correlated co-expression of EGFRvIII and PTEN in tumour cells with responsiveness to EGFR kinase inhibitors, erlotinib and gefitinib (Mellinghoff *et al.* 2005). There are several glioma therapies currently in clinical trial phase; a phase II trial involving the PDGFR kinase inhibitor nilotinib which targets BCR-ABL in recurrent malignant gliomas, a phase II trial involving the TKI dasatinib targeting PDGFR and SRC kinase in recurrent glioblastoma patients, and a phase III trial involving temozolomide in combination with bevacizumab, an antibody which targets VEGF in patients with newly diagnosed glioblastoma or gliosarcoma .

Effect of Temozolomide on Glioma Invasion

Temozolomide is an alkylating drug, which causes DNA methylation at the O6 position of guanine and crosslinks between DNA strands, which results in cell death. Temozolomide is currently the first line chemotherapeutic drug for glioblastomas, resulting in a median survival of around 16 months (Stupp *et al.* 2002). However, tested on the majority of cell cultures it had a 10 to 30% inhibitory effect on glioma invasion (Figs. 3.4.2 to 3.4.17). Surprisingly, temozolomide increased invasion activity in 4 cell cultures (Figs. 3.4.2, 3.4.3, 3.4.10, 3.4.13), which needs to be further assessed. Improved clinical outcome after temozolomide treatment has been associated with promoter methylation of MGMT (or loss of MGMT) and Loss of Heterozygosity (LOH) of 1p and 19q in patients with glioblastoma, anaplastic astrocytoma and oligoastrocytomas. The DNA repair enzyme MGMT reverses the alkylating effect of temozolomide, resulting in increased resistance to temozolomide (Ishii *et al.* 2007). Temozolomide treatment in glioblastoma patients, who have the

methylated MGMT promoter has been promising, and has shown an increase in progression free survival (PFS), PFS and overall survival were longer in patients with tumours with MGMT promoter methylation (13.4 and 23.2 months) *versus* those without MGMT promoter methylation (3.4 and 13.1 months) (Stupp *et al.* 2010). The allelic losses of 1p and 19q are associated with sensitivity of brain tumours to radiotherapy and chemotherapy (Ishii *et al.* 2007). In particular, LOH in 1p and promoter methylation of MGMT was associated with longer progression free survival in glioma (Ishii *et al.* 2007). It is possible the glioblastomas whose invasion was not affected by temozolomide or in fact increased, could have expression of MGMT, allowing them to repair the DNA damage caused by temozolomide; the presence of MGMT needs to be tested in these cultures to clarify this. It is also possible that these early passage cultures contain populations of stem cells, these cells are known to be resistant to chemotherapy and radiation (as discussed in section 2) (Bao *et al.* 2006; Chua *et al.* 2008). The expression of MGMT and the detection of LOH of 1p19q in the glioma cell cultures may explain the resistance to temozolomide, it would also be interesting to check for the stem cell marker CD133, to check for the presence of stem cells in the cultures.

Using an established glioma cell line, U87MG, Gunther *et al*, showed found an IC_{50} of 50 μM with temozolomide after 8 days (Gunther *et al.* 2003), in the present study an established cell line SNB-19 had an IC_{50} with temozolomide of 30 μM after 7 days, and with the low passage glioma cultures the IC_{50} results for temozoloimde were much higher ranging from 198.3 to 1146 μM. It appears that early passage glioma cultures are a lot more resistant to temozolomide than glioma cell lines. This could explain why temozolomide treatment is not as clinically effective as *in vitro* results appear.

Others have found an improvement with temozolomide treatment by combining it with other inhibitors. Demuth *et al,* 2007 found that inhibition of mitogen-activated protein kinase (MAPK) kinase 3 (MKK3) signalling through a novel treatment combination of p38 inhibitor plus temozolomide heightens the vulnerability of glioma to chemotherapy (Demuth *et al.* 2007). They also found that members of the MAPK family are strong promoters of tumour invasion,

progression, and therefore associated with poor patient survival (Demuth *et al.* 2007). Dasatinib targets drug-resistant tumours with mutant BCR-ABL, KIT, and EGFR by blocking tyrosine phosphorylation sites that are critical in tumorigenesis. Milano *et al*, found that levels of phosphorylated SRC, AKT, and ribosomal protein S6 were decreased in cell lines treated with low nanomolar concentrations of dasatinib at baseline and following stimulation with EGF (Milano *et al.* 2009). An increased sensitivity to dasatinib was noted in glioma cells with functional PTEN (Milano *et al.* 2009) and their invasive potential was reduced in the presence of dasatinib. A combination of glioma cells with dasatinib and temozolomide resulted in a significant increase in cell cycle disruption and autophagic cell death (Milano *et al.* 2009).

Effect of Docetaxel on Glioma Invasion

Docetaxel strongly inhibited the invasion activity of most cell cultures (Fig. 3.4.2 to 3.4.17). In a previous section it has also been shown that docetaxel also strongly inhibits proliferation in glioma, possibly showing docetaxel to be a very effective chemotherapeutic drug for treating glioma (section 3). Docetaxel is a cytotoxic taxane that inhibits depolymerisation of microtubules, thereby interrupting cell proliferation and inhibiting cell motility (Bissery *et al.* 1995). Docetaxel is used in the treatment of various forms of cancer and is one of the most effective chemotherapeutic agents for non-small cell lung cancer (Burris *et al.* 1995). As second line treatment in phase II trials in recurrent glioblastoma, systemic docetaxel showed very little response which is probably due to the poor penetration of the BBB (Forsyth *et al.* 1996; Kemper *et al.* 2003; Kemper *et al.* 2004). Local delivery of docetaxel in an animal model resulted in a significant improvement in survival (Sampath *et al.* 2006).

Kogashiwa *et al*, showed that docetaxel suppressed filopodia formation in head and neck cancer, and suppressed two-dimensional (2D) cell migration and 3D cell invasion by decreasing Cdc42 activities in HEp-2 cells (Kogashiwa *et al.* 2010). Actin filament polymerization, elongation, and contraction, are thought to provide the major driving forces for cell migration (Ridley *et al.* 2003). Cdc42 controls the

polarity of actin in the microtubules through distinct signal transduction pathways (Cau and Hall 2005). Abnormal tubulin bundles induced by docetaxel may lead to suppression of Cdc42 and decreased transport of Cdc42 to the plasma membrane (Kogashiwa *et al.* 2010). Decreased Cdc42 activity was likely to affect actin filament formation, resulting in decreased filopodia. These results suggest that docetaxel treatment has the benefit of reducing local invasion in addition to its ability to cause apoptosis.

Effect of Erlotinib and Gefitinib on Glioma Invasion

Overall erlotinib and gefitinib as a single drug treatments did not have a strong effect on invasion (Fig. 3.4.2 to 3.4.17), while in 3 cultures the combination of erlotinib with docetaxel (Fig. 3.4.2) or with temozolomide (Figs. 3.4.5 and 3.4.16) was more potent than each drug alone. Gefitinib even increased invasion in 4 high-grade glioma cultures (Figs. 3.4.2, 3.4.13, 3.4.14, and 3.4.15). A combination of temozolomide and gefitinib inhibited invasion activity of 2 cultures by 43% and 36% (Figs. 3.4.5 and 3.4.15); which might be due to the presence of methylated MGMT making them more sensitive to temozolomide.

Inhibition of EGFR alone may not be sufficient to inhibit invasion in glioma. Mutated forms of EGFR, i.e. EGFRvIII (Haas-Kogan *et al.* 2005) and other growth factors such as PDGFR and VEGFR (Schlessinger 2000) may have a more significant role to play in cell survival and invasion. Bevacizumab, a monoclonal antibody targeting VEGFR is showing promising results in glioma (Friedman *et al.* 2009; Kreisl *et al.* 2009). Erlotinib is currently being combined with dasatinib in a phase I/II clinical trial in advanced NSCLC patients (Haura *et al.* 2010). Dasatinib specifically targets Src family kinase (SFK) proteins which are activated in cancer and coordinate growth, survival, invasion, and angiogenesis. It is known that Src kinase and EGFR signalling is coordinated, therefore it may be more effective to target both pathways in patients with advanced non-small-cell lung cancer, and possibly also in other cancers including glioma.

Guillamo *et al*, used a panel of six human malignant gliomas from established xenografts and showed that gefitinib reduced cell invasion in EGFR

amplified tumours and PTEN LOH seemed to be a determinant of resistance. They have also shown that inhibition of angiogenesis by gefitinib seems independent of EGFR (Guillamo *et al.* 2009). All cultures tested in this study express EGFR (section 3.4) and PTEN; however it is not clear if PTEN is mutated resulting in loss of function, making the cultures resistant to gefitinib. Mellinghoff *et al*, examined the effect of erlotinib and gefitinib in 49 patients with recurrent malignant glioma, and found only a 10-20% response which was correlated response with the co-expression of EGFRvIII and PTEN (Mellinghoff *et al.* 2005).

Gefitinib has been shown to be effective in lung cancer patients carrying mutations in exons 19 and 21 of the EGFR tyrosine kinase domain. These mutations were not found in a study involving 95 gliomas including glioblastomas, anaplastic oligodendrogliomas, and low-grade gliomas, which might explain the limited success of gefitinib in glioma treatment (Marie *et al.* 2005). There have been some encouraging results with TKIs and chemotherapeutic drugs in non-small cell lung cancer (NSCLC), however response appears to be due to specific activated EGFR mutations (Mack *et al.* 2009). Mack *et al*, have shown that activating mutations in the EGFR are associated with enhanced response to EGFR tyrosine kinase inhibitors in NSCLC, whereas KRAS mutations translate into poor patient outcomes (Mack *et al.* 2009). They found EGFR mutations in 10 of 49 patients (20%), six (12%) had single activating mutations in EGFR, associated with improved progression-free survival (median, 18.3 months), four patients had a *de novo* T790M resistance mutation (median progression-free survival, 3.9 months) (Mack *et al.* 2009). KRAS mutations were detected in two patients, both of whom had rapid progressive disease (Mack *et al.* 2009), which may not be present in all cancers.

Effect of Imatinib on Glioma Invasion

Most of the cultures tested express PDGFR-β, C-abl and C-Kit. Imatinib as a single drug had a strong inhibitory effect on invasion in most cell cultures (Fig. 3.4.2 to 3.4.17), which is promising, imatinib blocks invasion through PDGFR inhibition (Aoki *et al.* 2007; Abouantoun and Macdonald 2009). It has been reported that small amounts of imatinib in the plasma can cross the BBB (Bihorel *et al.* 2007), this

could possibly be overcome by treatments such as convection enhanced delivery which bypasses the BBB (Chamberlain 2006). Imatinib combined with docetaxel decreased invasion by an additional 14% in one glioblastoma cell culture (Fig. 3.4.3). In a previous section it has been shown that the combination of imatinib and docetaxel produces a strong apoptotic effect in glioma cell cultures as well as decreasing proliferation and invasion in glioma. Docetaxel causes G2/M cell cycle arrest (Gucluler and Baran 2009) and imatinib induces cell cycle arrest at the G0-G1 or G2/M phase in glioma cells (Ren *et al.* 2009). As imatinib and docetaxel individually strongly inhibit invasion in these newly established glioma cell cultures, it would be interesting to see if a combined effect of both drugs would also strongly inhibit proliferation with each culture.

Angiogenesis is an important hallmark of glioblastomas involving microvascular proliferation (Paul Kleihues 1997), this process is initiated by growth factors including VEGF, FGF and PDGF which activate several pathways controlling glioma formation. Abouantoun and Macdonald, have shown that PDGFRB tyrosine kinase activity is critical for migration and invasion of medulloblastoma cells possibly by transactivating EGFR (Abouantoun and Macdonald 2009). Aoki *et al*, have shown that PDGF-BB enhanced the invasive activity of malignant peripheral nerve sheath tumour cells schwannomas and neurofibromas through PDGFR phosphorylation which can be inhibited by imatinib (Aoki *et al.* 2007).

3.4 Summary and Conclusion

Overall with the glioma cultures, there was not a strong increased effect on inhibition of invasion with the TKIs erlotinib, gefitinib and imatinib combined with the chemotherapeutic drugs docetaxel or temozolomide. Temozolomide showed some inhibition of invasion in some of the glioma cultures however, it was worrying to see that temozolomide increased invasion in 4 of the cultures. Docetaxel treatment on the other hand had a very strong inhibitory effect on invasion with the majority of the cultures. It was shown previously that docetaxel also inhibits proliferation in these cultures; possibly indicating that docetaxel would be a more effective chemotherapeutic drug for glioma than temozolomide. Erlotinib and gefitinib had a weak inhibitory effect on invasion of the cultures. Imatinib had a strong inhibitory effect on glioma cultures.

It is possible that single drug treatments of either imatinib or docetaxel may have a strong inhibitory effect on glioma invasion, using convection enhanced delivery to overcome the BBB.

3.5 Expression of Protein Targeted by TKIs in High-Grade Glioma, in relation to their response to these Inhibitors

As previously mentioned glioma cultures were generated from tumour biopsy samples. In collaboration with Rachel Howley, a Ph.D student from Beaumont hospital, Dublin, 26 high-grade gliomas were choosen (20 glioblastomas, 2 secondary glioblastomas, and 4 grade III astrocytomas) to analyse the correlation between responsiveness to TKIs and the expression of specific protein targets of the PI3K/Akt pathway which are targeted by tyrosine kinase inhibitors. Rachel carried out immunocytochemical analysis with each culture. The expression of these targets was examined in each individual culture (Figs. 3.5.6-28). The targets included PDGFR-α, PDGFR-β, phosphorylated C-Abl (p-C-Abl), phosphorylated C-Kit (p-C-Kit), all of which are specific targets of imatinib; EGFR and EGFRvIII, specific targets of erlotinib and gefitinib; and some downstream targets of EGFR and PDGFR including phosphorylated Akt (p-Akt), the tumour suppressor gene PTEN and a downstream protein of MTOR phosphorylated p70S6K (p-p70S6K). The expression of each target protein was given an immunocytochemical score (see section 2.12.4). The overall expression levels in the cultures were 92.3% PDGFR-α and PDGFR-β, 61.5% for p-C-Abl, 61.5% for p-C-Kit, 88.4% for EGFR, 65.3% for p-Akt, 84.6% for p-p70S6K and 100% for PTEN.

The age profile of these patients was between 22 to 78 years, and survival ranged from 1 month to several years (Table 3.5.1). Figure 3.5.1 shows the Kaplan Meier graph for survival data. The lowest survival time was seen with the primary glioblastomas, the secondary glioblastomas and the grade III astrocytomas had a longer survival time.

Table 3.5.1 Patient age, gender and survival time.

Cell Culture	Tumour Type	Age at onset	Gender	Survival Time (months)
N060913	Primary Glioblastoma	67	F	10
N060978	Primary Glioblastoma	54	F	3
N061007	Primary Glioblastoma	75	M	1
N061092	Primary Glioblastoma	78	M	6
N070126	Primary Glioblastoma	56	M	28
N070152	Primary Glioblastoma	52	M	5
N070293	Primary Glioblastoma	38	M	>36
5070454	Primary Glioblastoma	73	F	3
N070859	Primary Glioblastoma	55	M	12
N070865	Primary Glioblastoma	70	M	5
N071026	Primary Glioblastoma	46	M	10
N071144	Primary Glioblastoma	53	M	8
N071271	Primary Glioblastoma	59	M	11
N080501	Primary Glioblastoma	60	M	18
N080533	Primary Glioblastoma	55	F	15
N080540	Primary Glioblastoma	51	M	?>12
N080558	Primary Glioblastoma	64	M	5
N080869	Primary Glioblastoma	54	F	>20
N080923	Primary Glioblastoma	61	M	15
N080943	Primary Glioblastoma	62	F	>19
N060893	Secondary Glioblastoma	40	M	>138
N070701	Secondary Glioblastoma	39	F	>56
N070201	Grade III Astrocytoma	42	M	>36
N070229	Grade III Astrocytoma	22	M	>36
N070237	Grade III Astrocytoma	33	M	55
N070788	Grade III Astrocytoma	38	F	>31

?: we do not have the survival information for this patient post 12 months. >: greater than. M: male. F: female.

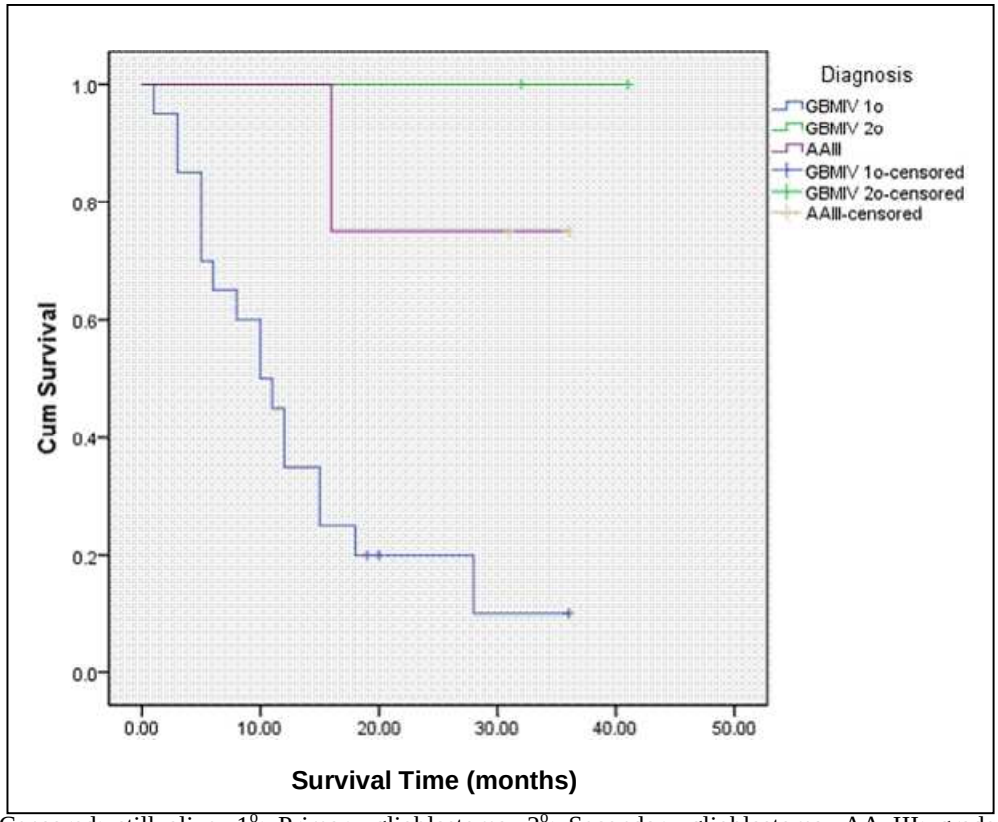

Censored: still alive. 1^{o}: Primary glioblastoma, 2^{o}: Secondary glioblastoma, AA III: grade III anaplastic astrocytoma. Cum: cumulative.

Fig. 3.5.1 Kaplan Meier graph showing the difference in survival time of the primary glioblastomas with secondary glioblastomas and grade III anaplastic astrocytomas used in our study. The cumulative survival was plotted on the y-axis with a value of 1 representing 100% of the cohort alive; with each death the line stepped down, a steeper drop represented a worse outcome. The vertical lines that cross each arm are patients still alive, and survival time is only known up to that point.

3.5.1 Response of High-Grade Gliomas to the TKIs

Using IC_{50} toxicity assays the cultures were classified as responders or non-responders to Erlotinib, gefitinib, and imatinib (see section 3.2.2). TKI responsiveness was classified as follows: if the IC_{50} concentrations for the culture was less than or equal to 10 μM for erlotinib, and 20 μM for both gefitinib and imatinib these were responders, non-responders had IC_{50} values greater than these concentrations. Of the 26 high-grade glioma cultures, 7 were non-responders to any of the TKIs tested, 3 responded to erlotinib, 6 to gefitinib, and 3 to imatinib (Table 3.5.2). There were also 4 which responded to both erlotinib and gefitinib, 1 to erlotinib and imatinib, 1 to gefitinib and imatinib, and 1 which responded to erlotinib, gefitinib and imatinib (Table 3.5.2). The ICC expression of specific protein targets of the PI3K/Akt pathway is shown for each individual culture; the cultures are grouped in regard to their TKI responsiveness (Figs. 3.5.29-44).

Table 3.5.2 Response of high-grade gliomas to the TKIs, erlotinib, gefitinib and imatinib.

Cell Culture	Tumour Type	Response to TKIs
N070229	Grade III Astrocytoma	Non-responder
N070237	Grade III Astrocytoma	Non-responder
N070788	Grade III Astrocytoma	Non-responder
N070859	Primary Glioblastoma	Non-responder
N070865	Primary Glioblastoma	Non-responder
N080558	Primary Glioblastoma	Non-responder
N080943	Primary Glioblastoma	Non-responder
N060913	Primary Glioblastoma	Erlotinib
N061007	Primary Glioblastoma	Erlotinib
N061092	Primary Glioblastoma	Erlotinib
N060893	Secondary Glioblastoma	Gefitinib
N070126	Primary Glioblastoma	Gefitinib
N070293	Primary Glioblastoma	Gefitinib
N071271	Primary Glioblastoma	Gefitinib
N080501	Primary Glioblastoma	Gefitinib
N080533	Primary Glioblastoma	Gefitinib
N060978	Primary Glioblastoma	Erlotinib & Gefitinib
N070152	Primary Glioblastoma	Erlotinib & Gefitinib
N071144	Primary Glioblastoma	Erlotinib & Gefitinib
N080923	Primary Glioblastoma	Erlotinib & Gefitinib
N070201	Grade III Astrocytoma	Erlotinib & Imatinib
N070454	Primary Glioblastoma	Imatinib
N071026	Primary Glioblastoma	Imatinib
N080869	Primary Glioblastoma	Imatinib
N080540	Primary Glioblastoma	Gefitinib & Imatinib
N070701	Secondary Glioblastoma	Erlotinib, Gefitinib & Imatinib

3.5.1 Non-Responders to Tyrosine Kinase Inhibitors

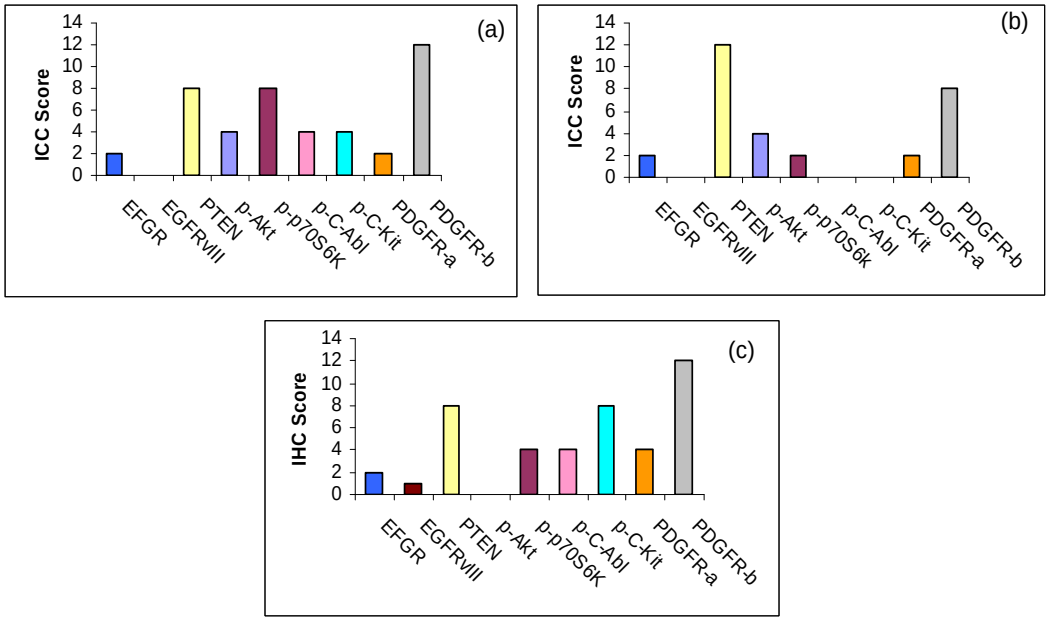

Fig. 3.5.2 PI3K/Akt pathway targets of 3 grade III astrocytomas N070229 (a), N070237 (b) and N070788 (c) which were non-responders to the TKIs.

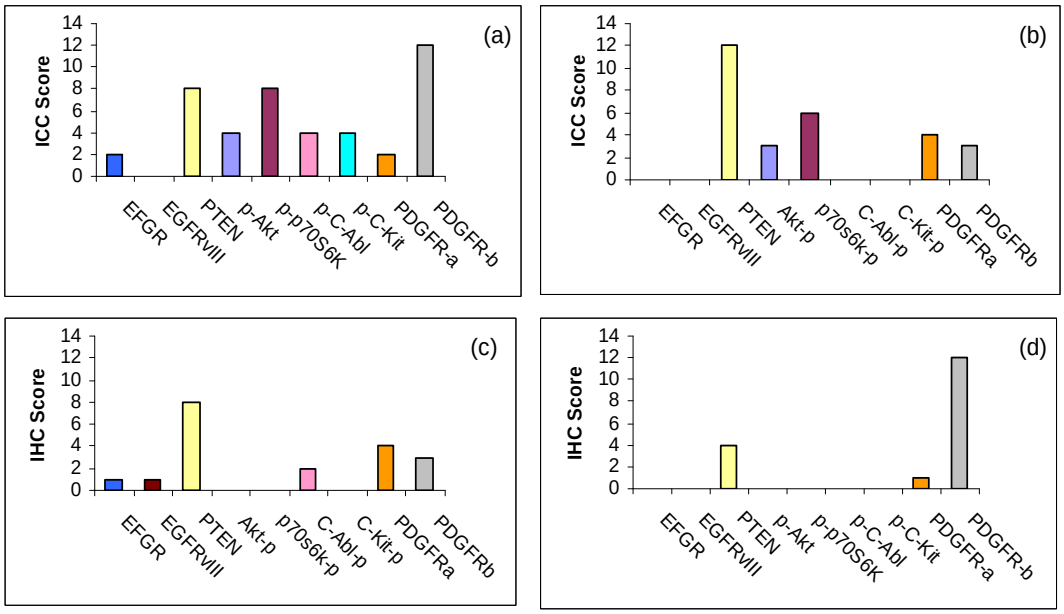

Fig. 3.5.3 PI3K/Akt pathway targets for 4 primary glioblastoma cultures N070865 (a), N080558 (b) N080943 (c) and N070859 (d) which were non-responders to the TKIs.

3.5.2 Erlotinib responders

Table 3.5.3 IC_{50} values of erlotinib for cultures which responded to erlotinib.

Cell Culture	IC_{50} for Erlotinib
N060913	7.2 μM
N061007	9.1 μM
N061092	9.3 μM

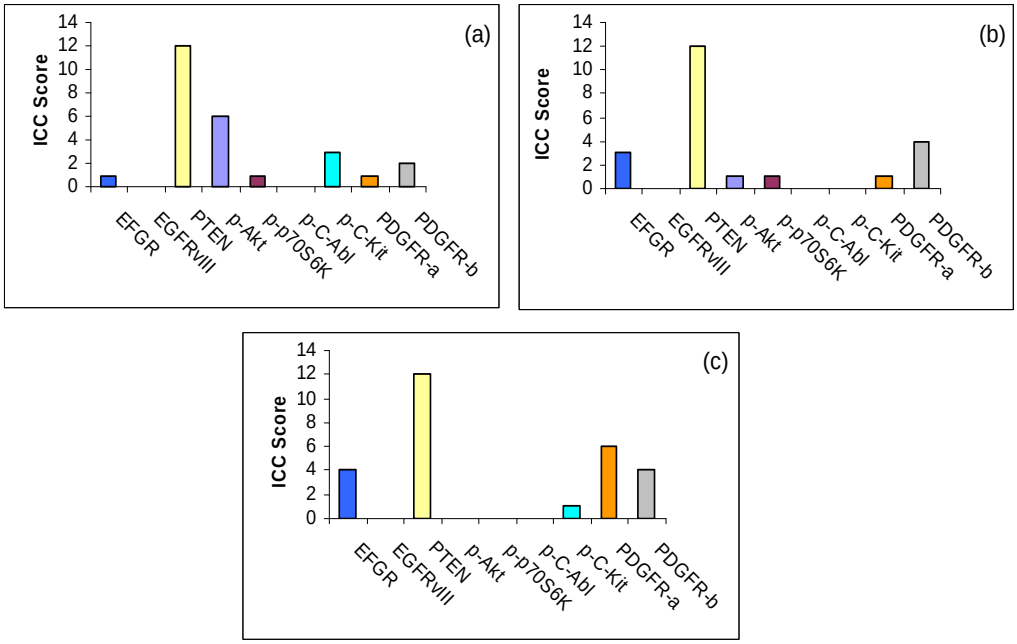

Fig. 3.5.4 PI3K/Akt pathway targets for 3 primary glioblastoma cultures N060913 (a), N061007 (b) and N061092 (c) which responded to erlotinib.

3.5.3 Gefitinib Responders

Table 3.5.4 IC_{50} values of gefitinib for cultures which responded to gefitinib.

Cell Culture	IC_{50} for Gefitinib
N060893	16.8 µM
N070126	20 µM
N070293	18.3 µM
N071271	16.7 µM
N080501	16.9 µM
N080533	16.7 µM

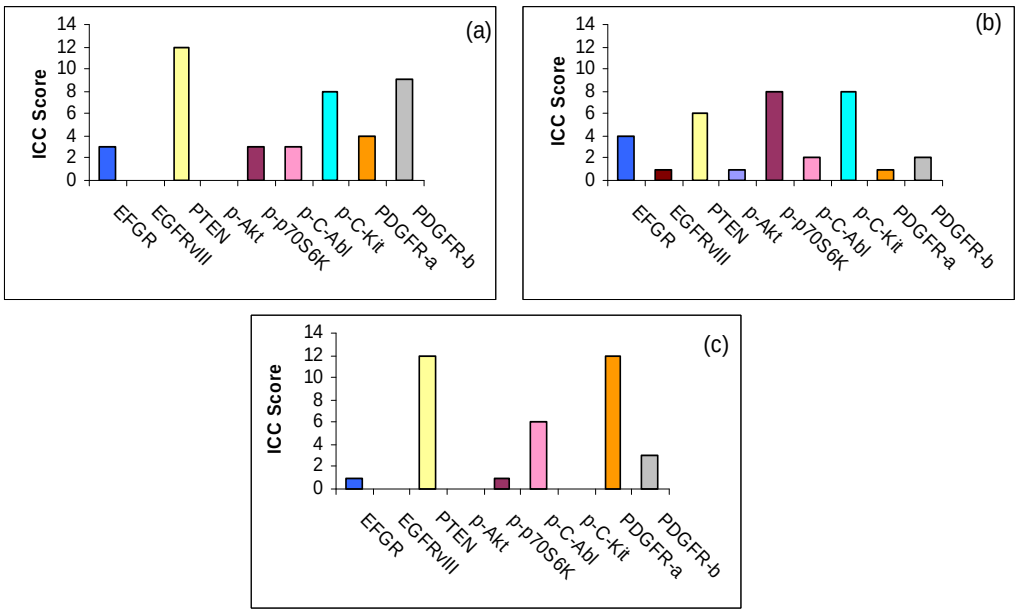

Fig. 3.5.5 PI3K/Akt pathway targets for a secondary glioblastoma N060893 (a), and 2 primary glioblastomas N070126 (b) and N070293 (c) which responded to gefitinib.

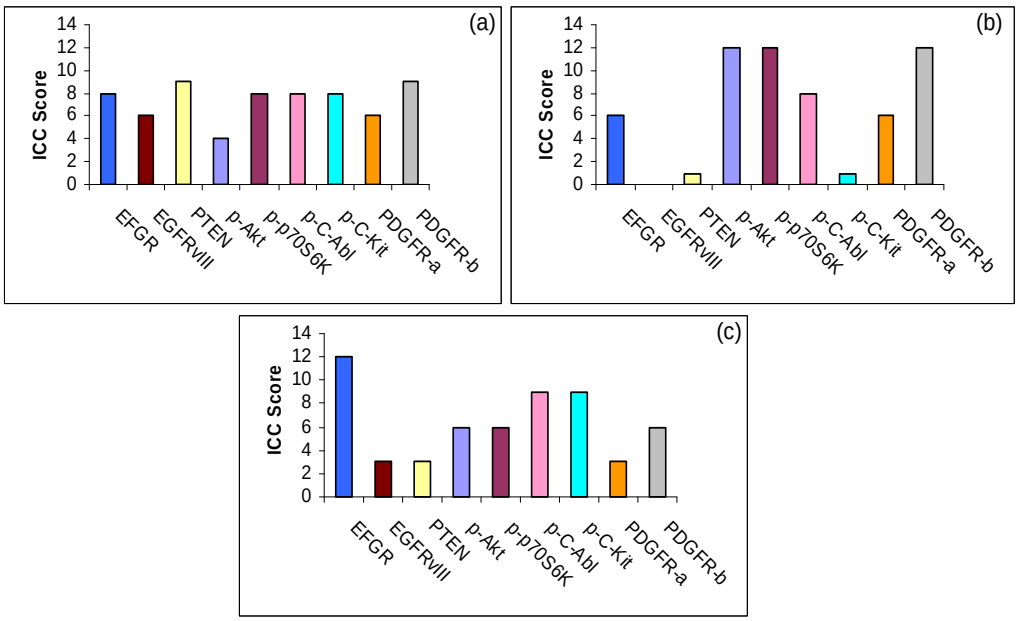

Fig. 3.5.6 PI3K/Akt pathway targets for 3 primary glioblastomas N071271 (a), N080501 (b), and N080533 (c) which responded to gefitinib.

3.5.4 Responders to Erlotinib and Gefitinib

Table 3.5.5 IC_{50} values of gefitinib and erlotinib for cultures which responded to erlotinib and gefitinib.

Cell Culture	IC_{50} for Erlotinib	IC_{50} for Gefitinib
N060978	9.5 µM	17.2 µM
N070152	6.5 µM	17 µM
N071144	9.3 µM	19.5 µM
N080923	7.2 µM	15.2 µM

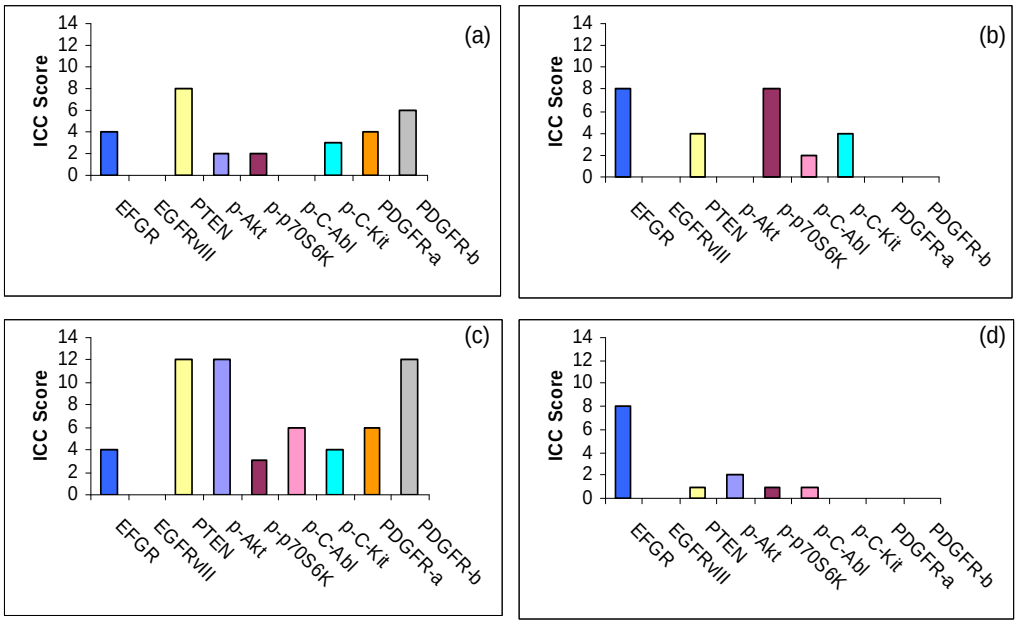

Fig. 3.5.7 PI3K/Akt pathway targets for 4 primary glioblastomas N060978 (a), N070152 (b), N071144 (c) and N080923 (d) which responded to both erlotinib and gefitinib.

3.5.5 Responders to Imatinib

Table 3.5.6 IC_{50} values of imatinib for cell cultures which responded to imatinib.

Cell Culture	IC_{50} for Imatinib
N070454	16.7 µM
N071026	19.6 µM
N080869	14 µM

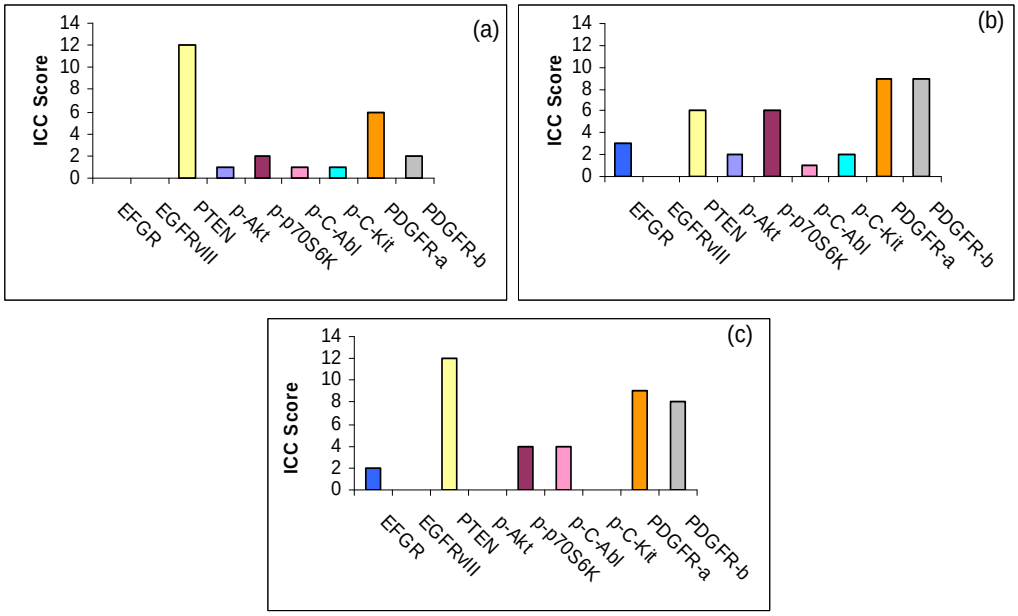

Fig. 3.5.8 PI3K/Akt pathway targets for 3 primary glioblastomas N070454 (a), N071026 (b), and N080869 (c) which responded to imatinib.

3.5.6 Responder to Erlotinib and Imatinib

Table 3.5.7 IC_{50} value of erlotinib and imatinib for N070201.

Cell Culture	IC_{50} for Erlotinib	IC_{50} for Imatinib
N070201	8.4 μM	20 μM

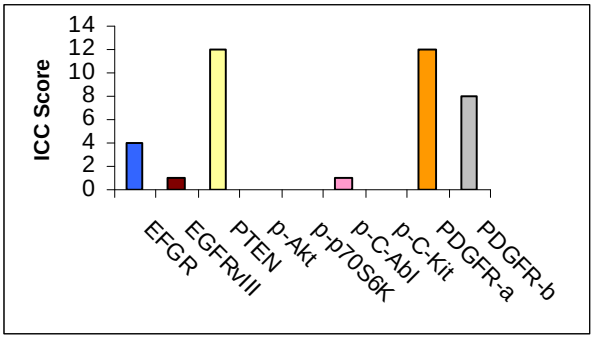

Fig. 3.5.9 PI3K/Akt pathway targets for a grade III astrocytoma N070201 which responded to both erlotinib and imatinib.

3.5.7 Responder to Gefitinib and Imatinib

Table 3.5.8 IC_{50} value of gefitinib and imatinib for N080540.

Cell Culture	IC_{50} for Gefitinib	IC_{50} for Imatinib
N080540	18.5 μM	15.8 μM

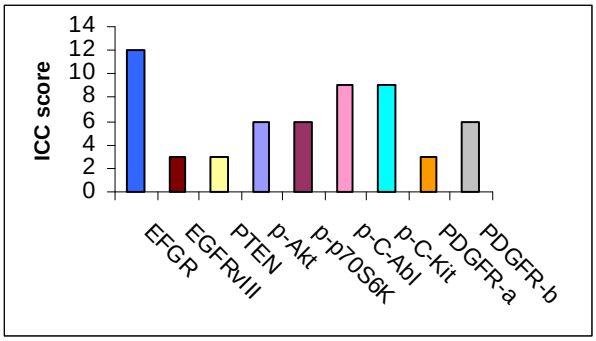

Fig. 3.5.10 PI3K/Akt pathway targets for a primary glioblastoma N080540.

3.5.8 Responder to Erlotinib, Gefitinib and Imatinib

Table 3.5.9 IC_{50} value of erlotinib, gefitinib, and imatinib for N070701.

Cell Culture	IC_{50} for Erlotinib	IC_{50} for Gefitinib	IC_{50} for Imatinib
N070701	7.9 μM	16.7 μM	14.4 μM

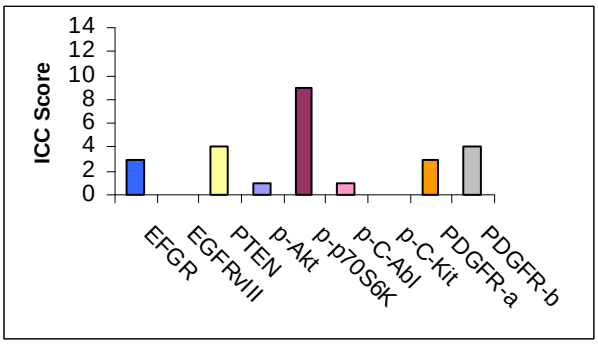

Fig. 3.5.11 PI3K/Akt pathway targets for a secondary glioblastoma N070701.

3.5.9 PI3K/Akt Pathway Proteins Expression and Response to Tyrosine Kinase Inhibitors

Receptor tyrosine kinases EGFR, PDGFR-α, PDGFR-β, C-Kit and a non-receptor tyrosine kinase C-Abl activate the PI3K/Akt pathway; the expression of these was examined by ICC.

EGFR is a specific target of erlotinib and gefitinib. The gefitinib and erlotinib responders had the highest EGFR expression; and lower expression of EGFR was found in the non-responders and imatinib responders (Fig. 3.5.13) (Table 3.5.10).

PDGFR is specifically targeted by imatinib. The non-responders had higher expression of PDGFR-β whereas the imatinib responders had higher PDGFR-α expression (Fig. 3.5.13) (Table 3.5.10). The responders to erlotinib and gefitinib had similar expression levels of PDGFR-α and PDGFR-β (Fig. 3.5.13) (Table 3.5.10).

KIT is a receptor tyrosine kinase which plays an important role in proliferation, differentiation, metastasis, and glioma development. C-Abl is an ubiquitously expressed non-receptor tyrosine kinase and is involved in cell cycle arrest and apoptosis. Overexpression of C-Abl in glioblastomas suggests an association with poor survival (Jiang *et al.* 2006). Overall, higher expression of p-C-Abl and p-C-Kit was found in gefitinib responders compared to non-responders and erlotinib or imatinib responders (Fig. 3.5.13) (Table 3.5.10).

PI3K/Akt pathway activation was examined by ICC expression of the tumour suppressor PTEN, p-Akt and p-p70S6K. PTEN is a tumour suppressor gene which inhibits cell growth, and negatively regulates the PI3K/Akt pathway. The PI3K/Akt pathway promotes cell survival and Akt promotes cell growth via MTOR signalling. MTOR also plays an important role in regulating protein translation through phosphorylation of p70S6K, a protein involved in ribosome biogenesis. Overall higher expression of p-Akt and p-p70S6K was found in the gefitinib responders (Figs. 3.5.14), (Table 3.5.11).

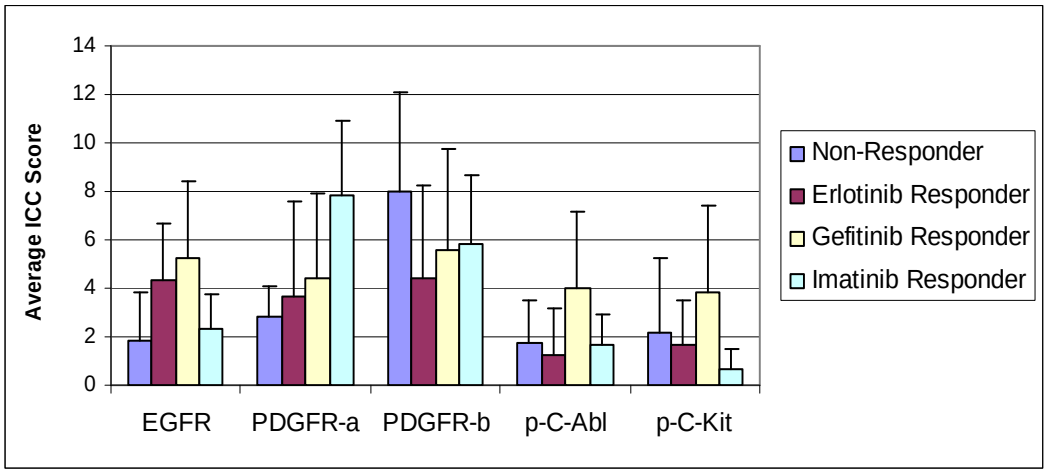

PDGFR-a: PDGFR-α. PDGFR-b: PDGFR-β

Fig. 3.5.12 Average ICC score of EGFR, PDGFR-α, PDGFR-β, p-C-Abl, and p-C-Kit for non-responders, and for responders to erlotinib, gefitinib, and imatinib. The standard deviations represent the variance of the ICC score within each group. Standard deviations were generated from Microsoft Excel software.

Table 3.5.10 Average ICC score of EGFR, PDFGR-α, PDGFR-β, p-C-Abl and p-C-Kit in high-grade gliomas.

Response to TKIs	EGFR	PDGFR-α	PDGFR-β	p-C-Abl	p-C-Kit
Non-responder	1.9 ± 2	2.9 ± 1.2	8 ± 4.1	1.7 ± 1.8	2.1 ± 3.1
Erlotinib responder	4.3 ± 2.3	3.7 ± 3.9	4.4 ± 3.8	1.2 ± 1.9	1.7 ± 1.8
Gefitinib responder	5.3 ± 3.2	4.4 ± 3.5	5.6 ± 4.2	4 ± 3.2	3.8 ± 3.6
Imatinib responder	2.3 ± 1.4	7.8 ± 3.1	5.8 ± 2.9	1.7 ± 1.2	0.7 ± 0.8

Highest average ICC score

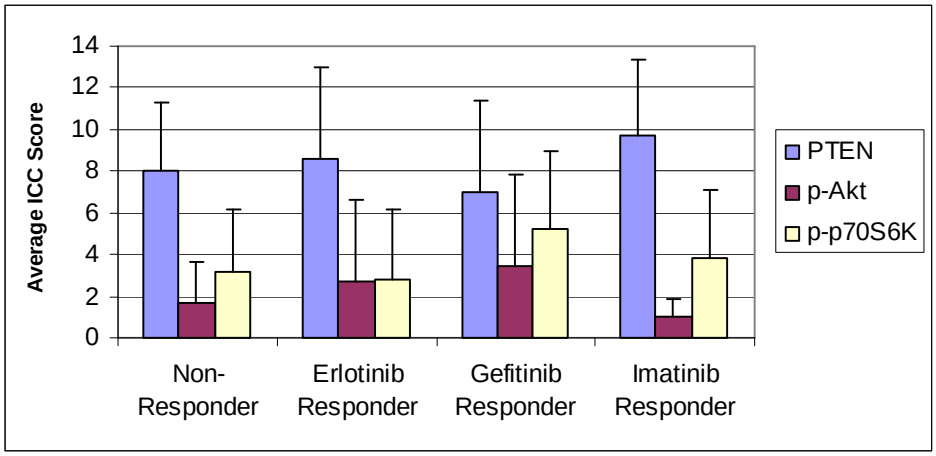

Fig. 3.5.13 Average ICC score of PTEN, p-Akt, and p-p70S6K for non-responders, erlotinib, gefitinib, and imatinib responders. The standard deviations represent the variance of the ICC score within each group. Standard deviations were generated from Microsoft Excel software.

Table 3.5.11 Average ICC score of PTEN, p-Akt and p-p70S6K in high-grade gliomas.

Response to TKIs	PTEN	p-Akt	p-p70S6K
Non-responder	8 ± 3.3	1.7 ± 1.9	3.1 ± 3
Erlotinib responder	8.6 ± 4.4	2.7 ± 4	2.1 ± 3.4
Gefitinib responder	7 ± 4.4	3.5 ± 4.3	5.3 ± 3.7
Imatinib responder	9.7 ± 3.7	1 ± 0.9	3.8 ± 3.3

Highest average ICC score

3.5.10 Bioinformatic Analysis for PI3K/Akt Pathway Proteins in Non-Responders and Responders to Tyrosine Kinase Inhibitors

The statistical analysis was carried out by a bioinformatician Dr. Colin Clarke from the NICB. The cohort included 26 high-grade glioma samples. This dataset was too small for supervised analysis; therefore hierarchical clustering analysis (HCA) and principal components analysis (PCA) were employed for multivariate statistics.

3.5.10.1 Hierarchical Clustering Analysis

Statistical analysis was used to analyse the large amount of data which were generated through ICC analysis. To stratify samples corresponding to a clinical trait or response to drug, the Ward's distance method with Euclidian was used (Lomo *et al.* 2008). HCA on cell culture ICC data resulted in two main groupings of samples; 11 samples with high and 15 with low PTEN expression (Fig. 3.5.14 vertical grouping). Clustering the marker again resulted in two additional clusters: PDGFR-α, PDGFR-β and PTEN grouped together; these markers contain the majority of high scores from the ICC analysis. The second cluster contains p-C-Kit, p-C-Abl, EGFRtot, EGFRvIII, p-p70S6K and p-Akt expression, and was defined by low ICC scores (Fig. 3.5.14 vertical grouping).

Cluster 1 had the highest PTEN and PDGFR-α expression. PDGFR-β expression was high in some of the cultures. Cluster 1 also had very little expression of EGFR, p-C-Kit, and p-C-Abl. There was low expression of downstream targets of the PI3K/Akt pathway, including p-p70S6K and p-Akt (Fig. 3.5.14) (Table 3.5.12).

Cluster 2 is characterized by higher PDGFR-β, EGFR, p-C-Kit and p-C-Abl expression as well as higher expression of downstream targets of the PI3K/Akt pathway including p-p70S6K and p-Akt (Fig. 3.5.14) (Table 3.5.13).

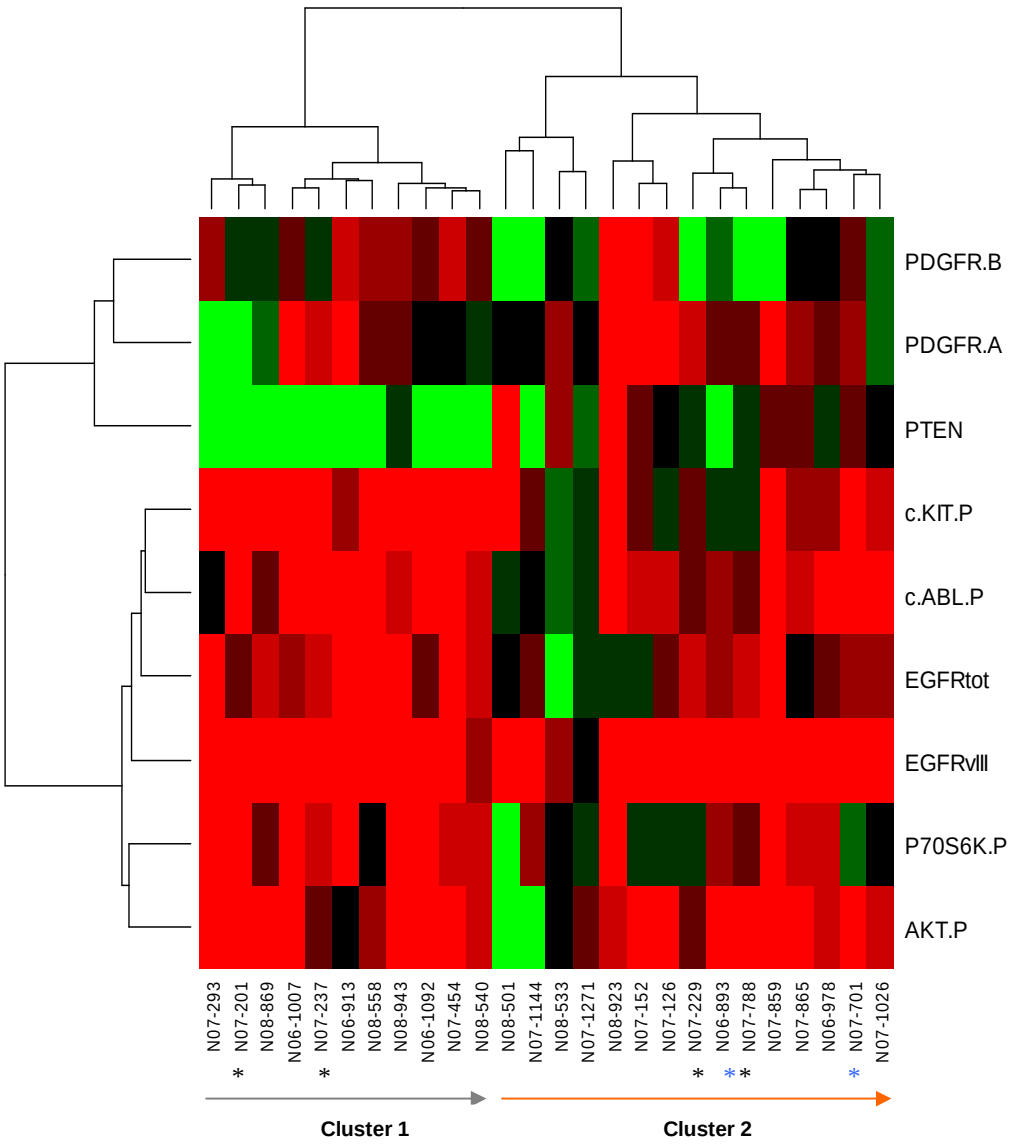

Bright green: high expression bright red: low expression black: in between.
*: Anaplastic astrocytoma. *: secondary glioblastoma. Cluster 1 is highlighted with a gray arrow, cluster 2 with an orange arrow.

Fig. 3.5.14 HCA and heatmap for cell culture ICC analysis of 26 high-grade glioma samples. The dendrogram depicts all cases individually in rows, and the interpretation of each protein in columns. PDGFR.A: PDGFRα; PDGFR.B: PDGFRβ; c.KIT.P: phosphorylated c-KIT; c.ABL.P: phosphorylated c-ABL; P70S6K.P: phosphorylated p70S6K; AKT.P: phosphorylated AKT.

Table 3.5.12 Characteristics of Cluster 1

Cell Culture	Tumour Grade	Survival Time (months)	Doubling Time (hrs)	Invasion	Erl	Gef	Imt
N070293	Primary Glioblastoma	>36	91.5	2	-	+	-
N070201	Grade III Astrocytoma	>36	59.4	0	+	-	+
N080869	Primary Glioblastoma	>20	115	2	-	-	+
N061007	Primary Glioblastoma	1	>168	1	+	-	-
N070237	Grade III Astrocytoma	55	88.45	0	-	-	-
N060913	Primary Glioblastoma	110	>168	1	+	-	-
N080558	Primary Glioblastoma	5	115.4	0	-	-	-
N080943	Primary Glioblastoma	>19	94.33	2	-	-	-
N061092	Primary Glioblastoma	6	100.5	2	+	-	-
N070454	Primary Glioblastoma	3	51.5	2	-	-	+
N080540	Primary Glioblastoma	>12	49.1	0	-	+	+

Erl: erlotinib, Gef: gefitinib, Imt: imatinib. -: non-responder, +: responder. Invasion. 2: very invasive, 1: some invasion, 0: no invasion.

Table 3.5.13 Characteristics of Cluster 1

Cell Culture	Tumour Grade	Survival Time (months)	Doubling Time (hrs)	Invasion	Erl	Gef	Imt
N080501	Primary Glioblastoma	18	107	1	-	+	-
N071144	Primary Glioblastoma	8	77.7	2	+	+	-
N080533	Primary Glioblastoma	15	62.58	2	-	+	-
N071271	Primary Glioblastoma	11	59.2	2	-	+	-
N080923	Primary Glioblastoma	15	56.2	0	+	+	-
N070152	Primary Glioblastoma	5	48.8	2	+	+	-
N070126	Primary Glioblastoma	28	82.54	0	-	+	-
N070229	Grade III Astrocytoma	>36	72.46	2	-	-	-
N060893	Secondary Glioblastoma	>138	88.13	1	-	+	-
N070788	Grade III Astrocytoma	>31	65.9	0	-	-	-
N070859	Primary Glioblastoma	12	56	1	-	-	-
N070865	Primary Glioblastoma	5	37.3	2	-	-	-
N060978	Primary Glioblastoma	3	99.3	0	+	+	-
N070701	Secondary Glioblastoma	>56	71.8	1	+	+	+
N071026	Primary Glioblastoma	10	74.52	2	-	-	+

Erl: erlotinib, Gef: gefitinib, Imt: imatinib. -: non-responder, +: responder. Invasion 2: very invasive, 1: some invasion, 0: no invasion

3.5.2 Correlation of Patient Survival Time with Hierarchial Cluster Analysis

Within the two main clusters received through HCA patient survival time was correlated with the expression of each protein from the PI3K/Akt pathway. Cluster 1 had a lower proliferation rate overall in comparison to cluster 2 (Table 3.5.12 and 3.5.13). Figures 3.5.15 to 3.5.22 show the relationship with each protein between the two clusters: cluster 2 had higher PDGFR-β expression than cluster 1; the majority of patients in cluster 2 with high PDGFR-β expression had a lower survival time (Fig. 3.5.15). There was significantly higher expression of PDGFR-β in cluster 2 ($p = 0.05$) (Table 3.5.14). PDGFR-α expression was not correlated with survival time in either cluster (Fig. 3.5.16). There was no significant difference in expression of PDGFR-α between the two clusters ($p = 0.067$) (Table 3.5.15).

High expression of PTEN in cluster 1 appears to be related to longer survival in 3 patients; whereas there was no correlation with PTEN and survival in cluster 2 (Fig. 3.5.17). There was higher expression of PTEN in cluster 1 than cluster 2, statistically significant ($p = 2.86E-05$) (Table 3.5.16).

In cluster 1 there was very little expression of p-C-Kit, (4 out of 11 cultures had expression); high expression of p-C-Kit was found in cluster 2 and seemed to correlate with lower survival time (Fig. 3.5.18), with higher expression of p-C-Kit in cluster 2 ($p = 0.0018$) (Table 3.5.17).

6 patients out of 11 in cluster 1 had no expression of p-C-Abl, while 13 out of 15 patients in cluster 2 expressed p-C-Abl and within this group 8 showed a correlation with lower survival (Fig. 3.5.19). There was no difference in expression of C-Abl between the clusters ($p = 0.074$) (Table 3.5.18).

While levels of EGFRtot expression in cluster 1 were very low, EGFRtot expression was much higher in cluster 2 and correlated with lower survival time (Fig. 3.5.20), a difference in EGFRtot expression was found between the two clusters ($p = 0.005$) (Table 3.5.19).

Very low expression of p-p70S6K was seen in cluster 1; 3 patients had no expression. In cluster 2 expression level of p-p70S6K was much higher and the

majority of the patients with high expression had a lower survival time (Fig. 3.5.21), ($p = 0.0046$) (Table 3.5.20).

There was little p-Akt expression overall. In cluster 2 strong expression of p-Akt was seen in two samples, which was accompanied with lower survival time (Fig. 3.5.22), there was no difference of expression of p-Akt between the two clusters ($p = 0.239$) (Table 3.5.21).

3.5.2.1 PDGFR-β Expression in Comparison to Patient Survival

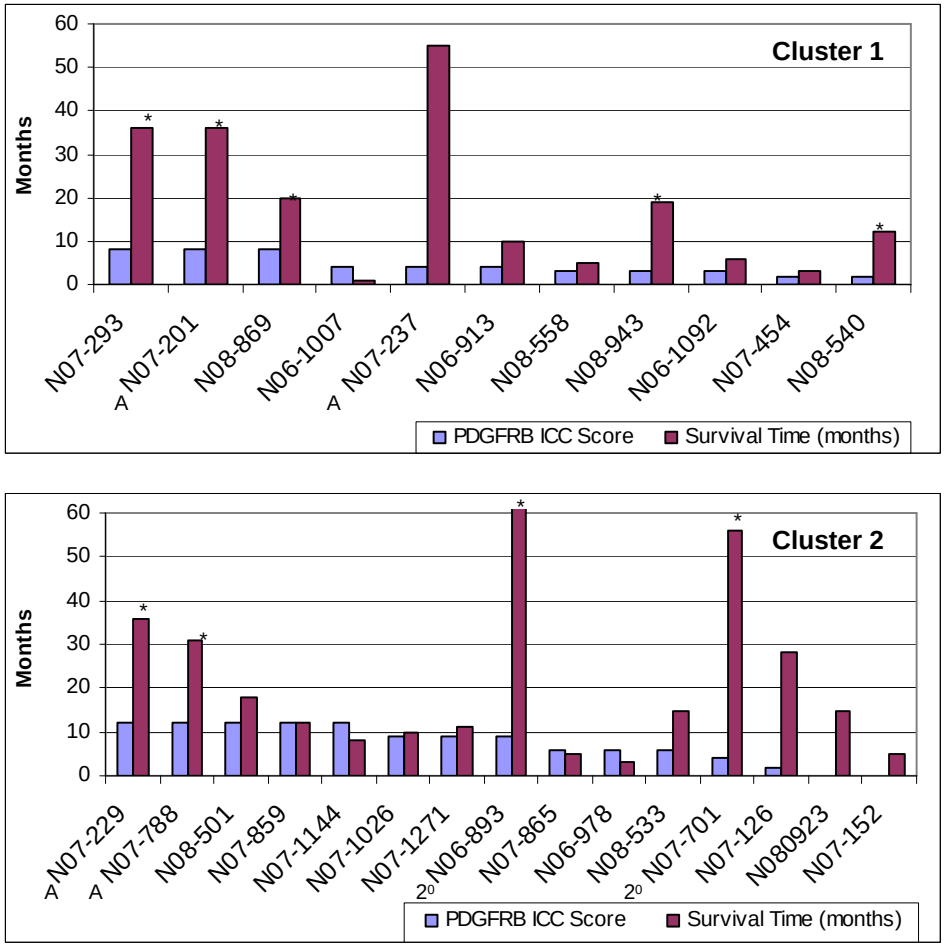

A: Grade III astrocytoma. 2^0: secondary glioblastoma. *: patient still alive. PDGFRB: PDGFR-β. N060893 had greater than 138 months survival.

Fig. 3.5.15 Survival time (months) of patients correlated with PDGFR-β ICC score in cluster 1 (a) and cluster 2 (b).

Table 3.5.14 Anova analysis of PDGFR-β ICC score, with cluster 1 and cluster 2.

Protein	Average ICC Score Cluster 1	Average ICC Score Cluster 2	P Value
PDGFR-β	4.5 ± 2.4	7.4 ± 4.4	0.05

Standard deviations represent variance within each cluster.

3.5.2.2 PDGFR-α Expression in Comparison to Patient Survival

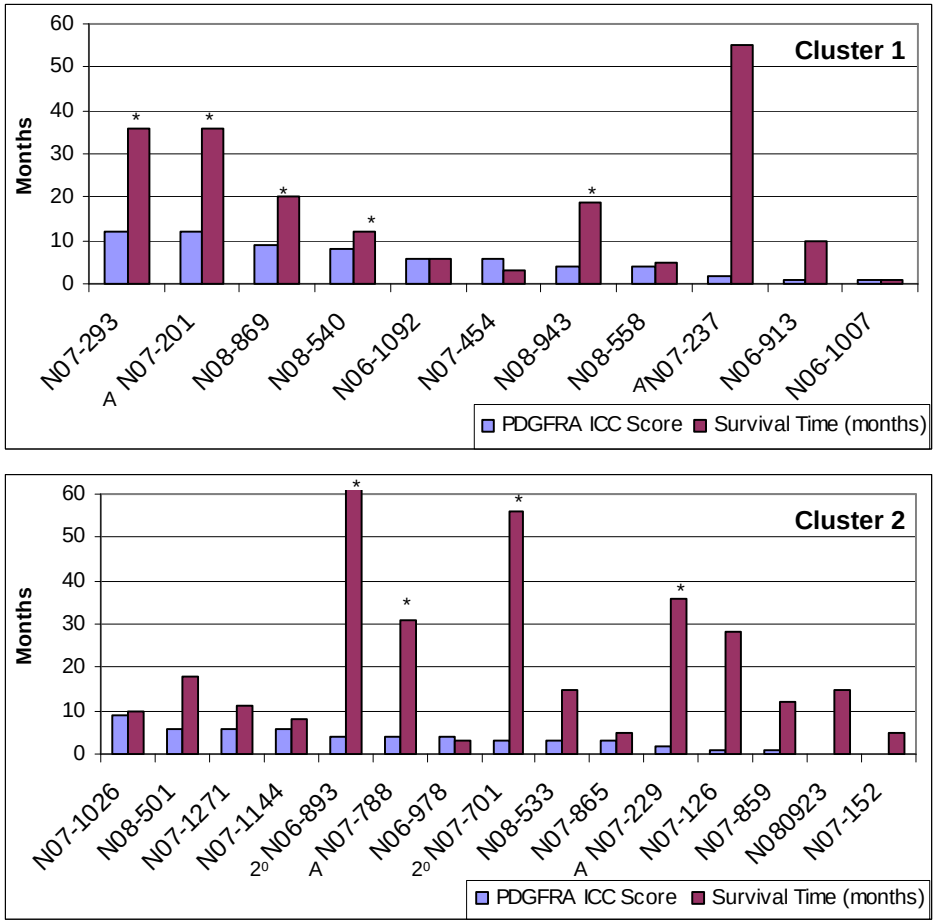

A: Grade III astrocytoma. 2^0: secondary glioblastoma. *: patient still alive. PDGFRA: PDGFR-α. N060893 had greater than 138 months survival

Fig. 3.5.16 Survival time in months of patients correlated with PDGFR-α ICC score in cluster 1 (a) and cluster 2 (b).

Table 3.5.15 Anova analysis of PDGFR-α ICC score, with cluster 1 and cluster 2.

Protein	Average ICC Score Cluster 1	Average ICC Score Cluster 2	P Value
PDGFR-α	5.9 ± 4.0	3.5 ± 2.5	0.067

Standard deviations represent variance within each cluster.

3.5.2.3 PTEN Expression in Comparison to Patient Survival

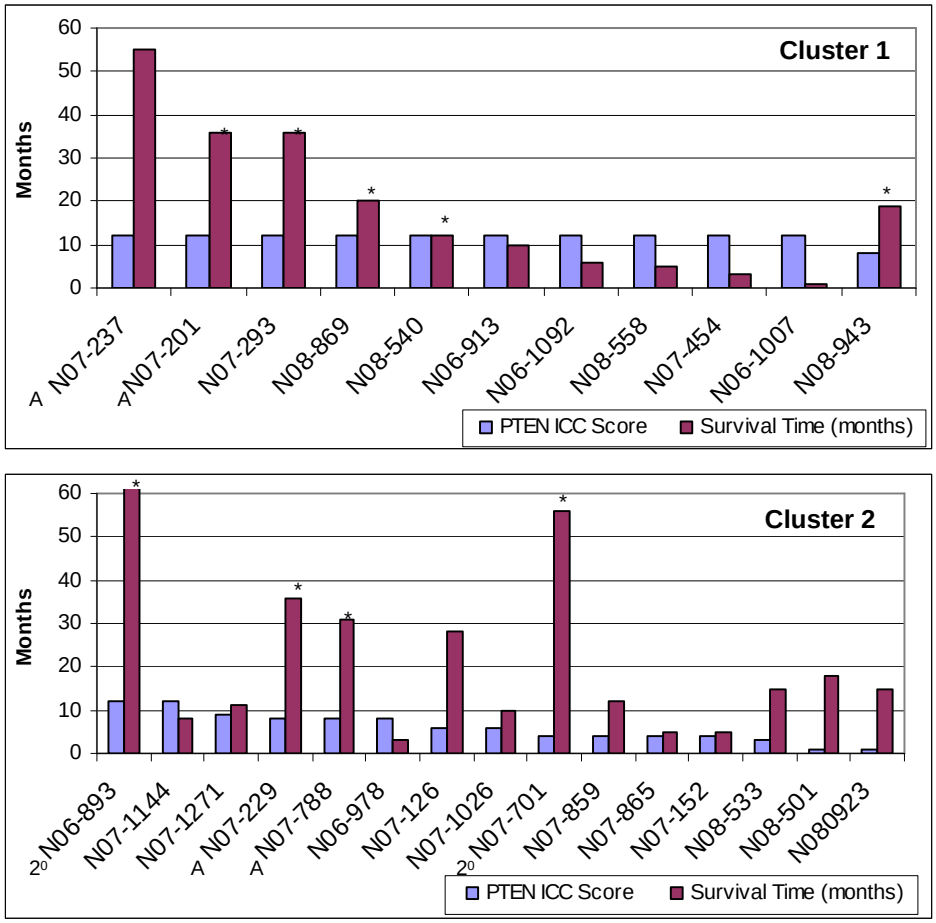

A: Grade III astrocytoma. 2^0: secondary glioblastoma. *: patient still alive. N060893 had greater than 138 months survival.

Fig. 3.5.17 Survival time in months of patients correlated with PTEN ICC score in cluster 1 (a) and cluster 2 (b).

Table 3.5.16 Anova analysis of PDGFR-α ICC score, with cluster 1 and cluster 2.

Protein	Average ICC Score Cluster 1	Average ICC Score Cluster 2	P Value
PTEN	11.6 ± 1.2	6.0 ± 3.5	2.86E-05

Standard deviations represent variance within each cluster.

3.5.2.4 p-C-Kit Expression in Comparison with Patient Survival

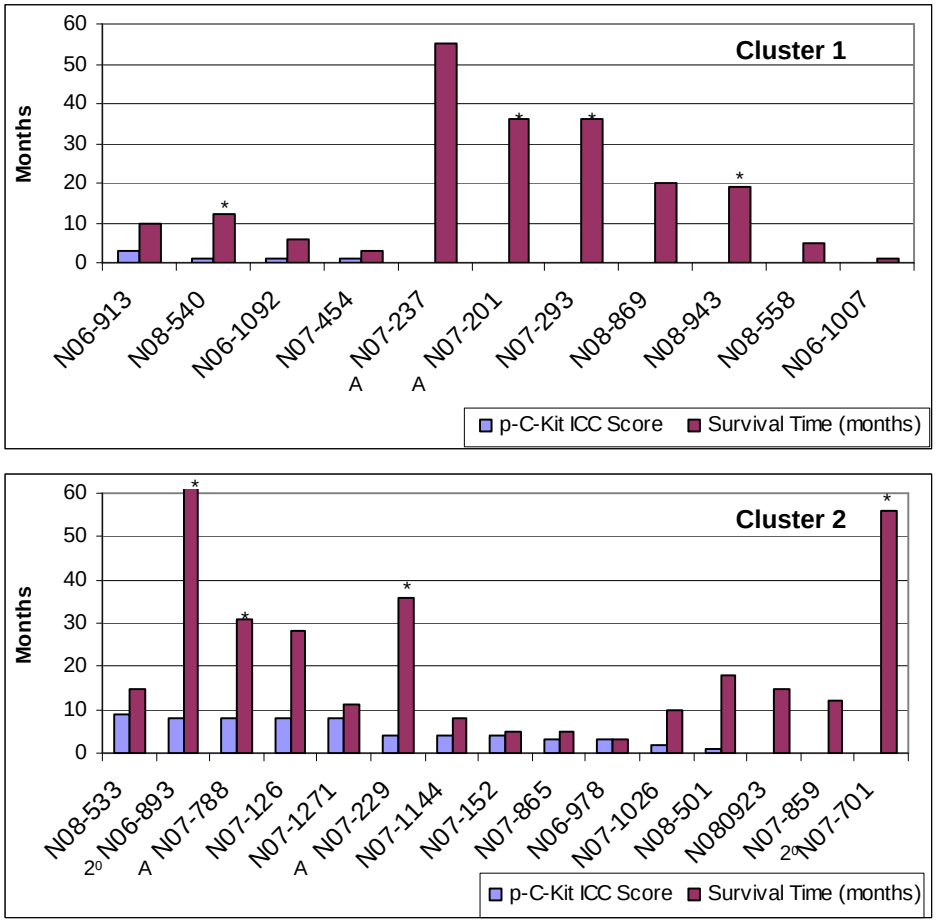

A: Grade III astrocytoma. 2^0: secondary glioblastoma. *: patient still alive. P-C-Kit: phosphorylated C-Kit. N060893 had greater than 138 months survival.

Fig. 3.5.18 Survival time in months of patients correlated with p-C-Kit ICC score in cluster 1 (a) and cluster 2 (b).

Table 3.5.17 Anova analysis of PDGFR-α ICC score, with cluster 1 and cluster 2.

Protein	Average ICC Score Cluster 1	Average ICC Score Cluster 2	P Value
C-Kit-P	0.5 ± 0.9	4.1 ± 3.3	0.0018

Standard deviations represent variance within each cluster.

3.5.2.5 p-C-Abl Expression in Comparison with Patient Survival

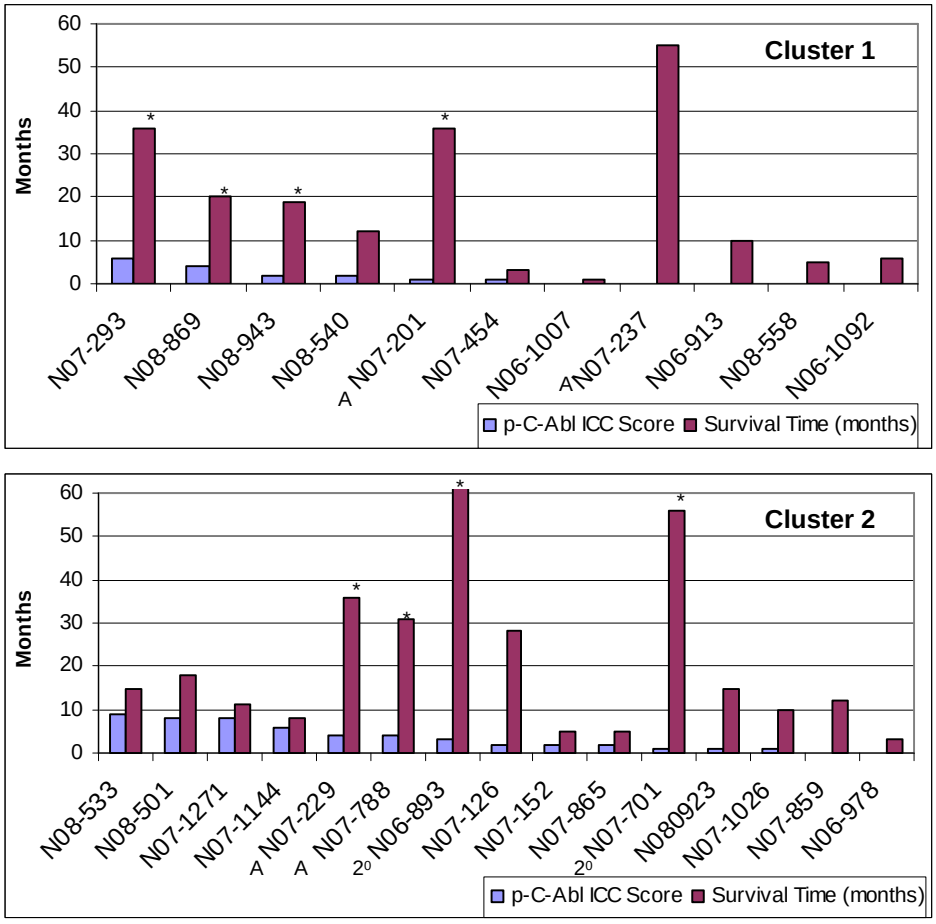

A: Grade III astrocytoma. 2^0: secondary glioblastoma. *: patient still alive. P-C-Abl: phosphorylated C-Abl. N060893 had greater than 138 months survival

Fig. 3.5.19 Survival time in months of patients correlated with p-C-Abl ICC score in cluster 1 (a) and cluster 2 (b).

Table 3.5.18 Anova analysis of p-C-Abl ICC score, with cluster 1 and cluster 2.

Protein	Average ICC Score Cluster 1	Average ICC Score Cluster 2	P Value
C-Abl-P	1.5 ± 2.0	3.4 ± 3.0	0.074

Standard deviations represent variance within each cluster.

3.5.2.6 EGFR Expression in Comparison with Patient Survival

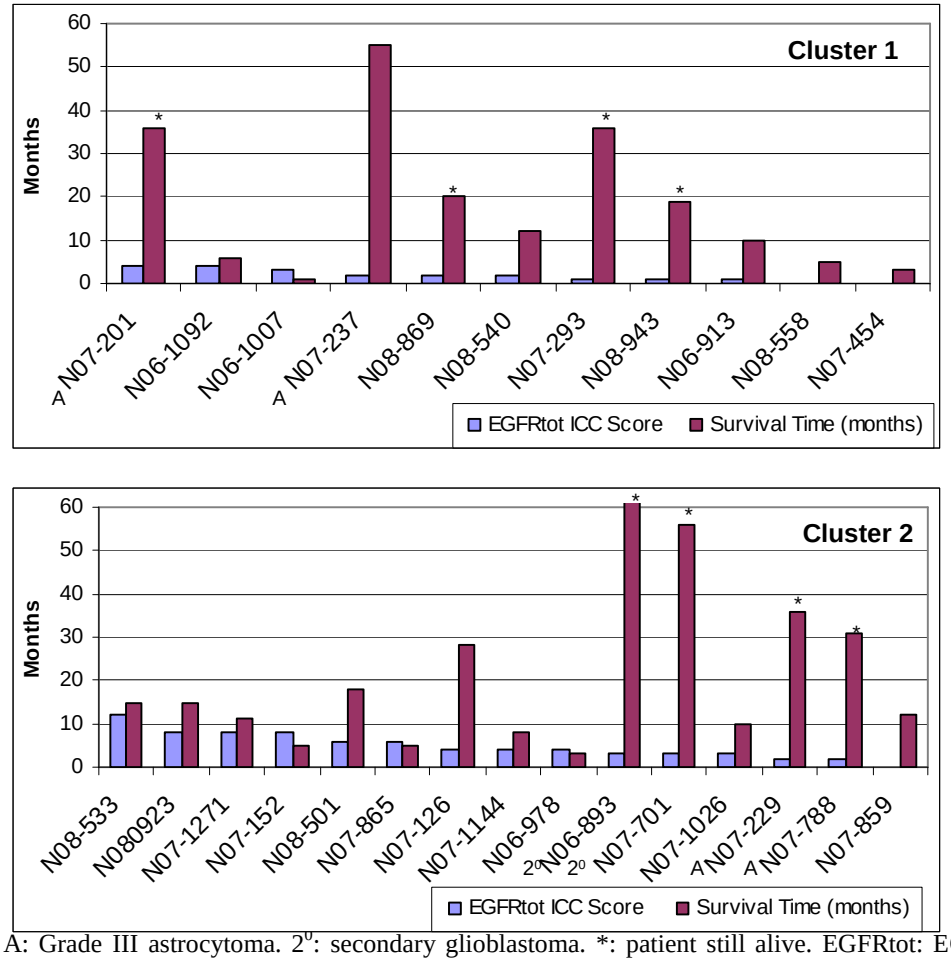

A: Grade III astrocytoma. 2^0: secondary glioblastoma. *: patient still alive. EGFRtot: EGFR total. N060893 had greater than 138 months survival

Fig. 3.5.20 Survival time in months of patients correlated with EGFRtot ICC score in cluster 1 (a) and cluster 2 (b).

Table 3.5.19 Anova analysis of EGFR ICC score, with cluster 1 and cluster 2.

Protein	Average ICC Score Cluster 1	Average ICC Score Cluster 2	P Value
EGFRtot	1.8 ± 1.4	4.9 ± 3.1	0.005

Standard deviations represent variance within each cluster.

3.5.2.7 p-p70S6K Expression in Comparison with Patient Survival

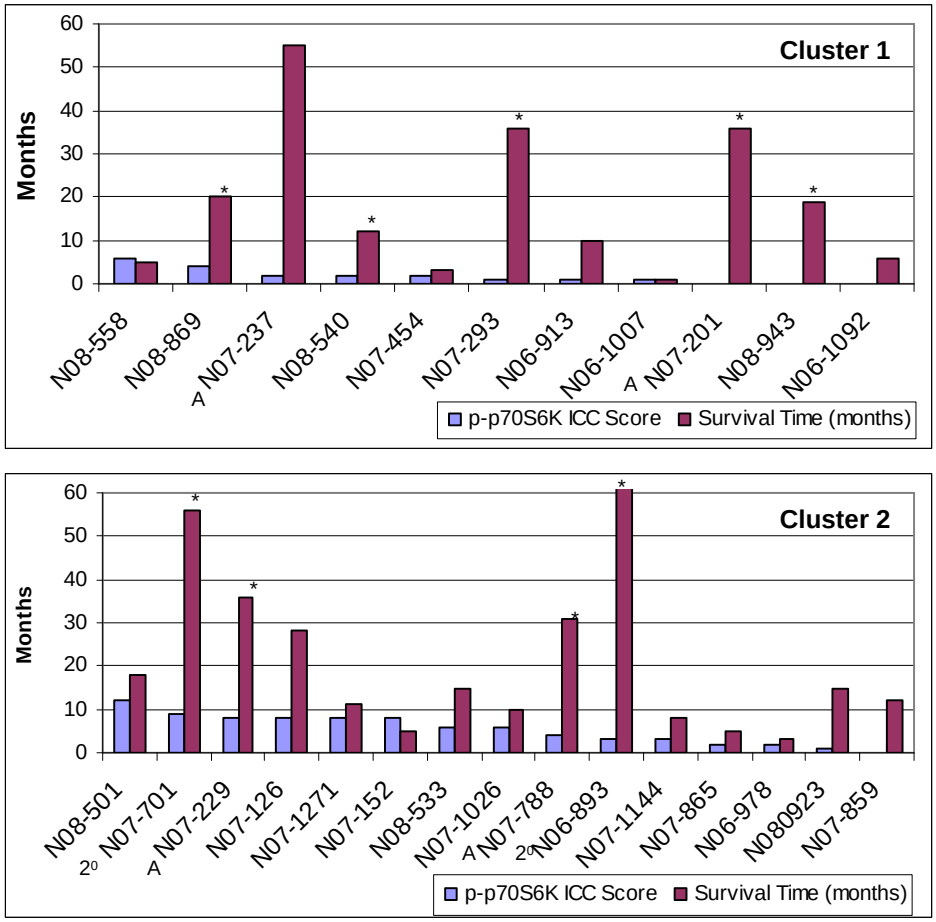

A: Grade III astrocytoma. 2^0: secondary glioblastoma. *: patient still alive. P-p70S6K: phosphorylated p70S6K. N060893 had greater than 138 months survival

Fig. 3.5.21 Survival time in months of patients correlated with p-p70S6K ICC score in cluster 1 (a) and cluster 2 (b).

Table 3.5.20 Anova analysis of p-p70S6K ICC score, with cluster 1 and cluster 2.

Protein	Average ICC Score Cluster 1	Average ICC Score Cluster 2	P Value
p-p70S6K	1.7 ± 1.8	5.3 ± 3.5	0.0046

Standard deviations represent variance within each cluster.

3.5.2.8 p-Akt Expression in Comparison with Patient survival

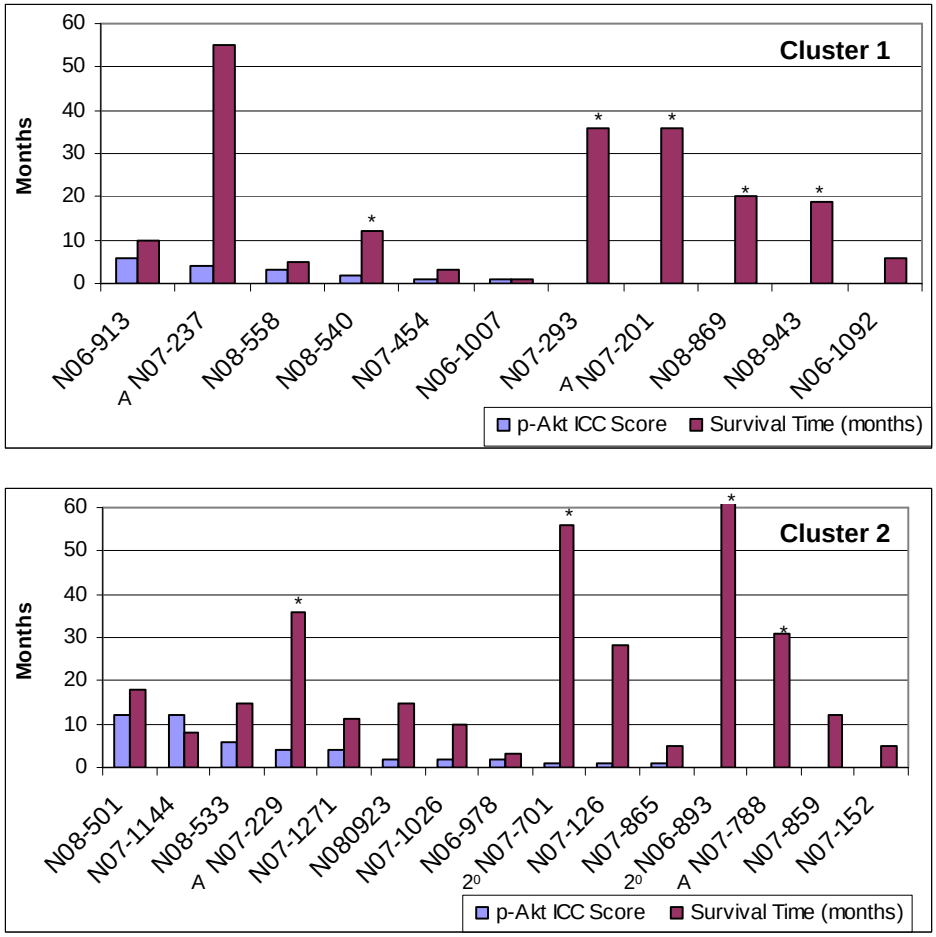

A: Grade III astrocytoma. 2^0: secondary glioblastoma. *: patient still alive. P-Akt: phosphorylated Akt. N060893 had greater than 138 months survival

Fig. 3.5.22 Survival time in months of patients correlated with p-Akt ICC score in cluster 1 (a) and cluster 2 (b).

Table 3.5.21 Anova analysis of p-Akt ICC score, with cluster 1 and cluster 2.

Protein	Average ICC Score Cluster 1	Average ICC Score Cluster 2	P Value
p-Akt	1.5 ± 2.0	3.4 ± 4.0	0.23

Standard deviations represent variance within each cluster.

3.5.11 Unsupervised Principal Components Analysis of Pathway Proteins response to Tyrosine Kinase Inhibitors

Unsupervised Principal components analysis (PCA) was applied to the ICC data to see if expression of certain proteins is associated with response to TKIs. 55 % of the variance in the dataset was retained in the first two principal components (Fig. 3.5.23). The biplot represents the grouping of the cell cultures in principle component space in relation to their expression of the proteins (Fig. 3.5.23).

Figure 3.5.24 shows the PCA score plot for responders (R) and non-responders to Erlotinib (NR). Fig 3.5.24 showed that there was a definitive separation between responders and non-responders to erlotinib treatment. The majority of responders cluster to the top right of the plots, suggesting that these samples were not influenced by the analysed proteins (Fig. 3.5.24). Most of the NR's cluster to the lower right of the plots associated with higher expression of PTEN and PDGFR-α.

With gefitinib there was stratification between responders and non-responders, with the latter clustering toward the right of the plot (Fig. 3.5.25). Again the NRs were associated with higher expression of PTEN and PDGFR-α. Within the responders to gefitinib one group clustered to the top right not being influenced by the protein tested; another group clustered to the bottom left characterized by high expression of the target proteins, p-p70S6K,p-C-Kit, p-Akt and p-C-Abl (Fig. 3.5.25).

Imatinib responders clustered toward the bottom right hand corner of the plot, which shows a strong influence by PTEN and PDGFR-α (Fig. 3.5.26).

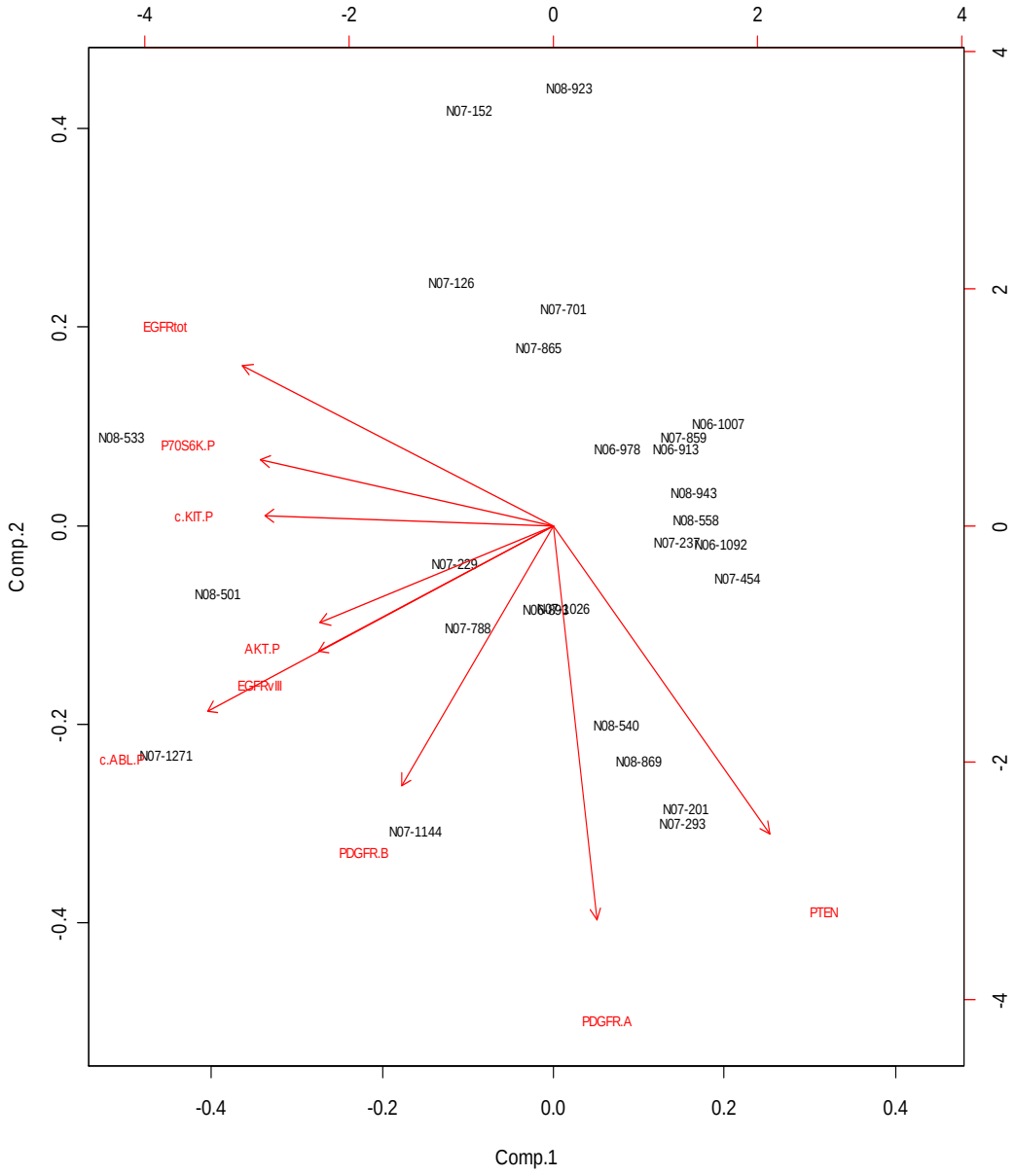

Fig. 3.5.23 Unsupervised PCA of 26 cell cultures. 55% of the variance in the dataset is retained in the first two principal components. The biplot represents the grouping of cell cultures in principle component space. The red arrows correspond to the influence of protein staining values on the separation of the samples. Each protein is labelled in red and each glioma cell culture is labelled in black. Each culture is positioned closest to the protein they had the highest expression of. The cultures which had little or no expression of the proteins lie to the right hand side of the arrows.

Determination of variable influence on response/non-response

Erlotinib

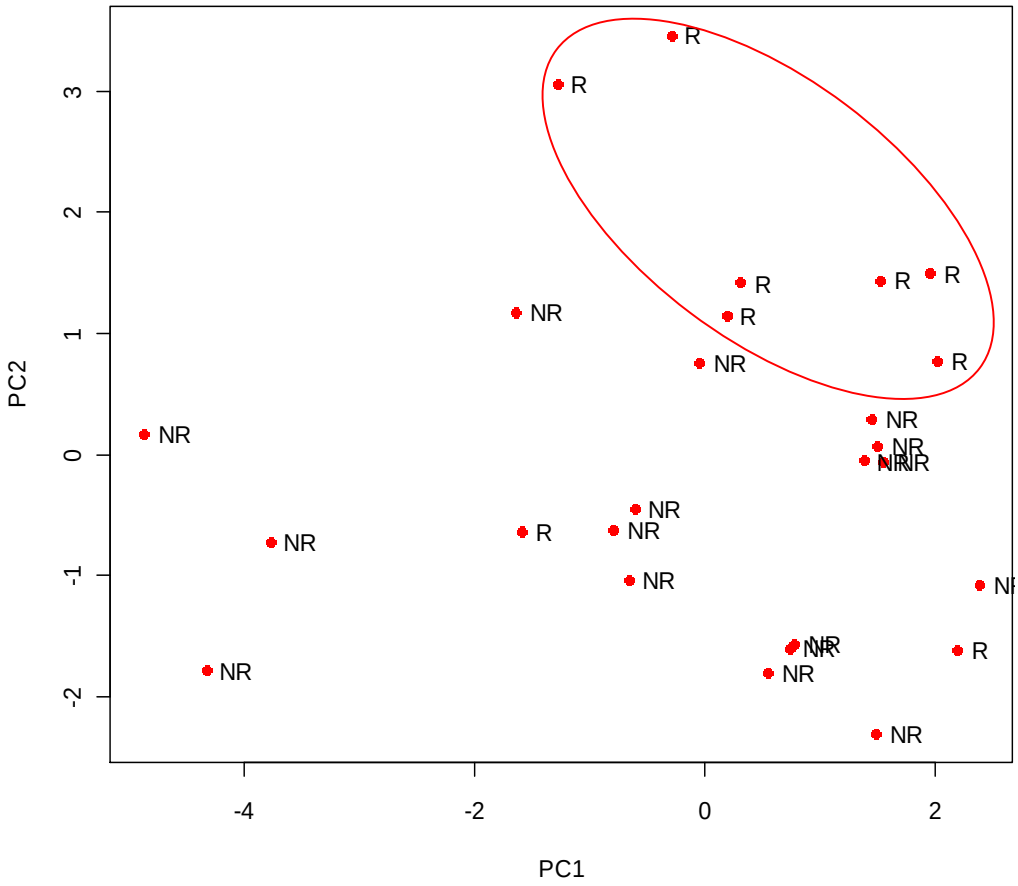

R: responder, NR: non-responder. PC1: principle component 1. PC2 : principle component 2.

Fig. 3.5.24 PCA scores plot of cell culture ICC. Samples are labelled according to their responsiveness to erlotinib. This plot is a replicate of figure 3.5.23, with the cultures labelled as responders or non-responders to erlotinib. The main cluster of erlotinib responders is circled in red, which is at the top right hand side of the plot, showing that responsiveness to erlotinib is not associated with expression of the proteins.

Gefitinib

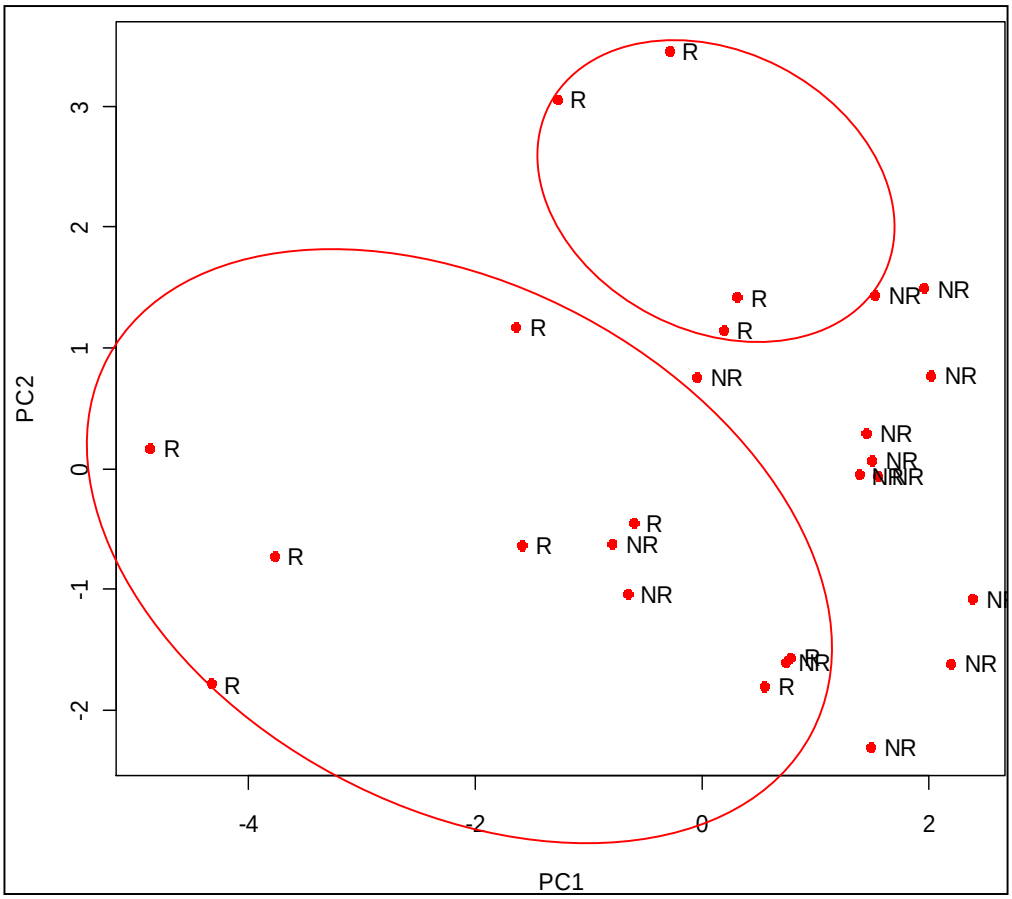

R: responder, NR: non-responder. PC1: principle component 1. PC2: principle component 2.

Fig. 3.5.25 PCA scores plot of of cell culture ICC. Samples were labelled according to their responsiveness to gefitinib. This plot has the same layout as figure 3.5.23, with the cultures labelled as responders or non-responders to gefitinib. The 2 main clusters of gefitinib responders are circled in red. There was a cluster of gefitinib responders that had high expression of some of the proteins (bottom left hand side) and a cluster which did not (top right hand side).

Imatinib

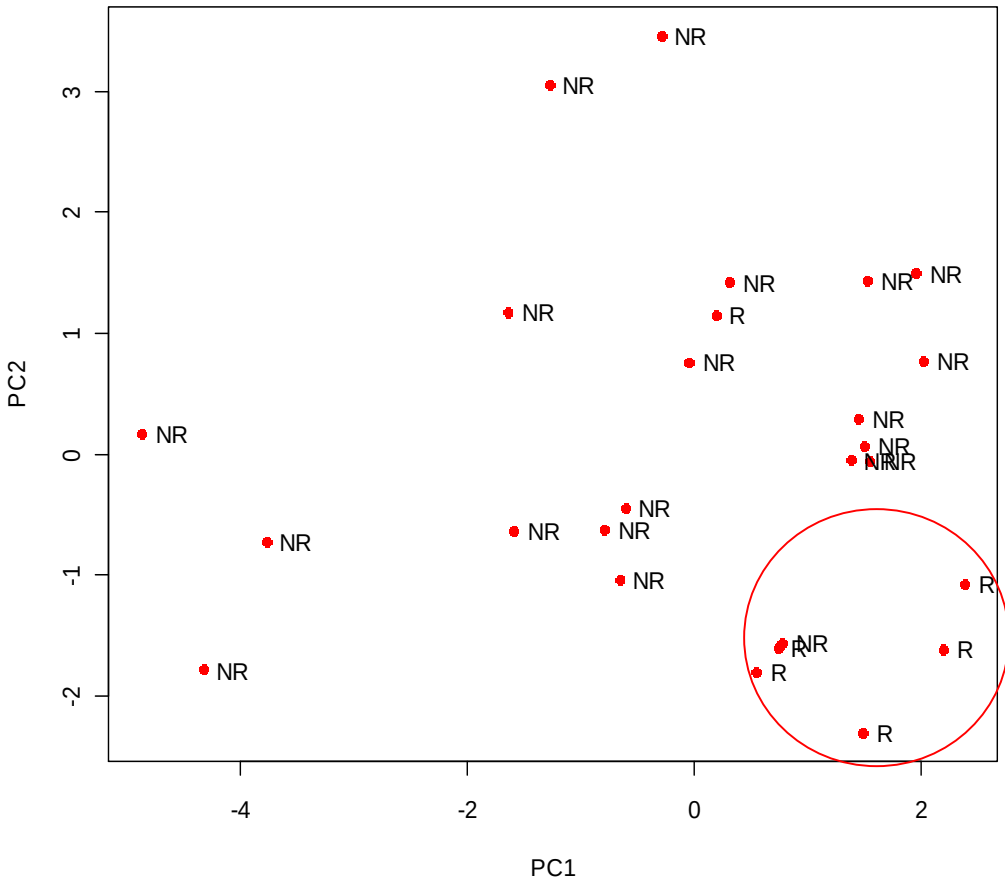

R: responder, NR: non-responder. PC1: principle component 1. PC2 : principle component 2.

Fig. 3.5.26 PCA scores plot of PC1 versus PC2 of cell culture ICC. Samples are labelled according to their response to imatinib. The cultures are labelled as responders or non-responders to imatinib and have the same grouping as figure 3.5.23. The majority of the imatinib responders are circled in red. The cluster of imatinib responders was at the bottom right hand side of the plot, this was due to the high expression of PTEN and PDGFR-α.

3.5 Discussion:

Expression of Proteins targeted by TKIs in High-Grade Glioma, in relation to their Response to these Inhibitors.

Overexpression of EGFR and PDGFR is frequently found in glioblastoma, which results in the activation of downstream kinases including phosphatidylinositol 3′-kinase (PI3K), Akt, and the mammalian target of rapamycin (MTOR). MTOR is a nutrient sensor which regulates cell growth and many cellular functions such as mRNA translation and metabolism (Shaw and Cantley 2006). MTOR has been shown to play a key role in tumour progression in various types of cancer including glioma (Seeliger *et al.* 2007), where it is activated by Akt (Riemenschneider *et al.* 2006). MTOR phosphorylates p70S6K, which regulates protein synthesis and has been shown to cause glioblastoma formation in mice (Holland *et al.* 2000), while its inhibition causes apoptosis (Hu *et al.* 2005). It was hypothesized that the expression of specific proteins targeted by TKIs in glioma cell cultures would correlate with their response to tyrosine kinase inhibitors. 26 newly developed high-grade glioma cell cultures were analysed by immunocytochemistry (ICC) (Table 3.5.1). The ICC work was carried out by a Ph.D student, Rachel Howley, in Beaumont Hospital, Dublin. The cell cultures were classified as responders or non-responders to the TKIs, erlotinib, gefitinib, and imatinib (Table 3.5.2) (see section 3.3.2).

EGFR was expressed in 88.4%, and EGFRvIII in 26.9% of the cultures. P-Akt was expressed in 65.3% and PTEN in 100% of the cultures. A similar expression level of Akt was found in glioblastoma cells by others where Akt was activated in 70% of gliomas (Alessi *et al.* 1996; Haas-Kogan *et al.* 1998). The expression of EGFR by ICC varied in the cultures; it was low in the non-responders and imatinib responders, and high in erlotinib and gefitinib responders (Fig. 3.5.12) (Table 3.5.10). PTEN expression did not appear to be a determinant of TKI responsiveness. Mellinghoff *et al*, found the inhibition of EGFR was successful in a sub-group of recurrent glioblastomas (Mellinghoff *et al.* 2005). Response was correlated with co-expression of the mutated form of EGFRvIII and PTEN; however, the detailed mechanism of action is still unknown (Mellinghoff *et al.*

2005). Sordella *et al*, found that in lung cancer cells EGFRvIII activates PI3K/AKT signalling and can sensitize cells to the EGFR inhibitor, gefitinib (Sordella *et al.* 2004); this has not been shown yet for glioblastomas. Overall a low amount of EGFRvIII was found in the cultures, 2 primary glioblastomas and 2 grade III astrocytomas had low EGFRvIII expression and PTEN expression, 1 of the primary glioblastomas was a gefitinib responder and 1 of these grade III astrocytomas was an erlotinib responder (Figs 3.5.2, 3.5.3 3.5.5 and 3.5.9). There were 2 primary glioblastomas with higher EGFRvIII expression who also expressed PTEN; both were responders to gefitinib (Fig. 3.5.6). It is thought that the loss of PTEN might promote resistance to EGFR kinase inhibitors (Bianco *et al.* 2003). High expression of PTEN was found in the majority of the cultures; however, it is unclear if it is functional. PTEN can be mutated with loss of function, which has been reported for about 30% of glioblastomas (Kleihues and Ohgaki 2000).

PDGFR-α Expression in Relation to Imatinib Responders in High-grade Glioma Cultures

PDGFR-α and PDGFR-β was expressed in 92.3% of the glioma cultures, p-C-Abl in 61.5%, and p-C-Kit in 61.5%. Non-responders had higher expression of PDGFR-β in comparison to the responders (Fig. 3.5.12) (Table 3.5.10). While PDGFR-α and PDGFR-β levels were similar in the responders to erlotinib and gefitinib (Fig. 3.5.12) (Table 3.5.10). The imatinib responders had higher PDGFR-α expression in comparison to the non-responders, erlotinib and gefitinib responders (Fig. 3.5.12) (Table 3.5.10). Responsiveness to imatinib in gliomas appears to correlate with high PDGFR-α expression; it may be possible to base imatinib treatment on PDGFR-α expression in glioma patients. Amplification of the *PDGFR*-α gene and/or overexpression of the receptor at the protein level, has been found in high-grade gliomas (Fleming *et al.* 1992; Kumabe *et al.* 1992; Smith *et al.* 2000), and in astrocytomas (Guha *et al.* 1995; Saxena *et al.* 1999). Therefore, this receptor may play a more generalized role in glioma formation, as it is not exclusive to glioblastomas, and non-responders had higher PDGFR-β expression indicating that PDGFR-β may be associated with a more resistant phenotype.

P-Akt, p-p70S6K, p-C-Abl and p-C-Kit Expression in Relation to Gefitinib Responders in High-Grade Glioma Cultures

A downstream protein of MTOR, p-p70S6K was expressed in 84.6% of the cultures and p-Akt in 65.3%. Li *et al*, found in a cohort of 36 glioblastoma patients expression levels of p-Akt (36.1%), p-MTOR (44.4%), and p-p70S6K (41.7%); in addition they found levels correlated with grade of malignancy (Li *et al.* 2010). Annovazzi *et al*, found mTOR, p-p70S6K, p-Akt expression in 64 malignant gliomas, and found the expression which was increased in higher grades of malignancy (Annovazzi *et al.* 2009).

In our cohort higher expression of p-p70S6K was found in the gefitinib responders, and lower expression in non-responders, erlotinib and imatinib responders (Fig. 3.5.13) (Table 3.5.11). MTOR can be regulated independently of PI3K (Tang *et al.* 2003), the MTOR-p70S6K pathway may play a more critical role in tumourigenesis, this would explain the higher expression of p-p70S6K in gefitinib responders. Gefitinib responders had a slightly lower PTEN expression in comparison to the other groups; PTEN may have loss of function in gefitinib responders.

In addition higher expression of p-C-Abl and p-C-Kit was found with gefitinib responders than with the non-responders, erlotinib or imatinib responders (Fig. 3.5.12) (Table 3.5.10). Jiang *et al*, showed that the over-expression of C-Abl has been found in glioblastomas compared but not in lower grade gliomas, suggesting an association with poor survival (Jiang *et al.* 2006). Stanulla *et al*, showed that the expression of C-Kit was found in the cytoplasm of glioma cell lines, suggesting its involvement in the autocrine growth regulation of glioma cells (Stanulla *et al.* 1995). It may also be that gliomas expressing higher levels of p-C-Kit and p-C-Abl are more responsive to gefitinib, because higher levels of expression of the phosphorylated protein targets of the PI3K/Akt pathway were found in the gefitinib responders indicated that the pathway was more active in gefitinib responders.

Bioinformatic Analysis of Proteins of the PI3K/Akt Pathway in Relation to Response to Tyrosine Kinase Inhibitors in High-Grade Glioma

Using hierarchical cluster analysis (HCA) and unsupervised principal components analysis (PCA) two distinct clusters of samples were found within the cohort. It is possible that the 2 clusters represent 2 different subgroups of high-grade gliomas. Brennan *et al*, took a cohort of 27 glioma samples and carried out proteomic analysis, to examine signal transduction pathways (Brennan *et al.* 2009). They compared their results with The Cancer Genome Atlas (Brennan *et al.* 2009), which contains expression data of 243 glioblastoma samples; 3 subclasses of glioblastoma emerged, one with high EGFR activation, another with high PDGFR activation, and a third had loss of the RAS regulator Neurofibromatosis type I (NF1) (Brennan *et al.* 2009). The EGFR signalling class had high notch pathway activation, the PDGF class had high levels of PDGFB ligand and phosphorylation of PDGFR-β and NF-kappa-B (NFκ-B). The class with loss of NF1 had lower MAPK and PI3K activation (Brennan *et al.* 2009). Cluster 2 from the present study may correspond to class 2, because it is characterized by high PDGFR-β expression (Brennan *et al.* 2009). It would be interesting to check the samples for NF1 loss and notch signalling by proteomic analysis to see if any of the samples correspond to the third class mentioned (Brennan *et al.* 2009). If glioma samples become classified into more specific subgroups based on protein expression and pathway signalling, a patient's treatment could become tailored with specific drugs to suit each individual, and possibly result in more effective treatment.

High expression of PTEN and PDGFR-α was characterized for cluster 1 (11 samples), while PDGFR-β, EGFR, p-C-Kit and p-C-Abl expression was predominant in cluster 2 (15 samples) (Fig. 3.5.14).

High EGFR and p-Akt expression correlated with low survival time in cluster 2 in glioblastomas (Figs. 3.5.20 and 3.5.22); these 2 biomarkers have been previously associated with poor prognosis in glioma (Shinojima *et al.* 2003). PDGFR-β, PDGFR-α, p-C-Kit and p-C-Abl expression did not correlate with survival in either cluster (Figs. 3.5.15, 3.5.16, 3.5.18 and 3.5.19). High expression of PTEN was found in all samples in cluster 1 (Fig. 3.5.17) the average doubling time

for cluster 1 was 100 hours whereas for cluster 2 it was 70 hours (Tables 3.5.12 and 3.5.13), this indicated that a loss of PTEN resulted in a higher proliferation rate. There were 10 gefitinib responders in cluster 2 (Table 3.5.13). P-C-Abl had no effect on survival in cluster 1; in cluster 2, 8 out of 15 patients with C-Abl expression had less than 20 months survival (Fig. 3.5.19). Overexpression of C-Abl has been found in glioblastomas compared to lower grade gliomas, suggesting an association with poor survival (Jiang *et al.* 2006). Higher levels of p-C-Kit expression have been associated with lower survival times in high-grade glioma (Sun *et al.* 2006). P-p70S6K expression in cluster 2 was found in 5 patients with survival of 10 months or less, and 4 patients with less than 20 months survival; it was not associated with survival in cluster 1 (Fig. 3.5.21). Higher expression of p70S6K in glioblastoma is associated with poor prognosis (Pelloski *et al.* 2006). P-Akt expression in cluster 1 was found in 5 patients with less than 12 months survival, and 4 patients who had no expression had greater than 19 months survival; with cluster 2, 4 patients with p-Akt expression had survival of 10 months or less, and 4 had less than 20 months survival (Fig. 3.5.22). The activation of Akt seems to be a consequence of the loss of PTEN function (Wu *et al.* 1998).

Amplification of the *PDGFR-α* gene and/or overexpression of the receptor at the protein level, has been found in high-grade gliomas (Fleming *et al.* 1992; Kumabe *et al.* 1992; Smith *et al.* 2000). Expression and amplification of the PDGFR-α gene have also been found in astrocytomas (Guha *et al.* 1995; Saxena *et al.* 1999). However, PDFGR-α expression did not have any effect on survival time in either cluster (Fig. 3.5.16). In addition PTEN also had no effect on survival (Fig. 3.5.17).

Unsupervised PCA of the culture data captures 55% of the variance in the dataset showing PTEN, PGDFR-α and PGDFR-β loading vectors in approximately the same direction (Fig. 3.5.23). All drug responses were separated using PCA based on the expression of various target proteins (Fig. 3.5.23). Non-responders and responders to erlotinib and gefitinib showed lower expression of PDGFR-α (Fig. 3.5.24 and 3.5.25); in contrast, higher expression was found in imatinib responders (Fig. 3.5.26). The majority of gefitinib responders were influenced by the proteins of

the PI3K/Akt pathway (Fig. 3.5.25); while erlotinib response may be characterised by lack of expression of those markers (Fig. 3.5.24), suggesting that erlotinib responsiveness may not be reliant on the PI3K/Akt pathway.

PI3K/Akt Pathway in High-Grade Glioma

In high-grade gliomas was examined; other pathways, and downstream proteins seem to be involved in glioma tumourigenesis, e.g. RAS/RAF signalling is found in gliomas (Jeuken *et al.* 2007). Copy number gains in the oncogenes BRAF, NRAS, KRAS, and HRAS and in growth factors EGF, PDGF, IGF, FGF, TGF have been found in 44% and 53% of gliomas, respectively (Jeuken *et al.* 2007). These copy number gains were most frequently found in WHO grade III and IV gliomas; phosphorylated MAPK, the activated downstream compound of the RAS/RAF pathway, was detected in most cases (Jeuken *et al.* 2007). Fan *et al*, found protein kinase C (PKC) to be a mediator of EGFR signalling to MTOR independently of Akt in glioma, separating MTOR from the Akt-signalling cascade (Fan *et al.* 2009). They used erlotinib to inhibit EGFR signalling, and found a correlation with decreased levels of phosphorylated MTOR (p-MTOR) and p70S6K in cells which expressed the wild type for PTEN (Fan *et al.* 2009). EGFR inhibition did not affect cells which expressed p-MTOR, p70S6K and mutant PTEN; the amount of p-Akt decreased with EGFR inhibition, however, Akt levels did not correlate with MTOR signalling (Fan *et al.* 2009). Activated MTOR correlated with the presence of activated Akt, in glioblastoma, MTOR is thought to have a stimulatory effect on PI3K/Akt (Choe *et al.* 2003). They identified an Akt-independent pathway, linking EGFR to MTOR which was dependent on PKC (Fan *et al.* 2009). They showed that by blocking or activating Akt there was no effect on proliferation or response to erlotinib in glioma, and the levels of EGFR correlated with p-p70S6K and PKC in glioblastoma, and but not with Akt (Fan *et al.* 2009). Furthermore the inhibition of PKC decreased the viability of glioma cells independently of EGFR or PTEN expression levels (Fan *et al.* 2009). Perhaps PKC is a more important signalling pathway in glioma; PKC inhibitors need to be examined in glioma and may have more promising results than PI3K/Akt inhibitors. In relation to TKI responsiveness

there is a need to look at all of the different pathways to gain a better understanding of cross talk between pathways, and biomarkers for responsiveness to TKIs.

3. 5 Summary and Conclusion

With 26 high-grade gliomas cultures correlation of expression of proteins from the PI3K/Akt pathway, resulted in statistically significant separation of responders and non-responders to TKIs. High PDGFR-α and PTEN expression correlated with imatinib responders. Higher expression of p-Akt, p-p70S6K, p-C-Abl and p-C-Kit was found with gefitinib responders. Possibly indicating that gefitinib responders have a more active PI3K/Akt pathway. Erlotinib responders and non-responders had much lower expression of the proteins from the PI3K/Akt pathway. They may be more dependent on other pathways for survival, such as the RAS/MAPK or PKC pathway.

There was a correlation with low survival and high EGFR and p-Akt expression, this was not surprising as over expression of EGFR and high levels of p-Akt have been reported to be associated with a poor prognosis in glioma.

3.6 MicroRNA

3.6.1 Taqman Low Density Array (TLDA) Analysis of Two Subsets of Primary Glioma Cultures

Within the cohort of primary glioblastoma cultures there were large differences in proliferation rate and invasive behaviour. The objective of this part of the project was to look for miRNAs that regulate proliferation and invasion in glioblastomas. Therefore, two pools were formed: pool 1 consisted of two invasive glioblastoma cultures with a high proliferation rate, and pool 2 contained two glioblastoma cultures with very little invasion activity and a much lower proliferation rate (Tables 3.6.1 and 3.6.2). TLDA analysis (section 2.14.1) was carried out on both pools, the expression of 365 miRNAs was measured. From the TLDA data miRNA expression was compared in pool 1 (fast, invasive) with pool 2 (slow, non-invasive). Proliferation rate was previously measured based on the doubling time of the cultures (see section 2.4.2); invasion was measured with the 3D spheroid invasion assay (see section 2.8). Previously with pool 2 biospheres (tissue pieces) (Fig. 3.3.10) of N070978 were found to be invasive, however, when the culture of N070978 was tested for invasion using the 3D collagen invasion assay it was non-invasive. Not all biospheres of N060913 were invasive, the cell culture of N060913 was not tested for invasion as it stopped proliferating. For clarity, pool 2 is referred to as non-invasive.

Pool 1 miRNA expression was designated as 100%. Using a cycle threshold (Ct) cut off of 34, out of 365 miRNAs, 82 were upregulated in Pool 2, and 34 were downregulated; of which 19 have been reported in the literature to be associated with glioma proliferation or invasion (Table 3.6.3). A fold change cut off of 2 or greater was then applied, this resulted in 62 miRNAs identified as upregulated in pool 2, and 13 downregulated in pool 2 in comparison to pool 1.

The Ct (section 2.14.2) cut off was 34, therefore anything at 34 or above was defined as not expressed or to have very low levels of a miRNA expressed. 13 miRNAs were undetected or present at very low levels in pool 1 (fast, invasive) in

comparison to pool 2 (slow, non-invasive) (Table 3.6.5). 13 miRNAs were undetected or present at very low levels in pool 2 in comparison to pool 1 (Table 3.6.6).

Table 3.6.1 TLDA plate with the fast, invasive **Pool 1**, with 2 invasive primary glioblastoma cultures with a fast proliferation rate.

Cell Culture	Tumour Type	Doubling Time (hrs)	Invasive Behaviour	Patient Survival Time (months)	Age
N070152	Primary Glioblastoma	55	Invasive	5	52
N070859	Primary Glioblastoma	55.98	Invasive	12	55

Table 3.6.2 TLDA plate with the slow non-invasive **Pool 2**, with 2 primary glioblastoma cultures, one non-invasive, and one slightly-invasive, both with a slow proliferation rate.

Cell Culture	Tumour Type	Doubling Time (hrs)	Invasive Behaviour	Patient Survival Time (months)	Age
N060978	Primary Glioblastoma	98.33	Non-invasive	3	54
N060913	Primary Glioblastoma	>168	Poorly-invasive	110	67

Table 3.6.3 Deregulated miRNAs identified in primary glioblastomas in the present study (in comparison to pool 1) and in other studies.

MiRNA	Our TLDA Analysis	Deregulation in Glioblastomas
MiR-125b	↑P2	↑ (Ciafre *et al.* 2005)
MiR-328	↑P2	↓ (Silber et al. 2008)
MiR-31	↑P2	↓ (Silber *et al.* 2008)
MiR-155	↓P2	↑ (Silber *et al.* 2008)
MiR-19a	↓P2	↑ (Malzkorn et al. 2010)
Mir-146b	↓P2	↓ (Xia *et al.* 2009)
MiR-323*	↑P2	↓ (Silber *et al.* 2008)
MiR-101*	↑P2	↓ (Silber *et al.* 2008)
MiR-181b*	↑P2	↓ (Ciafre *et al.* 2005)
MiR-218*	↑P2	↓ (Godlewski *et al.* 2008)
MiR-25*	↑P2	↓ (Ciafre *et al.* 2005)
MiR-330	↑P2	↑ (Gal et al. 2008)
MiR-34a	↑P2	↓ (Li *et al.* 2009)
MiR-107	Low P2	↑ (Gal *et al.* 2008)
MiR-9	Low P2	↑ (Malzkorn *et al.* 2010)
MiR-221*	↓P2	↑ (Zhang *et al.* 2009)
MiR-222*	↓P2	↑ (Zhang *et al.* 2009)
MiR-296*	↓P2	↑ (Wurdinger et al. 2008)
MiR-132*	↓P2	↓ (Silber *et al.* 2008)

↑: upregulated, ↓: downregulated. *: less than 2 fold dysregulated. P2: Pool 2 (slow, non-invasive glioblastomas). Low: very low levels detected or undetected.

MiRNAs previously reported in the literature to be associated with invasion or proliferation in glioblastoma, also found to be deregulated in the present study.

3.6.1.1 MiRNAs Upregulated in Pool 2 in Comparison to Pool 1

MiR-143 was the most highly upregulated miRNA in pool 2, with a 7.6-fold increase in expression in pool 2 in comparison to pool 1. Of the 62 miRNAs that were upregulated in pool 2 in comparison to pool 1, 20 of these miRNAs were greater than 3 fold upregulated (Fig. 3.6.1); 18 were greater than 2 fold upregulated in pool 2 (Fig. 3.6.2).

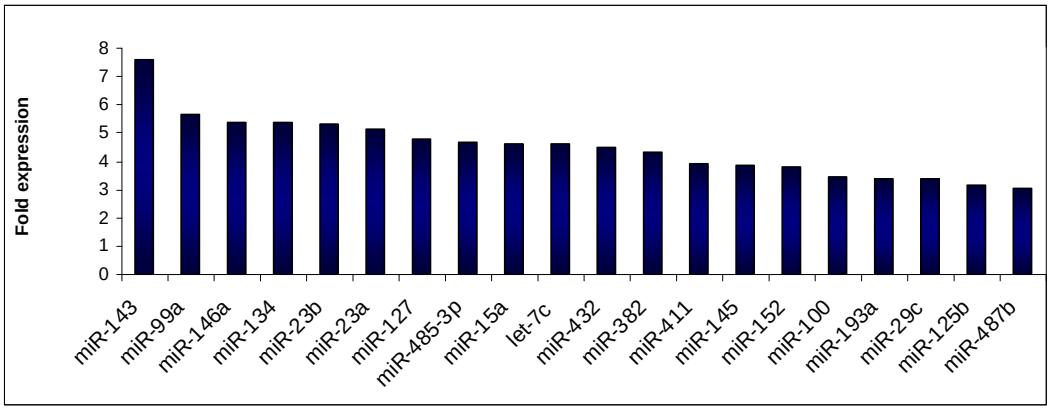

Fig. 3.6.1 20 MiRNAs greater than 3 fold upregulated in pool 2 in comparison to pool 1.

Table 3.6.4 miRNAs upregulated greater than 3 fold in pool 2 (slow, non-invasive) compared to pool 1 (fast, invasive), genes/function/cancer they are associated with.

miRNA	Fold Upregulated	Genes/Function/Cancer associated with
miR-143	7.59	**ERK5**: apoptosis (Akao et al. 2009). **DNMT3A**: (Ng et al. 2009) **FNDC3B**: invasion/migration & metastasis (Zhang et al. 2009) **KRAS**: growth (Chen et al. 2009). **ABL2**: C-Abl
miR-99a	5.67	**SAMSN1** and **USP25**: (Yamada et al. 2008). Downregulated in ovarian cancer (Nam et al. 2008)
miR-146a	5.37	**BRMS1**: invasion, migration and metastasis (Hurst et al. 2009) proliferation (Wang et al. 2008). **MMPs**: migration and invasion (Xia *et al.* 2009)
miR-134	5.36	Developmental in brain (Schratt et al. 2006)
miR-23b	5.31	**UPA** & **C-MET**: migration & proliferation (Salvi et al. 2009)
miR-23a	5.14	Apoptosis (Chhabra et al. 2009)
miR-127	4.80	**E2F3**, **NOTCH1**, **BCL6**, **ZFHX1B**, and **BCL2**: apoptosis, proliferation, cell-to-cell connection (Tryndyak et al. 2009)
miR-485-3p	4.65	?
miR-15a	4.61	Cell cycle arrest (Bandi et al. 2009). Proliferation (Calin et al. 2008)
Let-7c	4.61	Prostate cancer (Ozen et al. 2008)
miR-432	4.50	Muscle development and growth (McDaneld et al. 2009)
miR-382	4.30	?
miR-411	3.90	?
miR-145	3.88	**TP53**: apoptosis (Spizzo et al. 2009)
miR-152	3.79	?
miR-100	3.42	Oral cancer (Henson et al. 2009)
miR-193a	3.40	Tumour suppressor (Kozaki et al. 2008)
miR-29c	3.39	**TP53**: (Mraz et al. 2009)
miR-125b	3.15	**ErbB2**: proliferation and migration (Hofmann et al. 2009)
miR-487b	3.04	?

?: no information available on this. Genes are highlighted in bold. References are in parenthesis.

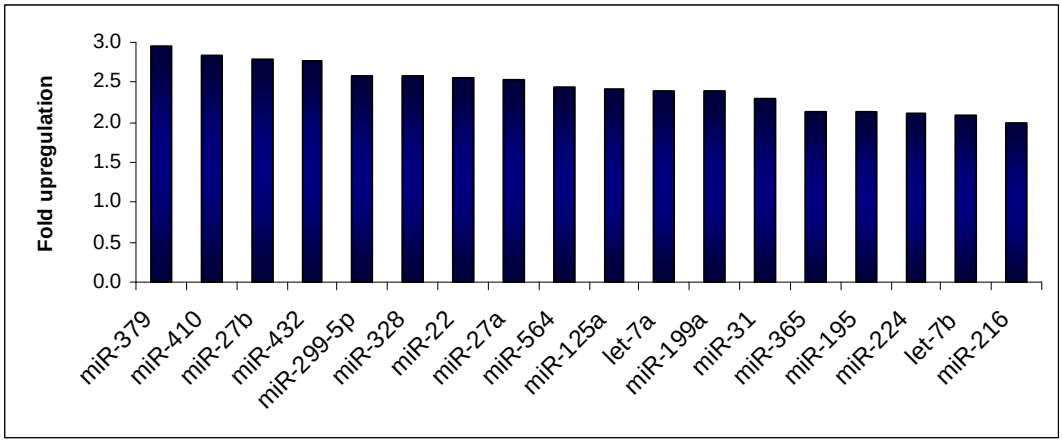

Fig. 3.6.2 18 miRNAs greater than 2 fold upregulated in pool 2 in comparison to pool 1.

3.6.1.2 MiRNAs Downregulated in Pool 2 in Comparison to Pool 1

13 miRNAs were 2 fold or greater downregulated in pool 2 (slow, non-invasive) in comparison to pool 1 (fast, invasive) (Fig. 3.6.3).

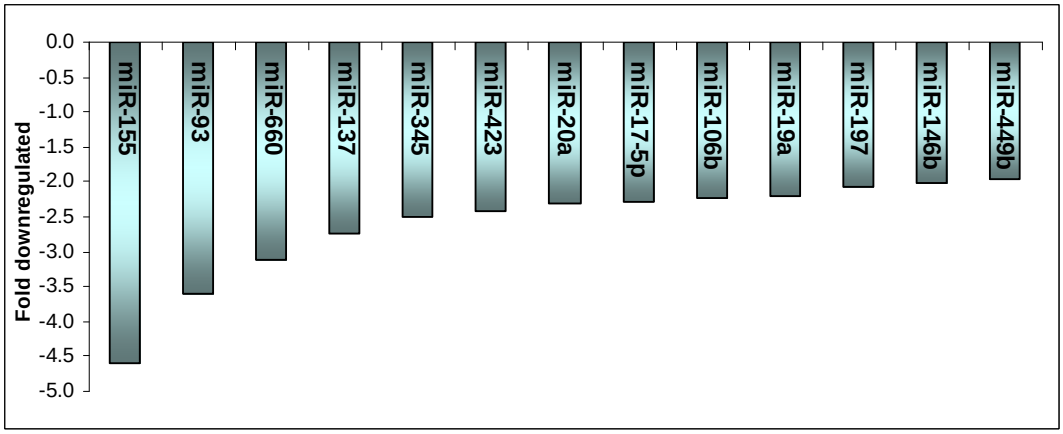

Fig. 3.6.3 13 miRNAs 2 fold or greater downregulated in pool 2 in comparison to pool 1.

Table 3.6.5 miRNAs downregulated 2 fold or greater in pool 2 (slow, non-invasive) compared to pool 1 (fast, invasive), genes/function/cancer they are associated with.

miRNA	Fold Downregulated	Genes/Function/Cancer associated with
miR-155	3.6	Targets the tumour suppressor genes:**TP53INP1** (Yeung et al. 2008), **FUS1** (Du et al. 2009), **BCL11B** (Karlsson et al. 2007), **PTPRD** (Veeriah et al. 2009), (Solomon et al. 2008), **CDKN1A** (Petrocca et al. 2008)
miR-93	4.6	**TP53INP1** (Gironella et al. 2007) **JARID2**: cell cycle regulator (Bolisetty et al. 2009)
miR-660	3.1	**RAB3GAP2**: neurodevelopment (Aligianis et al. 2006)
miR-137	2.8	High expression found in lymph node metastasis of colorectal cancer (Huang et al. 2009)
miR-345	2.5	Targets the tumour suppressor **CDKN2A** (Guled et al. 2009)
miR-423	2.4	Targets the tumour suppressor **CDKN2A** (Guled *et al.* 2009)
miR-20a	2.3	Promotes proliferation and invasion by targeting amyloid precursor protein (**APP**) in ovarian cancer (Fan *et al.* 2010)
miR-17-5p	2.3	Promotes breast cancer migration and invasion by suppression of **HBP1** (Li et al. 2010)
miR-106b	2.2	Functions as an oncogene by suppressing **p21** and **BIM** (Kan et al. 2009)
miR-19a	2.2	Involved in the malignant progression in glioma (Malzkorn *et al.* 2010)
miR-197	2.1	Regulates the expression of the tumour suppression gene FUS1 (Du *et al.* 2009)
miR-146b	2.0	Highly expressed in thyroid carcinoma (Chou *et al.* 2010)
miR-449b	2.0	?

?: no information available on this. Genes are highlighted in bold. References are in parenthesis.

3.6.1.3 MiRNAs Detected in the TLDA as Off or Very Low Levels Detected

The Ct cut off was 34 and above, therefore the closer the Ct was to 34 the lower the level of miRNA detected and the more likely for the miRNA to be off. 13 miRNAs were undetected or very low levels (Ct>33) detected in pool 1 (fast, invasive) in comparison to pool 2 (slow, non-invasive) (Table 3.6.6). 13 miRNAs were undetected or very low levels detected in pool 2 in comparison to pool 1 (Table 3.6.7).

Table 3.6.6 13 miRNAs off or very low levels detected in Pool 1 (fast, invasive) in comparison to Pool 2 (slow, non-invasive), genes/function/cancer they are associated with.

miRNA	Cycle Threshold Pool 2, Pool 1	Genes/Function/Cancer associated with
miR-193b	33.25, 33.97	**UPA**: invasion (Li et al. 2009)
miR-213	33.28, 33.97	?
miR-302b	32.29, 33.97	**CYCLIN D2**: pluripotency of embryonic stem cells (Lee et al. 2008)
miR-30e-5p	32.94, 34.67	?
miR-330	31.79, 33.94	**E2F1**: growth and apoptosis (Lee et al. 2009)
miR-433	32.40, 33.96	Gastric carcinoma (Luo et al. 2009)
miR-497	33.38, 36.94	Breast cancer (Yan et al. 2008)
miR-518f	31.96, undet	?
miR-564	32.93, 34.02	?
miR-646	32.96, undet	?
miR-654	32.99, undet	?
miR-34a	32.11, 33.96	**C-MET** and **NOTCH**: growth (Li *et al.* 2009)
miR-485-5p	32.49, 33.99	?

?: no information available on this. Genes are highlighted in bold. References are in parenthesis. Undet: undetermined.

Table 3.6.7 13 miRNAs off or very low levels detected in Pool 2 (slow, non-invasive) in comparison to Pool 1 (fast, invasive), genes/function/cancer they are associated with.

miRNA	Cycle Threshold Pool 1, Pool 2	Genes/Function/Cancer associated with
miR-10a	29.9, undet	**HOXB1** and **HOXB3**: metastasis (Weiss et al. 2009)
miR-219	32.9, undet	?
miR-501	32.9, undet	?
miR-107	29.3, 35.98	Head and neck cancer (Liu et al. 2009)
miR-589	32.9, undet	?
miR-9	28.3, 36.01	**CBX7**: (tumour suppressor) in glioma (Chao *et al.* 2008)
miR-182	30.4, 35.95	**FOXO3**: metastasis (Segura et al. 2009)
miR-18a	32.9, 33.99	Hepatocellular carcinoma (Liu et al. 2009)
miR-32	32.9, 34.26	**PTEN, BCL11B**: (tumour suppressor genes)
miR-424	32.5, 34.97	**BCL2L2**: antiapoptotic protein
miR-449	31.7, 36.99	?
miR-532	30.7, 33.96	?
miR-550	31.3, 35.97	?

?: no information available on this. Genes are highlighted in bold. References are in parenthesis. Undet: undetermined.

3.6.2 Predicted Genes for miRNA Groups

To date biological experiments have uncovered only a small fraction of all miRNA targeted genes (miTGs); therefore computational target prediction remains one of the key means to analyze the role of miRNAs in biological processes. 20 miRNAs were selected which were the most upregulated in pool 2 in comparison to pool 1 (Fig. 3.6.1) and a search was performed with this group of miRNAs using the DIANA LAB database (http://diana.cslab.ece.ntua.gr/?sec=software) (DNA intelligent analysis), which uses an algorithm to predict target genes for a group of miRNAs. The top ten genes predicted to be targeted by the 20 miRNAs most upregulated in pool 2 in comparison to pool 1 are listed; the target prediction is grouped by mRNA, ordered by descending number of expected sites for any of the selected miRNAs (Tables 3.6.8 (a) and (b)). In addition the 20 most upregulated miRNAs in pool 1 were selected (Tables 3.6.9 (a) and (b)), the top ten genes predicted to be targeted by this group of miRNAs are listed.

Table 3.6.8 (a) Top 10 predicted target genes using the DIANA LAB database (http://diana.cslab.ece.ntua.gr/?sec=software) for 20 miRNAs most upregulated in pool 2 (slow, non-invasive) in comparison to pool 1 (fast, invasive).

Gene	Name	Expected Number of miRNA binding sites
ONECUT2	One cut homeobox 2	18.4
TNRC6B	Trinucleotide repeat containing 6B	16.0
SH3TC2	SH3 domain and tetratricopeptide repeats 2	15.7
FLJ25778	Hypothetical protein FLJ25778	12.9
IGF1R	Insulin-like growth factor 1 receptor	12.4
BNC2	Basonuclin 2 zinc finger protein basonuclin	12.0
CC5	Chloride channel 5 (nephrolithiasis 2, X-linked	11.9
FLJ20309	Hypothetical protein	11.9
ACVR2B	Activin A receptor, type IIB	11.5
YOD1OTU	Deubiquinating enzyme 1 homolog (S. cerevisiae)	11.2

Table 3.6.8 (b) Published information for the top 10 predicted target genes with the DIANA LAB database (http://diana.cslab.ece.ntua.gr/?sec=software) for 20 miRNAs most upregulated in pool 2 (slow, non-invasive) in comparison to pool 1 (fast, invasive).

Gene	Published information
ONECUT2	Methylated in lymphoma (Pike *et al*. 2008), and lung cancer (Rauch *et al*. 2006)
TNRC6B	Associated with aggressive prostate cancer risk (Sun *et al.* 2009)
SH3TC2	Mutations in this gene result in autosomal recessive Charcot-Marie-Tooth disease type 4C (Lupo *et al*. 2009)
FLJ25778	Cell cycle regulator (Balaji *et al*. 2009)
IGF1R	IGF-I modulates proliferation and strongly stimulates migration of glioma cell lines in vitro (Schlenska-Lange *et al.* 2008)
BNC2	?
CC5	?
FLJ20309	?
ACVR2B	An activin type 2 receptor. Activins are dimeric growth and differentiation factors which belong to the transforming growth factor-beta (TGF-beta) superfamily of structurally related signaling proteins (Ishikawa *et al.* 1998)
YOD1 OTU	?

? no information available on this. References are in parenthesis.

Table 3.6.9 (a) Top 10 predicted target genes with the DIANA LAB database (http://diana.cslab.ece.ntua.gr/?sec=software) for 20 miRNAs most upregulated in pool 2 (slow, non-invasive) in comparison to pool 1 (fast, invasive).

Gene	Name	Expected Number of miRNA binding sites
ATXN1	Ataxin 1	11.2
TNRC6B	Trinucleotide repeat containing 6B	10.2
BNC2	Basonuclin 2 Zinc finger protein basonuclin-2	8.4
SH3TC2	SH3 domain and tetratricopeptide repeats 2	8.2
KLF12	Kruppel-like factor 12	8.2
TCF4	Transcription factor 4	7.7
FLJ25778	Hypothetical protein	7.2
AAK1	AP2 associated kinase 1	7.1
MECP2	Methyl CpG binding protein 2 (Rett syndrome)	6.9
NFIB	Nuclear factor I/B	6.5

Table 3.6.9 (b) Published information for the top 10 predicted target genes with the DIANA LAB database (http://diana.cslab.ece.ntua.gr/?sec=software) for 20 miRNAs most upregulated in pool 1 (fast, invasive) in comparison to pool 2 (slow, non-invasive).

Gene	Published information
ATXN1	Ataxin-1 mediates neurodegeneration (Tsuda *et al.* 2005)
TNRC6B	Required for miRNA function (Baillat and Shiekhattar 2009)
BNC2	Has the potential to generate nearly 90,000 mRNA isoforms encoding over 2000 different proteins (Vanhoutteghem and Djian 2007). Expressed in glioblastoma, a tumour suppressor gene (Nord *et al*. 2009).
SH3TC2	Mutations in this gene result in autosomal recessive Charcot-Marie-Tooth disease type 4C, a childhood-onset neurodegenerative disease characterized by demyelination of motor and sensory neurons (Lupo *et al.* 2009).
KLF12	Activator protein-2 alpha (AP-2 alpha) is a developmentally-regulated transcription factor and important regulator of gene expression during vertebrate development and carcinogenesis.
TCF4	Associated with the pathogenesis of colorectal cancer (Goel and Boland 2010).
FLJ25778	Cell-cycle regulator (Balaji *et al.* 2009).
AAK1	?
MECP2	Contributes to apoptosis (Bracaglia *et al*. 2009).
NFIB	?

? no information available on this. References are in parenthesis.

3.6.3 Top Ten miRNA Targets

From the TLDA data comparing pool 1 (fast, invasive) to pool 2 (slow, non-invasive) the top ten most interesting miRNA targets were selected (Table 3.6.10). In relation to pool 1, 3 miRNAs were chosen that were upregulated and 5 downregulated, 1 off in pool 1, and 1 off in pool 2 for functional analysis.

Table 3.6.10 Top ten most interesting miRNA targets differentially expressed in pool 1 (fast, invasive) in comparison to pool 2 (slow, non-invasive) from the TLDA analysis.

miRNA	Comparison	Gene targets/ Function
miR-93	3.6 fold ↓	Targets the tumour suppressor genes:**TP53INP1** (Yeung *et al.* 2008), **FUS1** (Du *et al.* 2009), **BCL11B** (Karlsson *et al.* 2007), **PTPRD** (Veeriah *et al.* 2009), (Solomon *et al.* 2008),**CDKN1A** (Petrocca *et al.* 2008)
miR-155	4.6 fold ↓	**TP53INP1** (Gironella *et al.* 2007) **JARID2**: cell cycle regulator (Bolisetty *et al.* 2009)
miR-660	3.1 fold ↓	**RAB3GAP2**: neurodevelopment (Aligianis *et al.* 2006)
miR-143	7.6 fold ↑	**ERK5**: apoptosis (Akao *et al.* 2009). **DNMT3A**: growth (Ng *et al.* 2009) **FNDC3B**: invasion/migration and metastasis (Zhang *et al.* 2009) **KRAS**: growth (Chen *et al.* 2009). **ABL2**: growth
miR-99a	5.7 fold ↑	**SAMSN1** and **USP25** (Yamada *et al.* 2008)
miR-146a	5.4 fold ↑	**BRMS1**: metastasis, invasion and migration (Hurst *et al.* 2009) Growth (Wang *et al.* 2008). **MMPs**: glioma migration and invasion by (Xia et al. 2009)
miR-134	5.4 fold ↑	Developmental in brain (Coolen and Bally-Cuif 2009)
miR-23b	5.3 fold ↑	**UPA** and **C-MET**: migration and proliferation (Salvi *et al.* 2009)
miR-518f	Off P1 V P2 (*)	?
miR-10a	Off P2 V P1 (**)	**HOXB1** and **HOXB3**: metastasis (Weiss *et al*. 2009)

* Ct: 31.96, ** Ct: 29.96, Ct: cycle threshold, Off:Ct>34. ↓ downregulated in pool 2, ↑ upregulated in pool 2. Genes are highlighted in bold. ? no information available on this. References are in parenthesis.

3.6.3.1 Expression of miR-155 in Glioma Cultutres and Normal Human Astrocytes

The TLDA result identified that MiR-155 was 4.6 fold upregulated in pool 1 (fast, invasive) in comparison to pool 2 (slow, non-invasive). The presence of miR-155 was measured by qRT-PCR in normal human astrocytes, 5 primary glioblastomas, 1 grade II astrocytoma II culture, and one established glioblastoma cell line SNB-19 (Fig. 3.6.4 (a)) (Table 3.6.11). As a calibrator N070152A was used and this was set to 100% expression of miR-155. N070152 and N070859 were included in pool 1 and N060978 and N060913 in pool 2 of the TLDA analysis, which gave 4.6 fold downregulation of miR-155 in pool 2 in comparison to pool 1 (Fig. 3.6.4). However, N070859 showed downregulation of miR-155 in comparison to N070152, when miR-155 was expected to also be upregulated in N070859. In addition high expression of miR-155 was found in the normal human astrocytes, and very low expression of miR-155 in the established glioblastoma cell line SNB-19; the opposite effect was expected as miR-155 was found to be upregulated in the invasive pool with high proliferation.

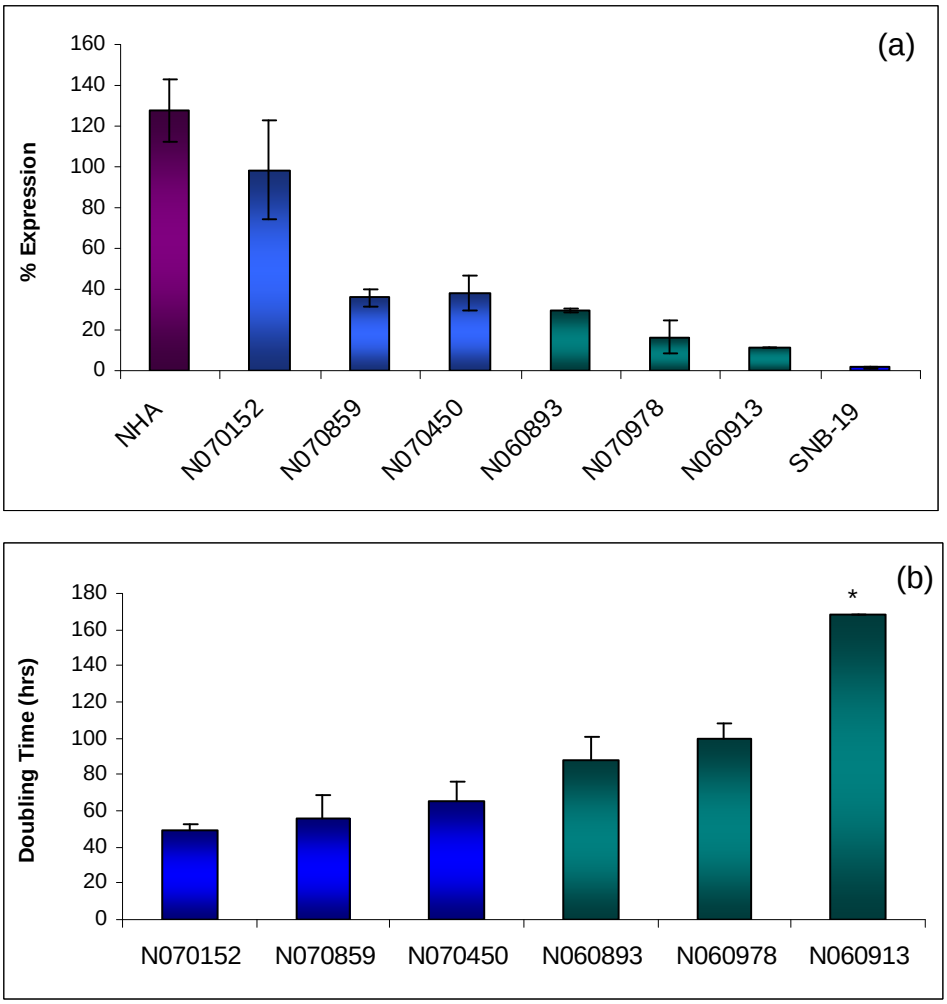

Invasive (blue), Non-invasive/poorly-invasive (green). *: doubling time >168 hrs.

Fig. 3.6.4 (a) MiR-155 expression by qRT-PCR in normal human astrocytes, 5 primary glioblastomas and 1 grade II astrocytoma II culture and one established glioblastoma cell line (SNB-19). N070152A was a calibrator sample taken as 100% expression of miR-155. Samples (with the exception of N060913, measured in technical triplicate (n=3)) were measured in technical and biological triplicate (n=3x3). (b) Doubling time of 3 invasive cultures and 3 cultures with less invasion; all of which have been measured for miR-155 expression. Standard deviations were generated using Microsoft excel software.

Table 3.6.11 Characteristics of primary glioma cultures validated with miR-155.

Cell Culture	Tumour Type	Doubling Time (hrs)	Invasive Behaviour	% Expression of miR-155
N070152	Primary Glioblastoma	55	Invasive	98.2
N070859	Primary Glioblastoma	56	Invasive	35.8
N070450	Grade II Astrocytoma	65.1	Invasive	37.8
N060893	Secondary Glioblastoma	88.1	Poorly-invasive	29.6
N060978	Primary Glioblastoma	98.3	Non-invasive	16.6
N060913	Primary Glioblastoma	>168	Poorly-invasive	11.1
SNB-19*	Glioblastoma	-	Invasive	1.7
NHA	-	-	Invasive	127.7

* SNB-19 is an established cell line known to have a fast proliferation rate.

3.6.3.2 Expression of miR-93 in Glioma Cultures and Normal Human Astrocytes

MiR-93 was 3.6 fold upregulated in Pool 1 (fast, invasive) compared to Pool 2 (slow, non-invasive) in the TLDA analysis (Fig. 3.6.5). The presence of miR-93 was validated by qRT-PCR in one established glioblastoma cell line SNB-19, 12 glioma cultures (8 glioblastomas, 2 grade III astrocytomas, 1 grade III oligoastrocytoma, 1 grade II oligodendroglioma), and in normal human astrocytes (Table 3.6.12). N070152A was used as a calibrator and taken as 100% expression of miR-93. N070152 was an invasive primary glioblastoma culture with a high proliferation rate, which was included in pool 1 of the TLDA analysis. 3 biological repeats of each culture were included with the exception of N060913 and N070314; these cultures had very slow proliferation rate and only one RNA sample was obtained from them. Cell cultures with high proliferation showed high expression levels of miR-93, 3 of the cultures with high miR-93 expression were also invasive (Fig. 3.6.5 (a)). Conversely miR-93 was down-regulated in cultures with lower proliferation and invasion rate, and in normal human astrocytes (Fig. 3.6.5 (a)). N070152 and N070859 were included in pool 1, and N060978 and N060913 in pool 2.

These results indicated that expression of miR-93 positively correlates with invasive gliomas with a high proliferation rate. Some of the cultures with high expression of miR-93 also had a low doubling time, i.e. a low proliferation rate, and some of the cultures with low expression of miR-93 had a high doubling time, i.e. a low proliferation rate (Fig. 3.6.5 (b)). Most of the cultures with low expression of miR-93 showed little or no invasion (Table 3.6.12).

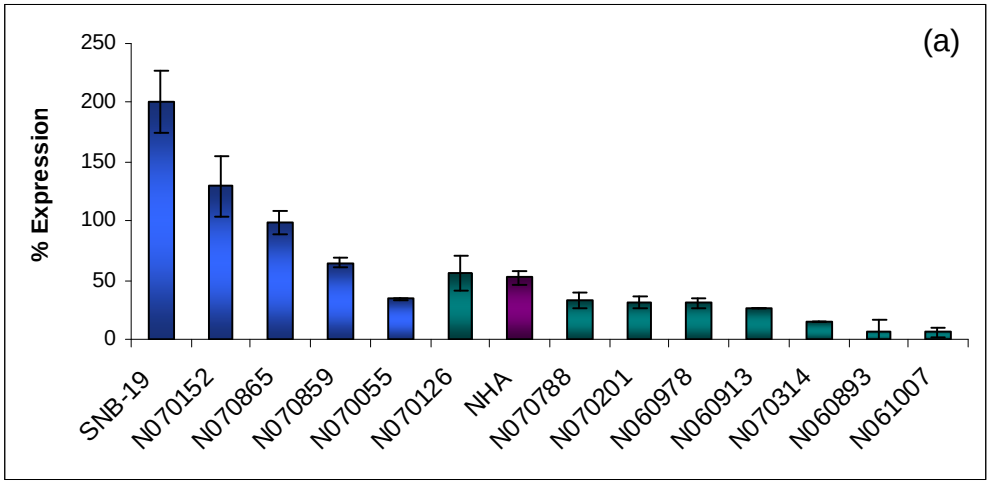

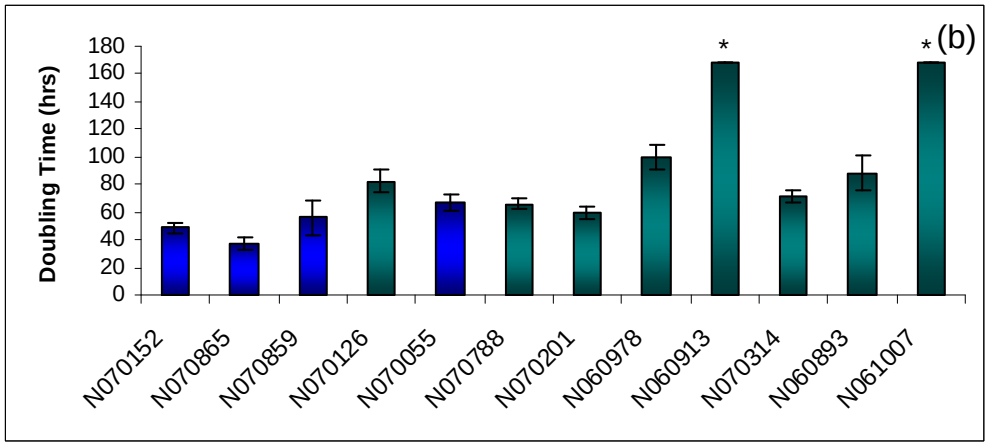

Invasive (blue), Non-invasive/poorly-invasive (green). *: doubling time >168 hrs.

Fig. 3.6.5 (a) Percentage expression of miR-93 in an established glioblastoma cell line SNB-19, normal human astrocytes (NHAs), and glioma cultures, N070152A was a calibrator sample taken as 100% expression of miR-93. Most cultures were measured in technical and biological triplicate (n=3x3) with the exception of N060913 and N070314, which were measured in technical triplicate only (n=3). (b) doubling time in glioma cultures. Standard deviations were generated using excel software.

Table 3.6.12 Doubling time and invasive behaviour of glioma cultures validated for miR-93 expression.

Cell Culture	Tumour Type	Doubling Time (hrs)	Invasive Behaviour	Percentage Expression of miR-93
SNB-19*	Primary Glioblastoma	-	Invasive	200.9
N070152	Primary Glioblastoma	55.0	Invasive	129.6
N070865	Primary Glioblastoma	37.3	Invasive	98.2
N070859	Primary Glioblastoma	56.0	Invasive	64.9
N070126	Primary Glioblastoma	82.5	Non-invasive	55.6
NHA	-	-	Invasive	52
N070055	Grade III Oligoastrocytoma	68.5	Invasive	34.4
N070788	Grade III Astrocytoma	65.7	Non-invasive	32.8
N070201	Grade III Astrocytoma	60.2	Non-invasive	31.0
N060978	Primary Glioblastoma	98.3	Non-invasive	30.6
N060913	Primary Glioblastoma	>168	Poorly-invasive	26.3
N070314	Grade II Oligodendroglioma	71.5	-	15.6
N060893	Secondary Glioblastoma	88.1	Poorly -invasive	5.9
N061007	Primary Glioblastoma	>168	Poorly -invasive	5.9

* SNB-19 is an established cell line known to have a fast proliferation rate.

3.6.3.3 Functional Validation of miR-93: Transfection of anti-miR-93 and pre-miR-93 into an Established Glioblastoma Cell Line

The established glioblastoma cell line SNB-19, an invasive cell line with a high proliferation rate showed upregulation of miR-93 (Fig. 3.6.5 (a)). SNB-19 was transiently transfected with anti-miR-93 and pre-miR-93 to examine the effect on proliferation when miR-93 expression was both decreased with anti-miR-93 and increased with pre-miR-93. The cells were seeded at 1X10E5/ ml, 1 ml per well in a 6 well plate for 3 days; with 2 µl of Neofx transfection reagent, and 30 nM of miRNA, negative pre-miR, negative anti-miR and siRNA (against kinesin). The media was changed 8 hours post- transfection. The cell numbers were then measured using the acid phosphatase assay (see section 2.4.1 B). Anti-miR-93 decreased proliferation by 13.2%; pre-miR-93 had no effect on proliferation (Fig. 3.6.6).

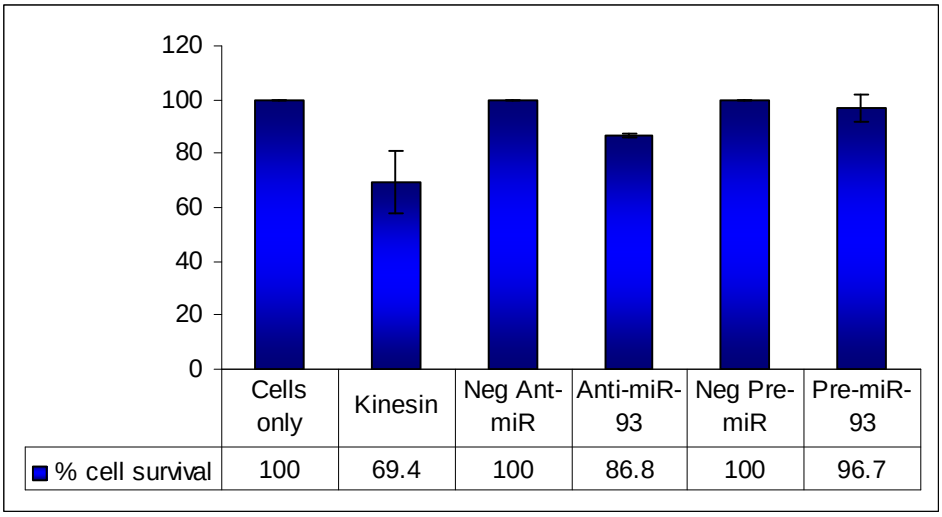

Fig. 3.6.6 Transient transfection of anti-miR-93 and pre-miR-93 into an established glioblastoma cell line SNB-19. 30 nM of miRNA, negative pre-miR, negative anti-miR and siRNA (against kinesin) with 2 µl of Neofx over a 3 day assay. Standard deviations were from 3 biologically individual assays (n=2X3). Standard deviations were generated using excel software.

3.6.3.4 Protein Targets of miR-93

We have shown miR-93 to be highly expressed in invasive glioblastomas with high proliferation, and low expression of miR-93 in non-invasive glioblastomas with low proliferation and in normal human astrocytes (Fig. 3.6.5 (a)).

Using the database microRNA.org (http://www.microrna. org/microrna/home.do) 4 tumour suppressor genes were identified which are targets of miR-93, tumour protein 53 inducible nuclear protein 1 (TP53INP1), B-cell CLL/lymphoma 11B (BCL11B), protein tyrosine phosphatase receptor type D (PTPRD), and cyclin-dependent kinase inhibitor 1A (CDKN1A) (Table 3.6.13). It was hypothesised that overexpression of miR-93 may decrease the expression of these tumour suppressor genes, resulting in increased proliferation and invasion in glioma cell cultures.

Table 3.6.13 Tumour suppressor genes targets predicted for miR-93 using the database microRNA.org (http://www.microrna.org/microrna/home.do).

Gene	Name	Background	Number of mRNA target sites for miR-93
TP53INP1	Tumour protein 53 inducible nuclear protein 1	Induces G1 arrest and increases p53-mediated apoptosis in leukaemia (Gironella *et al.* 2007; Yeung *et al.* 2008; Cano *et al.* 2009).	4
BCL11B	B-cell CL/lymphoma 11B (zinc finger protein)	Bcl11b functions as a tumour suppressor in myelogenous leukaemia, also found in brain tissue (Karlsson *et al.* 2007).	4
PTPRD	Protein tyrosine phosphatase, receptor type, D	Tumour suppressor gene found in GBM & leukaemia (Solomon *et al.* 2008; Veeriah *et al.* 2009).	3
CDKN1A	Cyclin-dependent kinase inhibitor 1A (P21 Cip1)	Impairs TGF beta tumour suppressor in gastric cancer (Petrocca *et al.* 2008).	1

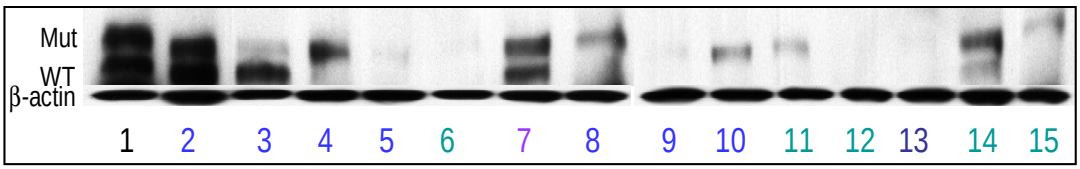

Fast (blue), slow (green), normal human astrocytes (violet). Mut: mutated form of BCL11B, WT: wild type BCL11B.

Fig. 3.6.7 Expression of BCL11B in glioma cell lines and normal human astrocytes.

The first target gene of miR-93 to be examined in the cultures was BCL11B. BCL11B was expressed in 5 out of 8 of the fast glioma cultures tested, the 4 fast cultures with the highest expression (lanes 2, 3, 4 and 8) were also invasive, while the fast culture with the lowest expression (lane 10) was non-invasive. Whereas BCL11B appeared to have lower expression in slower, non-invasive cell cultures with 3 out of 5 having expression 1 with high expression (lane 14) and 2 with lower expression (lanes 11 and 15) (Fig. 3.6.7).

Table 3.6.14 Characteristics of glioma cultures and normal human astrocytes of which have been tested for BCL11B expression in figure 3.6.7.

Lane	Sample	Origin	Doubling Time (Hours)	Invasive Behaviour
1	Positive control	Jurkat nuclear lysate (leukaemia cell line)	-	-
2	SNB-19*	Primary Glioblastoma	-	Invasive
3	N070152	Primary Glioblastoma	55	Invasive
4	N070865	Primary Glioblastoma	37.3	Invasive
5	N070859	Primary Glioblastoma	56	Invasive
6	N070126	Primary Glioblastoma	82.5	Non-invasive
7	NHA	Normal Human Astrocytes	-	Invasive
8	N070055	Grade III Oligoastrocytoma	68.5	Invasive
9	N070788	Grade III Astrocytoma	65.7	Non-invasive
10	N070201	Grade III Astrocytoma	60.2	Non-invasive
11	N060978	Primary Glioblastoma	98.3	Non-invasive
12	N060913	Primary Glioblastoma	>168	Poorly invasive
13	N070314	Grade II Oligodendroglioma	71.5	-
14	N060893	Primary Glioblastoma	88.1	Non-invasive
15	N061007	Primary Glioblastoma	>168	Poorly-invasive

* SNB-19 is an established cell line known to have a fast proliferation rate.

3.6.3.5 Expression of miR-23b in Glioma Cell Cultures and Normal Human Astrocytes

To further examine miR-23b expression in glioma using qRT-PCR we measured the expression of miR-23b in 4 glioma cell lines and in normal human astrocytes. N070152 and N070859 were the two cultures included in pool 1 of the TLDA analysis and N060978 and N060913 were included in pool 2. N070152 and N070859 (fast, invasive cultures from pool 1) had much lower expression of miR-23b in comparison to N060978 and N0600913 (slow, non-invasive cultures from pool 2); over twice as much miR-23b was expressed in the slow non-invasive cultures. N070152 had lower expression of miR-23b in comparison to the NHAs; however N070859 had a similar expression level of miR-23b to that of the NHAs (Fig. 3.6.8).

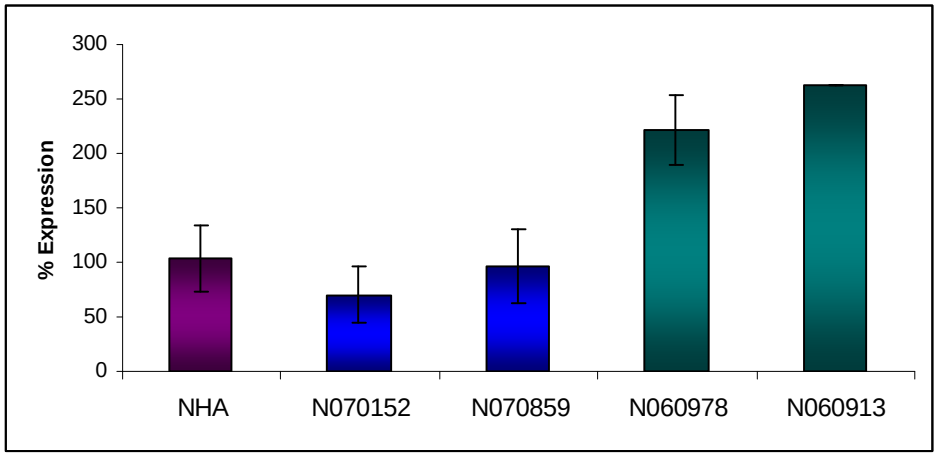

NHA: normal human astrocytes (violet), Invasive high proliferation rate (blue), Non-invasive low proliferation rate (green).

Fig. 3.6.8 Percentage expression measured by qRT-PCR of miR-23b in glioma cultures and normal human astrocytes. N070152A was taken as a calibrator sample as 100% expression of miR-23b. Each sample was measured in technical triplicate (n=3); in addition N070152 and NHAs were measured biological triplicate (n=3x3), N070859 and N060978 in biological duplicate (n=3x2). Standard deviations were generated using excel software.

3.6.3.6 Functional Validation of miR-23b: Transfection of pre-miR-23b with an Established Glioblastoma Cell Line

MiR-23b was 5.3 fold upregulated in pool 2 (slow, non-invasive) in comparison to pool 1 (fast, invasive) of the TLDA analysis. It was thought that by increasing the expression of miR-23b in glioma cells this would decrease proliferation. Therefore SNB-19 was transiently transfected with pre-miR-23b. Pre-miR-23b decreased proliferation by 30% (Fig. 3.6.9). The cells were seeded at 1X10E5/ ml, 1 ml per well, in a 6 well plate for 3 days with 2 µl of lipofectamine 2000 transfection reagent. 50 nM of miRNA, negative pre-miR, negative and siRNA (against kinesin) was used. The media was changed 8 hours post-transfection. The cell number was then measured using the acid phosphatase assay (see section 2.4.1 B). It was decided to examine if the effect on proliferation with pre-miR-23b could be further increased, therefore the assay length was increased to 5 days; the concentration of the cells was decreased to 2X10E4/ ml so that the control would not become confluent, proliferation was decreased by 40% compared to the negative pre-miR control (Fig. 3.6.10).

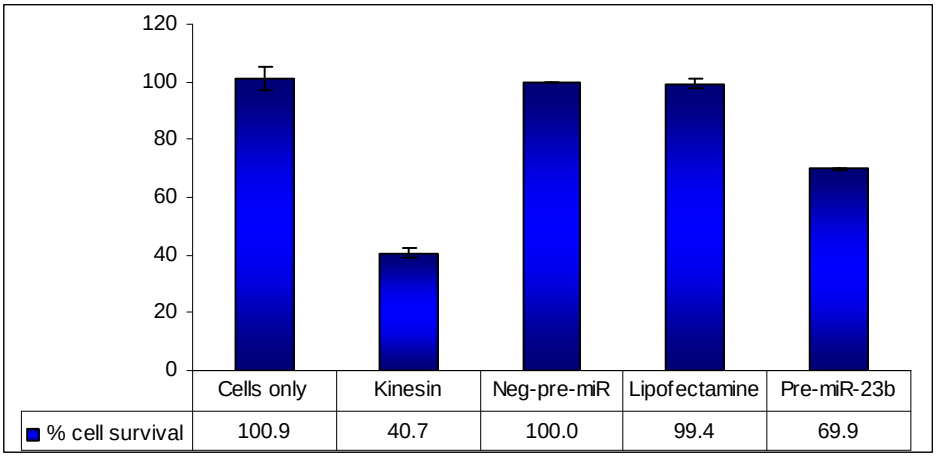

Fig. 3.6.9 Transient transfection of SNB-19 with pre-miR-23b in comparison to the negative pre-miR control, with 2 µl of lipofectamine 2000. 50 nM of miRNA, negative pre-miR or siRNA (against kinesin) were used. Standard deviations were of three biologically individual assays (n=2x3). Standard deviations were generated using excel software.

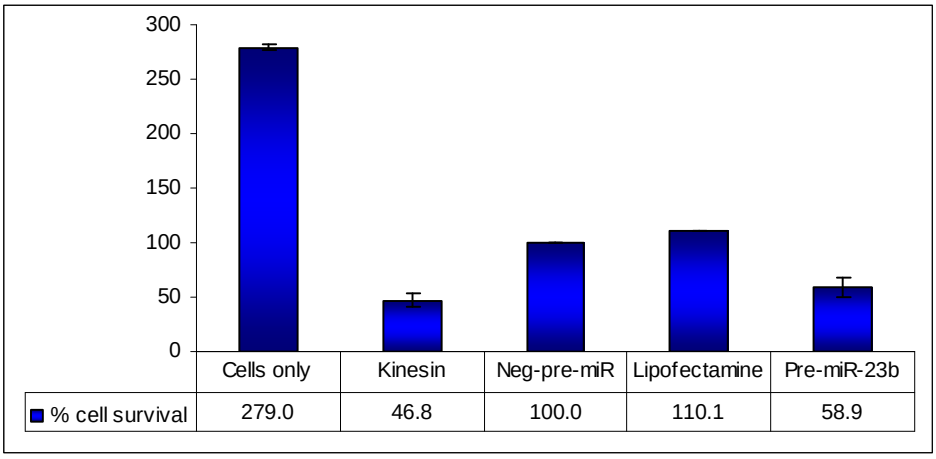

Fig. 3.6.10 Transient transfection of SNB-19 with pre-miR-23b in comparison to the negative pre-miR control, with 2 µl of lipofectamine. 50 nM of miRNA, negative pre-miR and siRNA (against kinesin) were used. Standard deviations were of two biologically individual assays (n=2x2). Standard deviations were generated using excel software.

3.6.3.7 Expression of miR-23b in SNB-19 Cells Post Transfection

After transient transfection of the glioma cell line SNB-19 with pre-miR-23b RNA was extracted from the cells to measure the amount of miR-23b in the cells post-transfection (see section 2.14.3). miR-23b expression was analysed by qRT-PCR. There was much higher levels (over twice as much) of miR-23b in the cells transfected with pre-miR-23b in comparison to the control cells and the cells transfected with the negative pre-miR (Fig. 3.6.11).

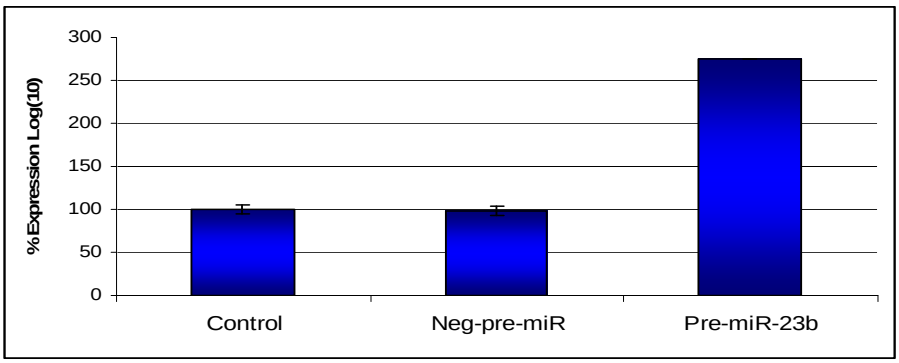

Fig. 3.6.11 Expression of miR-23b by qRT-PCR in SNB-19, post transfection with pre-miR-23b. Negative pre-miR was used as a control. Each sample was measured in technical triplicate (n=2). Standard deviations were generated using excel software.

3.6.3.8 Gene Targets of miR-23b

By increasing expression of miR-23b in the glioma cell line SNB-19 strong inhibition of proliferation was found. It was decided to look for target genes of miR-23b using 3 different databases, TargetScan (http://www.targetscan.org/), MicroRNA.org (http://www.microrna.org/) and DIANA LAB (http://diana.cslab.ece.ntua.gr/). In addition the literature was checked for information on these genes to find the most likely candidates. The genes chosen were associated with a malignant phenotype, i.e. miR-23b inhibition of the gene would be advantageous to glioma progression. The selection was also based on the best alignment of the miR-23b sequence with the target gene, and the most mRNA sites. In total 15 strong potential target genes were found for miR-23b, and 7 were chosen for further examination (Tables 3.6.15 - 3.6.17). Using the website (http://blast.ncbi.nlm.nih.gov/) primers were designed for the following genes SEMaphorin 6D (SEMA6D), X-linked Inhibitor of Apoptosis (XIAP), SMAD family member 5 (SMAD5), Mitogen-Activated Protein Kinase Kinase Kinase Kinase 4 (MAP4K4), B-cell CLL/Lymphoma 2 (BCL2), MNNG (N-Methyl-N'-nitro-N-nitroso-guanidine) HOS Tranforming gene (MET), and Platelet Derived Growth Factor Alpha (PDGFA) (see Table 2.14.12). The expression of these 7 genes was examined by qRT-PCR in SNB-19 cells which had been transfected with pre-miR-23b. A small bit of genomic DNA carried over from the RNA extraction, which resulted in PCR product in the negative control (no enzyme included in the RT reaction). This made it difficult to determine the difference between significant PCR product and product derived from genomic DNA (Fig. 3.6.12-3.6.25). However with XIAP there was a large difference between PCR product cycle number and genomic DNA cycle number for us to clearly identify product (Fig. 3.6.14). There was a 65.3% knockdown of XIAP after transfecting SNB-19 with pre-miR-23b (Fig. 3.6.15). The PCR amplicons were ran out on a 2.5% agarose gel to check for primer-dimers (PD); none were found (Fig. 3.6.26).

Table 3.6.15 Potential target genes found for miR-23b using the Target Scan database (http://www.targetscan.org/).

Number of conserved mRNA sites	Gene	Function	Publications
3	**SEMA6D**	Regulates proliferation and invasion.	(Toyofuku *et al.* 2004; Kinsella *et al.* 2011)
2	**RAB39B**	RAS oncogene family involved in early pathogenetic events of neoplastic germ cell formation.	(Biermann *et al*. 2007)
2	**MAP4K4**	Expression associated with worse prognosis in pancreatic cancer. Associated with lymph node metastasis in colorectal cancer. Overexpressed in pancreatic cancer. Promigratory kinase in ovarian cancer. Upregulated in glioma.	(Liang *et al*. 2008) (Hao *et al*. 2010) (Badea *et al*. 2008) (Collins *et al.* 2006) (Ramnarain *et al*. 2006)
2	**XIAP**	Inhibits apoptosis. Expressed in glioma.	(Dubrez-Daloz *et* al. 2008) (Wagenknecht *et al*. 1999)
1	**MAP3K9**	May play a role in esophageal cancer.	(Chen *et al*. 2008)
1	**TGFA**	Transforming growth factor alpha. Upregulated in glioma.	(Ramnarain *et al.* 2006)
1	**PDGFA**	Overexpressed in glioma increases proliferation.	(Martinho *et* al. 2009)

? no information available on this. References are in parenthesis.

Table 3.6.16 Potential target genes found for miR-23b using the MicroRNA.org database (http://www.microrna.org/microrna/home.do).

Number of conserved mRNA sites	Gene	Function	Publications
3	**SMAD5**	TGFbeta-stimulated Smad1/5 phosphorylation mediates the pro-migratory TGFbeta switch in mammary epithelial cells (breast cancer) Increased expression in HCC	(Liu *et al*. 2009) (Zimonjic *et al*. 2003)
3	**XIAP/BIRC4**	Inhibits apoptosis Expressed in glioma	(Dubrez-Daloz *et al.* 2008) (Wagenknecht *et al.* 1999)
2	**MAP3K7IP3**	?	?
2	**MET**	Regulates migration and proliferation	(Salvi *et al.* 2009)
2	**MAP4K4**	Expression associated with worse prognosis in pancreatic cancer. Associated with lymph node metastasis in colorectal cancer. Overexpressed in pancreatic cancer. Promigratory kinase in ovarian cancer.	(Liang *et al.* 2008) (Hao *et al.* 2010) (Badea *et al.* 2008) (Collins *et al.* 2006)
2	**BCL2**	Causes brain tumours resistance to chemotherapy. Increases proliferation in glioma.	(Tyagi *et al*. 2002) (Roth *et al*. 2000)
2	**SEMA6D**	Regulates proliferation and invasion.	(Toyofuku *et al.* 2004)
1	**TGFA**	Transforming growth factor alpha Upregulated in glioma.	(Ramnarain *et al.* 2006)
1	**PDGFA**	Overexpressed in glioma increase proliferation.	(Martinho *et al.* 2009)

? no information available on this. References are in parenthesis.

Table 3.6.17 Potential target genes found for miR-23b using the DIANA LAB database (http://diana.cslab.ece.ntua.gr/?sec=software).

MiTG score	Gene	Function	Publications
19.7	**SEMA6D**	Regulates proliferation and invasion.	(Toyofuku *et al.* 2004)
19	**XIAP/BIRC4**	Inhibits apoptosis. Expressed in glioma.	(Dubrez-Daloz *et al.* 2008) (Wagenknecht *et al.* 1999)
16.7	**MAP3K1**	?	?
11.9	**MYCT1**	c-myc overexpressed in cancer.	(Dang 2010)
11.4	**MAP3K7IP3**	?	?
10.4	**BCL2**	Makes brain tumours resistant to chemotherapy. Increases proliferation in glioma.	(Tyagi *et al.* 2002) (Roth *et al.* 2000)
10.3	**TGFBR3**	?	?
9.2	**SMAD5**	TGFbeta-stimulated Smad1/5 phosphorylation mediates the pro-migratory TGFbeta switch in mammary epithelial cells (breast cancer). Increased expression in HCC.	(Liu *et al.* 2009) (Zimonjic *et al.* 2003)
9	**MET**	Regulates migration and proliferation.	(Salvi *et al.* 2009)
8.8	**MAP4K3**	?	?

? no information available on this. References are in parenthesis.

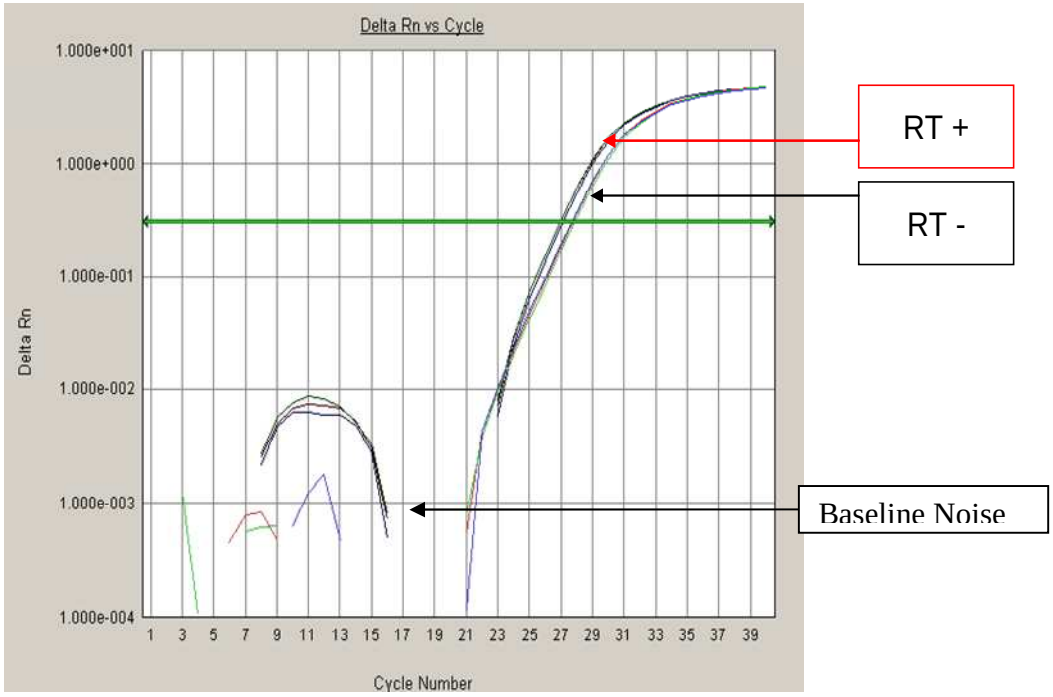

Fig. 3.6.12 Cycle numbers of the expression of SEMA6D measured by qRT-PCR in SNB-19 cells (RT+) and in the negative RT control (RT-). Each sample was measured in triplicate (n=3).

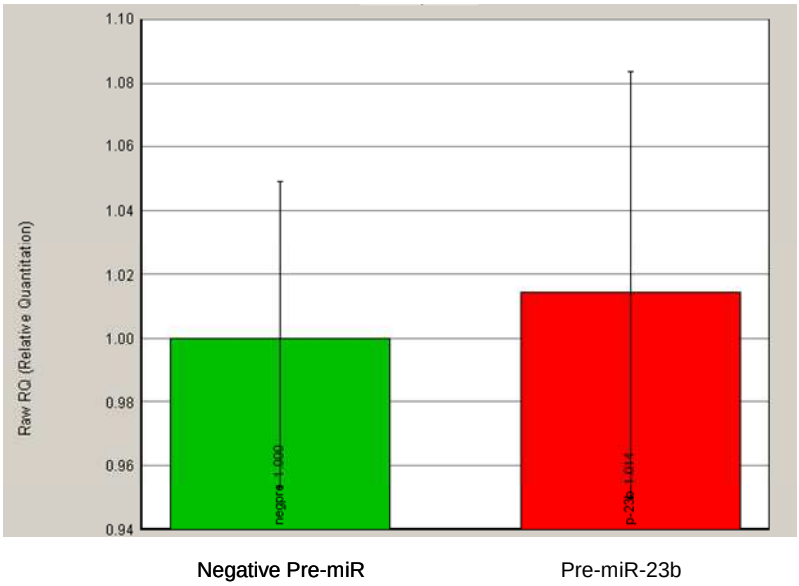

Fig. 3.6.13 Expression of SEMA6D measured by qRT-PCR in SNB-19 cells transfected with pre-miR-23b. Negative pre-miR was used as a control; each sample was measured in technical triplicate (n=3). Standard deviations were generated with SDS applied biosystem.

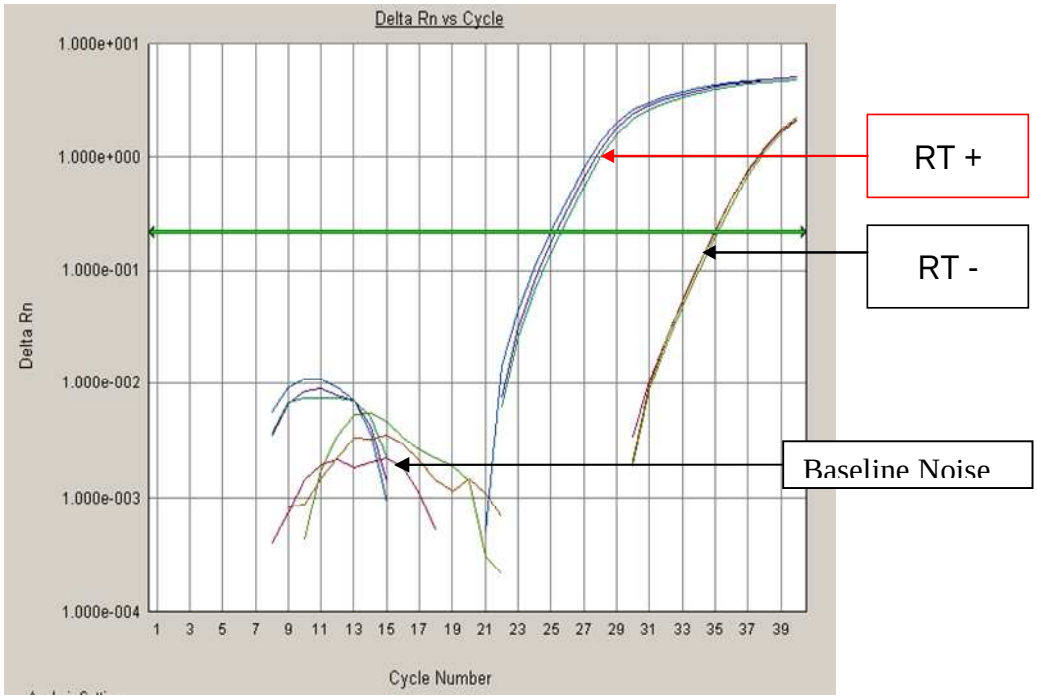

Fig. 3.6.14 Cycle numbers of the expression of XIAP measured by qRT-PCR in SNB-19 cells (RT+) and in the negative RT control (RT-). Each sample was measured in technical triplicate (n=3).

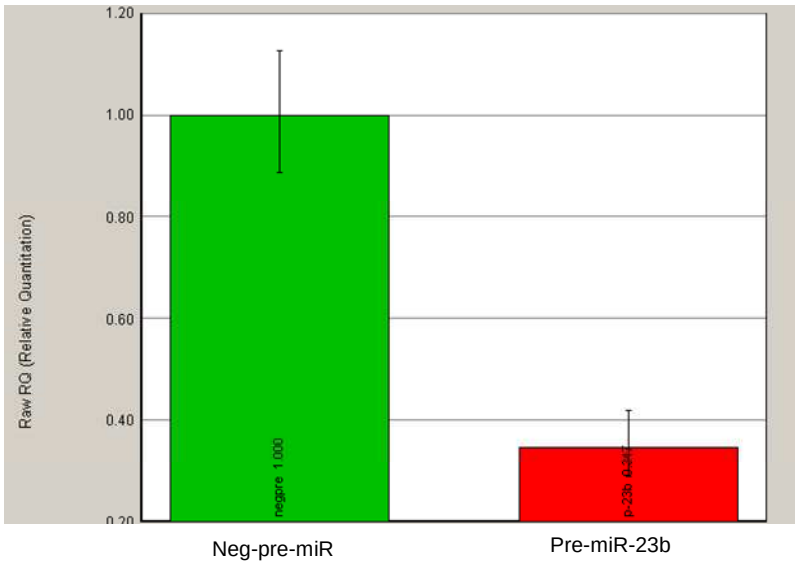

Fig. 3.6.15 Expression of XIAP measured by qRT-PCR in SNB-19 cells transfected with pre-miR-23b. Negative pre-miR was used as a control; each sample was measured in technical triplicate (n=3). Standard deviations were generated with SDS applied biosystem software.

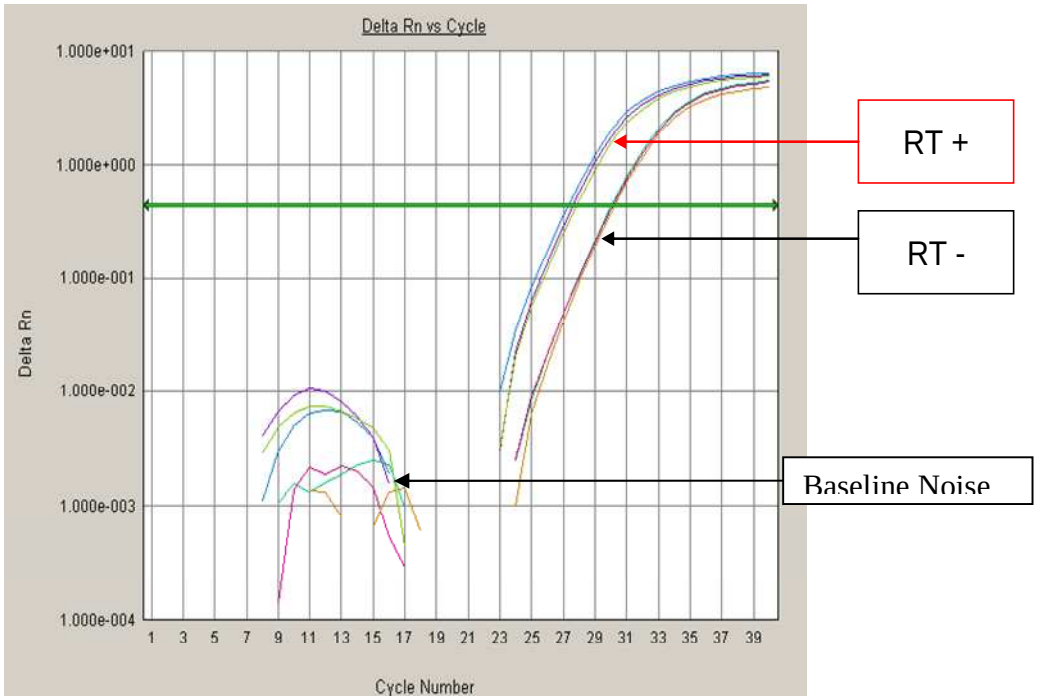

Fig. 3.6.16 Cycle numbers of the expression of SMAD5 measured by qRT-PCR in SNB-19 cells (RT+) and in the negative RT control (RT-). Each sample was measured in technical triplicate.

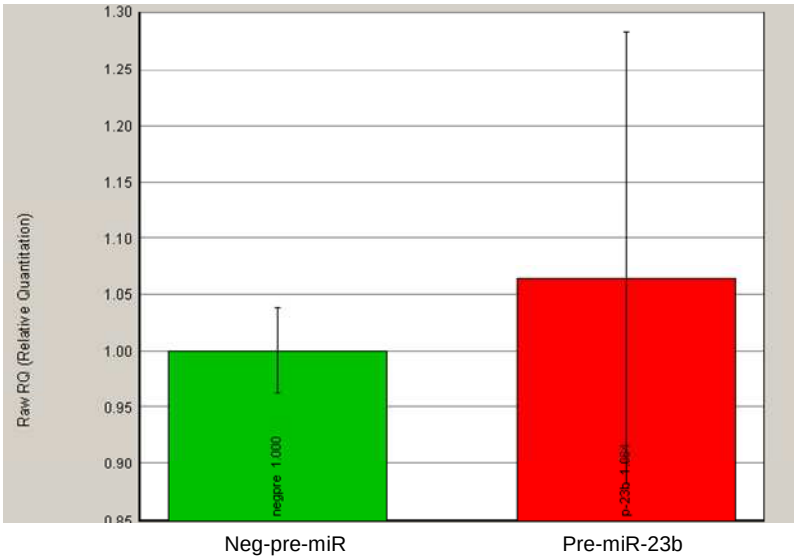

Fig. 3.6.17 Expression of SMAD5 measured by qRT-PCR in SNB-19 cells transfected with pre-miR-23b. Negative pre-miR was used as a control; each sample was measured in technical triplicate (n=3). Standard deviations were generated with SDS applied biosystem software.

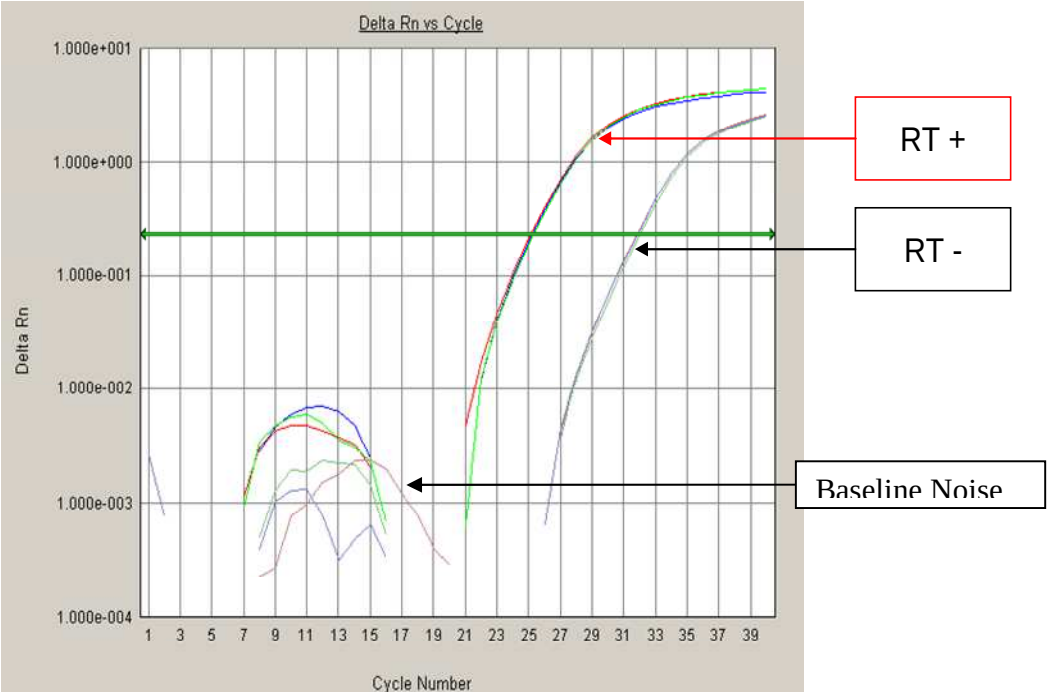

Fig. 3.6.18 Cycle numbers of the expression of MAP4K4 measured by qRT-PCR in SNB-19 cells (RT+) and in the negative RT control (RT-). Each sample was measured in technical triplicate (n=3).

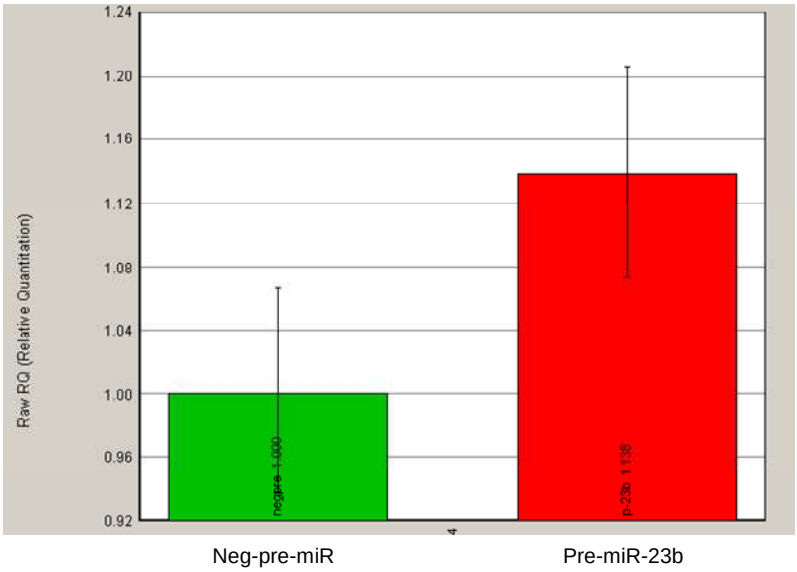

Fig. 3.6.19 Expression of MAP4K4 measured by qRT-PCR in SNB-19 cells transfected with pre-miR-23b. Negative pre-miR was used as a control; each sample was measured in technical triplicate (n=3). Standard deviations were generated with SDS applied biosystem software.

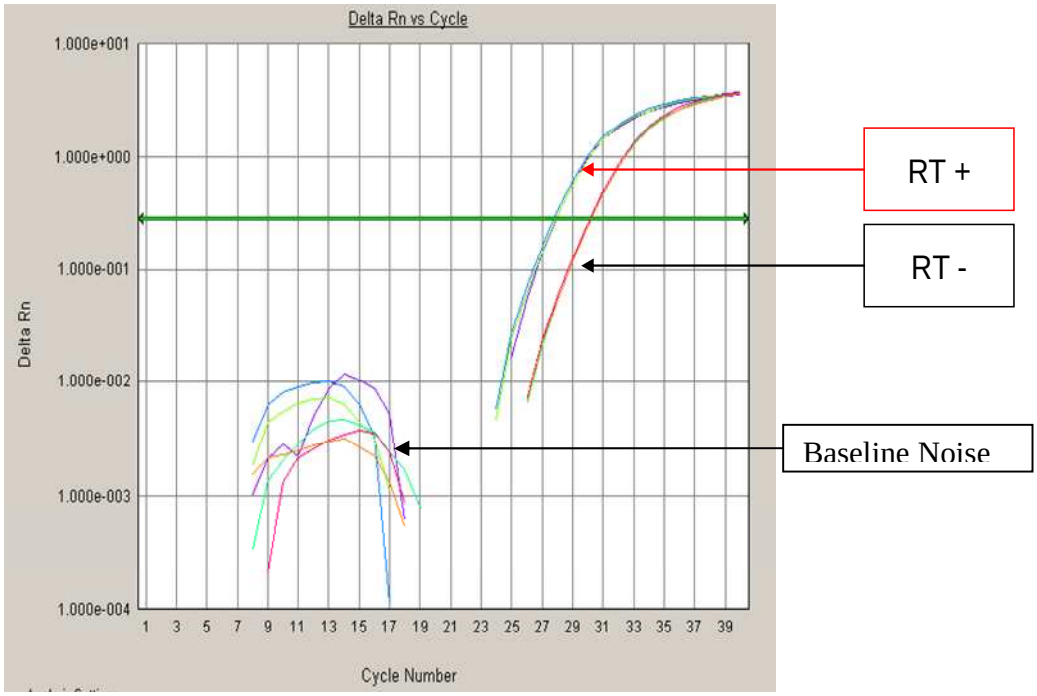

Fig. 3.6.20 Cycle numbers of the expression of BCL2 measured by qRT-PCR in SNB-19 cells (RT+) and in the negative RT control (RT-). Each sample was measured in technical triplicate (n=3).

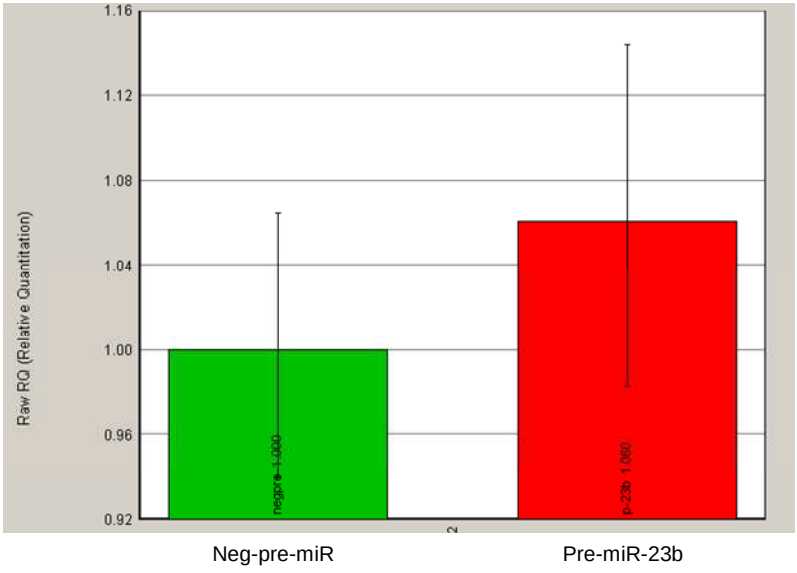

Fig. 3.6.21 Expression of BCL2 measured by qRT-PCR in SNB-19 cells transfected with pre-miR-23b. Negative pre-miR was used as a control, each samples was measured in technical triplicate (n=3). Standard deviations were generated with SDS applied biosystem software.

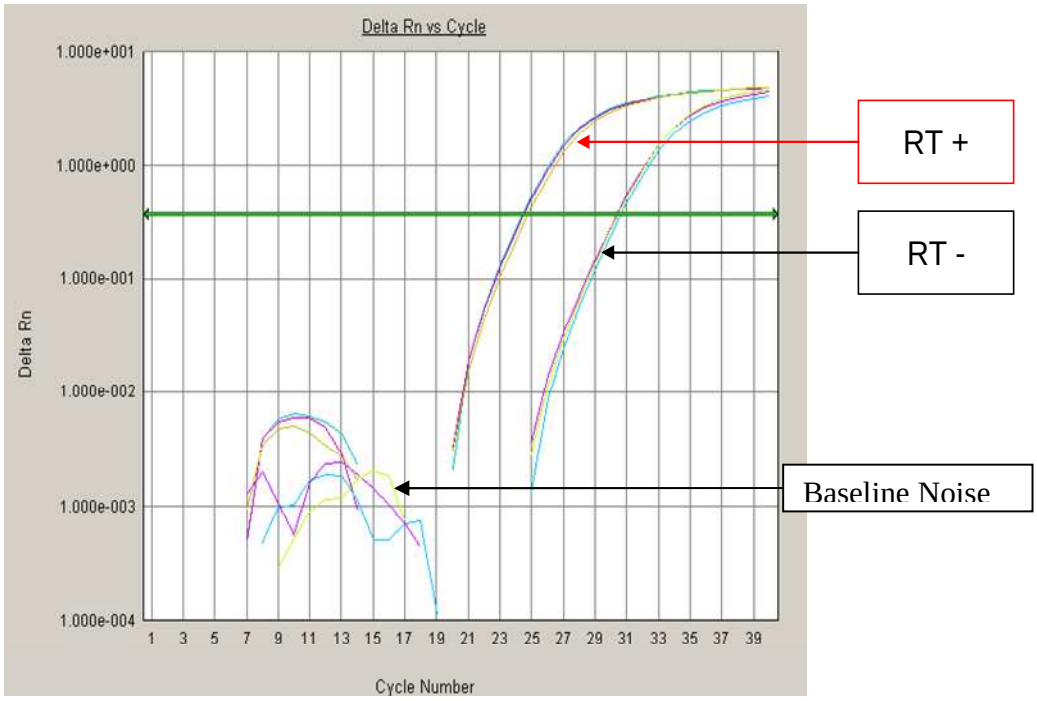

Fig. 3.6.22 Cycle numbers of the expression of MET measured by qRT-PCR in SNB-19 cells (RT+) and in the negative RT control (RT-). Each sample was measured in technical triplicate (n=3).

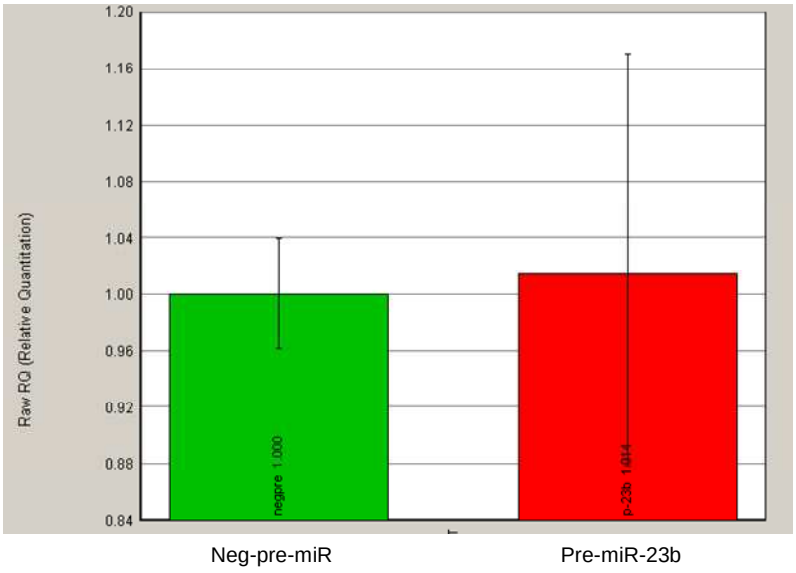

Fig. 3.6.23 Expression of MET measured by qRT-PCR in SNB-19 cells transfected with pre-miR-23b. Negative pre-miR was used as a control; each sample was measured in technical triplicate (n=3). Standard deviations were generated with SDS applied biosystem software.

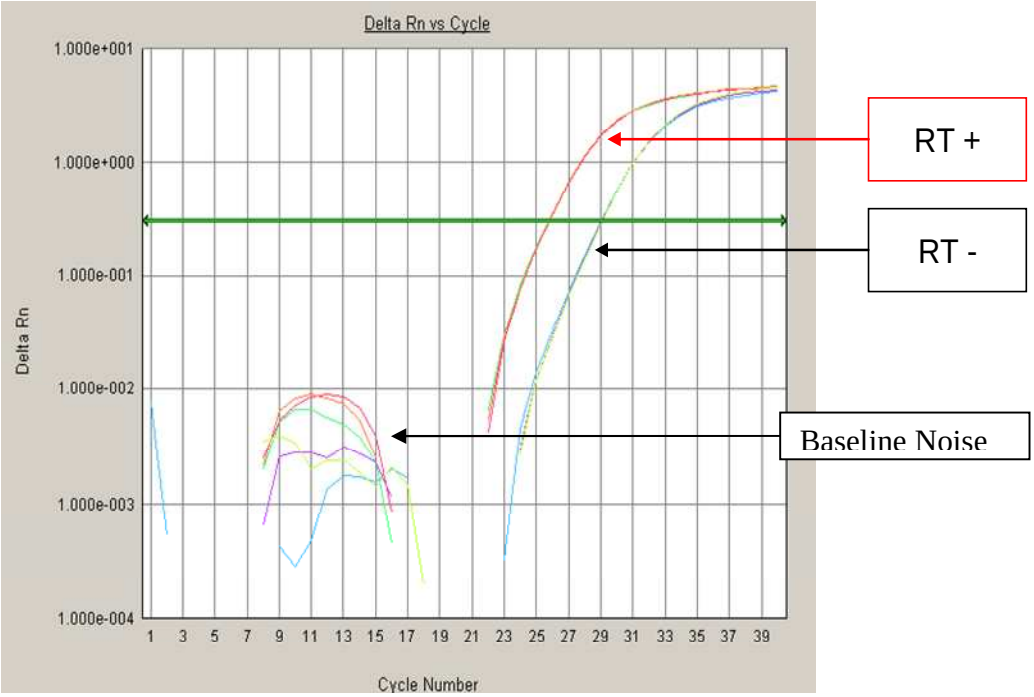

Fig. 3.6.24 Cycle numbers of the expression of PDGFA measured by qRT-PCR in SNB-19 cells (RT+) and in the negative RT control (RT-). Each sample was measured in technical triplicate (n=3).

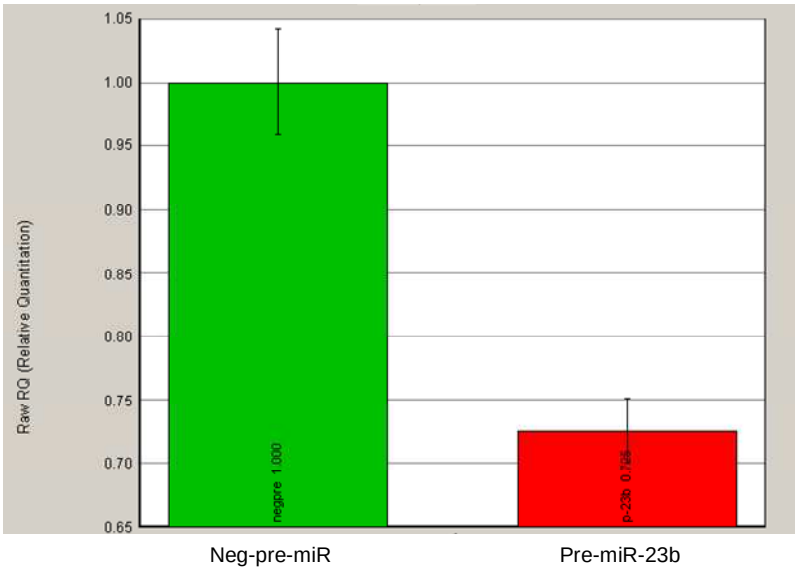

Fig. 3.6.25 Expression of PDGFA measured by qRT-PCR in SNB-19 cells transfected with pre-miR-23b. Negative pre-miR was used as a control, each samples was measured in technical triplicate (n=3). Standard deviations were generated with SDS applied biosystem software.

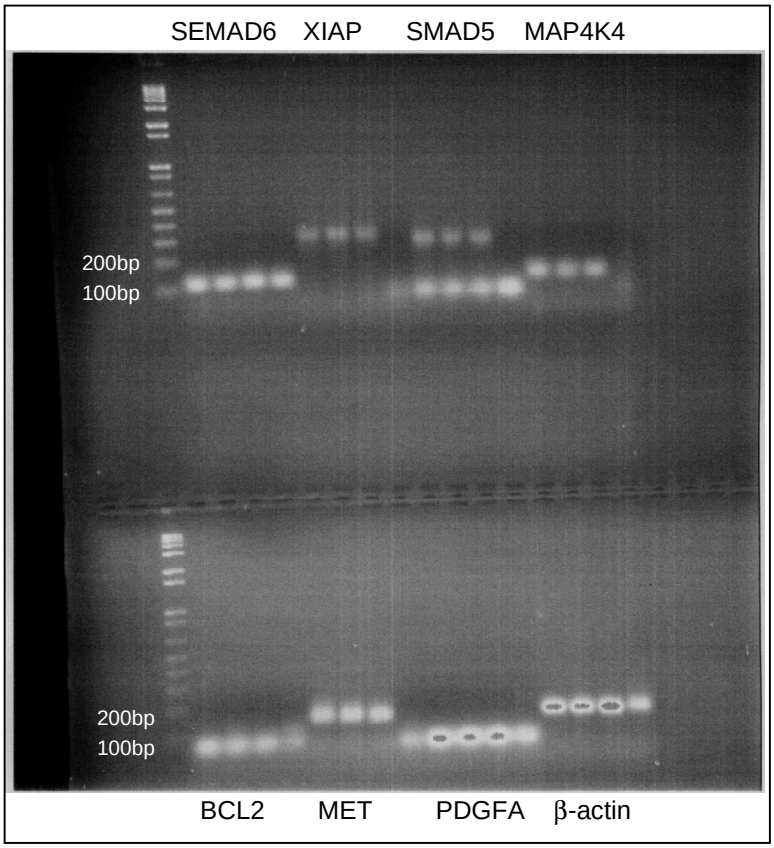

Fig. 3.6.26 PCR amplicons run on a 2.5% agarose gel. First lane contains marker. Lane 1-4 of each gene has (1) control (cells only), (2) negative pre-miR, (3) pre-miR-23b, (4) negative control for RT reaction (no enzyme). Where there is no band present in lane 4 there was very little DNA contamination during the RNA extraction.

3.6.3.9 Effect of miR-93 and miR-23b on Invasion Activity of Glioma

MiR-93 had higher expression in fast, invasive glioma cultures. The effect of anti-miR-93 was tested on the invasion activity of the established glioma cell line SNB-19 after they had been transfected with anti-miR-93 (see section 2.14.3), to see if by decreasing the expression of miR-93 we could also decrease invasion. There was no decrease in invasion activity in cells transfected with anti-miR-93 in comparison to the negative anti-miR control. The transfection reagent, lipofectamine had a strong inhibitory effect on invasion (Fig. 3.6.27). We also looked at the effect of pre-miR-23b on invasion activity (see section 2.9) of SNB-19; to see if by increasing the amount of miR-23b in the cells would decrease invasion. It did not appear that miR-23b had any specific effect on invasion; however the cells were very sensitive to the negative pre-miR control which had a strong inhibitory effect on invasion (Fig. 3.6.28).

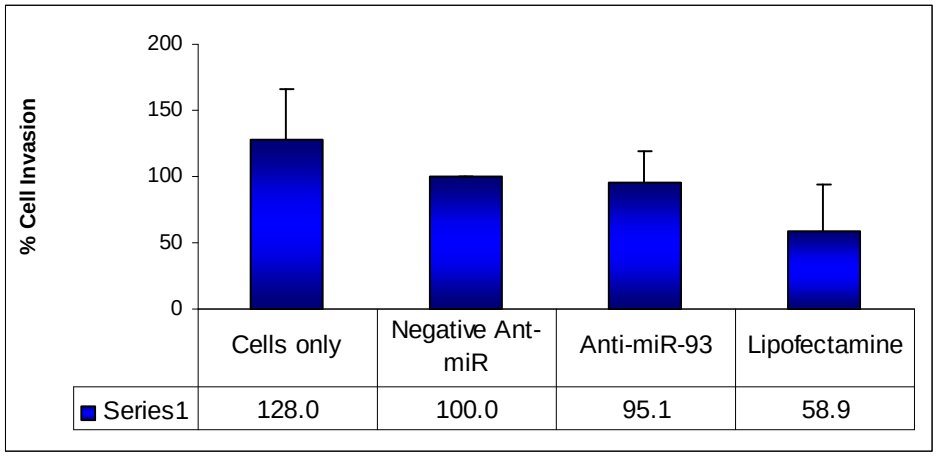

Fig. 3.6.27 Invasion of SNB-19 post transfection with anti-miR-93. 3 biologically individual assays were carried out (n=2x3). Standard deviations were generated using excel software.

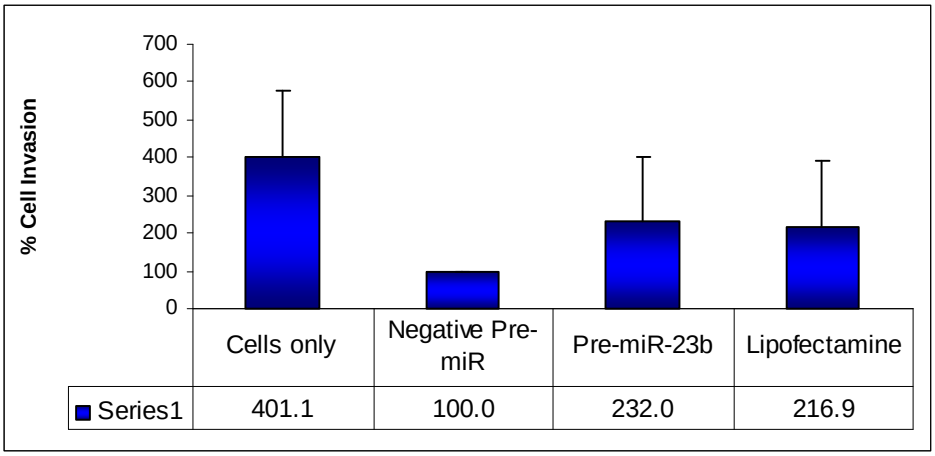

Fig. 3.6.28 Invasion of SNB-19 post transfection with pre-miR-23b. 3 biologically individual assays were carried out (n=2x3). Standard deviations were generated using excel software.

3.6 Discussion

MiRNA Expression in Gliomas

Introduction

As miRNAs control important processes such as differentiation, cell growth and cell death, they hold great promise for targeted cancer therapy. MiRNAs are small non-coding regulatory RNA fragments of 20-22 nucleotides. 721 human miRNAs have been identified and thought to regulate at least 30% of genes (Lewis *et al.* 2005). They bind mRNA through partial homology and can potentially regulate the expression of multiple targets, most of which are still largely unknown. MiRNAs are thought to act as master regulators, which orchestrate networks of gene signalling. Every type of analysed tumour has shown significantly different miRNA profiles in comparison to normal cells from the same tissue.

Several miRNAs have already been reported to regulate glioma proliferation and invasion. Knockdown of miR-221/222 has reduced growth and invasion in glioma cells due to downregulation of the anti-apoptotic gene BCL2 and the upregulation of negative regulators of the cell cycle including connexin43, p27, p57, PUMA, caspase-3, PTEN, TIPM3 and Bax (Gillies and Lorimer 2007; Medina *et al.* 2008; Zhang *et al.* 2009; Zhang *et al.* 2009). Mir-21 also plays a key role in glioma and other cancers as an anti-apoptotic factor (Chan *et al.* 2005; Chen *et al.* 2008; Ohno *et al.* 2009). MiR-181a and miR-181b act as tumour suppressors in glioma leading to growth inhibition, apoptosis and invasion inhibition (Shi *et al.* 2008).

Very little is known about miRNA interactions with cellular pathways in brain tumours; however, some miRNAs have been shown to be directly involved in pathway regulation in glioma. MiRNAs have been associated with the Notch pathway, which plays key roles in nervous system development and in brain tumours (Kefas *et al.* 2009). A neuronally expressed miRNA, miR-326 was upregulated following Notch-1 knockdown, and was not only suppressed by Notch but also inhibited Notch proteins and activity, indicating a feedback loop (Kefas *et al.* 2009). Transfection of miR-326 into both established and stem cell-like glioma lines and *in vivo* in a xenograft model was cytotoxic, and rescue was obtained with

Notch restoration (Kefas *et al.* 2009). MiR-326 partially mediated the toxic effects of Notch knockdown (Kefas *et al.* 2009). MiR-34a is a transcriptional target of p53, and is down-regulated in some cancer cell lines (Li *et al.* 2009). Transfection of miR-34a down-regulated c-Met in human glioma and medulloblastoma cells and Notch-1, Notch-2, and CDK6 protein expressions in glioma and stem cells, and strongly inhibited *in vivo* glioma xenograft growth (Li *et al.* 2009). MiR-34a in glioma and medulloblastoma cell lines strongly inhibited cell proliferation, cell cycle progression, survival, and invasion (Li *et al.* 2009). MiR-34a suppresses brain tumour growth by targeting c-Met and Notch in glioma cells and stem cells (Li *et al.* 2009).

MiR-21 is an important oncogene that targets a network of p53, TGF-beta, and tumour suppressor genes in glioblastoma cells (Zhu *et al.* 2007; Papagiannakopoulos *et al.* 2008). Type I interferons (IFNs) are involved in double-stranded RNA responses. IFN-beta treatment reduced miR-21 expression in glioma cells, and IFN-beta suppressed the growth of glioma-initiating cell-derived intracranial tumours; downregulation of miR-21 contributes to the antitumor effects of IFN-beta and miR-21 expression is negatively regulated by STAT3 activation (Ohno *et al.* 2009), it also inhibits the EGFR pathway independently of PTEN status (Zhou *et al.*).

The most common genetic alterations found in glioblastoma include EGFR activation and AKT pathways (Wong *et al.* 1987; Haas-Kogan *et al.* 1998). In glioblastoma cells, transfection of miR-7 decreased the level of EGFR and upstream regulators of the AKT pathway, insulin receptor substrate 1 (IRS1) and insulin receptor substrate 2 (IRS2); these cells had increased apoptosis and reduced invasion (Kefas *et al.* 2008). This would suggest that miR-7 regulates the EGFR and AKT pathways. MiR-7 is a potential tumour suppressor in glioblastoma targeting critical cancer pathways. MiR-7 decreased viability and invasiveness of primary glioblastoma lines and is a regulator of major cancer pathways suggesting that it has therapeutic potential for glioblastoma (Kefas *et al.* 2008).

MiR-26a is a direct regulator of PTEN expression and is frequently amplified in human glioma, most often in association with monoallelic PTEN loss

(Huse *et al.* 2009). MiR-26a-mediated PTEN repression in a murine glioma model both enhances *de novo* tumour formation and precludes loss of heterozygosity and the PTEN locus (Huse *et al.* 2009).

TLDA Screening of MiRNAs in Glioma

The expression of 365 miRNAs in 2 sets of primary glioblastomas was screened by TLDA, one set contained 2 primary invasive glioblastoma cultures with a high proliferation rate (pool 1) (Table 3.6.1), and one contained 2 non-invasive glioblastomas with a low proliferation rate (pool 2) (Table 3.6.2). The most extreme characteristics were chosen from the newly developed glioma cultures, i.e. the most invasive with the highest proliferation rate, and the least invasive with the lowest proliferation rate. It is thought that glioma cells favour one phenotype, that is they are either highly invasive or highly proliferative, known as the go or grow hypothesis, however some of the glioma samples in the present study had both high proliferation and were also invasive. There was no significant correlation between invasion and proliferation within the cohort of glioma cultures, i.e. a highly invasive culture was not necessarily a slow proliferating one, and a low amount of invasion did not always correlate with a fast proliferating culture. These characteristics may have been determined by the section of the tumour that the biopsy sample was removed from, i.e. a highly invasive section which would have resulted in an invasive cell population, or a highly proliferative section which would have given a highly proliferative population, as brain tumours contain a very heterogeneous population, and each section of a tumour has been shown to have specific functions (Deisboeck *et al.* 2001; Huang *et al.* 2008). It is possible that the glioblastoma cultures in pool 1 contained cells from a highly invasive area as well as cells from a highly proliferative area of the tumour, and the cultures in pool 2 may have contained cells from a low invasive and low proliferative areas.

From the TLDA data it was found that 62 miRNAs were upregulated in pool 2 (Fig. 3.6.1 and 3.6.2) (Table 3.6.4), and 13 were downregulated in pool 2 in comparison to pool 1 (Fig 3.6.3) (Table 3.6.5). 13 miRNAs were also found to be off

or have very low levels of detection in pool 1 in comparison to pool 2 (Table 3.6.6), and 13 in pool 2 in comparison to pool 1 (Table 3.6.7).

Godlewski *et al*, identified MiRNA-451 as a conditional switch controlling glioma cell proliferation and migration (Godlewski *et al.* 2010). MiR-451 levels were regulated by glucose, with abundant energy miR-451 expression is high (Godlewski *et al.* 2010). MiR-451 suppresses AMP-activated protein kinase (AMPK) signalling, which leads to high proliferation rates in cells with continual MTOR activation (Godlewski *et al.* 2010). With low amounts of glucose present, miR-451 downregulation is necessary for AMPK pathway activation, leading to suppressed proliferation rates, increased cell survival, and migration (Godlewski *et al.* 2010). This is known as the "go or grow hypothesis" (Hatzikirou *et al.* 2010), it is possible that miR-451 levels are lower in pool 2 cell lines and this could explain their low proliferation rate.

Silber *et al*, looked at 192 human miRNAs in anaplastic astrocytomas and primary glioblastomas, from human tissue samples in comparison to normal brain tissue, and found 4 upregulated and 25 miRNAs downregulated in glioma (Silber *et al.* 2008). They found that transfection of miR-124 or miR-137 induced G1 cell cycle arrest in glioblastoma cells, which was associated with decreased expression of cyclin-dependent kinase 6 and phosphorylated retinoblastoma (pSer 807/811) proteins (Silber *et al.* 2008). Ciafre *et al*, examined the expression of 245 miRNAs in glioblastoma tissue and cell lines in comparison to normal brain by microarray, and found 9 upregulated and 4 downregulated miRNAs (Ciafre *et al.* 2005). They found miR-221 to be strongly upregulated in glioblastoma, and miR-128, miR-181a, miR-181b, and miR-181c were downregulated (Ciafre *et al.* 2005). Godlewski *et al*, looked at miRNA expression with a microarray using glioblastoma tissue in comparison to normal brain and found 8 upregulated and 11 downregulated miRNAs (Godlewski *et al.* 2008). They found that miR-128 targeted the Bmi-1 oncogene/stem cell renewal factor and inhibited glioma proliferation and self renewal (Godlewski *et al.* 2008). 19 of the miRNAs dysregulated in our study have been reported in the literature to be associated with glioma proliferation or invasion (Table 3.6.3). A high number of miRNAs were upregulated in pool 2, i.e.

downregulated in pool 1 the fast, invasive phenotype. Most of the miRNA profiling studies on glioblastomas have focused on comparing normal brain with glioblastomas; however the present study differs in that it related fast, invasive glioblastomas to slow, non-invasive glioblastomas and examined the deregulation of miRNAs between these phenotypes. To our knowledge this type of study has not been carried out before.

MiR-143 was the highest upregulated miRNA in pool 2 in comparison to pool 1 (over 7 fold) (Fig. 3.6.1) (Table 3.6.4). Ng *et al*, found overexpression of miR-143 is significant in suppressing colorectal cancer cell growth through inhibition of translation of the oncogene KRAS (Chen *et al.* 2009), and DNA methyltranferase 3A (Ng *et al.* 2009). Clape *et al*, have shown that increased expression of miR-143 in prostate cancer inhibited cell proliferation this was partly due to the inhibition of extracellular signal-regulated kinase-5 (ERK5) activity (Clape *et al.* 2009). The expression of miR-143 has also been shown to suppress growth and induce apoptosis in leukaemia (Akao *et al.* 2009) and B-cell lymphoma (Akao *et al.* 2007). Unfortunately, no effect was seen on proliferation with miR-143 in a transient transfection, however miR-143 is known to cluster with miR-145 (Parmacek 2009), therefore it may be necessary for these 2 miRNAs to function at the same time (i.e. to transfect both miR-143 and miR-145 at the same time); miR-145 was also upregulated in pool 2 (3.8 fold) (Table 3.6.4).

Predicted Genes for miRNA Groups from TLDA Analysis

Based on the hypothesis that groups of differentially expressed miRNAs may regulate the same genes the algorithm from the DIANA LAB database was applied (http://diana.cslab.ece.ntua.gr/?sec=software), to identify potential genes targeted by the 20 most upregulated miRNAs in Pool 1 and in Pool 2. With Pool 1 the top 2 targeted genes were ataxin 1 (ATXN1) and trinucleotide repeat containing 6B (TNRC6B) (Table 3.6.8). Tsuda *et al*, found that ATXN1 mediates neurodegeneration through its interaction with Gfi-1/Senseless proteins (Tsuda *et al.* 2005), Crespo-Barreto *et al*, found that partial loss of ATXN1 function contributes to the pathogenesis of Spinocerebellar ataxia type 1 (SCA1), an inherited

neurodegenerative disease caused by expansion of a CAG repeat that encodes a polyglutamine tract in ATXN1 (Crespo-Barreto *et al.* 2010). Sun *et al*, found that TNRC6B is associated with aggressive prostate cancer, Balliat *et al*, discovered that a single nucleotide polymorphism at 22q13 located within the TNRC6B gene has been associated with prostate cancer risk (Sun *et al.* 2009); TNRC6B is required for miRNA-mediated mRNA degradation function (Baillat and Shiekhattar 2009). With Pool 2 the top 2 targeted genes were one cut homeobox 2 (ONECUT2) and again TNRC6B (Table 3.6.9); Pike *et al*, found ONECUT2 to be methylated in lymphoma (Pike *et al.* 2008) and Rauch et al, found it methylated in lung cancer (Rauch *et al.* 2006) and it may also play a role in glioma. TNRC6B appears to be targeted by both pools and could possibly be significant in regulating miRNA function in glioma.

miR-155 Expression in Glioma

From the TLDA analysis miR-155 was found to be downregulated in slow, non-invasive glioblastomas in comparison to fast, invasive glioblastomas (Fig. 3.6.3) (Table 3.6.5). High expression of miR-155 was found in the normal human astrocytes, and low expression in the established glioblastoma cell line SNB-19; 1 primary glioblastoma (N070152) had high expression of miR-155 and all of the other cell lines had low expression of miR-155 (Fig. 3.6.4) (Table 3.6.11). It was expected that miR-155 would have had high expression in all fast, invasive cultures; this was not the case as the highest expression was found in NHAs. As there were 2 pooled cell cultures in the fast, invasive pool, and miR-155 expression in N070152 was more than twice that of N070859, this diluted out the low miR-155 expression in N070859.

With high miR-155 expression in NHA's, and 1 out of 4 fast, invasive glioma cultures, it was decided that miR-155 would not be an ideal miRNA target to follow up in fast, invasive glioblastomas. Yeung *et al*, showed miR-155 binds to the mRNA of TP53INP1, which regulates P53 activity, a known tumour suppressor gene which functions in glioma (Yeung *et al.* 2008), and may be over-expressed in a number of glioblastomas with low P53 activity, but not in all glioblastomas.

miR-93 Expression in Glioma

From the TLDA analysis miR-93 was found to be 3.6 fold downregulated in slow, non-invasive glioblastomas in comparison to fast, invasive glioblastomas (Fig. 3.6.3) (Table 3.6.5). The expression of miR-93 was validated by qRT-PCR in one established glioblastoma cell line SNB-19, 12 glioma cultures including 8 primary glioblastomas, 1 secondary glioblastoma, 1 grade III oligoastrocytoma and 1 grade II oligodendroglioma, and in NHAs (Fig. 3.6.5) (Table 3.6.12). As expected miR-93 was upregulated in all 3 fast, proliferating and invasive cultures and was downregulated in all non-invasive, slow proliferating cultures as well as in NHAs (Fig. 3.6.5). This indicated that miR-93 might play an important role in regulating invasion and proliferation in gliomas. Yeung *et al*, have also shown that miR-93 binds to the mRNA of TP53INP1, which regulates P53 activity (Yeung *et al.* 2008), and may also be over-expressed in a number of glioblastomas with low P53 activity.

Functional Validation of miR-93 in an Established Glioblastoma Cell Line

As miR-93 was found to be overexpressed in fast invasive glioma cells by qRT-PCR, the functional effect of miR-93 was then examined in an established glioblastoma cell line SNB-19. SNB-19 was transiently transfected with anti-miR-93, and a 13.2% decrease in proliferation was found (Fig. 3.6.6). The effect of anti-miR-93 on invasion activity needs to be examined in SNB-19.

It was hypothesized that the overexpression of miR-93 in fast proliferating invasive glioma cells results in a downregulation of TP53INP1, and an increase in proliferation. TP53INP1 regulates P53 activity; a tumour suppressor gene which functions in glioma. Increased miR-93 expression would lead to downregulation of P53 and increased proliferation. Using the microRNA.org database (http://www.microrna.org/microrna/home.do) 4 tumour suppressor genes were identified which are potential targets of miR-93: tumour protein 53 inducible nuclear protein 1 (TP53INP1), B-cell CLL/lymphoma 11B (BCL11B), protein tyrosine phosphatase receptor type D (PTPRD), and cyclin-dependent kinase inhibitor 1A (CDKN1A) (Table 3.6.13). Yeung *et al*, found that knockdown the expression of

both miR-93 and miR-130b resulted in enhanced TP53INP1 expression causing apoptosis in leukaemia (Yeung *et al.* 2008). Cano *et al*, have shown that TP53INP1 induces p53-driven oxidative stress response, that possesses both a p53-independent intracellular reactive oxygen species regulatory function, and a p53-dependent transcription regulatory function (Cano *et al.* 2009). Gironella *et al*, found dramatically reduced expression of TP53INP1 in pancreatic cancer (Gironella *et al.* 2007). Karlsson *et al*, found BCL11B to be a tumour suppressor in leukaemia (Karlsson *et al.* 2007); and Veeriah *et al*, and Solomon *et al*, also found PTPRD to function as a tumour suppressor gene in leukaemia (Solomon *et al.* 2008; Veeriah *et al.* 2009). Petrocca *et al*, showed that CDKN1A acts as a tumour suppressor in gastric cancer by inhibiting TGF beta (Petrocca *et al.* 2008).

The expression of BCL11B, a target of miR-93 was examined by western blot. It was found that BCL11B was expressed in all cultures tested. 5 out of 8 of the fast glioblastoma cultures had high expression of BCL11B. 1 out of 4 slow cultures had high expression of BCL11B (Fig. 3.6.7) (Table 3.6.14). Higher expression of miR-93 in fast, invasive glioma cultures correlates with higher expression of BCL11B (Fig. 3.6.5). Inhibition of this tumour suppressor gene favours glioma progression. Western blot analysis of the other tumour suppressor genes, including TP53INP1, CDKN1A, and PTPRD would confirm if these genes are expressed in the cultures. It would be interesting to analyse the expression of all 4 tumour suppressor genes after SNB-19 cells had been transfected with anti-miR-93, to see if the expression of these genes is increased when miR-93 expression is decreased.

Functional Validation of miR-23b in an Established Glioblastoma Cell Line

From the TLDA analysis miR-23b was found to be 5.3 fold upregulated in pool 2 (slow, non-invasive), that is it was downregulated in pool 1 (fast, invasive) (Fig. 3.6.1) (Table 3.6.4). The expression of miR-23b was also examined by qRT-PCR in 4 glioma cell cultures, 2 of which were included in pool 1 (fast, invasive) of the TLDA analysis, and 2 which were in pool 2 (slow, non-invasive); in addition the expression of miR-23b was examined in NHAs. Twice as much miR-23b was expressed in pool 2 cultures as in pool 1 cultures. The pool 1 cultures had a similar

expression level of miR-23b to that of the NHAs (Fig. 3.6.8). It was previously shown that NHAs are invasive.

By increasing the expression of miR-23b in a transient transfection assay pre-miR-23b decreased proliferation by 30% in a glioma cell line over 3 days, and by up to 40% in a 5 day assay. This is a strong inhibition of proliferation for one miRNA with a transient transfection over a short period of time. The expression of miR-23b was examined by qRT-PCR in SNB-19 cells post transfection with pre-miR-23b, this confirmed very high levels of miR-23b in the cells in comparison to the non-transfected parental cell line. This confirmed the inhibition of proliferation was due to the increase in the amount of miR-23b transfected into the cells.

As such a strong effect was observed the next step included finding target genes of miR-23b using 3 different databases, TargetScan (http://www.targetscan.org/), MicroRNA.org (http://www.microrna.org/microrna/home.do) and DIANA LAB (http://diana.cslab.ece.ntua.gr/?sec=software). These databases predict thousands of potential gene targets for each individual miRNA, and although they predict target genes based on target sequence conservation homology and/or with miRNAs, there is no guarantee that these genes are in fact targets of these miRNAs. In addition the literature was examined for information on these genes, particularly information which supported the malignant glioma phenotype i.e. invasion and proliferation; by increasing miR-23b expression and downregulating the target gene that would be advantageous to glioma progression. The selection was based on the best alignment and the most potential mRNA sites of the miR-23b sequence within the target gene. The list was comprised of 15 potential target genes for miR-23b, and 7 genes were chosen for further examination.

Using the website http://blast.ncbi.nlm.nih.gov/Blast.cgi primers were designed for the 7 genes: semaphorin 6D (SEMA6D), X-linked inhibitor of apoptosis (XIAP), SMAD family member 5 (SMAD5), mitogen-activated protein kinase kinase kinase kinase 4 (MAP4K4), B-cell lymphoma 2 (BCL2), met proto-oncogene (hepatocyte growth factor receptor) (MET), and platelet-derived growth factor subunit A (PDGFA) (Table 3.8.15). Toyofuku *et al*, have shown SEMAD6 to be involved in cardiac morphogenesis, and to have a migration-promoting activity

on outgrowing cells of cardiac explants (Toyofuku *et al.* 2004). XIAP is known to inhibit apoptosis in many cancer types (Dubrez-Daloz *et al.* 2008). Liu *et al*, have found that SMAD5 mediates the pro-migratory TGF-beta switch in breast cancer mammary epithelial cells (Liu *et al.* 2009), Zimonjic *et al*, found increased expression of SMAD5 in human hepatocellular carcinoma (Zimonjic *et al.* 2003). Liang *et al*, and Badae *et al*, found MAP4K4 expression to be associated with poor prognosis in pancreatic cancer (Badea *et al.* 2008; Liang *et al.* 2008). Hao *et al*, found MAP4K4 to be associated with metastasis in colorectal cancer (Hao *et al.* 2010). BCL2 is an anti-apoptotic gene, Tygai *et al*, found that BCL2 was involved in brain tumour resistance to chemotherapy (Tyagi *et al.* 2002), and Roth *et al*, showed that overexpression of BCL2 increased proliferation in glioma (Roth *et al.* 2000). Salvi *et al*, found that overexpression of miR-23b led to decreased migration and proliferation abilities of human hepatocellular carcinoma cells (Salvi *et al.* 2009).

QRT-PCR was then carried out for each of the 7 target genes in SNB-19 cells which had been transfected with pre-miR-23b. Due to a small amount of genomic DNA contamination during the RNA extraction, it was only possible to measure the PCR product from MAP4K4 and XIAP, as there was sufficient separation of the cycle threshold number from amplicons generated from RNA and that of the genomic DNA.

The PCR amplicons were resolved on a 2.5% agarose gel to check for additional bands including primer-dimers (PD), there were none present. A PD is a potential by-product in PCR, it consists of primer molecules that have attached to each other due to strings of complementary bases in the primers. No bands were expected in lane 4 for each gene (RT negative control), which was the case with XIAP, SMAD5, MAP4K4, and MET; however bands derived from genomic DNA were present in the gel for BCL2, PDGFA and B-actin, which were not as strong as lanes 1 to 3, but the band in lane 4 for SEMAD6 was strong. The presence of a band in lane 4 indicated the presence of genomic DNA in our PCR reaction. However with the exception of SEMAD6 the fourth band was either absent or fainter than the other bands, confirming that sufficient amplicons were amplified specifically for the

target genes. To prevent DNA contamination the extracted RNA could have been treated with DNase (an enzyme which digests DNA) to remove any DNA carried over in the RNA extraction.

QRT-PCR showed that a 65.3% knockdown of XIAP was achieved with overexpression of miR-23b in the glioma cell line SNB-19. This was a very strong inhibitory effect with a single miRNA. The ability of cancer cells to resist apoptosis is crucial for development, progression, and treatment resistance. XIAP is the most potent member of the inhibitor of apoptosis (IAP) family (Deveraux and Reed 1999). XIAP is a direct inhibitor of cell death proteases, it directly inhibits caspase-3 and 7; these caspases are highly conserved throughout the animal kingdom (Deveraux *et al.* 1997). These have a protective effect against irradiation and anti-cancer drugs (LaCasse *et al.* 1998). Shi *et al*, have shown miR-21 to also target caspase-3 in addition to targeting caspase-9 in glioma, leading to cell growth suppression and invasion reduction (Shi *et al.* 2008). XIAP could potentially play a very significant role in glioma progression. As the present study has shown miR-23b to be decreased in invasive glioblastoma with a high proliferation rate, it is possible that a decrease of miR-23b expression in glioblastomas and subsequent unregulated expression of XIAP, has led to the ability of glioblastomas to evade apoptosis, which has possibly contributed to resistance and malignant progression in glioblastoma.

Future work will include the confirmation by western blot, of decreased protein levels of XIAP in SNB-19 cells overexpressing miR-23b. Further confirmation of XIAP as a target gene for miR-23b would include cloning of 3 stably transfected plasmids (Fig. 4.12.3) each containing an XIAP 3'UTR with one of the 3 potential binding sites for miR-23b (Fig. 4.12.2), downstream of a reporter gene e.g. luciferase or GFP; this could then be transfected into glioblastoma cells with pre-miR negative and pre-miR-23b. MiR-23b would then bind to the 3' UTR of the XIAP gene, and downregulate the gene. Binding of miR-23b would reduce luciferase expression levels if XIAP is a specific target of miR-23b in glioma cells. This would confirm XIAP as a target of miR-23b, and also determine the exact binding site of miR-23b on the XIAP gene.

It would also be interesting to check the presence of miR-23b in the lower grade tumours, as it has only been examined in the higher grade tumours. This would indicate if miR-23b is associated with malignant progression in glioma.

58 - aucacauugccagggauuacc - 78

(http://mirbase.org/cgi-bin/mirna_entry.pl?acc=MI0000439)

Fig 4.12.1 Mature sequence of hsa-miR-23b.

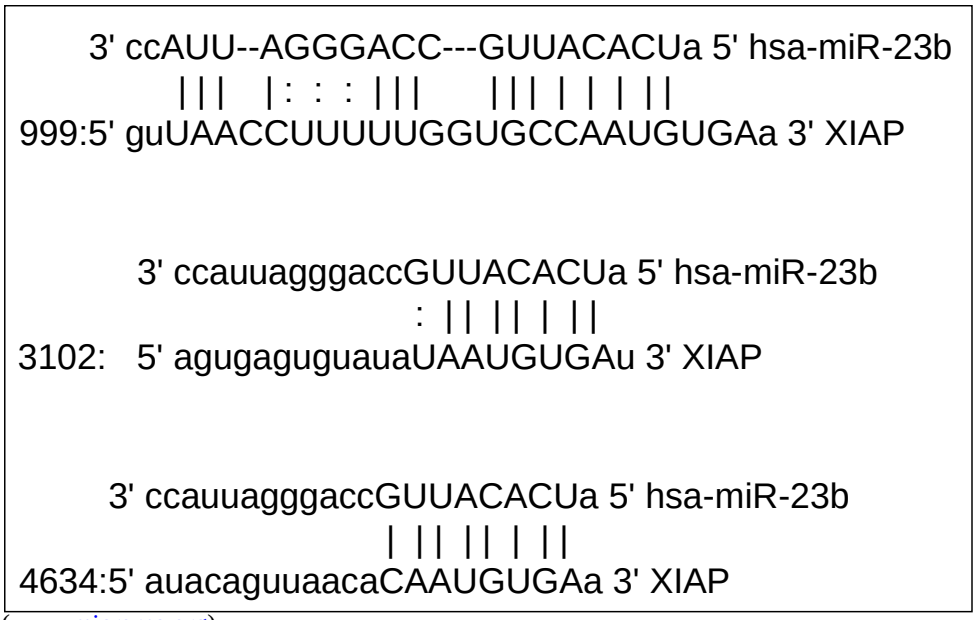

(www.microrna.org)

Fig. 4.12.2 Three predicted binding sites of miR-23b in the coding sequence for the XIAP gene.

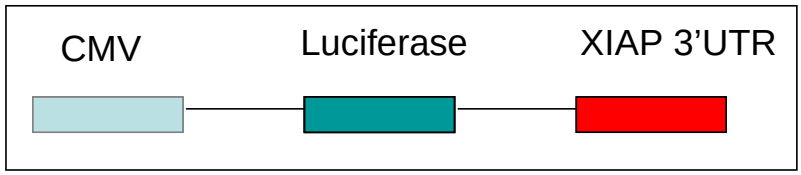

CMV: cytomegalovirus. XIAP: X-linked inhibitor of apoptosis 3'UTR: 3 prime untranslated region.

Fig. 4.12.3 Plasmid containing XIAP 3'UTR, and the reporter gene luciferase.

Effect of miR-93 and miR-23b on Invasion Activity of Glioma

The effect of anti-miR-93 was examined on the invasion activity of SNB-19 to see if by decreasing the expression of miR-93 that this could also decrease invasion. No effect on invasion was found (Fig. 3.8.27). Increasing the expression of miR-23b with pre-miR-23b to try to decrease invasion in SNB-19 had no effect (Fig. 3.8.28). Unfortunately the cell line SNB-19 was sensitive to the transfection reagent lipofectamine 2000; this alone had a strong inhibitory effect on invasion. In addition the negative control for pre-miR had an even stronger inhibitory effect on invasion; this made it difficult to accurately measure invasion activity when SNB-19 was transfected with miR-93 and miR-23b. However, as miR-93 and miR-23b have previously been shown to directly inhibit proliferation it is possible they may also inhibit invasion, as it has been discussed that glioma cells can switch from a proliferative to an invasive state and vice versa depending on environmental influences. Unfortunately it was not possible to measure invasion with SNB-19 post transfection with the reagent lipofectamine 2000. It may have damaged the membrane of the cells irreversibly and prevented invasion activity. Other methods of transfection need to be examined that leave the cell membrane intact, such as different transfection reagents or sonication.

3.6 Summary and Conclusion

miRNA Expression in Gliomas

(1) From the TLDA analysis 62 miRNAs were upregulated in non-invasive glioblastomas with slow proliferation and 13 were downregulated in comparison to invasive glioblastomas with fast proliferation.

(2) MiR-155 was 4.6 fold downregulated in slow, non-invasive glioblastomas; however, its expression did not correlate with a fast invasive phenotype.

(3) MiR-93 was 3.59 fold downregulated in slow, non-invasive glioblastomas in comparison to fast invasive glioblastomas. MiR-93 overexpression correlated with high proliferation and invasiveness in 12 glioma cultures, 1 established cell line, and in normal human astrocytes. Anti-miR-93 downregulated proliferation by 13.2 % in an established glioblastoma cell line, SNB-19. MiR-93 plays a role in proliferation in gliomas.

(4) High expression of the tumour suppressor gene BCL11B, in fast invasive glioma cultures correlated with high expression of miR-93, suggesting that miR-93 targets BCL11B.

(5) MiR-23b was 5.3 fold upregulated in slow, non-invasive glioblastomas. Overexpression of miR-23b resulted in a 30% decrease of proliferation over 3 days, and 40% over 5 days. Twice as much miR-23b expression was found in the slow, non-invasive glioblastoma pool in comparison to the fast, invasive glioblastoma pool. Overexpression of miR-23b resulted in a 65% knockdown at mRNA level of XIAP, the most potent human inhibitor of apoptosis, which is responsible for resistance to treatment in a variety of cancer types. Therefore, miR-23b might be a promising candidate for the development of new targeted treatment options.

Section 4.0 Future Plans

4.1 The Effect of Imatinib and Docetaxel on Glioma

(1) It is possible that this study identified a mutated form of BCR-Abl in the established glioma cell line SNB-19, which accounts for the resistance of this cell line to imatinib. This mutated protein should be analysed further by mass spectrometry. In addition, it would be interesting to screen the newly developed glioma cultures for this mutation.

(2) The strongly synergistic effect of the combination of imatinib and docetaxel shown in glioma cells should be validated in the newly developed primary cultures.

4.2 Temozolomide Resistant Cell Line SNB-19

The temozolomide resistant cell line SNB-19-Tmz, developed in this study should be further characterized with regard to its proliferation and invasion behaviour and its expression profile of the glial marker GFAP, and the stem cell markers nestin and CD133. It would also be interesting to examine the MGMT and the P53 status, as both are playing a role in drug resistance. By searching for possible mutations or deletions in proteins of the PI3K/Akt pathway it would enable us to explore another mechanism of resistance in this temozolomide resistant cell line.

4.3 Response of Glioma Cell Lines to Tyrosine Kinases

(1) As the response to TKIs with the glioma cultures was not correlated with specific targets of the TKIs, it would be interesting to look at single nucleotide polymorphism (SNP) analysis in each culture to identify mutations indicative of responders or non-responders to TKIs.

(2) The expression of targets involved in the PI3K/Akt pathway was examined in relation to responders and non-responders to TKIs. By examining other pathways, which might be involved in glioma tumourigenesis, such as the PKC, and MAPK pathways, this would give a better idea of glioma dependency on such pathways.

4.4 MiRNA

(1) Validation of other miRNAs identified in the TLDA analysis in all newly developed glioma cultures and the NHAs, to identify additional miRNAs involved in the regulation of proliferation and invasion in glioma.

(2) Western blot analysis of XIAP in SNB-19 cells post transfection with pre- miR-23b, to measure the amount of protein knockdown with miR-23b.

(3) Investigation of the phenotypical effect resulting from miRNA-23b overexpression by using a stable transfection system. By cloning a plasmid containing the XIAP 3'UTR containing binding sites for miR-23b, and a luciferase reporter gene into glioma cells, this would allow us to identify if XIAP is a specific target of miR-23b.

Section 5.0 References

ABTA. American Brain tumour Association, 2009 American Brain tumour Association.

NCRI. National cancer registry Ireland, © National Cancer Registry, 2006.

Abouantoun, T. J. and T. J. Macdonald (2009). "Imatinib blocks migration and invasion of medulloblastoma cells by concurrently inhibiting activation of platelet-derived growth factor receptor and transactivation of epidermal growth factor receptor." *Mol Cancer Ther* **8**(5): 1137-47.

Abrams, T. J., L. J. Murray, E. Pesenti, V. W. Holway, T. Colombo, L. B. Lee, J. M. Cherrington and N. K. Pryer (2003). "Preclinical evaluation of the tyrosine kinase inhibitor SU11248 as a single agent and in combination with "standard of care" therapeutic agents for the treatment of breast cancer." *Mol Cancer Ther* **2**(10): 1011-21.

Adams, V. R. and M. Leggas (2007). "Sunitinib malate for the treatment of metastatic renal cell carcinoma and gastrointestinal stromal tumors." *Clin Ther* **29**(7): 1338-53.

Adnane, J., P. Gaudray, C. A. Dionne, G. Crumley, M. Jaye, J. Schlessinger, P. Jeanteur, D. Birnbaum and C. Theillet (1991). "BEK and FLG, two receptors to members of the FGF family, are amplified in subsets of human breast cancers." *Oncogene* **6**(4): 659-63.

Agarwal, S., R. Sane, J. L. Gallardo, J. R. Ohlfest and W. F. Elmquist (2010). "Distribution of gefitinib to the brain is limited by P-glycoprotein (ABCB1) and breast cancer resistance protein (ABCG2)-mediated active efflux." *J Pharmacol Exp Ther* **334**(1): 147-55.

Akao, Y., Y. Nakagawa, A. Iio and T. Naoe (2009). "Role of microRNA-143 in Fas-mediated apoptosis in human T-cell leukemia Jurkat cells." *Leuk Res* **33**(11): 1530-8.

Akao, Y., Y. Nakagawa, Y. Kitade, T. Kinoshita and T. Naoe (2007). "Downregulation of microRNAs-143 and -145 in B-cell malignancies." *Cancer Sci* **98**(12): 1914-20.

Akbar, U., T. Jones, J. Winestone, M. Michael, A. Shukla, Y. Sun and C. Duntsch (2009). "Delivery of temozolomide to the tumor bed via biodegradable gel matrices in a novel model of intracranial glioma with resection." *J Neurooncol* **94**(2): 203-12.

Albini, A., I. Paglieri, G. Orengo, S. Carlone, M. G. Aluigi, R. DeMarchi, C. Matteucci, A. Mantovani, F. Carozzi, S. Donini and R. Benelli (1997). "The beta-core fragment of human chorionic gonadotrophin inhibits growth of Kaposi's sarcoma-derived cells and a new immortalized Kaposi's sarcoma cell line." *Aids* **11**(6): 713-21.

Alessi, D. R., F. B. Caudwell, M. Andjelkovic, B. A. Hemmings and P. Cohen (1996). "Molecular basis for the substrate specificity of protein kinase B; comparison with MAPKAP kinase-1 and p70 S6 kinase." *FEBS Lett* **399**(3): 333-8.

Ali, I. U., L. M. Schriml and M. Dean (1999). "Mutational spectra of PTEN/MMAC1 gene: a tumor suppressor with lipid phosphatase activity." *J Natl Cancer Inst* **91**(22): 1922-32.

Aligianis, I. A., N. V. Morgan, M. Mione, C. A. Johnson, E. Rosser, R. C. Hennekam, G. Adams, R. C. Trembath, D. T. Pilz, N. Stoodley, A. T. Moore, S. Wilson and E. R. Maher (2006). "Mutation in Rab3 GTPase-activating protein (RAB3GAP) noncatalytic subunit in a kindred with Martsolf syndrome." *Am J Hum Genet* **78**(4): 702-7.

Allikmets, R., L. M. Schriml, A. Hutchinson, V. Romano-Spica and M. Dean (1998). "A human placenta-specific ATP-binding cassette gene (ABCP) on chromosome 4q22 that is involved in multidrug resistance." *Cancer Res* **58**(23): 5337-9.

Amberger, V. R., V. Avellana-Adalid, T. Hensel, A. Baron-van Evercooren and M. E. Schwab (1997). "Oligodendrocyte-type 2 astrocyte progenitors use a metalloendoprotease to spread and migrate on CNS myelin." *Eur J Neurosci* **9**(1): 151-62.

Ambion www.ambion.com.

Annovazzi, L., M. Mellai, V. Caldera, G. Valente, L. Tessitore and D. Schiffer (2009). "mTOR, S6 and AKT expression in relation to proliferation and apoptosis/autophagy in glioma." *Anticancer Res* **29**(8): 3087-94.

Aoki, H., Y. Takada, S. Kondo, R. Sawaya, B. B. Aggarwal and Y. Kondo (2007). "Evidence that curcumin suppresses the growth of malignant gliomas in vitro and in vivo through induction of autophagy: role of Akt and extracellular signal-regulated kinase signaling pathways." *Mol Pharmacol* **72**(1): 29-39.

Aoki, M., K. Nabeshima, K. Koga, M. Hamasaki, J. Suzumiya, K. Tamura and H. Iwasaki (2007). "Imatinib mesylate inhibits cell invasion of malignant peripheral nerve sheath tumor induced by platelet-derived growth factor-BB." *Lab Invest* **87**(8): 767-79.

Auger, N., J. Thillet, K. Wanherdrick, A. Idbaih, M. E. Legrier, B. Dutrillaux, M. Sanson and M. F. Poupon (2006). "Genetic alterations associated with acquired temozolomide resistance in SNB-19, a human glioma cell line." *Mol Cancer Ther* **5**(9): 2182-92.

Badea, L., V. Herlea, S. O. Dima, T. Dumitrascu and I. Popescu (2008). "Combined gene expression analysis of whole-tissue and microdissected pancreatic ductal adenocarcinoma identifies genes specifically overexpressed in tumor epithelia." *Hepatogastroenterology* **55**(88): 2016-27.

Baehrecke, E. H. (2003). "miRNAs: micro managers of programmed cell death." *Curr Biol* **13**(12): R473-5.

Baillat, D. and R. Shiekhattar (2009). "Functional dissection of the human TNRC6 (GW182-related) family of proteins." *Mol Cell Biol* **29**(15): 4144-55.

Balaji, S., L. M. Iyer and L. Aravind (2009). "HPC2 and ubinuclein define a novel family of histone chaperones conserved throughout eukaryotes." *Mol Biosyst* **5**(3): 269-75.

Bandi, N., S. Zbinden, M. Gugger, M. Arnold, V. Kocher, L. Hasan, A. Kappeler, T. Brunner and E. Vassella (2009). "miR-15a and miR-16 are implicated in cell

cycle regulation in a Rb-dependent manner and are frequently deleted or down-regulated in non-small cell lung cancer." *Cancer Res* **69**(13): 5553-9.

Bao, S., Q. Wu, R. E. McLendon, Y. Hao, Q. Shi, A. B. Hjelmeland, M. W. Dewhirst, D. D. Bigner and J. N. Rich (2006). "Glioma stem cells promote radioresistance by preferential activation of the DNA damage response." *Nature* **444**(7120): 756-60.

Bartolovic, K., S. Balabanov, U. Hartmann, M. Komor, A. M. Boehmler, H. J. Buhring, R. Mohle, D. Hoelzer, L. Kanz, W. K. Hofmann and T. H. Brummendorf (2004). "Inhibitory effect of imatinib on normal progenitor cells in vitro." *Blood* **103**(2): 523-9.

Bauer, G. (2000). "Reactive oxygen and nitrogen species: efficient, selective, and interactive signals during intercellular induction of apoptosis." *Anticancer Res* **20**(6B): 4115-39.

Baumann, N. and D. Pham-Dinh (2001). "Biology of oligodendrocyte and myelin in the mammalian central nervous system." *Physiol Rev* **81**(2): 871-927.

Benbest www.benbest.com/nutrceut/AntiOxidants.html.

Bianco, R., I. Shin, C. A. Ritter, F. M. Yakes, A. Basso, N. Rosen, J. Tsurutani, P. A. Dennis, G. B. Mills and C. L. Arteaga (2003). "Loss of PTEN/MMAC1/TEP in EGF receptor-expressing tumor cells counteracts the antitumor action of EGFR tyrosine kinase inhibitors." *Oncogene* **22**(18): 2812-22.

Biermann, K., L. C. Heukamp, K. Steger, H. Zhou, F. E. Franke, I. Guetgemann, V. Sonnack, R. Brehm, J. Berg, P. J. Bastian, S. C. Muller, L. Wang-Eckert, H. Schorle and R. Buttner (2007). "Gene expression profiling identifies new biological markers of neoplastic germ cells." *Anticancer Res* **27**(5A): 3091-100.

Bihorel, S., G. Camenisch, M. Lemaire and J. M. Scherrmann (2007). "Influence of breast cancer resistance protein (Abcg2) and p-glycoprotein (Abcb1a) on the transport of imatinib mesylate (Gleevec) across the mouse blood-brain barrier." *J Neurochem* **102**(6): 1749-57.

Bihorel, S., G. Camenisch, M. Lemaire and J. M. Scherrmann (2007). "Modulation of the brain distribution of imatinib and its metabolites in mice by valspodar, zosuquidar and elacridar." *Pharm Res* **24**(9): 1720-8.

Bissery, M. C., G. Nohynek, G. J. Sanderink and F. Lavelle (1995). "Docetaxel (Taxotere): a review of preclinical and clinical experience. Part I: Preclinical experience." *Anticancer Drugs* **6**(3): 339-55, 363-8.

Blom, T., H. Fox, A. Angers-Loustau, K. Peltonen, L. Kerosuo, K. Wartiovaara, M. Linja, O. A. Janne, P. Kovanen, H. Haapasalo and N. N. Nupponen (2008). "KIT overexpression induces proliferation in astrocytes in an imatinib-responsive manner and associates with proliferation index in gliomas." *Int J Cancer* **123**(4): 793-800.

Boddy, A. V., J. Sludden, M. J. Griffin, C. Garner, J. Kendrick, P. Mistry, C. Dutreix, D. R. Newell and S. G. O'Brien (2007). "Pharmacokinetic investigation of imatinib using accelerator mass spectrometry in patients with chronic myeloid leukemia." *Clin Cancer Res* **13**(14): 4164-9.

Bohler, T., J. Waiser, H. Hepburn, J. Gaedeke, C. Lehmann, P. Hambach, K. Budde and H. H. Neumayer (2000). "TNF-alpha and IL-1alpha induce apoptosis in subconfluent rat mesangial cells. Evidence for the involvement of hydrogen peroxide and lipid peroxidation as second messengers." *Cytokine* **12**(7): 986-91.

Bolisetty, M. T., G. Dy, W. Tam and K. L. Beemon (2009). "Reticuloendotheliosis virus strain T induces miR-155, which targets JARID2 and promotes cell survival." *J Virol* **83**(23): 12009-17.

Bracaglia, G., B. Conca, A. Bergo, L. Rusconi, Z. Zhou, M. E. Greenberg, N. Landsberger, S. Soddu and C. Kilstrup-Nielsen (2009). "Methyl-CpG-binding protein 2 is phosphorylated by homeodomain-interacting protein kinase 2 and contributes to apoptosis." *EMBO Rep* **10**(12): 1327-33.

Brennan, C., H. Momota, D. Hambardzumyan, T. Ozawa, A. Tandon, A. Pedraza and E. Holland (2009). "Glioblastoma subclasses can be defined by activity among signal transduction pathways and associated genomic alterations." *PLoS One* **4**(11): e7752.

Bronger, H., J. Konig, K. Kopplow, H. H. Steiner, R. Ahmadi, C. Herold-Mende, D. Keppler and A. T. Nies (2005). "ABCC drug efflux pumps and organic anion uptake transporters in human gliomas and the blood-tumor barrier." *Cancer Res* **65**(24): 11419-28.

Broniscer, A., J. C. Panetta, M. O'Shaughnessy, C. Fraga, F. Bai, M. J. Krasin, A. Gajjar and C. F. Stewart (2007). "Plasma and cerebrospinal fluid pharmacokinetics of erlotinib and its active metabolite OSI-420." *Clin Cancer Res* **13**(5): 1511-5.

Brunner, T. B., S. M. Hahn, A. K. Gupta, R. J. Muschel, W. G. McKenna and E. J. Bernhard (2003). "Farnesyltransferase inhibitors: an overview of the results of preclinical and clinical investigations." *Cancer Res* **63**(18): 5656-68.

Burris, H. A., 3rd, S. Fields and N. Peacock (1995). "Docetaxel (Taxotere) in combination: a step forward." *Semin Oncol* **22**(6 Suppl 13): 35-40.

Cai, X. M., B. B. Tao, L. Y. Wang, Y. L. Liang, J. W. Jin, Y. Yang, Y. L. Hu and X. L. Zha (2005). "Protein phosphatase activity of PTEN inhibited the invasion of glioma cells with epidermal growth factor receptor mutation type III expression." *Int J Cancer* **117**(6): 905-12.

Calatozzolo, C., M. Gelati, E. Ciusani, F. L. Sciacca, B. Pollo, L. Cajola, C. Marras, A. Silvani, L. Vitellaro-Zuccarello, D. Croci, A. Boiardi and A. Salmaggi (2005). "Expression of drug resistance proteins Pgp, MRP1, MRP3, MRP5 and GST-pi in human glioma." *J Neurooncol* **74**(2): 113-21.

Calin, G. A., A. Cimmino, M. Fabbri, M. Ferracin, S. E. Wojcik, M. Shimizu, C. Taccioli, N. Zanesi, R. Garzon, R. I. Aqeilan, H. Alder, S. Volinia, L. Rassenti, X. Liu, C. G. Liu, T. J. Kipps, M. Negrini and C. M. Croce (2008). "MiR-15a and miR-16-1 cluster functions in human leukemia." *Proc Natl Acad Sci U S A* **105**(13): 5166-71.

Cano, C. E., J. Gommeaux, S. Pietri, M. Culcasi, S. Garcia, M. Seux, S. Barelier, S. Vasseur, R. P. Spoto, M. J. Pebusque, N. J. Dusetti, J. L. Iovanna and A. Carrier (2009). "Tumor protein 53-induced nuclear protein 1 is a major mediator of p53 antioxidant function." *Cancer Res* **69**(1): 219-26.

Cappuzzo, F., E. Magrini, G. L. Ceresoli, S. Bartolini, E. Rossi, V. Ludovini, V. Gregorc, C. Ligorio, A. Cancellieri, S. Damiani, A. Spreafico, C. T. Paties, L. Lombardo, C. Calandri, G. Bellezza, M. Tonato and L. Crino (2004). "Akt phosphorylation and gefitinib efficacy in patients with advanced non-small-cell lung cancer." *J Natl Cancer Inst* **96**(15): 1133-41.

Cau, J. and A. Hall (2005). "Cdc42 controls the polarity of the actin and microtubule cytoskeletons through two distinct signal transduction pathways." *J Cell Sci* **118**(Pt 12): 2579-87.

Cemeus, C., T. T. Zhao, G. M. Barrett, I. A. Lorimer and J. Dimitroulakos (2008). "Lovastatin enhances gefitinib activity in glioblastoma cells irrespective of EGFRvIII and PTEN status." *J Neurooncol* **90**(1): 9-17.

Chamberlain, M. C. (2006). "Treatment options for glioblastoma." *Neurosurg Focus* **20**(4): E2.

Chan, J. A., A. M. Krichevsky and K. S. Kosik (2005). "MicroRNA-21 is an antiapoptotic factor in human glioblastoma cells." *Cancer Res* **65**(14): 6029-33.

Chao, T. F., Y. Zhang, X. Q. Yan, B. Yin, Y. H. Gong, J. G. Yuan, B. Q. Qiang and X. Z. Peng (2008). "[MiR-9 regulates the expression of CBX7 in human glioma]." *Zhongguo Yi Xue Ke Xue Yuan Xue Bao* **30**(3): 268-74.

Chemblink www.chemblink.com.

Chen, J., L. Guo, D. A. Peiffer, L. Zhou, O. T. Chan, M. Bibikova, E. Wickham-Garcia, S. H. Lu, Q. Zhan, J. Wang-Rodriguez, W. Jiang and J. B. Fan (2008). "Genomic profiling of 766 cancer-related genes in archived esophageal normal and carcinoma tissues." *Int J Cancer* **122**(10): 2249-54.

Chen, M. Y., R. R. Lonser, P. F. Morrison, L. S. Governale and E. H. Oldfield (1999). "Variables affecting convection-enhanced delivery to the striatum: a systematic examination of rate of infusion, cannula size, infusate concentration, and tissue-cannula sealing time." *J Neurosurg* **90**(2): 315-20.

Chen, X., X. Guo, H. Zhang, Y. Xiang, J. Chen, Y. Yin, X. Cai, K. Wang, G. Wang, Y. Ba, L. Zhu, J. Wang, R. Yang, Y. Zhang, Z. Ren, K. Zen, J. Zhang and C. Y. Zhang (2009). "Role of miR-143 targeting KRAS in colorectal tumorigenesis." *Oncogene* **28**(10): 1385-92.

Chen, Y., W. Liu, T. Chao, Y. Zhang, X. Yan, Y. Gong, B. Qiang, J. Yuan, M. Sun and X. Peng (2008). "MicroRNA-21 down-regulates the expression of tumor suppressor PDCD4 in human glioblastoma cell T98G." *Cancer Lett* **272**(2): 197-205.

Chhabra, R., Y. K. Adlakha, M. Hariharan, V. Scaria and N. Saini (2009). "Upregulation of miR-23a approximately 27a approximately 24-2 cluster induces caspase-dependent and -independent apoptosis in human embryonic kidney cells." *PLoS One* **4**(6): e5848.

Choe, G., S. Horvath, T. F. Cloughesy, K. Crosby, D. Seligson, A. Palotie, L. Inge, B. L. Smith, C. L. Sawyers and P. S. Mischel (2003). "Analysis of the phosphatidylinositol 3'-kinase signaling pathway in glioblastoma patients in vivo." *Cancer Res* **63**(11): 2742-6.

Chou, C. K., R. F. Chen, F. F. Chou, H. W. Chang, Y. J. Chen, Y. F. Lee, K. D. Yang, J. T. Cheng, C. C. Huang and R. T. Liu (2010). "miR-146b is highly

expressed in adult papillary thyroid carcinomas with high risk features including extrathyroidal invasion and the BRAF(V600E) mutation." *Thyroid* **20**(5): 489-94.

Chou, T. C. and P. Talalay (1984). "Quantitative analysis of dose-effect relationships: the combined effects of multiple drugs or enzyme inhibitors." *Adv Enzyme Regul* **22**: 27-55.

Chua, C., N. Zaiden, K. H. Chong, S. J. See, M. C. Wong, B. T. Ang and C. Tang (2008). "Characterization of a side population of astrocytoma cells in response to temozolomide." *J Neurosurg* **109**(5): 856-66.

Ciafre, S. A., S. Galardi, A. Mangiola, M. Ferracin, C. G. Liu, G. Sabatino, M. Negrini, G. Maira, C. M. Croce and M. G. Farace (2005). "Extensive modulation of a set of microRNAs in primary glioblastoma." *Biochem Biophys Res Commun* **334**(4): 1351-8.

Clape, C., V. Fritz, C. Henriquet, F. Apparailly, P. L. Fernandez, F. Iborra, C. Avances, M. Villalba, S. Culine and L. Fajas (2009). "miR-143 interferes with ERK5 signaling, and abrogates prostate cancer progression in mice." *PLoS One* **4**(10): e7542.

Collins, C. S., J. Hong, L. Sapinoso, Y. Zhou, Z. Liu, K. Micklash, P. G. Schultz and G. M. Hampton (2006). "A small interfering RNA screen for modulators of tumor cell motility identifies MAP4K4 as a promigratory kinase." *Proc Natl Acad Sci U S A* **103**(10): 3775-80.

Coolen, M. and L. Bally-Cuif (2009). "MicroRNAs in brain development and physiology." *Curr Opin Neurobiol* **19**(5):461-70.

Crespo-Barreto, J., J. D. Fryer, C. A. Shaw, H. T. Orr and H. Y. Zoghbi (2010). "Partial loss of ataxin-1 function contributes to transcriptional dysregulation in spinocerebellar ataxia type 1 pathogenesis." *PLoS Genet* **6**(7): e1001021.

Cui, J. G., Y. Zhao, P. Sethi, Y. Y. Li, A. Mahta, F. Culicchia and W. J. Lukiw (2009). "Micro-RNA-128 (miRNA-128) down-regulation in glioblastoma targets ARP5 (ANGPTL6), Bmi-1 and E2F-3a, key regulators of brain cell proliferation." *J Neurooncol* **98**(3): 297-304.

Cui, Q., Z. Yu, E. O. Purisima and E. Wang (2006). "Principles of microRNA regulation of a human cellular signaling network." *Mol Syst Biol* **2**: 46.

Cuneo, K. C., L. Geng, A. Fu, D. Orton, D. E. Hallahan and A. B. Chakravarthy (2008). "SU11248 (sunitinib) sensitizes pancreatic cancer to the cytotoxic effects of ionizing radiation." *Int J Radiat Oncol Biol Phys* **71**(3): 873-9.

Dahmane, N., P. Sanchez, Y. Gitton, V. Palma, T. Sun, M. Beyna, H. Weiner and A. Ruiz i Altaba (2001). "The Sonic Hedgehog-Gli pathway regulates dorsal brain growth and tumorigenesis." *Development* **128**(24): 5201-12.

Dang, C. V. (2010). "Rethinking the Warburg effect with Myc micromanaging glutamine metabolism." *Cancer Res* **70**(3): 859-62.

Debinski, W. (2002). "Local treatment of brain tumors with targeted chimera cytotoxic proteins." *Cancer Invest* **20**(5-6): 801-9.

Decleves, X., S. Bihorel, M. Debray, S. Yousif, G. Camenisch and J. M. Scherrmann (2008). "ABC transporters and the accumulation of imatinib and its active metabolite CGP74588 in rat C6 glioma cells." *Pharmacol Res* **57**(3): 214-22.

Deisboeck, T. S., M. E. Berens, A. R. Kansal, S. Torquato, A. O. Stemmer-Rachamimov and E. A. Chiocca (2001). "Pattern of self-organization in tumour systems: complex growth dynamics in a novel brain tumour spheroid model." *Cell Prolif* **34**(2): 115-34.

Del Duca, D., T. Werbowetski and R. F. Del Maestro (2004). "Spheroid preparation from hanging drops: characterization of a model of brain tumor invasion." *J Neurooncol* **67**(3): 295-303.

Demayo, F., P. Minoo, C. G. Plopper, L. Schuger, J. Shannon and J. S. Torday (2002). "Mesenchymal-epithelial interactions in lung development and repair: are modeling and remodeling the same process?" *Am J Physiol Lung Cell Mol Physiol* **283**(3): L510-7.

Demeule, M., D. Shedid, E. Beaulieu, R. F. Del Maestro, A. Moghrabi, P. B. Ghosn, R. Moumdjian, F. Berthelet and R. Beliveau (2001). "Expression of multidrug-resistance P-glycoprotein (MDR1) in human brain tumors." *Int J Cancer* **93**(1): 62-6.

Demuth, T., L. B. Reavie, J. L. Rennert, M. Nakada, S. Nakada, D. B. Hoelzinger, C. E. Beaudry, A. N. Henrichs, E. M. Anderson and M. E. Berens (2007). "MAP-ing glioma invasion: mitogen-activated protein kinase kinase 3 and p38 drive glioma invasion and progression and predict patient survival." *Mol Cancer Ther* **6**(4): 1212-22.

Deveraux, Q. L. and J. C. Reed (1999). "IAP family proteins--suppressors of apoptosis." *Genes Dev* **13**(3): 239-52.

Deveraux, Q. L., R. Takahashi, G. S. Salvesen and J. C. Reed (1997). "X-linked IAP is a direct inhibitor of cell-death proteases." *Nature* **388**(6639): 300-4.

Diana lab "http://www.diana.cslab."

Dresemann, G. (2010). "Temozolomide in malignant glioma." *Onco Targets Ther* **7**(3): 139-46.

Druker, B. J. (2001). "Current treatment approaches for chronic myelogenous leukemia." *Cancer J* **7 Suppl 1**: S14-8.

Du, L., J. J. Schageman, M. C. Subauste, B. Saber, S. M. Hammond, L. Prudkin, Wistuba, II, L. Ji, J. A. Roth, J. D. Minna and A. Pertsemlidis (2009). "miR-93, miR-98, and miR-197 regulate expression of tumor suppressor gene FUS1." *Mol Cancer Res* **7**(8): 1234-43.

Dubrez-Daloz, L., A. Dupoux and J. Cartier (2008). "IAPs: more than just inhibitors of apoptosis proteins." *Cell Cycle* **7**(8): 1036-46.

Duesberg, P., R. Stindl and R. Hehlmann (2001). "Origin of multidrug resistance in cells with and without multidrug resistance genes: chromosome reassortments catalyzed by aneuploidy." *Proc Natl Acad Sci U S A* **98**(20): 11283-8.

Dziadziuszko, R., S. E. Witta, F. Cappuzzo, S. Park, K. Tanaka, P. V. Danenberg, A. E. Baron, L. Crino, W. A. Franklin, P. A. Bunn, Jr., M. Varella-Garcia, K. D. Danenberg and F. R. Hirsch (2006). "Epidermal growth factor receptor messenger RNA expression, gene dosage, and gefitinib sensitivity in non-small cell lung cancer." *Clin Cancer Res* **12**(10): 3078-84.

Endersby, R. and S. J. Baker (2008). "PTEN signaling in brain: neuropathology and tumorigenesis." *Oncogene* **27**(41): 5416-30.

Evers, R., M. Kool, A. J. Smith, L. van Deemter, M. de Haas and P. Borst (2000). "Inhibitory effect of the reversal agents V-104, GF120918 and Pluronic L61 on MDR1 Pgp-, MRP1- and MRP2-mediated transport." *Br J Cancer* **83**(3): 366-74.

Fan, Q. W., C. Cheng, Z. A. Knight, D. Haas-Kogan, D. Stokoe, C. D. James, F. McCormick, K. M. Shokat and W. A. Weiss (2009). "EGFR signals to mTOR through PKC and independently of Akt in glioma." *Sci Signal* **2**(55): ra4.

Fan, X., Y. Liu, J. Jiang, Z. Ma, H. Wu, T. Liu, M. Liu, X. Li and H. Tang (2010). "miR-20a promotes proliferation and invasion by targeting APP in human ovarian cancer cells." *Acta Biochim Biophys Sin (Shanghai)* **42**(5): 318-24.

Fleming, T. P., A. Saxena, W. C. Clark, J. T. Robertson, E. H. Oldfield, S. A. Aaronson and I. U. Ali (1992). "Amplification and/or overexpression of platelet-derived growth factor receptors and epidermal growth factor receptor in human glial tumors." *Cancer Res* **52**(16): 4550-3.

Forsyth, P., G. Cairncross, D. Stewart, M. Goodyear, N. Wainman and E. Eisenhauer (1996). "Phase II trial of docetaxel in patients with recurrent malignant glioma: a study of the National Cancer Institute of Canada Clinical Trials Group." *Invest New Drugs* **14**(2): 203-6.

Fracasso, P. M., L. J. Goldstein, D. P. de Alwis, J. S. Rader, M. A. Arquette, S. A. Goodner, L. P. Wright, C. L. Fears, R. J. Gazak, V. A. Andre, M. F. Burgess, C. A. Slapak and J. H. Schellens (2004). "Phase I study of docetaxel in combination with the P-glycoprotein inhibitor, zosuquidar, in resistant malignancies." *Clin Cancer Res* **10**(21): 7220-8.

Francis Ali-Osman, D. (2005). Brain Tumors. Durham, Humana Press Inc, 999 Riverview Drive, Suite 208, Totowa, New Jersey 07512.

Franke, T. F., S. I. Yang, T. O. Chan, K. Datta, A. Kazlauskas, D. K. Morrison, D. R. Kaplan and P. N. Tsichlis (1995). "The Protein-Kinase Encoded by the Akt Protooncogene Is a Target of the Pdgf-Activated Phosphatidylinositol 3-Kinase." *Cell* **81**(5): 727-736.

Frankel, R. H., W. Bayona, M. Koslow and E. W. Newcomb (1992). "p53 mutations in human malignant gliomas: comparison of loss of heterozygosity with mutation frequency." *Cancer Res* **52**(6): 1427-33.

Frederick, L., X. Y. Wang, G. Eley and C. D. James (2000). "Diversity and frequency of epidermal growth factor receptor mutations in human glioblastomas." *Cancer Res* **60**(5): 1383-7.

Friedman, H. S., M. D. Prados, P. Y. Wen, T. Mikkelsen, D. Schiff, L. E. Abrey, W. K. Yung, N. Paleologos, M. K. Nicholas, R. Jensen, J. Vredenburgh, J. Huang, M. Zheng and T. Cloughesy (2009). "Bevacizumab alone and in combination with irinotecan in recurrent glioblastoma." *J Clin Oncol* **27**(28): 4733-40.

Furukawa, K., Y. Kumon, H. Harada, S. Kohno, S. Nagato, M. Teraoka, S. Fujiwara, K. Nakagawa, K. Hamada and T. Ohnishi (2006). "PTEN gene transfer suppresses the invasive potential of human malignant gliomas by regulating cell invasion-related molecules." *Int J Oncol* **29**(1): 73-81.

Gal, H., G. Pandi, A. A. Kanner, Z. Ram, G. Lithwick-Yanai, N. Amariglio, G. Rechavi and D. Givol (2008). "MIR-451 and Imatinib mesylate inhibit tumor growth of Glioblastoma stem cells." *Biochem Biophys Res Commun* **376**(1): 86-90.

Galceran, J., C. Sustmann, S. C. Hsu, S. Folberth and R. Grosschedl (2004). "LEF1-mediated regulation of Delta-like1 links Wnt and Notch signaling in somitogenesis." *Genes Dev* **18**(22): 2718-23.

Geoerger, B., K. Kerr, C. B. Tang, K. M. Fung, B. Powell, L. N. Sutton, P. C. Phillips and A. J. Janss (2001). "Antitumor activity of the rapamycin analog CCI-779 in human primitive neuroectodermal tumor/medulloblastoma models as single agent and in combination chemotherapy." *Cancer Res* **61**(4): 1527-32.

Giannopoulou, E., K. Dimitropoulos, A. A. Argyriou, A. K. Koutras, F. Dimitrakopoulos and H. P. Kalofonos (2010). "An in vitro study, evaluating the effect of sunitinib and/or lapatinib on two glioma cell lines." *Invest New Drugs* **28**(5): 554-60.

Giese, A., R. Bjerkvig, M. E. Berens and M. Westphal (2003). "Cost of migration: invasion of malignant gliomas and implications for treatment." *J Clin Oncol* **21**(8): 1624-36.

Giese, A., M. A. Loo, N. Tran, D. Haskett, S. W. Coons and M. E. Berens (1996). "Dichotomy of astrocytoma migration and proliferation." *Int J Cancer* **67**(2): 275-82.

Gilg, A. G., S. L. Tye, L. B. Tolliver, W. G. Wheeler, R. P. Visconti, J. D. Duncan, F. V. Kostova, L. N. Bolds, B. P. Toole and B. L. Maria (2008). "Targeting hyaluronan interactions in malignant gliomas and their drug-resistant multipotent progenitors." *Clin Cancer Res* **14**(6): 1804-13.

Gillies, J. K. and I. A. Lorimer (2007). "Regulation of p27Kip1 by miRNA 221/222 in glioblastoma." *Cell Cycle* **6**(16): 2005-9.

Gironella, M., M. Seux, M. J. Xie, C. Cano, R. Tomasini, J. Gommeaux, S. Garcia, J. Nowak, M. L. Yeung, K. T. Jeang, A. Chaix, L. Fazli, Y. Motoo, Q. Wang, P. Rocchi, A. Russo, M. Gleave, J. C. Dagorn, J. L. Iovanna, A. Carrier, M. J. Pebusque and N. J. Dusetti (2007). "Tumor protein 53-induced nuclear protein 1 expression is repressed by miR-155, and its restoration inhibits pancreatic tumor development." *Proc Natl Acad Sci U S A* **104**(41): 16170-5.

Glass, T. L., T. J. Liu and W. K. Yung (2000). "Inhibition of cell growth in human glioblastoma cell lines by farnesyltransferase inhibitor SCH66336." *Neuro Oncol* **2**(3): 151-8.

Godlewski, J., A. Bronisz, M. O. Nowicki, E. A. Chiocca and S. Lawler (2010). "microRNA-451: A conditional switch controlling glioma cell proliferation and migration." *Cell Cycle* **9**(14): 2742-8.

Godlewski, J., M. O. Nowicki, A. Bronisz, S. Williams, A. Otsuki, G. Nuovo, A. Raychaudhury, H. B. Newton, E. A. Chiocca and S. Lawler (2008). "Targeting of the Bmi-1 oncogene/stem cell renewal factor by microRNA-128 inhibits glioma proliferation and self-renewal." *Cancer Res* **68**(22): 9125-30.

Goel, A. and C. R. Boland (2010). "Recent insights into the pathogenesis of colorectal cancer." *Curr Opin Gastroenterol* **26**(1): 47-52.

Golembieski, W. A., S. L. Thomas, C. R. Schultz, C. K. Yunker, H. M. McClung, N. Lemke, S. Cazacu, T. Barker, E. H. Sage, C. Brodie and S. A. Rempel (2008). "HSP27 mediates SPARC-induced changes in glioma morphology, migration, and invasion." *Glia* **56**(10): 1061-75.

Gucluler, G. and Y. Baran (2009). "Docetaxel enhances the cytotoxic effects of imatinib on Philadelphia positive human chronic myeloid leukemia cells." *Hematology* **14**(3): 139-44.

Guha, A., K. Dashner, P. M. Black, J. A. Wagner and C. D. Stiles (1995). "Expression of PDGF and PDGF receptors in human astrocytoma operation specimens supports the existence of an autocrine loop." *Int J Cancer* **60**(2): 168-73.

Guha, A., D. Glowacka, R. Carroll, K. Dashner, P. M. Black and C. D. Stiles (1995). "Expression of platelet derived growth factor and platelet derived growth factor receptor mRNA in a glioblastoma from a patient with Li-Fraumeni syndrome." *J Neurol Neurosurg Psychiatry* **58**(6): 711-4.

Guillamo, J. S., S. de Bouard, S. Valable, L. Marteau, P. Leuraud, Y. Marie, M. F. Poupon, J. J. Parienti, E. Raymond and M. Peschanski (2009). "Molecular mechanisms underlying effects of epidermal growth factor receptor inhibition on invasion, proliferation, and angiogenesis in experimental glioma." *Clin Cancer Res* **15**(11): 3697-704.

Guled, M., L. Lahti, P. M. Lindholm, K. Salmenkivi, I. Bagwan, A. G. Nicholson and S. Knuutila (2009). "CDKN2A, NF2, and JUN are dysregulated among other genes by miRNAs in malignant mesothelioma -A miRNA microarray analysis." *Genes Chromosomes Cancer* **48**(7): 615-23.

Gullick, J. D. H. a. W. J. (2008). EGFR Signaling Networks in cancer Therapy, Humana Press, c/o Springer Science + Business Media, LLC, 233 Spring Street, New York, NY 10013, USA.

Gunther, W., E. Pawlak, R. Damasceno, H. Arnold and A. J. Terzis (2003). "Temozolomide induces apoptosis and senescence in glioma cells cultured as multicellular spheroids." *Br J Cancer* **88**(3): 463-9.

Haas-Kogan, D., N. Shalev, M. Wong, G. Mills, G. Yount and D. Stokoe (1998). "Protein kinase B (PKB/Akt) activity is elevated in glioblastoma cells due to mutation of the tumor suppressor PTEN/MMAC." *Curr Biol* **8**(21): 1195-8.

Haas-Kogan, D. A., M. D. Prados, T. Tihan, D. A. Eberhard, N. Jelluma, N. D. Arvold, R. Baumber, K. R. Lamborn, A. Kapadia, M. Malec, M. S. Berger and D. Stokoe (2005). "Epidermal growth factor receptor, protein kinase B/Akt, and glioma response to erlotinib." *J Natl Cancer Inst* **97**(12): 880-7.

Haberler, C., E. Gelpi, C. Marosi, K. Rossler, P. Birner, H. Budka and J. A. Hainfellner (2006). "Immunohistochemical analysis of platelet-derived growth factor receptor-alpha, -beta, c-kit, c-abl, and arg proteins in glioblastoma: possible implications for patient selection for imatinib mesylate therapy." *J Neurooncol* **76**(2): 105-9.

Hagerstrand, D., G. Hesselager, S. Achterberg, U. Wickenberg Bolin, M. Kowanetz, M. Kastemar, C. H. Heldin, A. Isaksson, M. Nister and A. Ostman (2006).

"Characterization of an imatinib-sensitive subset of high-grade human glioma cultures." *Oncogene* **25**(35): 4913-22.

Hamel, W., M. Westphal and H. M. Shepard (1992). "Protooncogene Expression in Human Glioma Derived Cell-Lines." *International Journal of Oncology* **1**(6): 673-682.

Hao, J. M., J. Z. Chen, H. M. Sui, X. Q. Si-Ma, G. Q. Li, C. Liu, J. L. Li, Y. Q. Ding and J. M. Li (2010). "A five-gene signature as a potential predictor of metastasis and survival in colorectal cancer." *J Pathol* **220**(4): 475-89.

Harry, G. J., M. Billingsley, A. Bruinink, I. L. Campbell, W. Classen, D. C. Dorman, C. Galli, D. Ray, R. A. Smith and H. A. Tilson (1998). "In vitro techniques for the assessment of neurotoxicity." *Environ Health Perspect* **106 Suppl 1**: 131-58.

Hatzikirou, H., D. Basanta, M. Simon, K. Schaller and A. Deutsch (2010). "'Go or Grow': the key to the emergence of invasion in tumour progression?" *Math Med Biol* **epub ahead of print**.

Haura, E. B., T. Tanvetyanon, A. Chiappori, C. Williams, G. Simon, S. Antonia, J. Gray, S. Litschauer, L. Tetteh, A. Neuger, L. Song, B. Rawal, M. J. Schell and G. Bepler (2010). "Phase I/II study of the Src inhibitor dasatinib in combination with erlotinib in advanced non-small-cell lung cancer." *J Clin Oncol* **28**(8): 1387-94.

Heimberger, A. B., R. Hlatky, D. Suki, D. Yang, J. Weinberg, M. Gilbert, R. Sawaya and K. Aldape (2005). "Prognostic effect of epidermal growth factor receptor and EGFRvIII in glioblastoma multiforme patients." *Clin Cancer Res* **11**(4): 1462-6.

Henson, B. J., S. Bhattacharjee, D. M. O'Dee, E. Feingold and S. M. Gollin (2009). "Decreased expression of miR-125b and miR-100 in oral cancer cells contributes to malignancy." *Genes Chromosomes Cancer* **48**(7): 569-82.

Hermanson, M., K. Funa, M. Hartman, L. Claesson-Welsh, C. H. Heldin, B. Westermark and M. Nister (1992). "Platelet-derived growth factor and its receptors in human glioma tissue: expression of messenger RNA and protein suggests the presence of autocrine and paracrine loops." *Cancer Res* **52**(11): 3213-9.

Hesselager, G. and E. C. Holland (2003). "Using mice to decipher the molecular genetics of brain tumors." *Neurosurgery* **53**(3): 685-94; discussion 695.

NIH http://ehis.niehs.nih.gov/.

Hirsch, F. R., M. Varella-Garcia, J. McCoy, H. West, A. C. Xavier, P. Gumerlock, P. A. Bunn, Jr., W. A. Franklin, J. Crowley and D. R. Gandara (2005). "Increased epidermal growth factor receptor gene copy number detected by fluorescence in situ hybridization associates with increased sensitivity to gefitinib in patients with bronchioloalveolar carcinoma subtypes: a Southwest Oncology Group Study." *J Clin Oncol* **23**(28): 6838-45.

Hirschmann-Jax, C., A. E. Foster, G. G. Wulf, J. G. Nuchtern, T. W. Jax, U. Gobel, M. A. Goodell and M. K. Brenner (2004). "A distinct "side population" of cells with high drug efflux capacity in human tumor cells." *Proc Natl Acad Sci U S A* **101**(39): 14228-33.

Hofer, S. and K. Frei (2007). "Gefitinib concentrations in human glioblastoma tissue." *J Neurooncol* **82**(2): 175-6.

Hofmann, M. H., J. Heinrich, G. Radziwil and K. Moelling (2009). "A short hairpin DNA analogous to miR-125b inhibits C-Raf expression, proliferation, and survival of breast cancer cells." *Mol Cancer Res* **7**(10): 1635-44.

Holland, E. C., J. Celestino, C. Dai, L. Schaefer, R. E. Sawaya and G. N. Fuller (2000). "Combined activation of Ras and Akt in neural progenitors induces glioblastoma formation in mice." *Nat Genet* **25**(1): 55-7.

Hu, X., P. P. Pandolfi, Y. Li, J. A. Koutcher, M. Rosenblum and E. C. Holland (2005). "mTOR promotes survival and astrocytic characteristics induced by Pten/AKT signaling in glioblastoma." *Neoplasia* **7**(4): 356-68.

Huang, S., D. Vader, Z. Wang, A. Stemmer-Rachamimov, D. A. Weitz, G. Dai, B. R. Rosen and T. S. Deisboeck (2008). "Using magnetic resonance microscopy to study the growth dynamics of a glioma spheroid in collagen I: A case study." *BMC Med Imaging* **8**: 3.

Huang, Z. M., J. Yang, X. Y. Shen, X. Y. Zhang, F. S. Meng, J. T. Xu, B. F. Zhang and H. J. Gao (2009). "MicroRNA expression profile in non-cancerous colonic tissue associated with lymph node metastasis of colon cancer." *J Dig Dis* **10**(3): 188-94.

Hurst, D. R., M. D. Edmonds, G. K. Scott, C. C. Benz, K. S. Vaidya and D. R. Welch (2009). "Breast cancer metastasis suppressor 1 up-regulates miR-146, which suppresses breast cancer metastasis." *Cancer Res* **69**(4): 1279-83.

Huse, J. T., C. Brennan, D. Hambardzumyan, B. Wee, J. Pena, S. H. Rouhanifard, C. Sohn-Lee, C. le Sage, R. Agami, T. Tuschl and E. C. Holland (2009). "The PTEN-regulating microRNA miR-26a is amplified in high-grade glioma and facilitates gliomagenesis in vivo." *Genes Dev* **23**(11): 1327-37.

Hwang, S. L., C. Y. Chai, H. J. Lin and S. L. Howng (1997). "Expression of epidermal growth factor receptors and c-erbB-2 proteins in human astrocytic tumors." *Kaohsiung J Med Sci* **13**(7): 417-24.

Hynes, N. E. and H. A. Lane (2005). "ERBB receptors and cancer: the complexity of targeted inhibitors." *Nat Rev Cancer* **5**(5): 341-54.

Ishii, D., A. Natsume, T. Wakabayashi, H. Hatano, Y. Asano, H. Takeuchi, S. Shimato, M. Ito, M. Fujii and J. Yoshida (2007). "Efficacy of temozolomide is correlated with 1p loss and methylation of the deoxyribonucleic acid repair gene MGMT in malignant gliomas." *Neurol Med Chir (Tokyo)* **47**(8): 341-9; discussion 350.

Ishikawa, S., M. Kai, Y. Murata, M. Tamari, Y. Daigo, T. Murano, M. Ogawa and Y. Nakamura (1998). "Genomic organization and mapping of the human activin receptor type IIB (hActR-IIB) gene." *J Hum Genet* **43**(2): 132-4.

Jemal, A., T. Murray, E. Ward, A. Samuels, R. C. Tiwari, A. Ghafoor, E. J. Feuer and M. J. Thun (2005). "Cancer statistics, 2005." *CA Cancer J Clin* **55**(1): 10-30.

Jeuken, J., C. van den Broecke, S. Gijsen, S. Boots-Sprenger and P. Wesseling (2007). "RAS/RAF pathway activation in gliomas: the result of copy number gains rather than activating mutations." *Acta Neuropathol* **114**(2): 121-33.

Jiang, R., C. Mircean, I. Shmulevich, D. Cogdell, Y. Jia, I. Tabus, K. Aldape, R. Sawaya, J. M. Bruner, G. N. Fuller and W. Zhang (2006). "Pathway alterations during glioma progression revealed by reverse phase protein lysate arrays." *Proteomics* **6**(10): 2964-71.

Johnston, R. J. and O. Hobert (2003). "A microRNA controlling left/right neuronal asymmetry in Caenorhabditis elegans." *Nature* **426**(6968): 845-9.

Kan, T., F. Sato, T. Ito, N. Matsumura, S. David, Y. Cheng, R. Agarwal, B. C. Paun, Z. Jin, A. V. Olaru, F. M. Selaru, J. P. Hamilton, J. Yang, J. M. Abraham, Y. Mori and S. J. Meltzer (2009). "The miR-106b-25 polycistron, activated by genomic amplification, functions as an oncogene by suppressing p21 and Bim." *Gastroenterology* **136**(5): 1689-700.

Kanakaraj, P., S. Raj, S. A. Khan and S. Bishayee (1991). "Ligand-induced interaction between alpha- and beta-type platelet-derived growth factor (PDGF) receptors: role of receptor heterodimers in kinase activation." *Biochemistry* **30**(7): 1761-7.

Kanda, Y., K. Mitani, M. Kurokawa, T. Yamagata, Y. Yazaki and H. Hirai (1998). "Overexpression of the MEN/ELL protein, an RNA polymerase II elongation factor, results in transformation of Rat1 cells with dependence on the lysine-rich region." *J Biol Chem* **273**(9): 5248-52.

Karlsson, A., A. Nordigarden, J. I. Jonsson and P. Soderkvist (2007). "Bcl11b mutations identified in murine lymphomas increase the proliferation rate of hematopoietic progenitor cells." *BMC Cancer* **7**: 195.

Kato, Y., D. A. Holm, B. Okollie and D. Artemov (2010). "Noninvasive detection of temozolomide in brain tumor xenografts by magnetic resonance spectroscopy." *Neuro Oncol* **12**(1): 71-9.

Katz, D., A. Segal, Y. Alberton, O. Jurim, P. Reissman, R. Catane and N. I. Cherny (2004). "Neoadjuvant imatinib for unresectable gastrointestinal stromal tumor." *Anticancer Drugs* **15**(6): 599-602.

Kawataki, T., E. Sato, T. Sato and H. Kinouchi (2010). "Anaplastic ganglioglioma with malignant features in both neuronal and glial components--case report." *Neurol Med Chir (Tokyo)* **50**(3): 228-31.

Kefas, B., L. Comeau, D. H. Floyd, O. Seleverstov, J. Godlewski, T. Schmittgen, J. Jiang, C. G. diPierro, Y. Li, E. A. Chiocca, J. Lee, H. Fine, R. Abounader, S. Lawler and B. Purow (2009). "The neuronal microRNA miR-326 acts in a feedback loop with notch and has therapeutic potential against brain tumors." *J Neurosci* **29**(48): 15161-8.

Kefas, B., J. Godlewski, L. Comeau, Y. Li, R. Abounader, M. Hawkinson, J. Lee, H. Fine, E. A. Chiocca, S. Lawler and B. Purow (2008). "microRNA-7 inhibits the epidermal growth factor receptor and the Akt pathway and is down-regulated in glioblastoma." *Cancer Res* **68**(10): 3566-72.

Kemper, E. M., A. E. van Zandbergen, C. Cleypool, H. A. Mos, W. Boogerd, J. H. Beijnen and O. van Tellingen (2003). "Increased penetration of paclitaxel into the brain by inhibition of P-Glycoprotein." *Clin Cancer Res* **9**(7): 2849-55.

Kemper, E. M., M. Verheij, W. Boogerd, J. H. Beijnen and O. van Tellingen (2004). "Improved penetration of docetaxel into the brain by co-administration of inhibitors of P-glycoprotein." *Eur J Cancer* **40**(8): 1269-74.

Khoshyomn, S., S. Lew, J. DeMattia, E. B. Singer and P. L. Penar (1999). "Brain tumor invasion rate measured in vitro does not correlate with Ki-67 expression." *J Neurooncol* **45**(2): 111-6.

Khvorova, A., A. Reynolds and S. D. Jayasena (2003). "Functional siRNAs and miRNAs exhibit strand bias." *Cell* **115**(2): 209-16.

Kilic, T., J. A. Alberta, P. R. Zdunek, M. Acar, P. Iannarelli, T. O'Reilly, E. Buchdunger, P. M. Black and C. D. Stiles (2000). "Intracranial inhibition of platelet-derived growth factor-mediated glioblastoma cell growth by an orally active kinase inhibitor of the 2-phenylaminopyrimidine class." *Cancer Res* **60**(18): 5143-50.

Kinsella, P., M. Clynes and V. Amberger-Murphy (2011). "Imatinib and docetaxel in combination can effectively inhibit glioma invasion in an in vitro 3D invasion assay." *J Neurooncol* **101**(2): 189-98.

Kitange, G. J., B. L. Carlson, M. A. Schroeder, P. A. Decker, B. W. Morlan, W. Wu, K. V. Ballman, C. Giannini and J. N. Sarkaria (2010). "Expression of CD74 in high grade gliomas: a potential role in temozolomide resistance." *J Neurooncol* **100**(2): 177-86.

Kleihues, P. and H. Ohgaki (2000). "Phenotype vs genotype in the evolution of astrocytic brain tumors." *Toxicol Pathol* **28**(1): 164-70.

Kogashiwa, Y., H. Sakurai, T. Kimura and N. Kohno (2010). "Docetaxel suppresses invasiveness of head and neck cancer cells in vitro." *Cancer Sci* **101**(6): 1382-6.

Kogiku, M., I. Ohsawa, K. Matsumoto, Y. Sugisaki, H. Takahashi, A. Teramoto and S. Ohta (2008). "Prognosis of glioma patients by combined immunostaining for survivin, Ki-67 and epidermal growth factor receptor." *J Clin Neurosci* **15**(11): 1198-203.

Kolenda, J., S. S. Jensen, C. Aaberg-Jessen, K. Christensen, C. Andersen, N. Brunner and B. W. Kristensen (2010). "Effects of hypoxia on expression of a panel of stem cell and chemoresistance markers in glioblastoma-derived spheroids." *J Neurooncol* **epub ahead of print**.

Komatsu, M., T. Takahashi, T. Abe, I. Takahashi, H. Ida and G. Takada (2001). "Evidence for the association of ultraviolet-C and H(2)O(2)-induced apoptosis with acid sphingomyelinase activation." *Biochim Biophys Acta* **1533**(1): 47-54.

Koukourakis, M. I., A. Giatromanolaki, S. Schiza, S. Kakolyris and V. Georgoulias (1999). "Concurrent twice-a-week docetaxel and radiotherapy: a dose escalation trial with immunological toxicity evaluation." *Int J Radiat Oncol Biol Phys* **43**(1): 107-14.

Kozaki, K., I. Imoto, S. Mogi, K. Omura and J. Inazawa (2008). "Exploration of tumor-suppressive microRNAs silenced by DNA hypermethylation in oral cancer." *Cancer Res* **68**(7): 2094-105.

Kreisl, T. N., L. Kim, K. Moore, P. Duic, C. Royce, I. Stroud, N. Garren, M. Mackey, J. A. Butman, K. Camphausen, J. Park, P. S. Albert and H. A. Fine

(2009). "Phase II trial of single-agent bevacizumab followed by bevacizumab plus irinotecan at tumor progression in recurrent glioblastoma." *J Clin Oncol* **27**(5): 740-5.

Krol, J., K. Sobczak, U. Wilczynska, M. Drath, A. Jasinska, D. Kaczynska and W. J. Krzyzosiak (2004). "Structural features of microRNA (miRNA) precursors and their relevance to miRNA biogenesis and small interfering RNA/short hairpin RNA design." *J Biol Chem* **279**(40): 42230-9.

Kumabe, T., Y. Sohma, T. Kayama, T. Yoshimoto and T. Yamamoto (1992). "Overexpression and amplification of alpha-PDGF receptor gene lacking exons coding for a portion of the extracellular region in a malignant glioma." *Tohoku J Exp Med* **168**(2): 265-9.

Laban, C., S. A. Bustin and P. J. Jenkins (2003). "The GH-IGF-I axis and breast cancer." *Trends Endocrinol Metab* **14**(1): 28-34.

LaCasse, E. C., S. Baird, R. G. Korneluk and A. E. MacKenzie (1998). "The inhibitors of apoptosis (IAPs) and their emerging role in cancer." *Oncogene* **17**(25): 3247-59.

le Coutre, P., K. A. Kreuzer, S. Pursche, M. Bonin, T. Leopold, G. Baskaynak, B. Dorken, G. Ehninger, O. Ottmann, A. Jenke, M. Bornhauser and E. Schleyer (2004). "Pharmacokinetics and cellular uptake of imatinib and its main metabolite CGP74588." *Cancer Chemother Pharmacol* **53**(4): 313-23.

Lee, J. C., I. Vivanco, R. Beroukhim, J. H. Huang, W. L. Feng, R. M. DeBiasi, K. Yoshimoto, J. C. King, P. Nghiemphu, Y. Yuza, Q. Xu, H. Greulich, R. K. Thomas, J. G. Paez, T. C. Peck, D. J. Linhart, K. A. Glatt, G. Getz, R. Onofrio, L. Ziaugra, R. L. Levine, S. Gabriel, T. Kawaguchi, K. O'Neill, H. Khan, L. M. Liau, S. F. Nelson, P. N. Rao, P. Mischel, R. O. Pieper, T. Cloughesy, D. J. Leahy, W. R. Sellers, C. L. Sawyers, M. Meyerson and I. K. Mellinghoff (2006). "Epidermal growth factor receptor activation in glioblastoma through novel missense mutations in the extracellular domain." *PLoS Med* **3**(12): e485.

Lee, K. H., Y. L. Chen, S. D. Yeh, M. Hsiao, J. T. Lin, Y. G. Goan and P. J. Lu (2009). "MicroRNA-330 acts as tumor suppressor and induces apoptosis of prostate cancer cells through E2F1-mediated suppression of Akt phosphorylation." *Oncogene* **28**(38): 3360-70.

Lee, N. S., J. S. Kim, W. J. Cho, M. R. Lee, R. Steiner, A. Gompers, D. Ling, J. Zhang, P. Strom, M. Behlke, S. H. Moon, P. M. Salvaterra, R. Jove and K. S. Kim (2008). "miR-302b maintains "stemness" of human embryonal carcinoma cells by post-transcriptional regulation of Cyclin D2 expression." *Biochem Biophys Res Commun* **377**(2): 434-40.

Lee, Y., C. Ahn, J. Han, H. Choi, J. Kim, J. Yim, J. Lee, P. Provost, O. Radmark, S. Kim and V. N. Kim (2003). "The nuclear RNase III Drosha initiates microRNA processing." *Nature* **425**(6956): 415-9.

Lee, Y., K. Jeon, J. T. Lee, S. Kim and V. N. Kim (2002). "MicroRNA maturation: stepwise processing and subcellular localization." *Embo J* **21**(17): 4663-70.

Leslie, E. M., R. G. Deeley and S. P. Cole (2005). "Multidrug resistance proteins: role of P-glycoprotein, MRP1, MRP2, and BCRP (ABCG2) in tissue defense." *Toxicol Appl Pharmacol* **204**(3): 216-37.

Levav-Cohen, Y., Z. Goldberg, V. Zuckerman, T. Grossman, S. Haupt and Y. Haupt (2005). "C-Abl as a modulator of p53." *Biochem Biophys Res Commun* **331**(3): 737-49.

Lewis, B. P., C. B. Burge and D. P. Bartel (2005). "Conserved seed pairing, often flanked by adenosines, indicates that thousands of human genes are microRNA targets." *Cell* **120**(1): 15-20.

Lewis, B. P., I. H. Shih, M. W. Jones-Rhoades, D. P. Bartel and C. B. Burge (2003). "Prediction of mammalian microRNA targets." *Cell* **115**(7): 787-98.

Li, H., C. Bian, L. Liao, J. Li and R. C. Zhao (2010). "miR-17-5p promotes human breast cancer cell migration and invasion through suppression of HBP1." *Breast Cancer Res Treat* **epub ahead of print**.

Li, L. and T. Xie (2005). "Stem cell niche: structure and function." *Annu Rev Cell Dev Biol* **21**: 605-31.

Li, X. F., P. J. Yan and Z. M. Shao (2009). "Downregulation of miR-193b contributes to enhance urokinase-type plasminogen activator (uPA) expression and tumor progression and invasion in human breast cancer." *Oncogene* **28**(44): 3937-48.

Li, X. Y., L. Q. Zhang, X. G. Zhang, X. Li, Y. B. Ren, X. Y. Ma, X. G. Li and L. X. Wang (2010). "Association between AKT/mTOR signalling pathway and malignancy grade of human gliomas." *J Neurooncol* **epub ahead of print**.

Li, Y., F. Guessous, Y. Zhang, C. Dipierro, B. Kefas, E. Johnson, L. Marcinkiewicz, J. Jiang, Y. Yang, T. D. Schmittgen, B. Lopes, D. Schiff, B. Purow and R. Abounader (2009). "MicroRNA-34a inhibits glioblastoma growth by targeting multiple oncogenes." *Cancer Res* **69**(19): 7569-76.

Liang, J. J., H. Wang, A. Rashid, T. H. Tan, R. F. Hwang, S. R. Hamilton, J. L. Abbruzzese and D. B. Evans (2008). "Expression of MAP4K4 is associated with worse prognosis in patients with stage II pancreatic ductal adenocarcinoma." *Clin Cancer Res* **14**(21): 7043-9.

Lindroos, P. M., P. G. Coin, A. Badgett, D. L. Morgan and J. C. Bonner (1997). "Alveolar macrophages stimulated with titanium dioxide, chrysotile asbestos, and residual oil fly ash upregulate the PDGF receptor-alpha on lung fibroblasts through an IL-1beta-dependent mechanism." *Am J Respir Cell Mol Biol* **16**(3): 283-92.

Liu, I. M., S. H. Schilling, K. A. Knouse, L. Choy, R. Derynck and X. F. Wang (2009). "TGFbeta-stimulated Smad1/5 phosphorylation requires the ALK5 L45 loop and mediates the pro-migratory TGFbeta switch." *Embo J* **28**(2): 88-98.

Liu, W. H., S. H. Yeh, C. C. Lu, S. L. Yu, H. Y. Chen, C. Y. Lin, D. S. Chen and P. J. Chen (2009). "MicroRNA-18a prevents estrogen receptor-alpha expression, promoting proliferation of hepatocellular carcinoma cells." *Gastroenterology* **136**(2): 683-93.

Liu, X., Z. Chen, J. Yu, J. Xia and X. Zhou (2009). "MicroRNA Profiling and Head and Neck Cancer." *Comp Funct Genomics*: 837514.

Liu, Z. J., M. Xiao, K. Balint, A. Soma, C. C. Pinnix, A. J. Capobianco, O. C. Velazquez and M. Herlyn (2006). "Inhibition of endothelial cell proliferation

by Notch1 signaling is mediated by repressing MAPK and PI3K/Akt pathways and requires MAML1." *Faseb J* **20**(7): 1009-11.

Livak, K. J., S. J. Flood, J. Marmaro, W. Giusti and K. Deetz (1995). "Oligonucleotides with fluorescent dyes at opposite ends provide a quenched probe system useful for detecting PCR product and nucleic acid hybridization." *PCR Methods Appl* **4**(6): 357-62.

Lokker, N. A., C. M. Sullivan, S. J. Hollenbach, M. A. Israel and N. A. Giese (2002). "Platelet-derived growth factor (PDGF) autocrine signaling regulates survival and mitogenic pathways in glioblastoma cells: evidence that the novel PDGF-C and PDGF-D ligands may play a role in the development of brain tumors." *Cancer Res* **62**(13): 3729-35.

Lomo, L., M. R. Nucci, K. R. Lee, M. C. Lin, M. S. Hirsch, C. P. Crum and G. L. Mutter (2008). "Histologic and immunohistochemical decision-making in endometrial adenocarcinoma." *Mod Pathol* **21**(8): 937-42.

Lorenzi, P. L., W. C. Reinhold, S. Varma, A. A. Hutchinson, Y. Pommier, S. J. Chanock and J. N. Weinstein (2009). "DNA fingerprinting of the NCI-60 cell line panel." *Mol Cancer Ther* **8**(4): 713-24.

Lund, E., S. Guttinger, A. Calado, J. E. Dahlberg and U. Kutay (2004). "Nuclear export of microRNA precursors." *Science* **303**(5654): 95-8.

Luo, H., H. Zhang, Z. Zhang, X. Zhang, B. Ning, J. Guo, N. Nie, B. Liu and X. Wu (2009). "Down-regulated miR-9 and miR-433 in human gastric carcinoma." *J Exp Clin Cancer Res* **28**: 82.

Lupo, V., M. I. Galindo, D. Martinez-Rubio, T. Sevilla, J. J. Vilchez, F. Palau and C. Espinos (2009). "Missense mutations in the SH3TC2 protein causing Charcot-Marie-Tooth disease type 4C affect its localization in the plasma membrane and endocytic pathway." *Hum Mol Genet* **18**(23): 4603-14.

Ma, J., M. Murphy, P. J. O'Dwyer, E. Berman, K. Reed and J. M. Gallo (2002). "Biochemical changes associated with a multidrug-resistant phenotype of a human glioma cell line with temozolomide-acquired resistance." *Biochem Pharmacol* **63**(7): 1219-28.

Mack, P. C., W. S. Holland, R. A. Burich, R. Sangha, L. J. Solis, Y. Li, L. A. Beckett, P. N. Lara, Jr., A. M. Davies and D. R. Gandara (2009). "EGFR mutations detected in plasma are associated with patient outcomes in erlotinib plus docetaxel-treated non-small cell lung cancer." *J Thorac Oncol* **4**(12): 1466-72.

Maher, E. A., F. B. Furnari, R. M. Bachoo, D. H. Rowitch, D. N. Louis, W. K. Cavenee and R. A. DePinho (2001). "Malignant glioma: genetics and biology of a grave matter." *Genes Dev* **15**(11): 1311-33.

Mahesparan, R., B. B. Tysnes, T. A. Read, P. O. Enger, R. Bjerkvig and M. Lund-Johansen (1999). "Extracellular matrix-induced cell migration from glioblastoma biopsy specimens in vitro." *Acta Neuropathol* **97**(3): 231-9.

Malzkorn, B., M. Wolter, F. Liesenberg, M. Grzendowski, K. Stuhler, H. E. Meyer and G. Reifenberger (2010). "Identification and functional characterization of microRNAs involved in the malignant progression of gliomas." *Brain Pathol* **20**(3): 539-50.

Marie, Y., A. F. Carpentier, A. M. Omuro, M. Sanson, J. Thillet, K. Hoang-Xuan and J. Y. Delattre (2005). "EGFR tyrosine kinase domain mutations in human gliomas." *Neurology* **64**(8): 1444-5.

Marroni, M., N. Marchi, L. Cucullo, N. J. Abbott, K. Signorelli and D. Janigro (2003). "Vascular and parenchymal mechanisms in multiple drug resistance: a lesson from human epilepsy." *Curr Drug Targets* **4**(4): 297-304.

Martinho, O., A. Longatto-Filho, M. B. Lambros, A. Martins, C. Pinheiro, A. Silva, F. Pardal, J. Amorim, A. Mackay, F. Milanezi, N. Tamber, K. Fenwick, A. Ashworth, J. S. Reis-Filho, J. M. Lopes and R. M. Reis (2009). "Expression, mutation and copy number analysis of platelet-derived growth factor receptor A (PDGFRA) and its ligand PDGFA in gliomas." *Br J Cancer* **101**(6): 973-82.

McDaneld, T. G., T. P. Smith, M. E. Doumit, J. R. Miles, L. L. Coutinho, T. S. Sonstegard, L. K. Matukumalli, D. J. Nonneman and R. T. Wiedmann (2009). "MicroRNA transcriptome profiles during swine skeletal muscle development." *BMC Genomics* **10**: 77.

Medina, R., S. K. Zaidi, C. G. Liu, J. L. Stein, A. J. van Wijnen, C. M. Croce and G. S. Stein (2008). "MicroRNAs 221 and 222 bypass quiescence and compromise cell survival." *Cancer Res* **68**(8): 2773-80.

Mellinghoff, I. K., M. Y. Wang, I. Vivanco, D. A. Haas-Kogan, S. Zhu, E. Q. Dia, K. V. Lu, K. Yoshimoto, J. H. Huang, D. J. Chute, B. L. Riggs, S. Horvath, L. M. Liau, W. K. Cavenee, P. N. Rao, R. Beroukhim, T. C. Peck, J. C. Lee, W. R. Sellers, D. Stokoe, M. Prados, T. F. Cloughesy, C. L. Sawyers and P. S. Mischel (2005). "Molecular determinants of the response of glioblastomas to EGFR kinase inhibitors." *N Engl J Med* **353**(19): 2012-24.

Miele, L. and B. Osborne (1999). "Arbiter of differentiation and death: Notch signaling meets apoptosis." *J Cell Physiol* **181**(3): 393-409.

Milano, V., Y. Piao, T. LaFortune and J. de Groot (2009). "Dasatinib-induced autophagy is enhanced in combination with temozolomide in glioma." *Mol Cancer Ther* **8**(2): 394-406.

Molina, J. R., Y. Hayashi, C. Stephens and M. M. Georgescu (2010). "Invasive glioblastoma cells acquire stemness and increased Akt activation." *Neoplasia* **12**(6): 453-63.

Mondy, J. S., V. Lindner, J. K. Miyashiro, B. C. Berk, R. H. Dean and R. L. Geary (1997). "Platelet-derived growth factor ligand and receptor expression in response to altered blood flow in vivo." *Circ Res* **81**(3): 320-7.

Mraz, M., K. Malinova, J. Kotaskova, S. Pavlova, B. Tichy, J. Malcikova, K. Stano Kozubik, J. Smardova, Y. Brychtova, M. Doubek, M. Trbusek, J. Mayer and S. Pospisilova (2009). "miR-34a, miR-29c and miR-17-5p are downregulated in CLL patients with TP53 abnormalities." *Leukemia* **23**(6): 1159-63.

Myer, M. S., G. Joone, M. R. Chasen and C. E. van Rensburg (1999). "The chemosensitizing potential of GF120918 is independent of the magnitude of P-glycoprotein-mediated resistance to conventional chemotherapeutic agents in a small cell lung cancer line." *Oncol Rep* **6**(1): 217-8.

Nagane, M., H. Lin, W. K. Cavenee and H. J. Huang (2001). "Aberrant receptor signaling in human malignant gliomas: mechanisms and therapeutic implications." *Cancer Lett* **162 Suppl**: S17-S21.

Nagar, B. (2007). "c-Abl tyrosine kinase and inhibition by the cancer drug imatinib (Gleevec/STI-571)." *J Nutr* **137**(6 Suppl 1): 1518S-1523S; discussion 1548S.

Nakagawa, T., K. Ido, T. Sakuma, H. Takeuchi, K. Sato and T. Kubota (2009). "Prognostic significance of the immunohistochemical expression of O6-methylguanine-DNA methyltransferase, P-glycoprotein, and multidrug resistance protein-1 in glioblastomas." *Neuropathology* **29**(4): 379-88.

Nakanishi, T., J. E. Karp, M. Tan, L. A. Doyle, T. Peters, W. Yang, D. Wei and D. D. Ross (2003). "Quantitative analysis of breast cancer resistance protein and cellular resistance to flavopiridol in acute leukemia patients." *Clin Cancer Res* **9**(9): 3320-8.

Nam, E. J., H. Yoon, S. W. Kim, H. Kim, Y. T. Kim, J. H. Kim, J. W. Kim and S. Kim (2008). "MicroRNA expression profiles in serous ovarian carcinoma." *Clin Cancer Res* **14**(9): 2690-5.

Narayana, A., J. G. Golfinos, I. Fischer, S. Raza, P. Kelly, E. Parker, E. A. Knopp, P. Medabalmi, D. Zagzag, P. Eagan and M. L. Gruber (2008). "Feasibility of using bevacizumab with radiation therapy and temozolomide in newly diagnosed high-grade glioma." *Int J Radiat Oncol Biol Phys* **72**(2): 383-9.

Narayana, A., P. Kelly, J. Golfinos, E. Parker, G. Johnson, E. Knopp, D. Zagzag, I. Fischer, S. Raza, P. Medabalmi, P. Eagan and M. L. Gruber (2009). "Antiangiogenic therapy using bevacizumab in recurrent high-grade glioma: impact on local control and patient survival." *J Neurosurg* **110**(1): 173-80.

Nelson, P., M. Kiriakidou, A. Sharma, E. Maniataki and Z. Mourelatos (2003). "The microRNA world: small is mighty." *Trends Biochem Sci* **28**(10): 534-40.

Neshat, M. S., I. K. Mellinghoff, C. Tran, B. Stiles, G. Thomas, R. Petersen, P. Frost, J. J. Gibbons, H. Wu and C. L. Sawyers (2001). "Enhanced sensitivity of PTEN-deficient tumors to inhibition of FRAP/mTOR." *Proc Natl Acad Sci U S A* **98**(18): 10314-9.

Newton, H. B. (2003). "Molecular neuro-oncology and development of targeted therapeutic strategies for brain tumors. Part 1: Growth factor and Ras signaling pathways." *Expert Rev Anticancer Ther* **3**(5): 595-614.

Newton, H. B. (2004). "Molecular neuro-oncology and the development of targeted therapeutic strategies for brain tumors. Part 3: brain tumor invasiveness." *Expert Rev Anticancer Ther* **4**(5): 803-21.

Ng, E. K., W. P. Tsang, S. S. Ng, H. C. Jin, J. Yu, J. J. Li, C. Rocken, M. P. Ebert, T. T. Kwok and J. J. Sung (2009). "MicroRNA-143 targets DNA methyltransferases 3A in colorectal cancer." *Br J Cancer* **101**(4): 699-706.

Nies, A. T. (2007). "The role of membrane transporters in drug delivery to brain tumors." *Cancer Lett* **254**(1): 11-29.

Nister, M., L. Claesson-Welsh, A. Eriksson, C. H. Heldin and B. Westermark (1991). "Differential expression of platelet-derived growth factor receptors in human malignant glioma cell lines." *J Biol Chem* **266**(25): 16755-63.

Nord, H., C. Hartmann, R. Andersson, U. Menzel, S. Pfeifer, A. Piotrowski, A. Bogdan, W. Kloc, J. Sandgren, T. Olofsson, G. Hesselager, E. Blomquist, J.

Komorowski, A. von Deimling, C. E. Bruder, J. P. Dumanski and T. Diaz de Stahl (2009). "Characterization of novel and complex genomic aberrations in glioblastoma using a 32K BAC array." *Neuro Oncol* **11**(6): 803-18.

Norden, A. D., J. Drappatz and P. Y. Wen (2008). "Antiangiogenic therapy in malignant gliomas." *Curr Opin Oncol* **20**(6): 652-61.

Ogiso, H., R. Ishitani, O. Nureki, S. Fukai, M. Yamanaka, J. H. Kim, K. Saito, A. Sakamoto, M. Inoue, M. Shirouzu and S. Yokoyama (2002). "Crystal structure of the complex of human epidermal growth factor and receptor extracellular domains." *Cell* **110**(6): 775-87.

Ohno, M., A. Natsume, Y. Kondo, H. Iwamizu, K. Motomura, H. Toda, M. Ito, T. Kato and T. Wakabayashi (2009). "The modulation of MicroRNAs by type I IFN through the activation of signal transducers and activators of transcription 3 in human glioma." *Mol Cancer Res* **7**(12): 2022-30.

Omuro, A. M., S. Faivre and E. Raymond (2007). "Lessons learned in the development of targeted therapy for malignant gliomas." *Mol Cancer Ther* **6**(7): 1909-19.

Ostermann, S., C. Csajka, T. Buclin, S. Leyvraz, F. Lejeune, L. A. Decosterd and R. Stupp (2004). "Plasma and cerebrospinal fluid population pharmacokinetics of temozolomide in malignant glioma patients." *Clin Cancer Res* **10**(11): 3728-36.

Ozen, M., C. J. Creighton, M. Ozdemir and M. Ittmann (2008). "Widespread deregulation of microRNA expression in human prostate cancer." *Oncogene* **27**(12): 1788-93.

Paez, J. G., P. A. Janne, J. C. Lee, S. Tracy, H. Greulich, S. Gabriel, P. Herman, F. J. Kaye, N. Lindeman, T. J. Boggon, K. Naoki, H. Sasaki, Y. Fujii, M. J. Eck, W. R. Sellers, B. E. Johnson and M. Meyerson (2004). "EGFR mutations in lung cancer: correlation with clinical response to gefitinib therapy." *Science* **304**(5676): 1497-500.

Pan E, P. M. (2004). "Translational research in neuro-oncology." *In: Perry MC, ed. Educational Book of the 40th Annual American Society of Clinical Oncology Meeting*.

Pao, W. and V. A. Miller (2005). "Epidermal growth factor receptor mutations, small-molecule kinase inhibitors, and non-small-cell lung cancer: current knowledge and future directions." *J Clin Oncol* **23**(11): 2556-68.

Papagiannakopoulos, T., A. Shapiro and K. S. Kosik (2008). "MicroRNA-21 targets a network of key tumor-suppressive pathways in glioblastoma cells." *Cancer Res* **68**(19): 8164-72.

Parmacek, M. S. (2009). "MicroRNA-modulated targeting of vascular smooth muscle cells." *J Clin Invest* **119**(9): 2526-8.

Pasquinelli, A. E., B. J. Reinhart, F. Slack, M. Q. Martindale, M. I. Kuroda, B. Maller, D. C. Hayward, E. E. Ball, B. Degnan, P. Muller, J. Spring, A. Srinivasan, M. Fishman, J. Finnerty, J. Corbo, M. Levine, P. Leahy, E. Davidson and G. Ruvkun (2000). "Conservation of the sequence and temporal expression of let-7 heterochronic regulatory RNA." *Nature* **408**(6808): 86-9.

Paul Kleihues, W. K. C. (1997). Pathology and Genetics of tumours of the Nervous System. Lyon, International Agency for Research on Cancer, 150 Cours Albert Thomas, 69372 Lyon, France.

Pelloski, C. E., E. Lin, L. Zhang, W. K. Yung, H. Colman, J. L. Liu, S. Y. Woo, A. B. Heimberger, D. Suki, M. Prados, S. Chang, F. G. Barker, 3rd, G. N. Fuller and K. D. Aldape (2006). "Prognostic associations of activated mitogen-activated protein kinase and Akt pathways in glioblastoma." *Clin Cancer Res* **12**(13): 3935-41.

Perry, J. R., K. Belanger, W. P. Mason, D. Fulton, P. Kavan, J. Easaw, C. Shields, S. Kirby, D. R. Macdonald, D. D. Eisenstat, B. Thiessen, P. Forsyth and J. F. Pouliot (2010). "Phase II trial of continuous dose-intense temozolomide in recurrent malignant glioma: RESCUE study." *J Clin Oncol* **28**(12): 2051-7.

Petrocca, F., R. Visone, M. R. Onelli, M. H. Shah, M. S. Nicoloso, I. de Martino, D. Iliopoulos, E. Pilozzi, C. G. Liu, M. Negrini, L. Cavazzini, S. Volinia, H. Alder, L. P. Ruco, G. Baldassarre, C. M. Croce and A. Vecchione (2008). "E2F1-regulated microRNAs impair TGFbeta-dependent cell-cycle arrest and apoptosis in gastric cancer." *Cancer Cell* **13**(3): 272-86.

Pike, B. L., T. C. Greiner, X. Wang, D. D. Weisenburger, Y. H. Hsu, G. Renaud, T. G. Wolfsberg, M. Kim, D. J. Weisenberger, K. D. Siegmund, W. Ye, S. Groshen, R. Mehrian-Shai, J. Delabie, W. C. Chan, P. W. Laird and J. G. Hacia (2008). "DNA methylation profiles in diffuse large B-cell lymphoma and their relationship to gene expression status." *Leukemia* **22**(5): 1035-43.

Pinzani, M., S. Milani, H. Herbst, R. DeFranco, C. Grappone, A. Gentilini, A. Caligiuri, G. Pellegrini, D. V. Ngo, R. G. Romanelli and P. Gentilini (1996). "Expression of platelet-derived growth factor and its receptors in normal human liver and during active hepatic fibrogenesis." *Am J Pathol* **148**(3): 785-800.

Pitman, M., B. Emery, M. Binder, S. Wang, H. Butzkueven and T. J. Kilpatrick (2004). "LIF receptor signaling modulates neural stem cell renewal." *Mol Cell Neurosci* **27**(3): 255-66.

Piva, R., P. Cavalla, S. Bortolotto, S. Cordera, P. Richiardi and D. Schiffer (1997). "p27/kip1 expression in human astrocytic gliomas." *Neurosci Lett* **234**(2-3): 127-30.

Plosker, G. L. and M. Hurst (2001). "Paclitaxel: a pharmacoeconomic review of its use in non-small cell lung cancer." *Pharmacoeconomics* **19**(11): 1111-34.

Ponten, A., X. Li, P. Thoren, K. Aase, T. Sjoblom, A. Ostman and U. Eriksson (2003). "Transgenic overexpression of platelet-derived growth factor-C in the mouse heart induces cardiac fibrosis, hypertrophy, and dilated cardiomyopathy." *Am J Pathol* **163**(2): 673-82.

Prados, M. D., S. M. Chang, N. Butowski, R. DeBoer, R. Parvataneni, H. Carliner, P. Kabuubi, J. Ayers-Ringler, J. Rabbitt, M. Page, A. Fedoroff, P. K. Sneed, M. S. Berger, M. W. McDermott, A. T. Parsa, S. Vandenberg, C. D. James, K. R. Lamborn, D. Stokoe and D. A. Haas-Kogan (2009). "Phase II study of erlotinib plus temozolomide during and after radiation therapy in patients with newly diagnosed glioblastoma multiforme or gliosarcoma." *J Clin Oncol* **27**(4): 579-84.

Qin, Y., S. Chen, B. Jiang, Q. Jiang, H. Jiang, J. Li, L. Li, Y. Lai, Y. Liu and X. Huang (2010). "Characteristics of BCR-ABL kinase domain point mutations in Chinese imatinib-resistant chronic myeloid leukemia patients." *Ann Hematol* **Epub ahead of print**.

Rabi, T. and A. Bishayee (2009). "d -Limonene sensitizes docetaxel-induced cytotoxicity in human prostate cancer cells: Generation of reactive oxygen species and induction of apoptosis." *J Carcinog* **8**: 9.

Ragel, B. T., W. T. Couldwell, D. L. Gillespie, M. M. Wendland, K. Whang and R. L. Jensen (2008). "A comparison of the cell lines used in meningioma research." *Surg Neurol* **70**(3): 295-307; discussion 307.

Ramnarain, D. B., S. Park, D. Y. Lee, K. J. Hatanpaa, S. O. Scoggin, H. Otu, T. A. Libermann, J. M. Raisanen, R. Ashfaq, E. T. Wong, J. Wu, R. Elliott and A. A. Habib (2006). "Differential gene expression analysis reveals generation of an autocrine loop by a mutant epidermal growth factor receptor in glioma cells." *Cancer Res* **66**(2): 867-74.

Rauch, T., H. Li, X. Wu and G. P. Pfeifer (2006). "MIRA-assisted microarray analysis, a new technology for the determination of DNA methylation patterns, identifies frequent methylation of homeodomain-containing genes in lung cancer cells." *Cancer Res* **66**(16): 7939-47.

Raymond, E., A. A. Brandes, C. Dittrich, P. Fumoleau, B. Coudert, P. M. Clement, M. Frenay, R. Rampling, R. Stupp, J. M. Kros, M. C. Heinrich, T. Gorlia, D. Lacombe and M. J. van den Bent (2008). "Phase II study of imatinib in patients with recurrent gliomas of various histologies: a European Organisation for Research and Treatment of Cancer Brain Tumor Group Study." *J Clin Oncol* **26**(28): 4659-65.

Reinhart, B. J., F. J. Slack, M. Basson, A. E. Pasquinelli, J. C. Bettinger, A. E. Rougvie, H. R. Horvitz and G. Ruvkun (2000). "The 21-nucleotide let-7 RNA regulates developmental timing in Caenorhabditis elegans." *Nature* **403**(6772): 901-6.

Ren, H., X. Tan, Y. Dong, A. Giese, T. C. Chou, N. Rainov and B. Yang (2009). "Differential effect of imatinib and synergism of combination treatment with chemotherapeutic agents in malignant glioma cells." *Basic Clin Pharmacol Toxicol* **104**(3): 241-52.

Ridley, A. J., M. A. Schwartz, K. Burridge, R. A. Firtel, M. H. Ginsberg, G. Borisy, J. T. Parsons and A. R. Horwitz (2003). "Cell migration: integrating signals from front to back." *Science* **302**(5651): 1704-9.

Riemenschneider, M. J., R. A. Betensky, S. M. Pasedag and D. N. Louis (2006). "AKT activation in human glioblastomas enhances proliferation via TSC2 and S6 kinase signaling." *Cancer Res* **66**(11): 5618-23.

Risau, W., H. Drexler, V. Mironov, A. Smits, A. Siegbahn, K. Funa and C. H. Heldin (1992). "Platelet-derived growth factor is angiogenic in vivo." *Growth Factors* **7**(4): 261-6.

Rivera, A. L., C. E. Pelloski, M. R. Gilbert, H. Colman, C. De La Cruz, E. P. Sulman, B. N. Bekele and K. D. Aldape (2010). "MGMT promoter methylation is predictive of response to radiotherapy and prognostic in the

absence of adjuvant alkylating chemotherapy for glioblastoma." *Neuro Oncol* **12**(2): 116-21.

Rooprai, H. K., T. E. van Meter, S. D. Robinson, A. King, G. J. Rucklidge and G. J. Pilkington (2003). "Expression of MMP-2 and -9 in short-term cultures of meningioma: influence of histological subtype." *Int J Mol Med* **12**(6): 977-81.

Roth, W., C. Grimmel, L. Rieger, H. Strik, S. Takayama, S. Krajewski, R. Meyermann, J. Dichgans, J. C. Reed and M. Weller (2000). "Bag-1 and Bcl-2 gene transfer in malignant glioma: modulation of cell cycle regulation and apoptosis." *Brain Pathol* **10**(2): 223-34.

Rudek, M. A., R. C. Donehower, P. Statkevich, V. K. Batra, D. L. Cutler and S. D. Baker (2004). "Temozolomide in patients with advanced cancer: phase I and pharmacokinetic study." *Pharmacotherapy* **24**(1): 16-25.

Rxlist http://www.rxlist.com.

Salvi, A., C. Sabelli, S. Moncini, M. Venturin, B. Arici, P. Riva, N. Portolani, S. M. Giulini, G. De Petro and S. Barlati (2009). "MicroRNA-23b mediates urokinase and c-met downmodulation and a decreased migration of human hepatocellular carcinoma cells." *Febs J* **276**(11): 2966-82.

Sampath, P., L. D. Rhines, F. DiMeco, B. M. Tyler, M. C. Park and H. Brem (2006). "Interstitial docetaxel (Taxotere), carmustine and combined interstitial therapy: a novel treatment for experimental malignant glioma." *Journal of Neuro-Oncology* **80**(1): 9-17.

Sampson, J. H., G. Akabani, G. E. Archer, D. D. Bigner, M. S. Berger, A. H. Friedman, H. S. Friedman, J. E. Herndon, 2nd, S. Kunwar, S. Marcus, R. E. McLendon, A. Paolino, K. Penne, J. Provenzale, J. Quinn, D. A. Reardon, J. Rich, T. Stenzel, S. Tourt-Uhlig, C. Wikstrand, T. Wong, R. Williams, F. Yuan, M. R. Zalutsky and I. Pastan (2003). "Progress report of a Phase I study of the intracerebral microinfusion of a recombinant chimeric protein composed of transforming growth factor (TGF)-alpha and a mutated form of the Pseudomonas exotoxin termed PE-38 (TP-38) for the treatment of malignant brain tumors." *J Neurooncol* **65**(1): 27-35.

Sanger "www.microrna.sanger.ac.uk/sequences."

Sanson, M., M. Napolitano, R. Yaya, F. Keime-Guibert, P. Broet, K. Hoang-Xuan and J. Y. Delattre (2000). "Second line chemotherapy with docetaxel in patients with recurrent malignant glioma: a phase II study." *J Neurooncol* **50**(3): 245-9.

Sarkaria, J. N., L. Yang, P. T. Grogan, G. J. Kitange, B. L. Carlson, M. A. Schroeder, E. Galanis, C. Giannini, W. Wu, E. B. Dinca and C. D. James (2007). "Identification of molecular characteristics correlated with glioblastoma sensitivity to EGFR kinase inhibition through use of an intracranial xenograft test panel." *Mol Cancer Ther* **6**(3): 1167-74.

Sasayama, T., M. Nishihara, T. Kondoh, K. Hosoda and E. Kohmura (2009). "MicroRNA-10b is overexpressed in malignant glioma and associated with tumor invasive factors, uPAR and RhoC." *Int J Cancer* **125**(6): 1407-13.

Saxena, A., L. M. Shriml, M. Dean and I. U. Ali (1999). "Comparative molecular genetic profiles of anaplastic astrocytomas/glioblastomas multiforme and their subsequent recurrences." *Oncogene* **18**(6): 1385-90.

Schaich, M., L. Kestel, M. Pfirrmann, K. Robel, T. Illmer, M. Kramer, C. Dill, G. Ehninger, G. Schackert and D. Krex (2009). "A MDR1 (ABCB1) gene single nucleotide polymorphism predicts outcome of temozolomide treatment in glioblastoma patients." *Ann Oncol* **20**(1): 175-81.

Schlenska-Lange, A., H. Knupfer, T. J. Lange, W. Kiess and M. Knupfer (2008). "Cell proliferation and migration in glioblastoma multiforme cell lines are influenced by insulin-like growth factor I in vitro." *Anticancer Res* **28**(2A): 1055-60.

Schlessinger, J. (1993). "How Receptor Tyrosine Kinases Activate Ras." *Trends in Biochemical Sciences* **18**(8): 273-275.

Schlessinger, J. (2000). "Cell signaling by receptor tyrosine kinases." *Cell* **103**(2): 211-25.

Schmelzle, T. and M. N. Hall (2000). "TOR, a central controller of cell growth." *Cell* **103**(2): 253-62.

Schratt, G. M., F. Tuebing, E. A. Nigh, C. G. Kane, M. E. Sabatini, M. Kiebler and M. E. Greenberg (2006). "A brain-specific microRNA regulates dendritic spine development." *Nature* **439**(7074): 283-9.

Schwarz, D. S., G. Hutvagner, T. Du, Z. Xu, N. Aronin and P. D. Zamore (2003). "Asymmetry in the assembly of the RNAi enzyme complex." *Cell* **115**(2): 199-208.

Seeliger, H., M. Guba, A. Kleespies, K. W. Jauch and C. J. Bruns (2007). "Role of mTOR in solid tumor systems: a therapeutical target against primary tumor growth, metastases, and angiogenesis." *Cancer Metastasis Rev* **26**(3-4): 611-21.

Segura, M. F., D. Hanniford, S. Menendez, L. Reavie, X. Zou, S. Alvarez-Diaz, J. Zakrzewski, E. Blochin, A. Rose, D. Bogunovic, D. Polsky, J. Wei, P. Lee, I. Belitskaya-Levy, N. Bhardwaj, I. Osman and E. Hernando (2009). "Aberrant miR-182 expression promotes melanoma metastasis by repressing FOXO3 and microphthalmia-associated transcription factor." *Proc Natl Acad Sci U S A* **106**(6): 1814-9.

Semenza, G. L. (2003). "Targeting HIF-1 for cancer therapy." *Nat Rev Cancer* **3**(10): 721-32.

Servidei, T., A. Riccardi, M. Sanguinetti, C. Dominici and R. Riccardi (2006). "Increased sensitivity to the platelet-derived growth factor (PDGF) receptor inhibitor STI571 in chemoresistant glioma cells is associated with enhanced PDGF-BB-mediated signaling and STI571-induced Akt inactivation." *J Cell Physiol* **208**(1): 220-8.

Shaw, R. J. and L. C. Cantley (2006). "Ras, PI(3)K and mTOR signalling controls tumour cell growth." *Nature* **441**(7092): 424-30.

Sherbenou, D. W. and B. J. Druker (2007). "Applying the discovery of the Philadelphia chromosome." *J Clin Invest* **117**(8): 2067-74.

Sherbenou, D. W., O. Hantschel, I. Kaupe, S. Willis, T. Bumm, L. P. Turaga, T. Lange, K. H. Dao, R. D. Press, B. J. Druker, G. Superti-Furga and M. W.

Deininger (2010). "BCR-ABL SH3-SH2 domain mutations in chronic myeloid leukemia patients on imatinib." *Blood* **116**(17): 3278-85.

Shi, L., Z. Cheng, J. Zhang, R. Li, Y. You and Z. Fu (2008). "[The mechanism of apoptosis in human U87 glioma cells induced by miR-21 antisense oligonucleotide]." *Zhonghua Yi Xue Yi Chuan Xue Za Zhi* **25**(5): 497-501.

Shi, L., Z. Cheng, J. Zhang, R. Li, P. Zhao, Z. Fu and Y. You (2008). "hsa-mir-181a and hsa-mir-181b function as tumor suppressors in human glioma cells." *Brain Res* **1236**: 185-93.

Shingu, T., K. Fujiwara, O. Bogler, Y. Akiyama, K. Moritake, N. Shinojima, Y. Tamada, T. Yokoyama and S. Kondo (2009). "Inhibition of autophagy at a late stage enhances imatinib-induced cytotoxicity in human malignant glioma cells." *Int J Cancer* **124**(5): 1060-71.

Shinojima, N., K. Tada, S. Shiraishi, T. Kamiryo, M. Kochi, H. Nakamura, K. Makino, H. Saya, H. Hirano, J. Kuratsu, K. Oka, Y. Ishimaru and Y. Ushio (2003). "Prognostic value of epidermal growth factor receptor in patients with glioblastoma multiforme." *Cancer Res* **63**(20): 6962-70.

Shlens, J. (2009). A Tutorial on Principal Component Analysis**:** http://www.snl.salk.edu/~shlens/pca.pdf.

Shteper, P. J. and D. Ben-Yehuda (2001). "Molecular evolution of chronic myeloid leukaemia." *Semin Cancer Biol* **11**(4): 313-23.

Silber, J., D. A. Lim, C. Petritsch, A. I. Persson, A. K. Maunakea, M. Yu, S. R. Vandenberg, D. G. Ginzinger, C. D. James, J. F. Costello, G. Bergers, W. A. Weiss, A. Alvarez-Buylla and J. G. Hodgson (2008). "miR-124 and miR-137 inhibit proliferation of glioblastoma multiforme cells and induce differentiation of brain tumor stem cells." *BMC Med* **6**: 14.

Smalheiser, N. R. (2003). "EST analyses predict the existence of a population of chimeric microRNA precursor-mRNA transcripts expressed in normal human and mouse tissues." *Genome Biol* **4**(7): 403.

Smith, J. S., X. Y. Wang, J. Qian, S. M. Hosek, B. W. Scheithauer, R. B. Jenkins and C. D. James (2000). "Amplification of the platelet-derived growth factor receptor-A (PDGFRA) gene occurs in oligodendrogliomas with grade IV anaplastic features." *J Neuropathol Exp Neurol* **59**(6): 495-503.

Solomon, D. A., J. S. Kim, J. C. Cronin, Z. Sibenaller, T. Ryken, S. A. Rosenberg, H. Ressom, W. Jean, D. Bigner, H. Yan, Y. Samuels and T. Waldman (2008). "Mutational inactivation of PTPRD in glioblastoma multiforme and malignant melanoma." *Cancer Res* **68**(24): 10300-6.

Sordella, R., D. W. Bell, D. A. Haber and J. Settleman (2004). "Gefitinib-sensitizing EGFR mutations in lung cancer activate anti-apoptotic pathways." *Science* **305**(5687): 1163-7.

Spizzo, R., M. S. Nicoloso, L. Lupini, Y. Lu, J. Fogarty, S. Rossi, B. Zagatti, M. Fabbri, A. Veronese, X. Liu, R. Davuluri, C. M. Croce, G. Mills, M. Negrini and G. A. Calin (2009). "miR-145 participates with TP53 in a death-promoting regulatory loop and targets estrogen receptor-alpha in human breast cancer cells." *Cell Death Differ* **17**(2): 246-54.

Stanulla, M., K. Welte, M. R. Hadam and T. Pietsch (1995). "Coexpression of stem cell factor and its receptor c-Kit in human malignant glioma cell lines." *Acta Neuropathol* **89**(2): 158-65.

Stokvis, E., H. Rosing, R. C. Causon, J. H. Schellens and J. H. Beijnen (2004). "Quantitative analysis of the P-glycoprotein inhibitor Elacridar (GF120918) in human and dog plasma using liquid chromatography with tandem mass spectrometric detection." *J Mass Spectrom* **39**(10): 1122-30.

Stupp, R., P. Y. Dietrich, S. Ostermann Kraljevic, A. Pica, I. Maillard, P. Maeder, R. Meuli, R. Janzer, G. Pizzolato, R. Miralbell, F. Porchet, L. Regli, N. de Tribolet, R. O. Mirimanoff and S. Leyvraz (2002). "Promising survival for patients with newly diagnosed glioblastoma multiforme treated with concomitant radiation plus temozolomide followed by adjuvant temozolomide." *J Clin Oncol* **20**(5): 1375-82.

Stupp, R., M. E. Hegi, B. Neyns, R. Goldbrunner, U. Schlegel, P. M. Clement, G. G. Grabenbauer, A. F. Ochsenbein, M. Simon, P. Y. Dietrich, T. Pietsch, C. Hicking, J. C. Tonn, A. C. Diserens, A. Pica, M. Hermisson, S. Krueger, M. Picard and M. Weller (2010). "Phase I/IIa study of cilengitide and temozolomide with concomitant radiotherapy followed by cilengitide and temozolomide maintenance therapy in patients with newly diagnosed glioblastoma." *J Clin Oncol* **28**(16): 2712-8.

Stupp, R., W. P. Mason, M. J. van den Bent, M. Weller, B. Fisher, M. J. Taphoorn, K. Belanger, A. A. Brandes, C. Marosi, U. Bogdahn, J. Curschmann, R. C. Janzer, S. K. Ludwin, T. Gorlia, A. Allgeier, D. Lacombe, J. G. Cairncross, E. Eisenhauer and R. O. Mirimanoff (2005). "Radiotherapy plus concomitant and adjuvant temozolomide for glioblastoma." *N Engl J Med* **352**(10): 987-96.

Sun, J., S. L. Zheng, F. Wiklund, S. D. Isaacs, G. Li, K. E. Wiley, S. T. Kim, Y. Zhu, Z. Zhang, F. C. Hsu, A. R. Turner, P. Stattin, W. Liu, J. W. Kim, D. Duggan, J. Carpten, W. Isaacs, H. Gronberg, J. Xu and B. L. Chang (2009). "Sequence variants at 22q13 are associated with prostate cancer risk." *Cancer Res* **69**(1): 10-5.

Sun, L., A. M. Hui, Q. Su, A. Vortmeyer, Y. Kotliarov, S. Pastorino, A. Passaniti, J. Menon, J. Walling, R. Bailey, M. Rosenblum, T. Mikkelsen and H. A. Fine (2006). "Neuronal and glioma-derived stem cell factor induces angiogenesis within the brain." *Cancer Cell* **9**(4): 287-300.

Swaisland, H. C., R. P. Smith, A. Laight, D. J. Kerr, M. Ranson, C. H. Wilder-Smith and T. Duvauchelle (2005). "Single-dose clinical pharmacokinetic studies of gefitinib." *Clin Pharmacokinet* **44**(11): 1165-77.

Takano, S., T. Yamashita and O. Ohneda (2010). "Molecular therapeutic targets for glioma angiogenesis." *J Oncol*: 351908.

Tang, X., L. Wang, C. G. Proud and C. P. Downes (2003). "Muscarinic receptor-mediated activation of p70 S6 kinase 1 (S6K1) in 1321N1 astrocytoma cells: permissive role of phosphoinositide 3-kinase." *Biochem J* **374**(Pt 1): 137-43.

Torp, S. H., E. Helseth, A. Dalen and G. Unsgaard (1991). "Epidermal growth factor receptor expression in human gliomas." *Cancer Immunol Immunother* **33**(1): 61-4.

Toth, K., M. M. Vaughan, N. S. Peress, H. K. Slocum and Y. M. Rustum (1996). "MDR1 P-glycoprotein is expressed by endothelial cells of newly formed capillaries in human gliomas but is not expressed in the neovasculature of other primary tumors." *Am J Pathol* **149**(3): 853-8.

Toyofuku, T., H. Zhang, A. Kumanogoh, N. Takegahara, F. Suto, J. Kamei, K. Aoki, M. Yabuki, M. Hori, H. Fujisawa and H. Kikutani (2004). "Dual roles of Sema6D in cardiac morphogenesis through region-specific association of its receptor, Plexin-A1, with off-track and vascular endothelial growth factor receptor type 2." *Genes Dev* **18**(4): 435-47.

Tryndyak, V. P., S. A. Ross, F. A. Beland and I. P. Pogribny (2009). "Down-regulation of the microRNAs miR-34a, miR-127, and miR-200b in rat liver during hepatocarcinogenesis induced by a methyl-deficient diet." *Mol Carcinog* **48**(6): 479-87.

Tsuda, H., H. Jafar-Nejad, A. J. Patel, Y. Sun, H. K. Chen, M. F. Rose, K. J. Venken, J. Botas, H. T. Orr, H. J. Bellen and H. Y. Zoghbi (2005). "The AXH domain of Ataxin-1 mediates neurodegeneration through its interaction with Gfi-1/Senseless proteins." *Cell* **122**(4): 633-44.

Tyagi, D., B. S. Sharma, S. K. Gupta, D. Kaul, R. K. Vasishta and V. K. Khosla (2002). "Expression of Bcl2 proto-oncogene in primary tumors of the central nervous system." *Neurol India* **50**(3): 290-4.

Ulasov, I. V., S. Nandi, M. Dey, A. M. Sonabend and M. S. Lesniak (2010). "Inhibition of Sonic hedgehog and Notch pathways enhances sensitivity of CD133(+) glioma stem cells to temozolomide therapy." *Mol Med* **Epub ahead of print**.

Valera, E. T., A. K. Lucio-Eterovic, L. Neder, C. A. Scrideli, H. R. Machado, C. G. Carlotti-Junior, R. G. Queiroz, F. J. Motta and L. G. Tone (2007). "Quantitative PCR analysis of the expression profile of genes related to multiple drug resistance in tumors of the central nervous system." *J Neurooncol* **85**(1): 1-10.

van den Bent, M. J., A. A. Brandes, R. Rampling, M. C. Kouwenhoven, J. M. Kros, A. F. Carpentier, P. M. Clement, M. Frenay, M. Campone, J. F. Baurain, J. P. Armand, M. J. Taphoorn, A. Tosoni, H. Kletzl, B. Klughammer, D. Lacombe and T. Gorlia (2009). "Randomized phase II trial of erlotinib versus temozolomide or carmustine in recurrent glioblastoma: EORTC brain tumor group study 26034." *J Clin Oncol* **27**(8): 1268-74.

van den Heuvel-Eibrink, M. M., B. van der Holt, A. K. Burnett, W. U. Knauf, M. F. Fey, G. E. Verhoef, E. Vellenga, G. J. Ossenkoppele, B. Lowenberg and P. Sonneveld (2007). "CD34-related coexpression of MDR1 and BCRP indicates a clinically resistant phenotype in patients with acute myeloid leukemia (AML) of older age." *Ann Hematol* **86**(5): 329-37.

Van Meir EG, H. C., Norden AD, Shu HK, Wen PY, Olson JJ. (2010). "Exciting new advances in neuro-oncology: the avenue to a cure for malignant glioma." *CA Cancer J Clin.* **60**(3): 166-93.

Van Meter, T. E., W. C. Broaddus, H. K. Rooprai, G. J. Pilkington and H. L. Fillmore (2004). "Induction of membrane-type-1 matrix metalloproteinase by

epidermal growth factor-mediated signaling in gliomas." *Neuro Oncol* **6**(3): 188-99.

Vanhoutteghem, A. and P. Djian (2007). "The human basonuclin 2 gene has the potential to generate nearly 90,000 mRNA isoforms encoding over 2000 different proteins." *Genomics* **89**(1): 44-58.

Veeriah, S., C. Brennan, S. Meng, B. Singh, J. A. Fagin, D. B. Solit, P. B. Paty, D. Rohle, I. Vivanco, J. Chmielecki, W. Pao, M. Ladanyi, W. L. Gerald, L. Liau, T. C. Cloughesy, P. S. Mischel, C. Sander, B. Taylor, N. Schultz, J. Major, A. Heguy, F. Fang, I. K. Mellinghoff and T. A. Chan (2009). "The tyrosine phosphatase PTPRD is a tumor suppressor that is frequently inactivated and mutated in glioblastoma and other human cancers." *Proc Natl Acad Sci U S A* **106**(23): 9435-40.

Virtua trials www.virtualtrials.com.

Vollmann, A., H. P. Vornlocher, T. Stempfl, G. Brockhoff, R. Apfel and U. Bogdahn (2006). "Effective silencing of EGFR with RNAi demonstrates non-EGFR dependent proliferation of glioma cells." *Int J Oncol* **28**(6): 1531-42.

Wagenknecht, B., T. Glaser, U. Naumann, S. Kugler, S. Isenmann, M. Bahr, R. Korneluk, P. Liston and M. Weller (1999). "Expression and biological activity of X-linked inhibitor of apoptosis (XIAP) in human malignant glioma." *Cell Death Differ* **6**(4): 370-6.

Wang, J., X. Wang, S. Jiang, P. Lin, J. Zhang, Y. Wu, Z. Xiong, J. J. Ren and H. Yang (2008). "Partial biological characterization of cancer stem-like cell line (WJ(2)) of human glioblastoma multiforme." *Cell Mol Neurobiol* **28**(7): 991-1003.

Wang, X., S. Tang, S. Y. Le, R. Lu, J. S. Rader, C. Meyers and Z. M. Zheng (2008). "Aberrant expression of oncogenic and tumor-suppressive microRNAs in cervical cancer is required for cancer cell growth." *PLoS One* **3**(7): e2557.

Weiss, F. U., I. J. Marques, J. M. Woltering, D. H. Vlecken, A. Aghdassi, L. I. Partecke, C. D. Heidecke, M. M. Lerch and C. P. Bagowski (2009). "Retinoic acid receptor antagonists inhibit miR-10a expression and block metastatic behavior of pancreatic cancer." *Gastroenterology* **137**(6): 2136-45 e1-7.

Wen, P. Y., W. K. Yung, K. R. Lamborn, P. L. Dahia, Y. Wang, B. Peng, L. E. Abrey, J. Raizer, T. F. Cloughesy, K. Fink, M. Gilbert, S. Chang, L. Junck, D. Schiff, F. Lieberman, H. A. Fine, M. Mehta, H. I. Robins, L. M. DeAngelis, M. D. Groves, V. K. Puduvalli, V. Levin, C. Conrad, E. A. Maher, K. Aldape, M. Hayes, L. Letvak, M. J. Egorin, R. Capdeville, R. Kaplan, A. J. Murgo, C. Stiles and M. D. Prados (2006). "Phase I/II study of imatinib mesylate for recurrent malignant gliomas: North American Brain Tumor Consortium Study 99-08." *Clin Cancer Res* **12**(16): 4899-907.

Westermark, B., C. H. Heldin and M. Nister (1995). "Platelet-derived growth factor in human glioma." *Glia* **15**(3): 257-63.

Wilcox, J. N., K. M. Smith, L. T. Williams, S. M. Schwartz and D. Gordon (1988). "Platelet-derived growth factor mRNA detection in human atherosclerotic plaques by in situ hybridization." *J Clin Invest* **82**(3): 1134-43.

Wong, A. J., S. H. Bigner, D. D. Bigner, K. W. Kinzler, S. R. Hamilton and B. Vogelstein (1987). "Increased expression of the epidermal growth factor receptor gene in malignant gliomas is invariably associated with gene amplification." *Proc Natl Acad Sci U S A* **84**(19): 6899-903.

Wong, M. L., A. H. Kaye and C. M. Hovens (2007). "Targeting malignant glioma survival signalling to improve clinical outcomes." *J Clin Neurosci* **14**(4): 301-8.

Wong, S. and O. N. Witte (2004). "The BCR-ABL story: bench to bedside and back." *Annu Rev Immunol* **22**: 247-306.

Woods, S. A., E. Marmor, M. Feldkamp, N. Lau, A. J. Apicelli, G. Boss, D. H. Gutmann and A. Guha (2002). "Aberrant G protein signaling in nervous system tumors." *J Neurosurg* **97**(3): 627-42.

Wu, X., K. Senechal, M. S. Neshat, Y. E. Whang and C. L. Sawyers (1998). "The PTEN/MMAC1 tumor suppressor phosphatase functions as a negative regulator of the phosphoinositide 3-kinase/Akt pathway." *Proc Natl Acad Sci U S A* **95**(26): 15587-91.

Wurdinger, T., B. A. Tannous, O. Saydam, J. Skog, S. Grau, J. Soutschek, R. Weissleder, X. O. Breakefield and A. M. Krichevsky (2008). "miR-296 regulates growth factor receptor overexpression in angiogenic endothelial cells." *Cancer Cell* **14**(5): 382-93.

Xia, H., Y. Qi, S. S. Ng, X. Chen, S. Chen, M. Fang, D. Li, Y. Zhao, R. Ge, G. Li, Y. Chen, M. L. He, H. F. Kung, L. Lai and M. C. Lin (2009). "MicroRNA-15b regulates cell cycle progression by targeting cyclins in glioma cells." *Biochem Biophys Res Commun* **380**(2): 205-10.

Xia, H., Y. Qi, S. S. Ng, X. Chen, D. Li, S. Chen, R. Ge, S. Jiang, G. Li, Y. Chen, M. L. He, H. F. Kung, L. Lai and M. C. Lin (2009). "microRNA-146b inhibits glioma cell migration and invasion by targeting MMPs." *Brain Res* **1269**: 158-65.

Xia, H. F., T. Z. He, C. M. Liu, Y. Cui, P. P. Song, X. H. Jin and X. Ma (2009). "MiR-125b expression affects the proliferation and apoptosis of human glioma cells by targeting Bmf." *Cell Physiol Biochem* **23**(4-6): 347-58.

Xie, D., D. Yin, H. J. Wang, G. T. Liu, R. Elashoff, K. Black and H. P. Koeffler (2004). "Levels of expression of CYR61 and CTGF are prognostic for tumor progression and survival of individuals with gliomas." *Clin Cancer Res* **10**(6): 2072-81.

Yamada, H., K. Yanagisawa, S. Tokumaru, A. Taguchi, Y. Nimura, H. Osada, M. Nagino and T. Takahashi (2008). "Detailed characterization of a homozygously deleted region corresponding to a candidate tumor suppressor locus at 21q11-21 in human lung cancer." *Genes Chromosomes Cancer* **47**(9): 810-8.

Yamamoto, N., A. Horiike, Y. Fujisaka, H. Murakami, T. Shimoyama, Y. Yamada and T. Tamura (2008). "Phase I dose-finding and pharmacokinetic study of the oral epidermal growth factor receptor tyrosine kinase inhibitor Ro50-8231 (erlotinib) in Japanese patients with solid tumors." *Cancer Chemother Pharmacol* **61**(3): 489-96.

Yan, L. X., X. F. Huang, Q. Shao, M. Y. Huang, L. Deng, Q. L. Wu, Y. X. Zeng and J. Y. Shao (2008). "MicroRNA miR-21 overexpression in human breast cancer is associated with advanced clinical stage, lymph node metastasis and patient poor prognosis." *Rna* **14**(11): 2348-60.

Yeung, M. L., J. Yasunaga, Y. Bennasser, N. Dusetti, D. Harris, N. Ahmad, M. Matsuoka and K. T. Jeang (2008). "Roles for microRNAs, miR-93 and miR-130b, and tumor protein 53-induced nuclear protein 1 tumor suppressor in cell growth dysregulation by human T-cell lymphotrophic virus 1." *Cancer Res* **68**(21): 8976-85.

Yi, R., Y. Qin, I. G. Macara and B. R. Cullen (2003). "Exportin-5 mediates the nuclear export of pre-microRNAs and short hairpin RNAs." *Genes Dev* **17**(24): 3011-6.

Yoh, K., G. Ishii, T. Yokose, Y. Minegishi, K. Tsuta, K. Goto, Y. Nishiwaki, T. Kodama, M. Suga and A. Ochiai (2004). "Breast cancer resistance protein impacts clinical outcome in platinum-based chemotherapy for advanced non-small cell lung cancer." *Clin Cancer Res* **10**(5): 1691-7.

Zandi, R., A. B. Larsen, P. Andersen, M. T. Stockhausen and H. S. Poulsen (2007). "Mechanisms for oncogenic activation of the epidermal growth factor receptor." *Cell Signal* **19**(10): 2013-23.

Zerbe, L. K., L. D. Dwyer-Nield, J. M. Fritz, E. F. Redente, R. J. Shroyer, E. Conklin, S. Kane, C. Tucker, S. G. Eckhardt, D. L. Gustafson, K. K. Iwata and A. M. Malkinson (2008). "Inhibition by erlotinib of primary lung adenocarcinoma at an early stage in male mice." *Cancer Chemother Pharmacol* **62**(4): 605-20.

Zhang, C., C. Kang, Y. You, P. Pu, W. Yang, P. Zhao, G. Wang, A. Zhang, Z. Jia, L. Han and H. Jiang (2009). "Co-suppression of miR-221/222 cluster suppresses human glioma cell growth by targeting p27kip1 in vitro and in vivo." *Int J Oncol* **34**(6): 1653-60.

Zhang, C. Z., C. S. Kang, P. Y. Pu, G. X. Wang, Z. F. Jia, A. L. Zhang, L. Han and P. Xu (2009). "[Inhibitory effect of knocking down microRNA-221 and microRNA-222 on glioma cell growth in vitro and in vivo]." *Zhonghua Zhong Liu Za Zhi* **31**(10): 721-6.

Zhang, X., S. Liu, T. Hu, Y. He and S. Sun (2009). "Up-regulated microRNA-143 transcribed by nuclear factor kappa B enhances hepatocarcinoma metastasis by repressing fibronectin expression." *Hepatology* **50**(2): 490-9.

Zhang, Y., T. Chao, R. Li, W. Liu, Y. Chen, X. Yan, Y. Gong, B. Yin, B. Qiang, J. Zhao, J. Yuan and X. Peng (2009). "MicroRNA-128 inhibits glioma cells proliferation by targeting transcription factor E2F3a." *J Mol Med* **87**(1): 43-51.

Zhou, X., Y. Ren, L. Moore, M. Mei, Y. You, P. Xu, B. Wang, G. Wang, Z. Jia, P. Pu, W. Zhang and C. Kang (2010) "Downregulation of miR-21 inhibits EGFR pathway and suppresses the growth of human glioblastoma cells independent of PTEN status." *Lab Invest* **90**(2): 144-55.

Zhu, S., M. L. Si, H. Wu and Y. Y. Mo (2007). "MicroRNA-21 targets the tumor suppressor gene tropomyosin 1 (TPM1)." *J Biol Chem* **282**(19): 14328-36.

Zhuo, Y., J. Zhang, M. Laboy and J. A. Lasky (2004). "Modulation of PDGF-C and PDGF-D expression during bleomycin-induced lung fibrosis." *Am J Physiol Lung Cell Mol Physiol* **286**(1): L182-8.

Ziegler, D. S., R. D. Wright, S. Kesari, M. E. Lemieux, M. A. Tran, M. Jain, L. Zawel and A. L. Kung (2008). "Resistance of human glioblastoma multiforme cells to growth factor inhibitors is overcome by blockade of inhibitor of apoptosis proteins." *J Clin Invest* **118**(9): 3109-22.

Zimonjic, D. B., M. E. Durkin, C. L. Keck-Waggoner, S. W. Park, S. S. Thorgeirsson and N. C. Popescu (2003). "SMAD5 gene expression, rearrangements, copy number, and amplification at fragile site FRA5C in human hepatocellular carcinoma." *Neoplasia* **5**(5): 390-6.